THE ORDOVICIAN SYSTEM IN THE IDA BAY AREA

by

C. E. Sharples

Thesis submitted in partial fulfilment of the requirements
for the degree of Bachelor of Science with Honours

Geology Department
University of Tasmania
Hobart

1979

FRONTISPIECE *Ken Morrison examining broken Speleothem whilst field assisting in Entrance Cave. Smaller stalagmite growing on the break indicates the long period which has passed since the speleothem broke. But then,*

"All things must pass..."

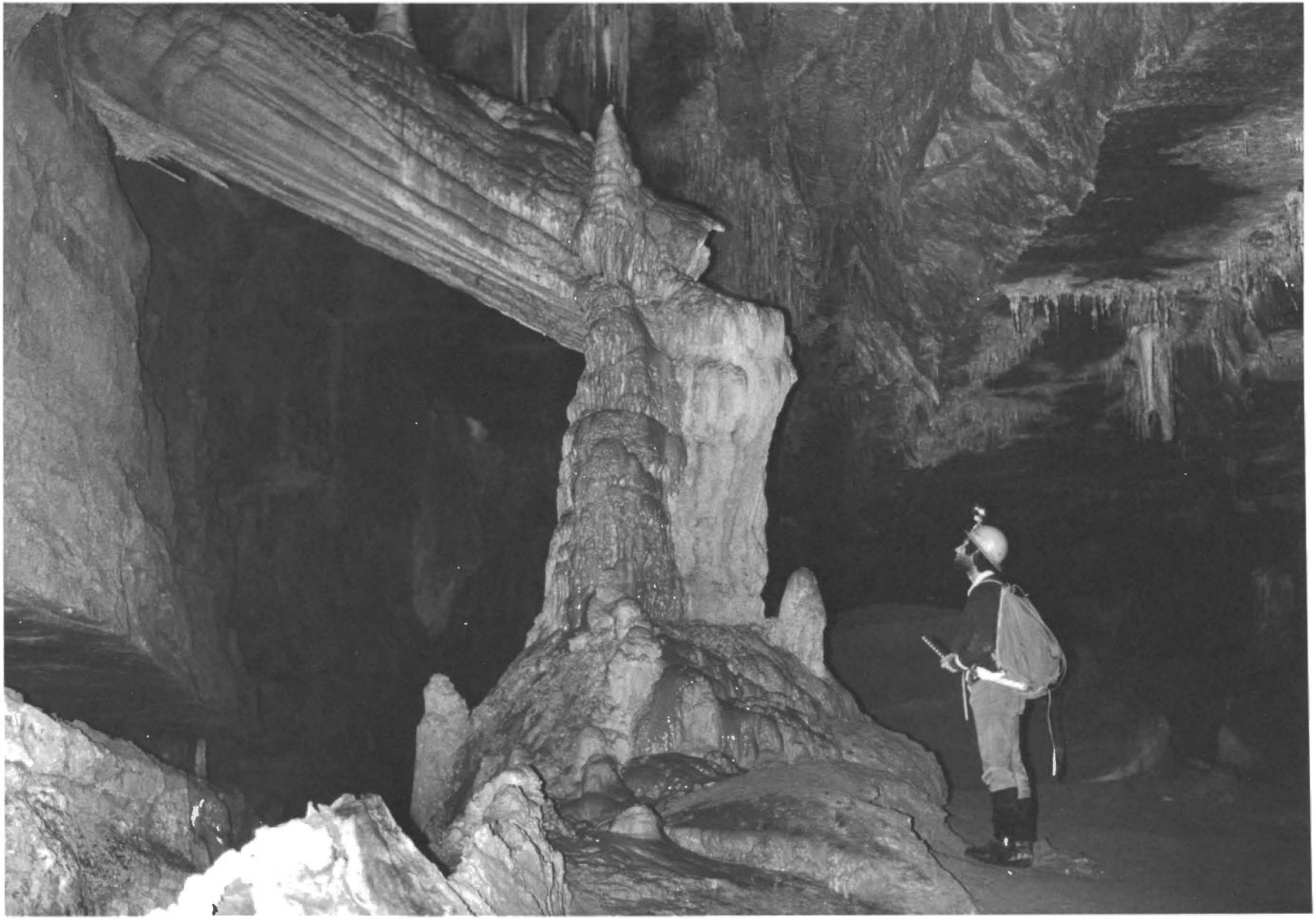

CONTENTS

LIST OF FIGURES

List of Figures (cont'd)

List of Figures (cont'd)

List of Figures (cont'd)

****

LIST OF TABLES

ACKNOWLEDGEMENTS

I wish to thank Dr M.R. Banks (supervisor), Dr C.F. Burrett, Dr C.P. Rao and Mr A. Goede for their enthusiasm and willing assistance in the mapping, sedimentological and palaeontological aspects of this project.

In regard to the palaeomagnetic aspects of this project, I am indebted to Dr M.W. McElhinny and especially to Dr C.T. Klootwyk for the time they took to assist, guide and discuss the work undertaken at the Australian National University (Canberra). Discussions in Canberra with Dr Brian Embleton and Professor Henry Halls, and in Hobart with Dr W.D. Parkinson, were also of great assistance and are much appreciated.

Discussions with fellow post-graduate and honours students proved valuable, and thanks are also extended to the various people who acted as field assistants on my subterranean excursions.

The co-operation of Benders Transport Company in allowing access to Newlands Quarry, and of Mr and Mrs B. Keady of the Ida Bay Railway Company in providing accommodation, was greatly appreciated.

Many thanks must go to my parents, Bill and Theo Sharples, for footing the bill for the production of this thesis. I am also indebted to Mrs Paula Goninon whose typing has been most efficient and accurate.

ABSTRACT

Ordovician sedimentary rocks in the Ida Bay area occur in a north-south trending Tabberabberan anticline, and in some further outcrops having doubtful structural relationships. Early Ordovician quartzites containing gastropods are overlain on Marble Hill by 350 metres of limestone ranging in age from Late Chazyan to Trentonian.

Ten lithofacies are distinguished in the limestones on Marble Hill, most of which represent sediments deposited in depositional regression cycles in a prograding tidal flat environment. While the lower 240 metres of limestones represent supratidal-intertidal conditions, the upper 110 metres represent intertidal-subtidal conditions.

Siliceous sediments on Coal Hill, north of the Lune River, appear to represent Ordovician Limestones which have been completely silicified, probably by a process related to silcrete horizon formation.

A primary Ordovician magnetisation is no longer present in the limestones on Marble Hill; instead a secondary magnetisation of mid-Cretaceous age has overprinted previous magnetisations in the limestone, probably as a result of burial and increased heat flow related to the rifting of the Tasman Sea.

CHAPTER ONE

INTRODUCTION

1.1 Locality

The region referred to herein as "the Ida Bay area" is an area situated several kilometres west of Ida Bay proper (see fig. 1:2). The area is situated roughly 70km south of Hobart and is centred at about 146°26' East longitude, 43°26' South latitude. The study area extends approximately from the D'Entrecasteaux River in the south to the Coal Hill-Hastings Caves area in the north, and from the Ida Bay and Lune River townships in the east to the Gleichenia Creek-Lune River Junction in the west (see fig. 1:2).

Access to the area is by the Huon Highway which is sealed to within 4.5km before the Lune River bridge (fig. 1:2) and thereafter by reasonable unsealed roads. A network of forestry roads exists in the area, some of which are passable to normal vehicles, and some (e.g. east branch of the North Lune Road) to four wheel drive vehicles only. Old tramlines still marked on contemporary survey maps are almost completely overgrown and impassable. Conversely, walking tracks not marked on survey maps give access to areas of geological interest. (Moonlight Flats, Mesa Creek and Exit Cave tracks; see fig. 1:2). A disused railway on the northern side of Marble Hill and Lune Sugarloaf still gives access to outcrops.

FIG. 1.1 View Southwest from Hastings Caves Road - Catamaran Road Junction. Lune River and Lune River Plains in middle-ground. Background consists of (Left to Right) Lune Sugarloaf, Marble Hill, and eastern slopes of Moonlight Flats (in rain). Newlands Quarry is just visible in the Lune S.L.-Marble Hill saddle.

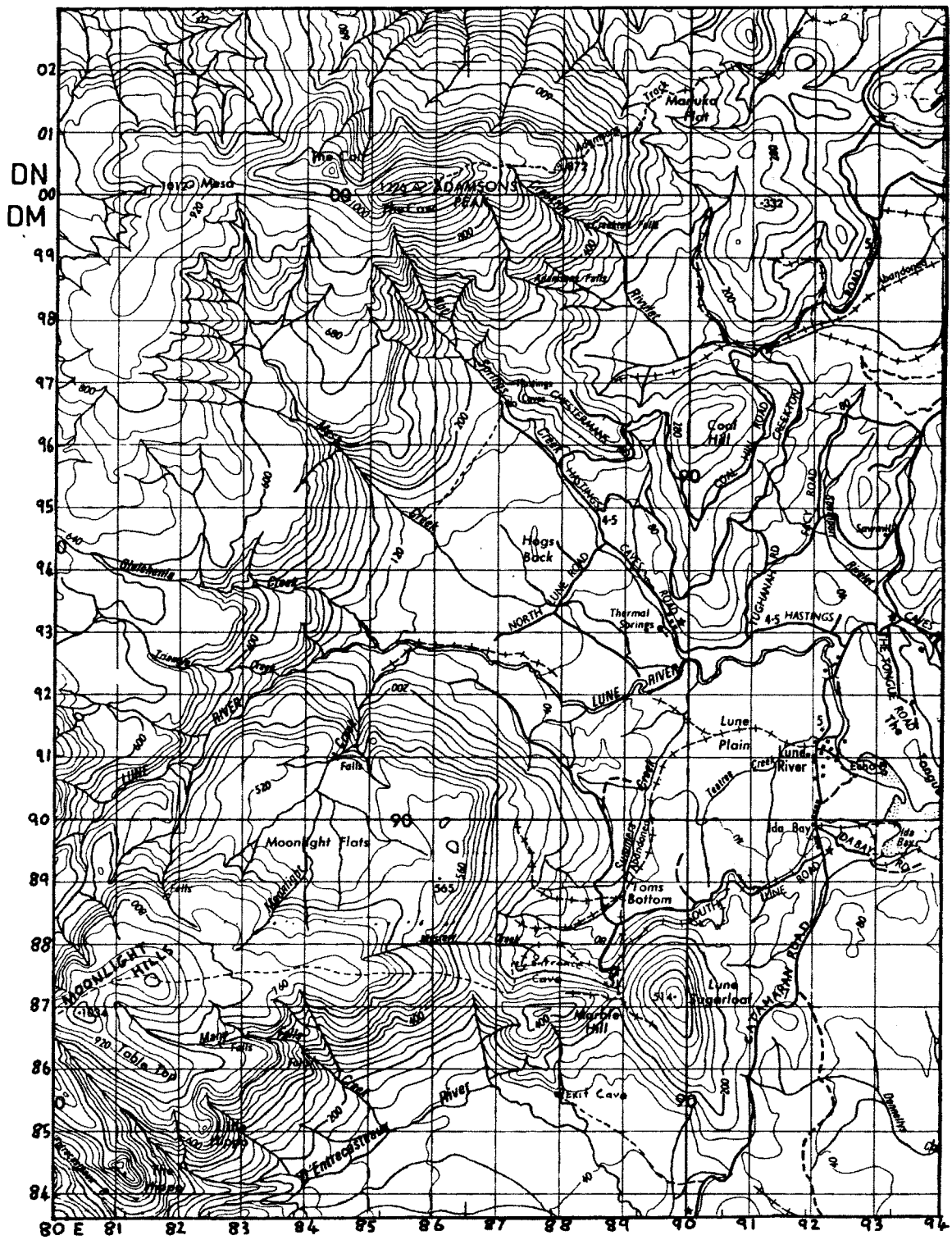

FIG.1:2 Ida Bay and surrounding areas

SCALE 1 : 100000

Kilometres 2 1 0 2 4 6 8 10 12 Kilometres

KEY

- Roads
- Tracks
- Railway
- Abandoned Railway

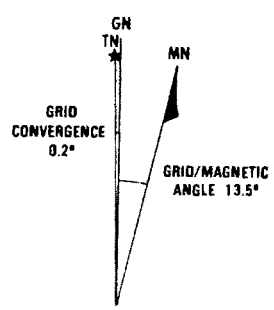

Locality

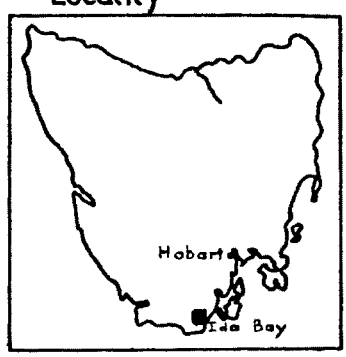

Most of the study area consists of low-lying plains surrounding the Lune River and covered with a mantle of alluvial sediments, resulting in a paucity of bedrock outcrops. This plain is surrounded on the north, south and west sides by steep hills whose sides are usually covered by slope deposits, again resulting in poor bedrock outcrop.

The Lune Plains are lightly vegetated to the east, but elsewhere the plains and hills are covered by forests of eucalyptus with a dense understorey, and by some myrtle forests.

The best bedrock exposures in the study area are man-made - road and rail cuttings, quarries, and costeans. The best of the natural exposures are in caves and a few riverside exposures.

The area of principal interest in this thesis is Marble Hill, in the south of the study area, which is a high spur extending eastwards from Moonlight Flats (see figs. 1:1, 1:3). Marble Hill is composed of Ordovician limestone with a cap of Permo-carboniferous tillite and other clastics. Road cuttings and quarries (one of which is presently being worked) on the northern side of the hill give good exposures of the limestone sequence.

An extensive cave system - the Entrance to Exit Cave system - extends beneath Marble Hill, and its geomorphology has been discussed by Goede (1969). (see Fig. 1:4). Parts of the cave system give good exposures of the limestone and were investigated in the present study.

In the past, Triassic coals have been mined in the Ida Bay region (Twelvetrees 1915) and silica has been quarried from the Ordovician quartzites of the Hogsback. (see Fig. 1:2). At present dolerite and slope deposits of a siliceous sediment (see chapter 2) are quarried on the Hastings Cave road for use as road metal, but the only major use of mineral resources in the area at present is the quarrying of limestone on Marble Hill for use by the Electrolytic Zinc Company, and the Carbide plant at Electrona.

1.2 Previous Work

The earliest published work on the Ida Bay region was produced by Twelvetrees (1915), who described the coal and limestone prospects of the area, together with a brief account of the regional geology as then known.

Unpublished work was done on the economic geology of the limestones by Nye (1926) and Dickenson (1945). Carey and Banks (1954) mentioned both the limestone and the underlying quartzite at the Hogsback, and gave a geological map of the area.

Everard (1957) summarised the geology and geomorphology of the Marble Hill area, and considerably improved the accuracy of the geological maps of that area as well as providing further chemical analyses of the limestones.

Refinements to knowledge of the boundaries of the limestone area on Marble Hill were added by Goede (1969) and Forsyth and Green (1976), the former also discussing the geomorphology of the caves beneath Marble Hill.

Öpik (1951) and Banks (1957, 1962) briefly mentioned the palaeontology of the limestones and speculated on their stratigraphic relations. More specifically, Teichert and Glenister (1952, 1953) described cephalopods from the limestones, Hill (1955) described corals, Banks and Johnston (1957) *Girvanella* and *?Macclurites*, Webby and Banks (1976) stromatophoroids, and Burrett (1978) conodonts.

The central and northern parts of the study area have hardly been worked on at all, as a result of which even the most recently published geological map of the area (Farmer 1975) contains major inaccuracies.

1.3 Scope of the Present Investigation

The present project can be broadly subdivided into three sections: regional geology, sedimentology/palaeontology/stratigraphy of the Ordovician limestones, and palaeomagnetism of the Ordovician limestones in the Ida Bay Region.

In view of the lack of detailed knowledge of the geology of areas north of Marble Hill it was decided to undertake regional mapping in order to set the limestones in the context of the area's overall geological structure. Although valuable knowledge has been gleaned from this work, the paucity of outcrop over large areas of the study region means that many aspects of the regional geology of the area around the Lune River remain a mystery.

Most previous palaeontological work on the Ida Bay Limestones has not been placed in a rigorous stratigraphic framework, and as such

has been of limited use in biostratigraphic correlation or erection of faunal assemblages. By making a detailed study of the stratigraphy of the limestones this study has set up a stratigraphic column which it is hoped will allow future studies to be placed within a stratigraphically controlled frame of reference. The present project has included a minor survey of the fossil forms present, with a view more to documenting some of the forms present and correlating with sequences elsewhere, rather than to making any real attempt at palaeoecological reconstruction.

The sedimentology of the limestones has been examined (although essentially from a petrographic point of view, with little geochemical work being done) in order to derive a depositional model for the limestones. This work will ultimately assist in palaeogeographical reconstructions of Tasmania in the middle-upper Ordovician.

Finally, a palaeomagnetic study of the rocks was undertaken in the hope of obtaining quantitative data on the palaeolatitude of Tasmania in the Ordovician. As shown in chapter five, however, a Cretaceous overprinting event has destroyed the primary magnetisation of the rocks.

1.4 Methods Employed

Details of stratigraphic, palaeontological, sedimentological and palaeomagnetic procedures employed in this work are discussed in the appropriate sections of this thesis.

1.5 Geographical Terminology Employed

In most cases the topographic nomenclature used in this thesis follows the usage on the 1:100,000 HUON map sheet (edition 3, 1977) produced by the Tasmanian Lands Department. In the past certain features have been known by several alternative names. Thus, "Marble Hill" (DM877869) has also been referred to as "Caves Hill" (e.g., in Everard 1957).

The only departure from the 1:100,000 map nomenclature in this thesis is that the main entrance and exit to the cave system beneath Marble Hill will be referred to as "Entrance Cave" (DM876878) and "Exit Cave" (DM880856) respectively, since these names appear to have gained wide currency amongst caverneers. In contrast, the HUON map sheet refers to Entrance Cave as the "Ida Bay Caves", and it has also been referred to as the "Mystery Creek Cave".

The limestone quarries on and near Marble Hill are named according to the usage of Forsyth and Green (1976). Thus, the western-most, disused, quarry at (DM874876) is referred to as "Blaneys Quarry", while the main quarry presently being worked at (DM888874) is called "Newlands Quarry". About one kilometre NNE of Newlands Quarry, at (DM893882), two small disused quarries occur just south of a disused railway line. These quarries are known as the "Lune Sugarloaf Quarries".

Co-ordinates given in this thesis refer to the arbitrary grid used on all metric lands department maps, and are prefixed by the universal grid reference letters DM.

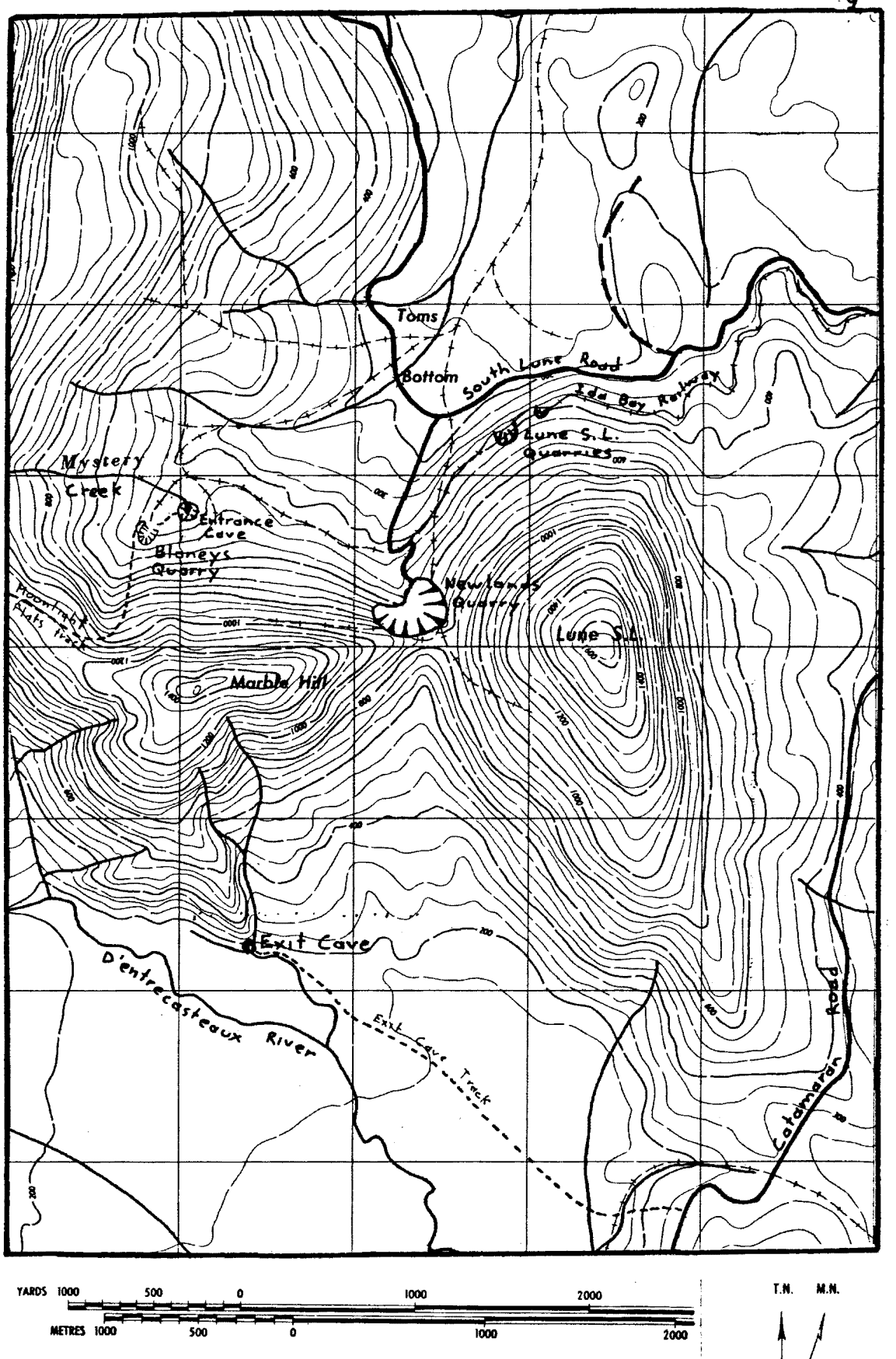

FIG. 1:3 Map of Marble Hill area. Contour interval is 50 feet. Most railways and tramways shown are now overgrown, except for the Ida Bay Railway which provides access to Blaney's Quarry.

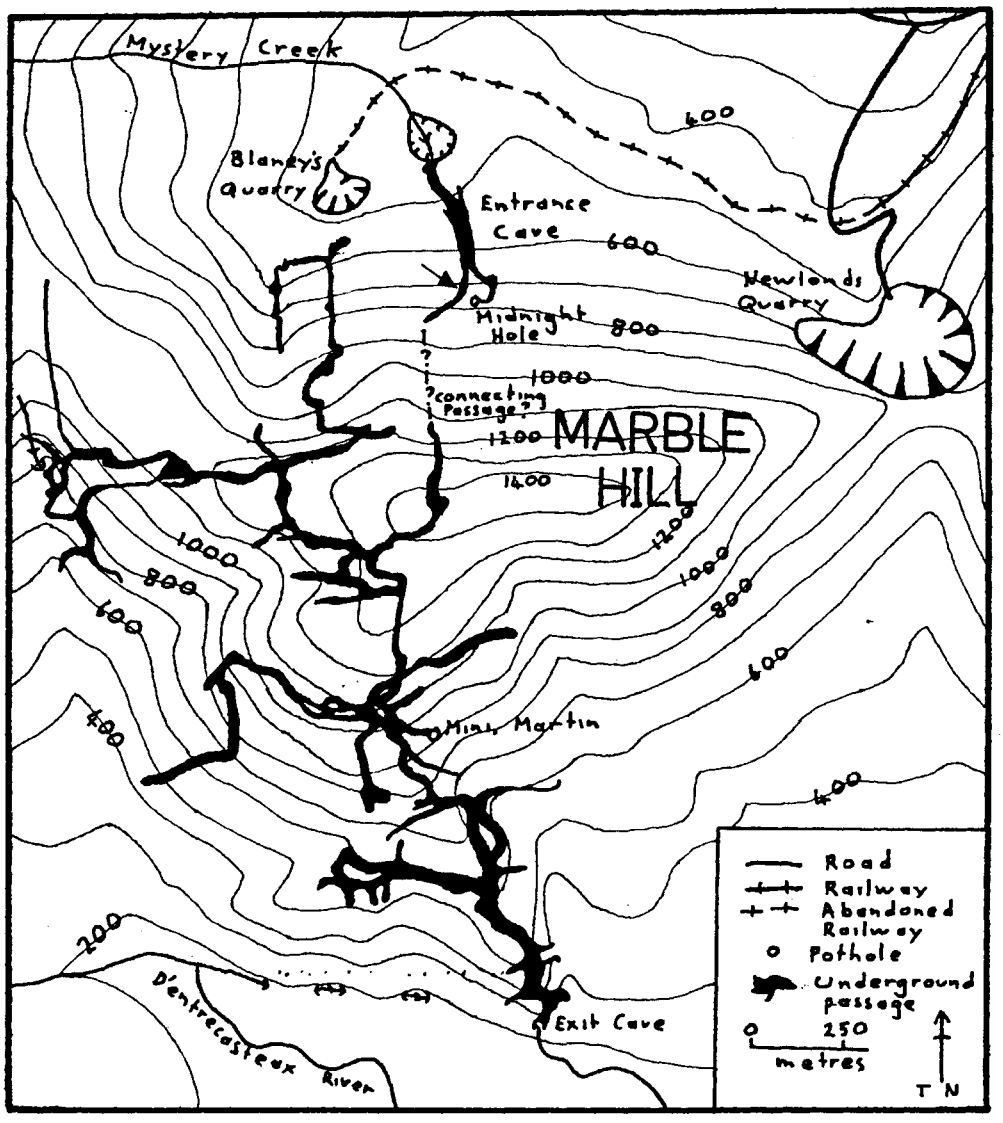

FIG.1:4 Map of Entrance-Exit Cave System beneath Marble Hill, taken (with alterations) from Goede (1969). Contours are in feet. Arrow to the left of Entrance Cave indicates point at the base of the stratigraphic section measured in Entrance Cave.

In the course of mapping, certain locations were numbered for ease of referring to them. (loc. 1, 2, etc.). These location numbers are used in the text, and are listed in appendix six, where their position and grid co-ordinates are given.

CHAPTER TWO

REGIONAL GEOLOGY

2.1 Precambrian

The only rocks of probable Precambrian age in the study region are the dolomites of the Hastings Caves Area. The quartzite at the Hogsback (DM875944) has previously been regarded as a precambrian quartzite conformably underlying the dolomites (Carey and Banks 1954, Spry 1957), but is now known to be of Ordovician age (section 2:2).

Dolomite occurs on the slopes of a ridge extending southeast from Adamsons Peak. It outcrops beneath a cap of Permo-carboniferous clastics and is best known on the south side of the ridge where several large caves are found. The dolomite probably outcrops on the northern side of the ridge, where karst features have also been reported.

On present evidence it is not possible to determine the structural relationship between the dolomite and the lower palaeozoic sediments of the area.

At the entrance to Newdegate Cave (DM872966) - also known as "Hastings Caves" - the dolomite is a pale yellow sediment showing no sedimentary features. Microscopically, the rock is a featureless dolomicrite. The rock is intensely fractured and has at least one

parting (Dip 34 degrees towards 340 degrees magnetic) which is probably jointing.

Better exposures occur in King George V Cave (DM993961) where bedding can be seen although details are obscured by the mudcoating on the cave walls. The bedding has gentle warping of a one metre wavelength, but has an average dip of 58 degrees towards 247 degrees magnetic. The dolomite is a fine grey sediment, finely laminated and with crossbedding, soft-sediment deformation and penecontemporaneous brecciation. Quartzite interbeds occur commonly within the dolomite, and are characterised by an extremely high surface relief compared to the dolomite. The quartzite beds may be one to ten centimetres thick, and commonly show fine internal lamination.

The sediments have a "boxwork" of planar quartz viens in a number of different orientations.

2.2 ?Early Ordovician Quartzites

White quartzites with minor conglomerates occur in an anticline trending north-south from the Hogsback (DM875944) to the base of Marble Hill (DM877869). The occurrence of fossils has demonstrated these beds to be Palaeozoic, rather than Precambrian as was previously thought. (Carey and Banks 1954).

The quartzites are best exposed on the Hogsback, a distinctive ridge comprising a part of the axis of the anticline. In a small quarry on the northwest side of the Hogsback (at DM87549458) the bedding dips 80 degrees towards 275 degrees magnetic, and crossbedding,

FIG. 2:3 Probable worm casts on a bedding plane in Early Ordovician quartzites on the Hogsback. Scale graduated in centimetres.

FIG. 2:4 The prominent ridge of The Hogsback, viewed from the south. Most outcrops are on the western side. (Shown in photograph). Adamsons Peak is visible in the background to the left of the Hogsback.

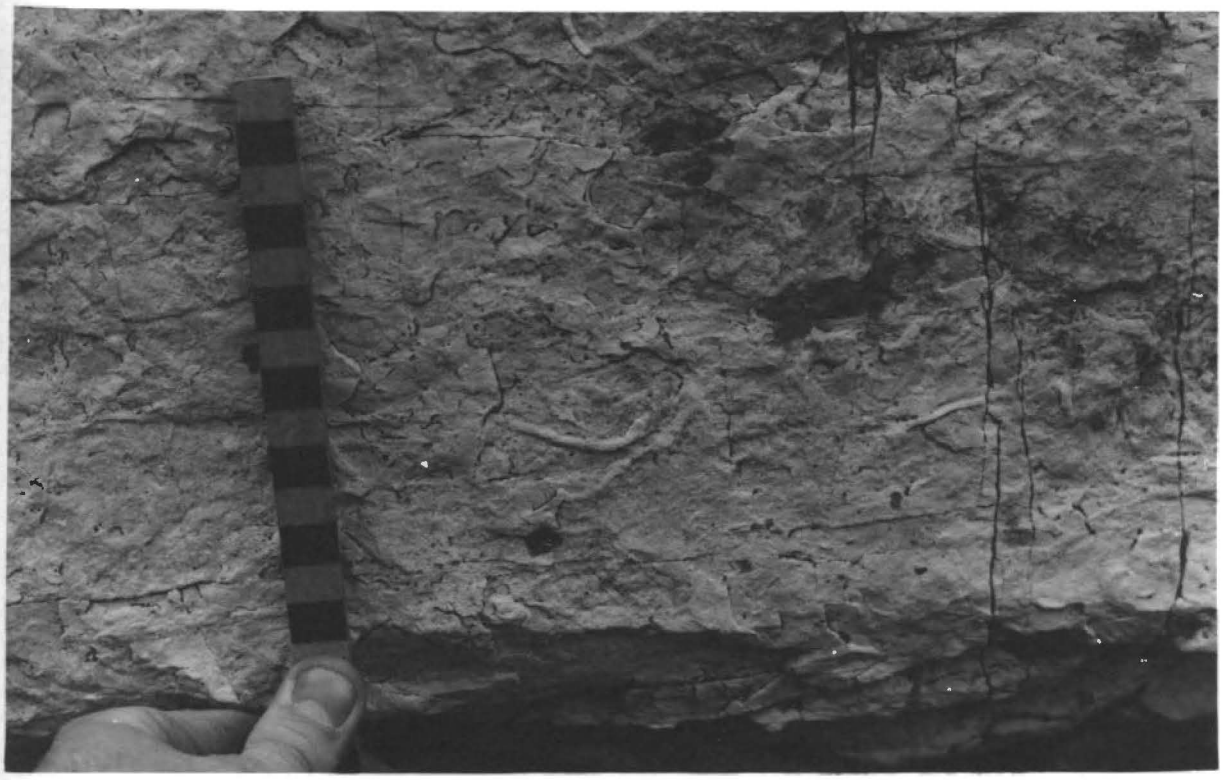

FIG. 2:5 Early Ordovician siliceous conglomerate in a Costean south of the Lune River, at DM88269135. Scale graduated in centimetres.

FIG. 2:6 Crossbedding and cut-and-fill structures in Early Ordovician quartzites exposed in a small quarry at DM87549458 on the Hogsback. Present day "up" is at the right and west is to the top of the photo. Prior to folding west was to left of photo. Crossbedding indicates currents derived from west, while cut-and-fill gives facing of beds. Scale graduated in centimetres.

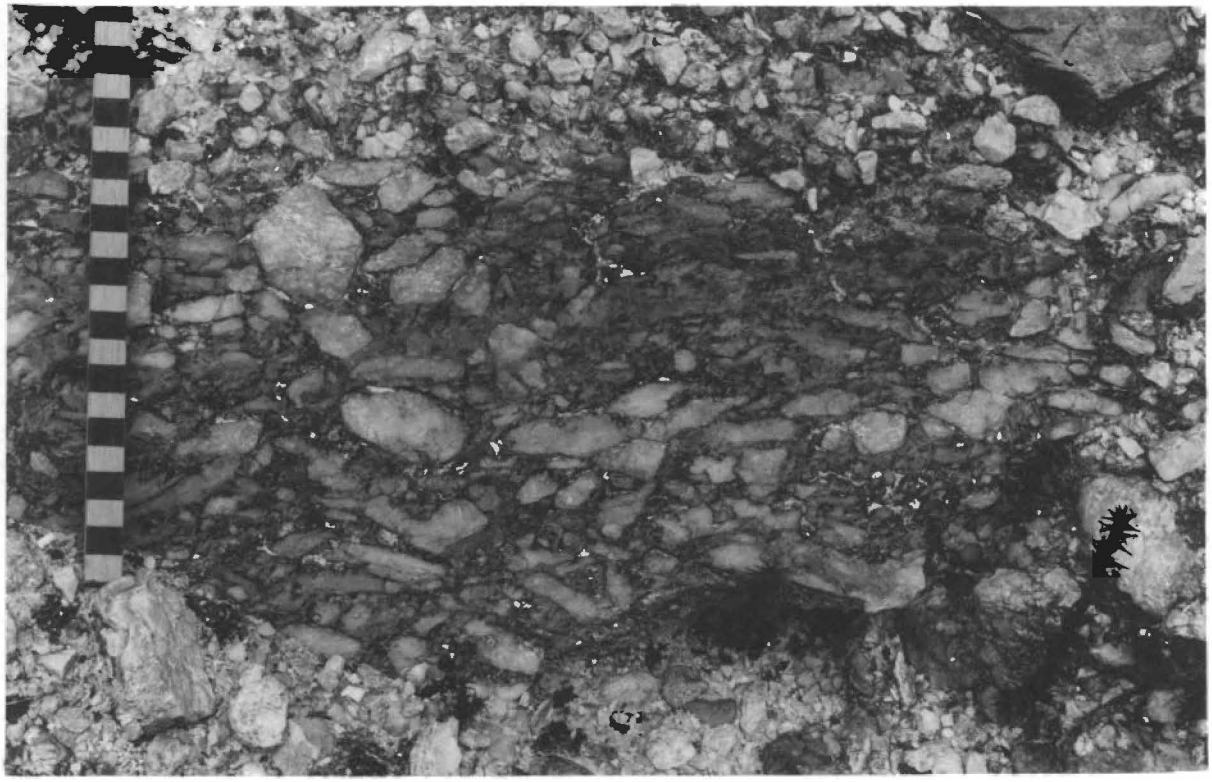

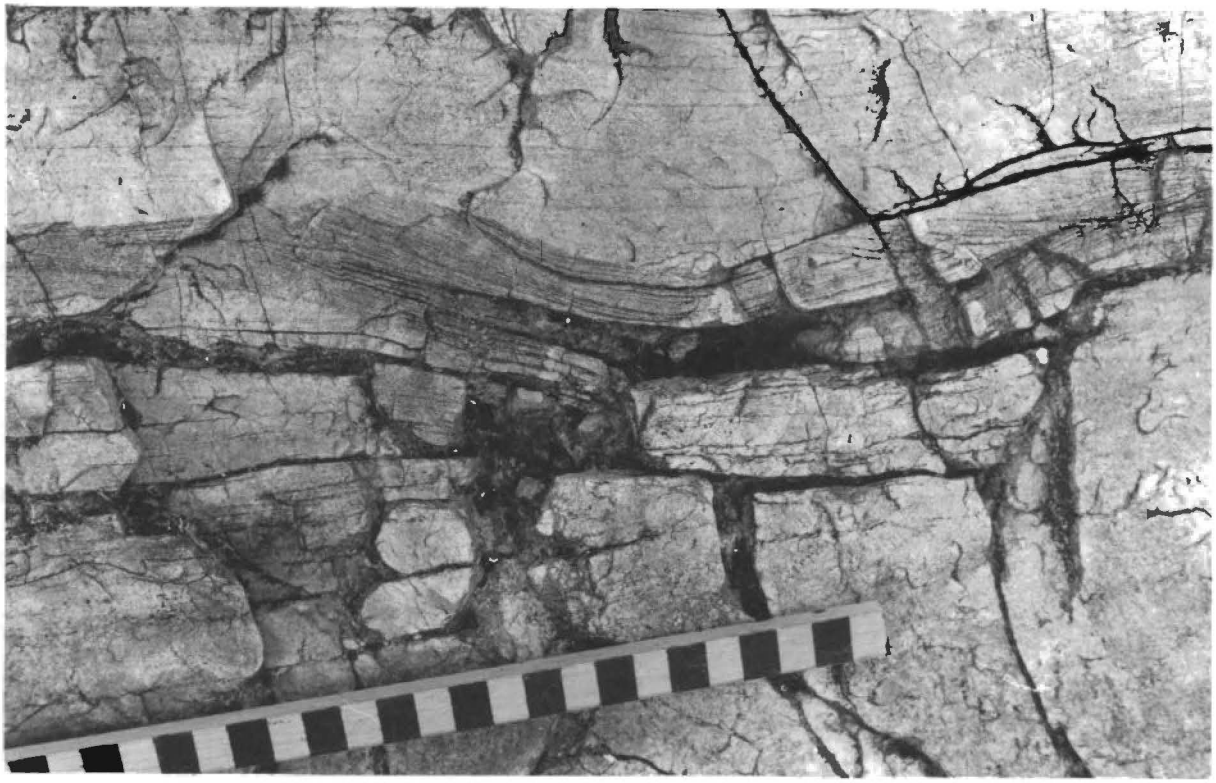

cut-and-fill structures (see Fig. 2:6), and load casts indicate that the "bedding-up" direction is towards 275 degrees. However, a mere fifteen metres or so to the west, on the ridge top, the bedding dips in the opposite direction. Near the southern end of the ridge a dip of 66 degrees towards 75 degrees magnetic was measured, and poor load casts indicate that "bedding-up" is towards 75 degrees. The Hogsback is thus an exposure of the tightly folded core of anticline. Slickensliding occurs on the Hogsback.

The quartzites on the Hogsback are hard white medium grained quartz arenites in beds commonly 0.2-0.2 metres thick. Fine laminations, small scale trough crossbeds and cut-and-fill structures occur, and worm casts are commonly exposed on bedding surfaces (see Fig. 2:3). Fossils are rare on the Hogsback, but one thin bed occurs in the small quarry at DM87549458 which contains gastropods and fragments of ?trilobites, ?brachiopods and other organisms. Fine conglomerate bands occur, containing rounded quartz pebbles up to 10mm diameter. Crossbedding indicates current transport from the west after unfolding of the anticlinal structure (see Fig. 2:6).

An outcrop of similar quartzites and fine conglomerates occurs just south of the Hogsback, on the North Lune Road at DM87759325, where the bedding dips at 52 degrees towards 72 degrees magnetic. In thin section, a typical specimen (48221) is seen to be a quartzarenite (Folk 1968) with a quartzitic texture of interlocking anhedral grains.

Some grains have "dustrings" (Carozzi 1960, p. 21) indicating secondary overgrowths of silica. (see Fig. 2:7).

Average grainsize is 0.2-0.4mm diameter, although grains up to 1.5mm diameter occur in a coarser band. The quartz is about 95 per cent monocrystalline grains, most of which show undulose extinction implying origin from a metamorphic terrain. A number of grains, including many of the larger grains, show non-undulose extinction and commonly have lines and bands of minute inclusions. These grains are possibly of igneous origin although this cannot be proven in the absence of other igneous minerals. Finely polycrystalline chert clasts comprise about five per cent of the slide.

South of the Lune River outcrops of quartzite occur in costeans and a road-gravel quarry off the South Lune Road, at DM882908. The quarry (location 14) does not give a good bedrock outcrop, but contains angular blocks of white quartzite with gastropods (Helicotomide gastropods, and other forms - see appendix three). The quartzite is of medium grainsize, with some laminations and planar crossbeds.

The costeans are cut into a ridge extending several hundred metres northwards from the quarry, and expose bedrock outcrops of quartzites similar to that in the quarry. One costean at DM88269135 exposes beds dipping at 53 degrees towards 70 degrees magnetic which include a coarse siliceous conglomerate (see Fig. 2:5). The conglomerate contains angular to subrounded and generally elongate clasts of quartz up to 4cm diameter.

Dips obtained from other costeans were: 41 degrees towards 65 degrees magnetic at DM88279113, and 59 degrees towards 85 degrees mag. at DM88259091.

No outcrop of quartzite is known in the area immediately to the north of Marble Hill, but its existence in that area is inferred from the abundance of white quartzite fragments in roadside cuttings along nearby parts of the South Lune Road (see Fig. 2:2). The occurrence of quartzite bedrock at the base of Marble Hill, if this inference is valid, implies that the quartzite lies stratigraphically immediately beneath the limestones, and that the quartzite-limestone transition is probably not too far beneath the limestones exposed in the Entrance-Exit Cave system.

Twelvetrees (1915, p.8) referred to quartzites and quartzite conglomerates of lower palaeozoic age "in the hills north of Ida Bay Caves". Twelvetrees records a cut put in (apparently) bedrock by prospectors, which exposed "white siliceous quartzites running north-north-east and dipping apparently in a north-westerly direction". Twelvetrees also refers to a locality "further west" where a cut had been put into a white quartz conglomerate containing angular and sub-cangular clasts of quartz. These beds dip west-south-west at an angle of 40 degrees. "Further west" agian, they are capped by "diabase" (dolerite) which crowns the crest of "the range". (Presumably "the range" refers to either Adamsons Peak or perhaps the Coal Hill area).

The area mentioned by Twelvetrees sounds like the area of siliceous slope deposits in the Coal Hill area (see section 2:4), but his description of quartz conglomerates sounds like a primary clastic sediment. If Twelvetrees was in fact talking about the Coal

FIG. 2:7 Early Ordovician quartzite under crossed nicols. Note syntaxial overgrowth on large quartz grain in centre of field.
48221 Mag. x 85

FIG. 2:8 Outcrop of Ordovician limestone on the Lune River, at location 15. Note sharp-edged *Rillenkarren*. Scale graduated in 0.1 metre units.

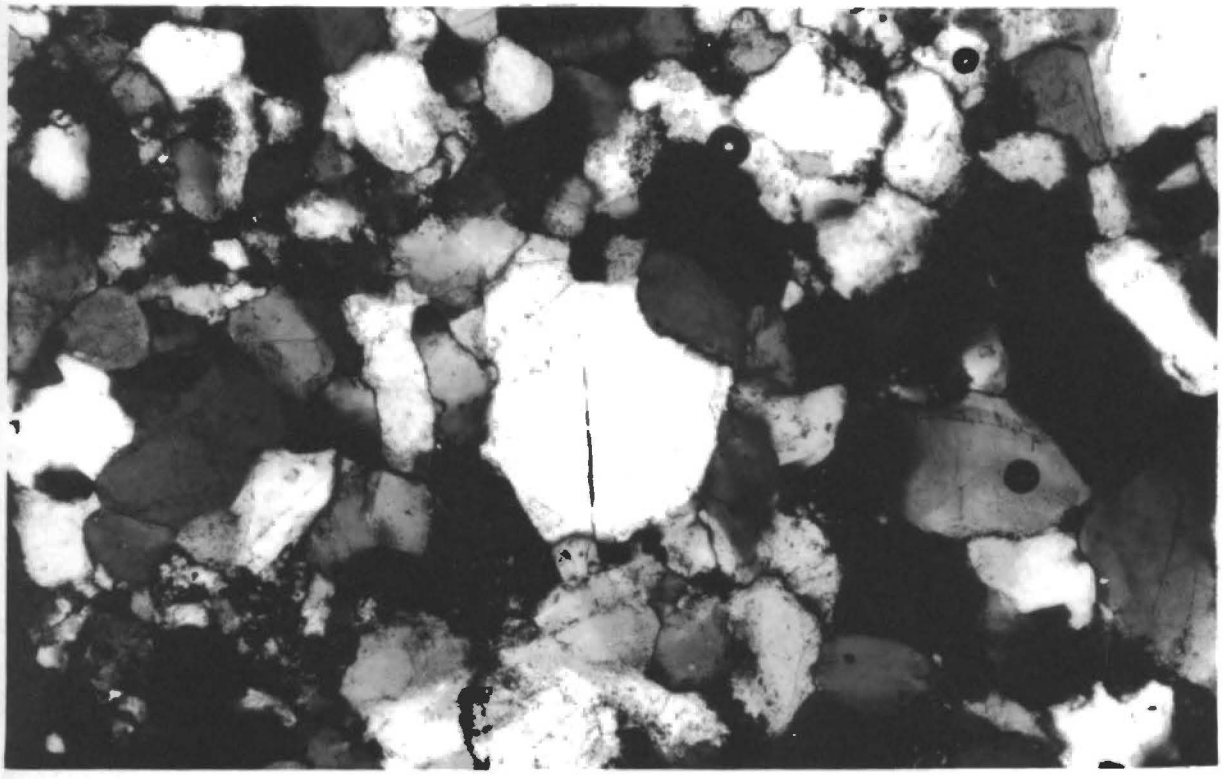

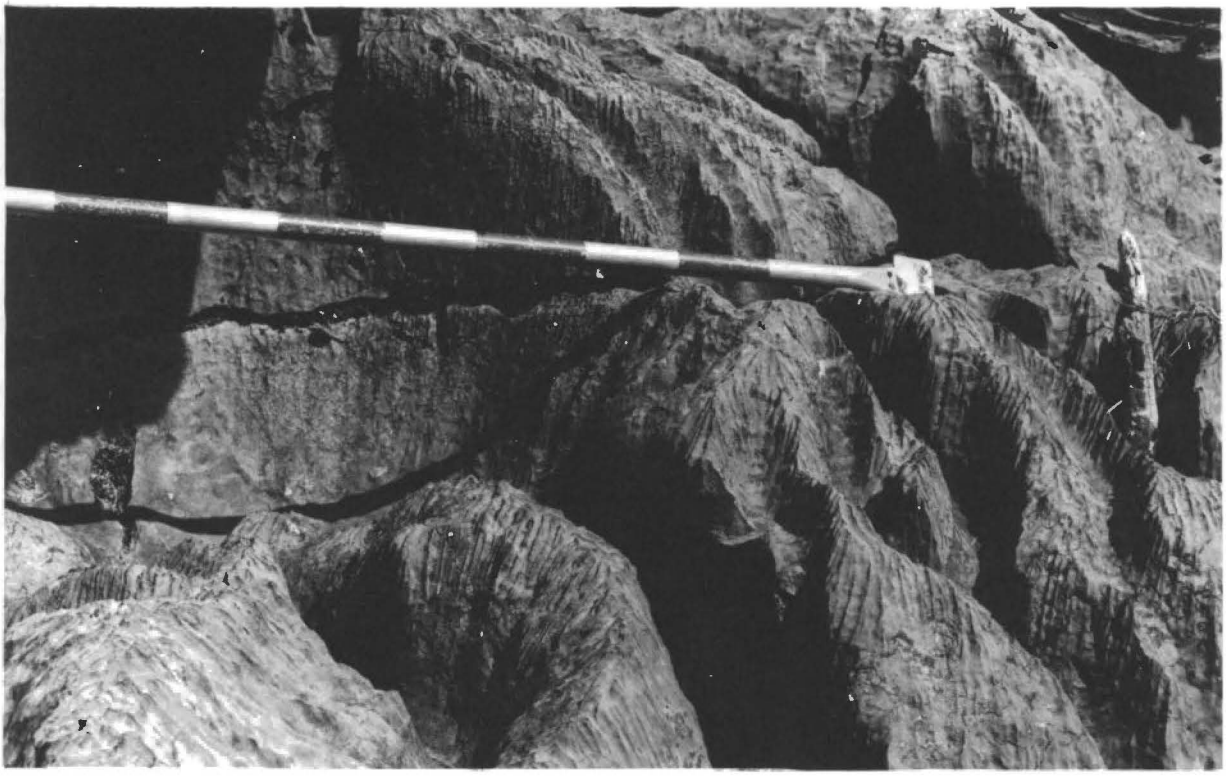

Hill area, it is possible that at least part of that area is underlain by primary terrigenous quartzites.

The occurrence of worm burrows and gastropods on the Hogsback and elsewhere indicates a near-marine (intertidal?) environment for the quartzites in the Ida Bay area. Sparse occurrences of trough crossbedding and minor conglomerates may indicate fluvial and intertidal channel activity (with derivation of sediments from a westerly direction?), but the geographically restricted nature of the quartzite outcrops precludes regional analysis of the sedimentary environments involved.

An Early Ordovician age for these quartzites is implied by their probable occurrence beneath the middle-late Ordovician limestones on Marble Hill.

2.3 Middle-Late Ordovician Limestones

1. Marble Hill and adjacent areas.

The Ordovician limestones which are the main subject of this thesis make up the bulk of Marble Hill (DM877869), where they are capped by a Permo-carboniferous sequence. The limestones also outcrop on the lower northern slopes of Lune Sugarloaf (DM898872), and are presumed to extend northwards and south-westwards from Marble Hill along the lower eastern and southeastern slopes of Moonlight Flats (DM845875) (see Fig.2:1).

The latter two extensions are not proven, however, and attempts by caverneers to find limestones on the southeast slopes below Moonlight

Flats have not been successful (A. Goede, *pers. comm.* 1979). It has been suggested that the near-linear stream channel at DM867866 may be the expression of a fault which downthrows strata to the west, resulting in little or no limestone outcrop. (See also section 2:12).

An east-west trending fault has also been suggested immediately to the north of Blaney's Quarry and Entrance Cave (Collins 1968) which would downthrow dolerite north of Mystery Creek (DM875879). There is no direct evidence known for this fault, however, and its existence is considered unlikely since there is evidence (see section 2:2) for Ordovician quartzites in the area in question.

Because the available outcrops in the Marble Hill area have already been noted by earlier workers, this study has not made any further refinements to knowledge of the boundaries of the limestone area, except to make what is considered a more reasonable extrapolation of the extent of limestone northwards and south-westwards than has previously been published. (Farmer 1975)

The sedimentology, palaeontology and stratigraphy of the limestones on Marble Hill are considered in detail in Chapter Three, Appendix Three and Chapter Four, respectively, of this thesis.

The limestones on Marble Hill are folded into a gentle anticline whose north-south trending axis is approximately co-incident with the Entrance-Exit Cave System (DM876878 to DM880856 - see Fig. 2:10). Northward and southward dip components in Entrance and Exit Caves, respectively, indicate that the anticline is warped into

a domal structure beneath Marble Hill. (See Fig. 2:9). The maximum recorded dips are 10 and 13 degrees towards the east on the easternmost limestone outcrops north of Lune Sugarloaf (see Fig.2:1). Steep dips towards the west are reported from small caves west of Blaney's Quarry (A. Goede, *pers. comm.*1979), but these outcrops were not relocated in the present investigation. In Blaney's Quarry the average dip is about eight degrees towards 314 degrees magnetic. This varies eastwards to a dip of five degrees towards 360 degrees magnetic in Entrance Cave. Local warping occurs in Newlands Quarry, but the average dip seems to be about six degrees towards 140 degrees magnetic.

A bed containing large oncolites in a dolomitic sediment (Lithofacies III) outcrops on the Moonlight Flats track well above Blaney's Quarry and not far below the unconformity at the top of the limestone. If this unit correlates with a similar unit on the road just below Newlands Quarry (as appears reasonable on structural grounds - see Fig. 2:10), then from its location on the Moonlight Flats track it is possible to estimate the stratigraphic height between the top beds exposed in Blaney's Quarry and the bottom beds exposed on the road below Newlands Quarry as being approximately 100 metres. (Due to patchiness of outcrop a section has not been measured up the Moonlight Flats track). Assuming this figure, and combining stratigraphic sections measured between the lowest exposed beds (at the top of Newlands Quarry) it appears that approximately 350 metres, stratigraphically, of Ordovician Limestone is exposed on Marble Hill. This represents the greatest thickness known to be attained by the limestone in the Ida Bay area.

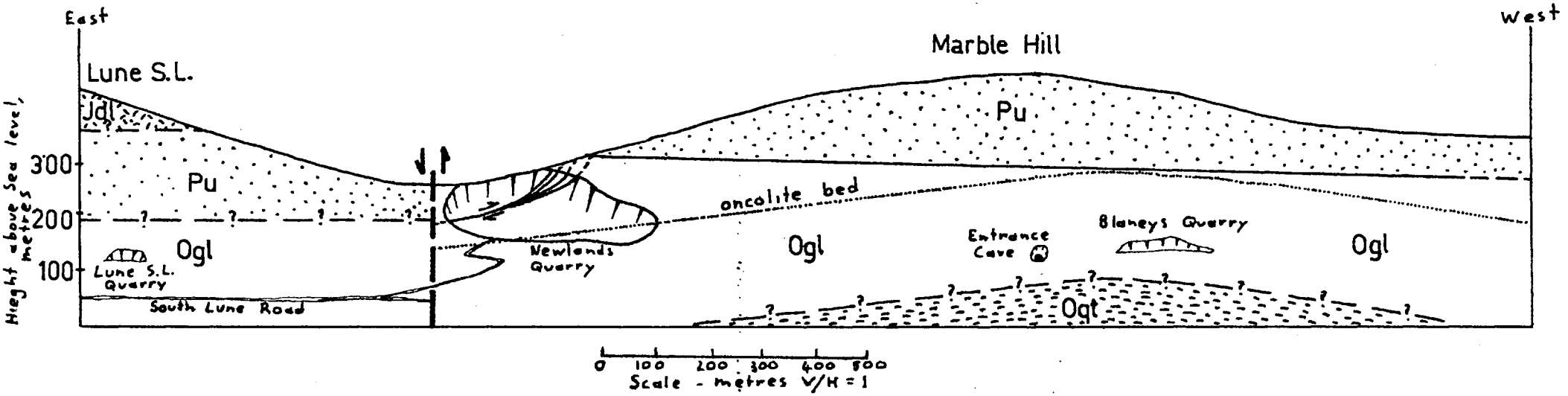

FIG. 2:10 East-west cross section through Marble Hill. Oncolite bed (at 240m - see Fig. 4:1) shows anticlinal structure of limestone.

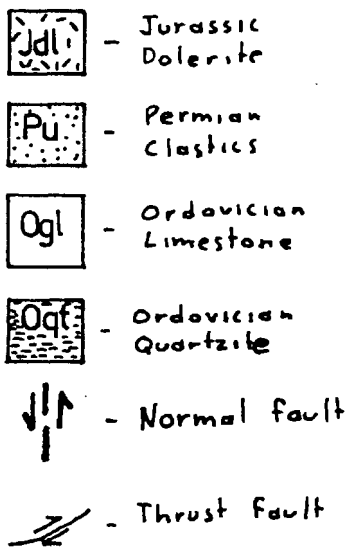

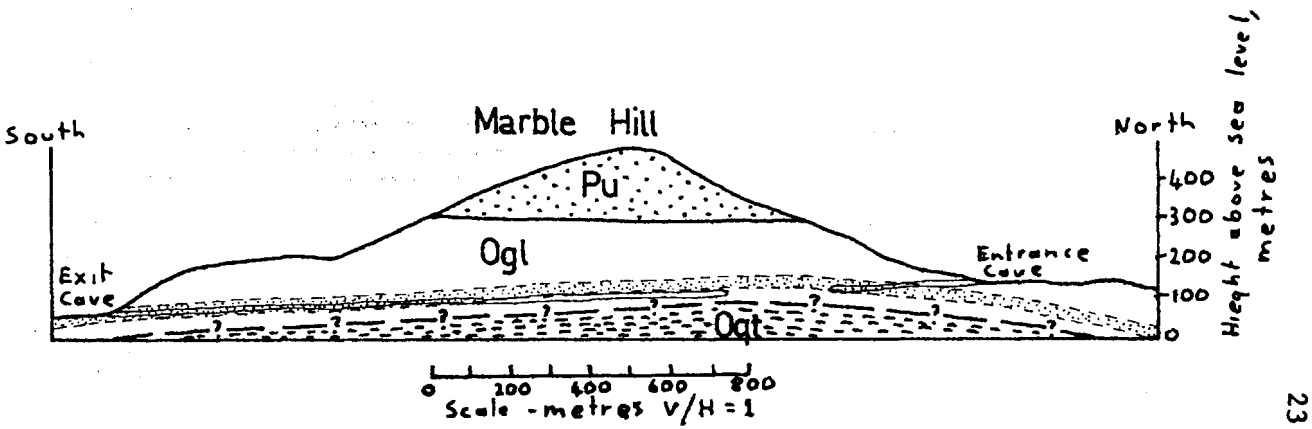

FIG. 2:9 North-South cross-section through Marble Hill, between entrance of Entrance Cave, and exit of Exit Cave. Birdseye limestone bed in caves shown, indicating domal warping of anticline.

The lowest beds observed during this project are the birdseye limestones of Lithofacies I (see Chapter 3) which extend to the bottom of Entrance Cave. (see Fig. 1:4). A similar Birdseye Limestone outcrops for at least the first 600 metres going northwards in from the main "exit" of Exit Cave, with neither an upper nor a lower boundary being seen in that distance. The birdseye limestones in Entrance and Exit Cave are regarded as belonging to the same unit on the grounds of their sedimentological similarity, the unusual thickness of the lithofacies in both caves, and the fact that the same unit would be expected to outcrop in both caves because of the domal structure of the Hill. (see Fig. 2:9). Because of the domal structure it is expected that stratigraphically lower units should outcrop further north inside Exit Cave, and indeed a 0.5 metre shale band, not known from above the birdseye unit in Entrance Cave, has been reported from deep inside Exit Cave. (A. Goede, *pers. comm.* 1979).

The base of the limestone, barring unknown structural complications, is probably not far beneath the Entrance-Exit Cave system (see Section 2:2), but any outcrop of the base is obscured by recent deposits on the north side of Marble Hill.

The limestone is overlain unconformably by Permo-carboniferous sediments. On Marble Hill the unconformity dips towards the west at a low angle. The unconformity outcrops at 300 metres altitude behind Newlands Quarry, and has been located at 290 metres altitude near Mini Martin pothole (Goede 1969, see also Fig. 1:4) and at about 277 metres altitude near Midnight Hole (*ibid.*). Another stream

goes underground just below the unconformity at about 235m altitude on the southwest side of the saddle between Moonlight Flats and Marble Hill (*ibid.*).

In the larger, westernmost, of the two Lune Sugarloaf quarries (at DM893882) burrowed micrites and biomicrites with Cephalopods, *Calathium, Solenopora, Tetradium, Bajgolia caespitosa, Pycnolithus* and Stromatoporoids outcrop below dolomitised brachiopod-rich micrites (c.f. Lithofacies VII, ch. 3?) and further burrowed micrites with trilobites and stromatoporoids. (see Fig. 2:11). The sediments dip at thirteen degrees towards seventy degrees magnetic.

Several outcrops of limestone occur on the South Lune Road below the Lune Sugarloaf quarries. The westernmost road outcrop, at DM890883, comprises algal-laminated and mudcracked limestone dipping at six degrees towards 95 degrees magnetic. Further east, at DM896886 and DM89758860, micrites with thick horizontal dolomite stringers and strophamenid-rich bioclastic bands dip at ten degrees towards ninety degrees magnetic. These latter outcrops resemble lithofacies VII sediments (Ch. 3) and have yielded large numbers of conodonts.

2. Lune River

A small outcrop of Ordovician limestone occurs on the Lune River at location 15 (DM880918), topographically below and immediately to the north of Early Ordovician quartzites (see Fig. 2:2). In view of the juxtaposition of these two lithofacies there is clearly major

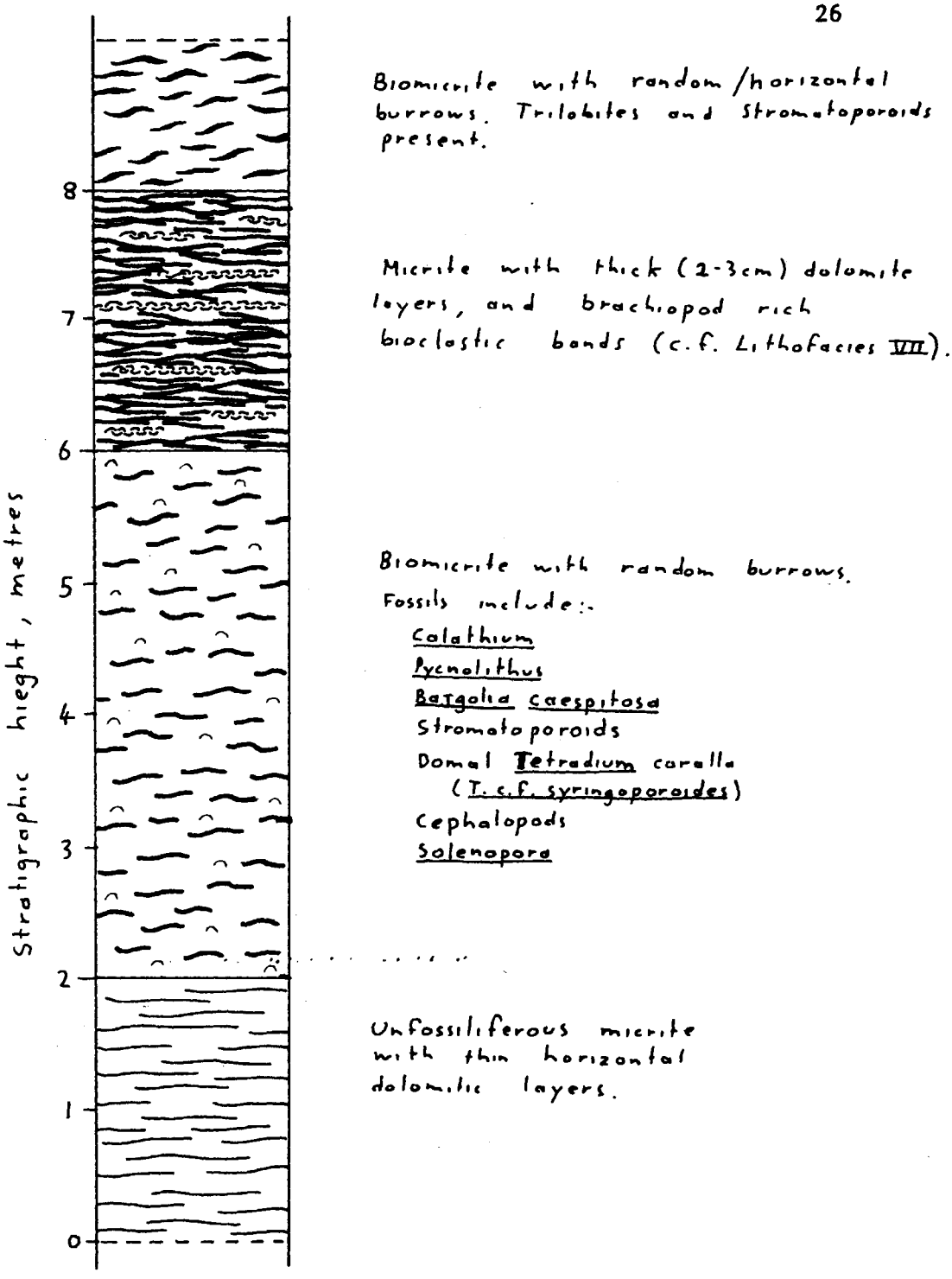

FIG. 2:11 Stratigraphic column measured up from floor of westernmost Lune Sugarloaf Quarry. Top of quarry face is inaccessible, so that stratigraphic column only covers lower half of quarry face.

structural complications in the area and indeed if two linear reaches of the Lune River, at around DM888918 and DM896921, result from a normal fault downthrowing to the north then this would account nicely for the outcrop pattern.

The limestone has sharp microkarst features - "rillenkarren" (see Fig. 2:8). The bedding is virtually horizontal, and the limestone appears in the field as an Intrabiomicrite containing *Bajgolia* or *Eofletcheria*, *Solenopora*, and other fossils. Minor oncolite development was noted, so that the lithofacies probably represents a shallow subtidal environment. Abundant conodonts have been obtained from this outcrop.

Microscopically, the limestone is a poorly washed intrabiosparite, with micritic patches grading into elongate spar patches about one centimetre thick, which may represent bioturbation. Intraclasts are rounded, and moderately well sorted, averaging 0.3-0.5mm diameter, and, together with fossil fragments in the same size range, are set in a fine spar matrix. (e.g., 48222).

3. Mesa Creek

Limestones of presumed Ordovician age are exposed in Mesa Creek at their unconformable contact with overlying Permo-carboniferous tillites. The dip of both the unconformity and the limestone changes considerably over a short distance.

At about DM84959542 the limestone dips at 22 degrees towards 120 degrees magnetic, and is overlain unconformably by over three

FIG. 2:12 Boulder of limestone in Mesa Creek, showing typical nature of sediment. Dark bands are argillaceous sediments. Scale graduated in centimetres. (N.B. Photo printed sidewards - top is to left)

FIG. 2:13 Unconformable contact between Permo-carboniferous tillite (above) and flat-lying Ordovician limestones (below) on Mesa Creek at about DM84809562. Geological hammer gives scale.

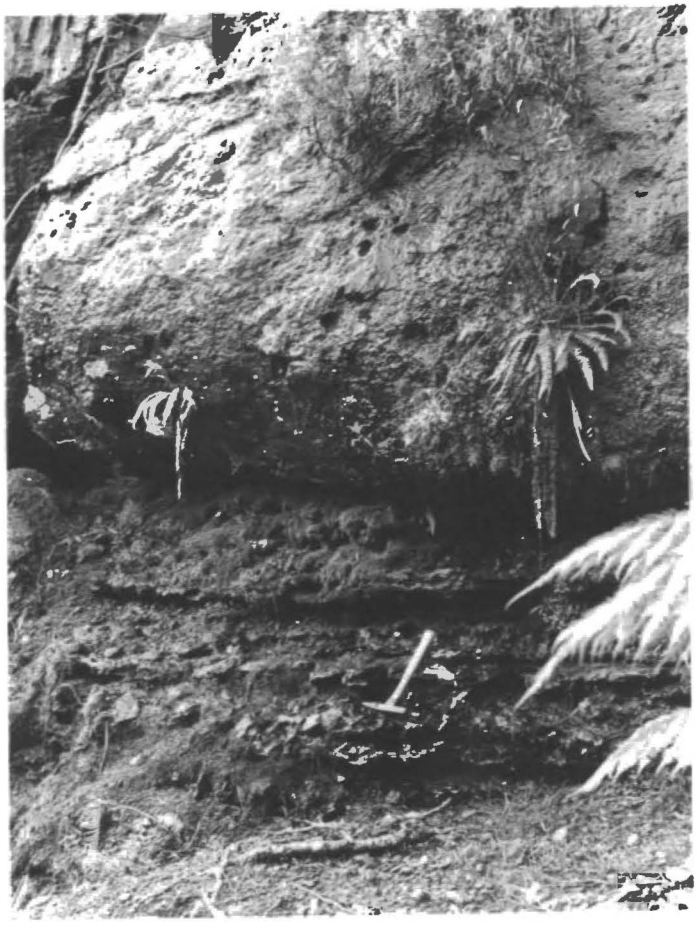

metres of tillite. The unconformity is irregular, transgressing some limestone beds and following others. Over 200 metres upstream at about DM84809562, the unconformity, which outcrops about ten metres above the stream bed, is horizontal and overlies near-horizontal limestone beds (see Fig. 2:13). The overlying tillite appears thinner than at DM84959542, grading up into a yellow-green mudstone after only a few metres.

There is about forty metres difference in topographic height between the two outcrops, and on the strength of the above facts, the pre-Permian topography of the area must have been quite uneven, with the upstream outcrop having been topographically higher than the downstream outcrop. The unevenness of the pre-Permian topography is apparently only local - the unconformity is much flatter on Marble Hill, and in fact the lower outcrop of the unconformity in Mesa Creek is at the same topographic height as the inferred position of the unconformity on Chestermans Road (see Fig. 2:1), so that the unconformity must be reasonably flat, or have only localised unevenness, between Mesa Creek and the Hastings Caves area.

The limestones outcropping on Mesa Creek are pale-brown weathering micrites with regular horizontal interbeds, averaging 1-3cm thick, of dark brown argillaceous material (see Fig. 2:12). Angular quartz grains up to 0.03mm diameter and dolomite rhombs of similar size occur in the argillaceous layers (e.g., 48223). Fossils are rare - a few shells occur, but only in one loose specimen (48224) was a concentrated band of fossils found. In 48224 a band

3cm thick contains broken fragments of trilobites, gastropods, bryozoa, ?algae, brachiopods and other organisms in an unwashed micrite matrix.

The scarcity of fossils and micritic nature of the sediment suggest a low energy intertidal environment of deposition, with periods of terrigenous clastic influx alternating regularly with periods of carbonate deposition.

Although no taxonomic work has been attempted on the fossils, the nearby occurrence of Ordovician limestones in a similar stratigraphic position suggests an Ordovician age for the limestones on Mesa Creek.

4. Hastings Caves area

An outcrop of limestone occurs southwest of Hastings Caves, at about DM866961 on the track to Mesa Creek. The limestone comprises algal-laminated and birdseye limestones similar to those on Marble Hill, and an Ordovician age is suspected.

The outcrop is a large 3-4 metre diameter block which, although perhaps not bedrock itself, implies bedrock nearby. The simplest interpretation is that this limestone outcrop is part of a belt continuous with the limestones on Mesa Creek, as shown on Fig. 2:1.

Recently published maps of the area (Farmer 1975) show a small northwest-southeast trending belt of limestone faulted against the dolomite at Hastings Caves. No evidence was found in the present study to support such an interpretation.

5. Coal Hill area

Blocks of unfossiliferous birdseye and algal-laminated limestones occur on the side of Creekton Road at DM903938. These limestones are very similar to the Ordovician limestones on Marble Hill and although no bedrock outcrop is seen, it is probable that they are locally derived since there is no obvious reason for them to have been carried into position by human activity.

To the west and north-west of this locality is a large area of siliceous sediments which may at least partly represent silicified Ordovician limestones (see Section 2:4).

6. Speculations on further extent of limestone.

The large area of flat low-lying alluvial plains around the D'entrecasteaux River, South of Marble Hill, is suggestive of topography developed on Ordovician limestones elsewhere in Tasmania (e.g., Vale of Rassellas, Olga River Valley). Since the D'entrecasteaux Plains are immediately south of, and topographically below, the lowest limestone outcrops on Marble Hill (at the "exit" of Exit Cave), it is highly likely that the plains are underlain by a significant area of limestone. Since the Exit Cave limestones are thought to be near the base of the limestone sequence (see Section 2:3) there would not be a very significant thickness of limestone beneath the D'entrecasteaux Plains unless the southward dipping trend of the limestones in Exit Cave continued to the south.

Other areas of low-lying topography near the present study area which could well be underlain by limestones (on account of their

topography and likely geological position) are the middle Catamaran River Plains, (around DM830780) and the South Cape Rivulet Plains (around DM825740).

2.4 Problematical Siliceous Sediments

Extensive superficial slope deposits of pebble-to-boulder size fragments of a white siliceous sediment, ostensibly a quartzite, occur north of the Hasting Caves Road, inbetween Coal Hill and Chesterman's Road (see Figs. 2:1, 2:17 and section 2:11). No fossils have been found in these rocks and they are characterised by a "honeycomb" appearance imparted by small angular or sub-angular "holes" (see Fig. 2:14). The holes are not the result of weathering around quartz veins, as might be expected, since microscopic examination indicates that such veins are comparatively rare. Their honeycomb appearance differentiates those rocks from white quartzites at the Hogsback and elsewhere (section 2:2).

Microscopic examination of a typical specimen (48225 from DM89209505) shows that the sediment is composed almost entirely of silica, forming an intergrown xenotopic groundmass in which individual grains average 0.2-0.3mm diameter. The ubiquity of intergrown grains and the apparent absence of detrital silica grains with or without syntaxial overgrowth rims seems to indicate that the grains are entirely a cement rather than being a cemented clastic sandstone.

Furthermore, the silica contains large numbers of irregular angular inclusions which give a "dirty" appearance to the sediment

FIG. 2:14 Macroscopic appearance of problematical siliceous sediment showing angular holes. Two probable quartz veins are visible in this specimen (parallel, trending from bottom left to top right of specimen), but all the remaining vein-like walls between holes are composed of fine-grained silica. (See text). Scale graduated in millimetres.
(N.B. Photo double exposed; ignore background!)

FIG. 2:15 Microscopic appearance of problematical siliceous sediment: 48225 under crossed nicols, showing fine grained nature of the quartz, and empty angular holes (dark) in sediment. Note that holes are clearly not the result of weathering around veins.
Mag. x 7

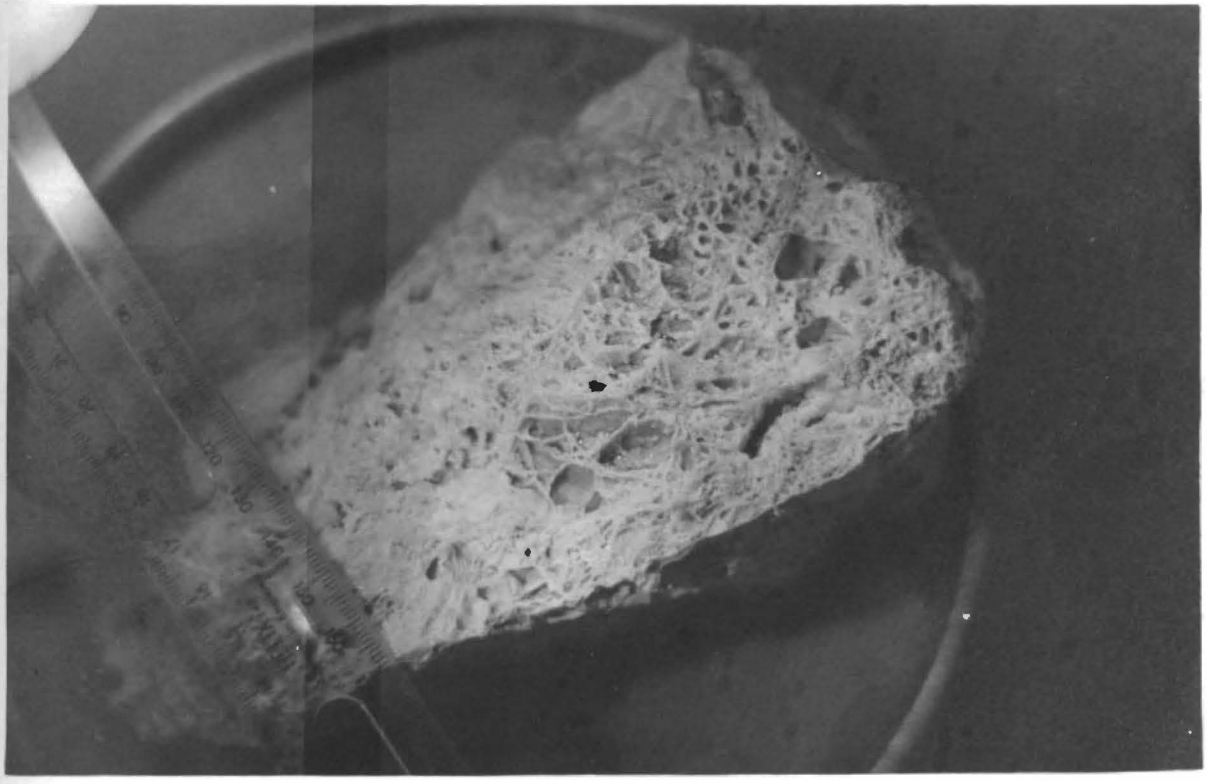

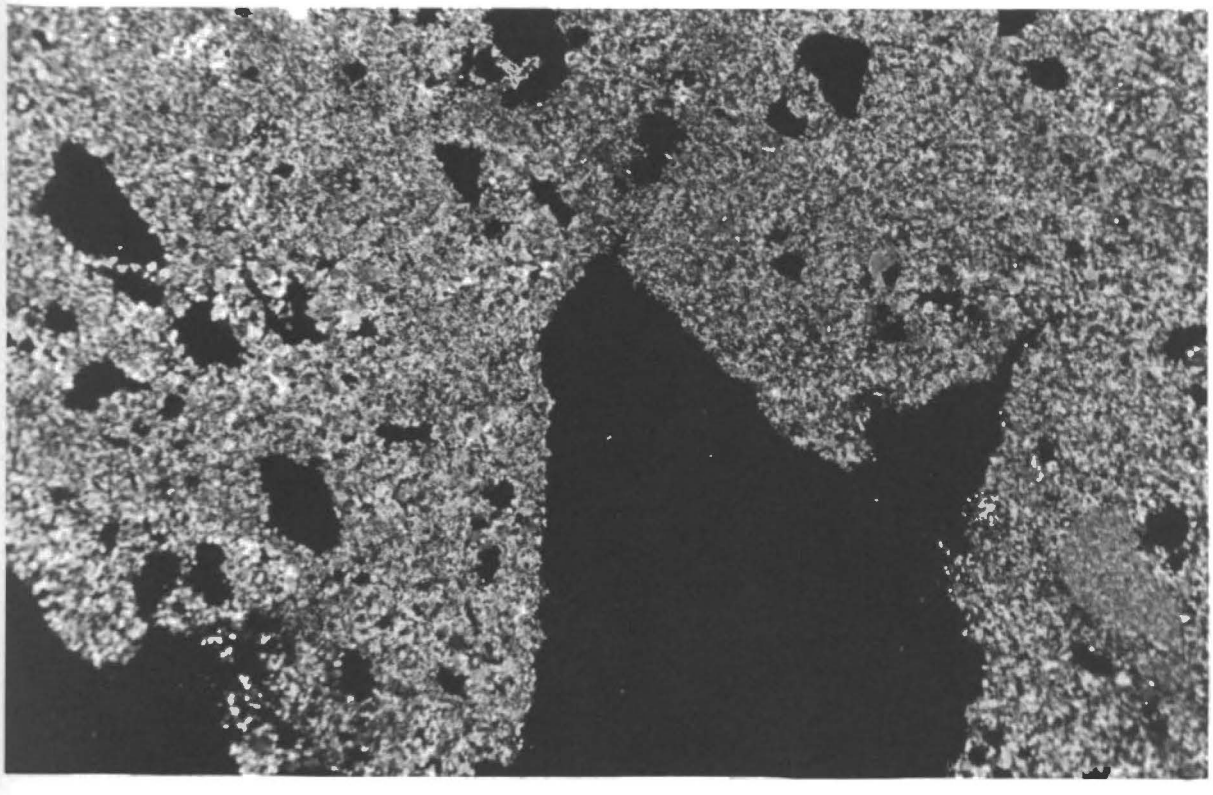

FIG. 2:16 Detail of problematical siliceous sediment. Middle-right part of photo shows fine-grained quartz with abundant inclusions and empty pits imparting "dirty" appearance. Coarser mosaic quartz on left fills an angular hole, and contains few inclusions. 48225 Mag. x 95

FIG. 2:17 Slope deposits containing blocks of problematical siliceous sediment, exposed in road-metal quarry at DM893939. Scale graduated in 0.1 metre units.

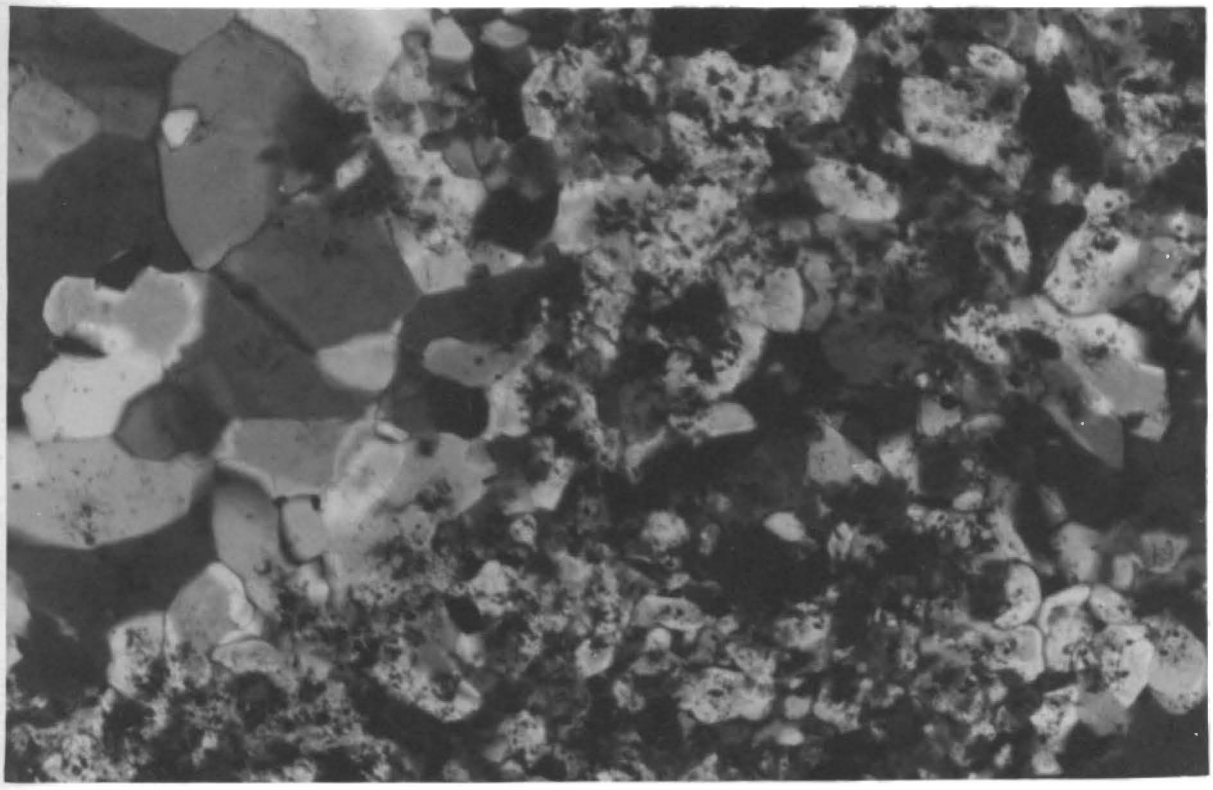

FIG. 2.18(a) Detail of inclusions in Silica grains in polished thin section of 48225. Dark patches are empty pits, unfilled outlines represent birefringent ? carbonate inclusions. Note rectangular zonal distribution of ? carbonate inclusions-relict of original grain? Field of view is approximately 0.3 millimetres diameter.

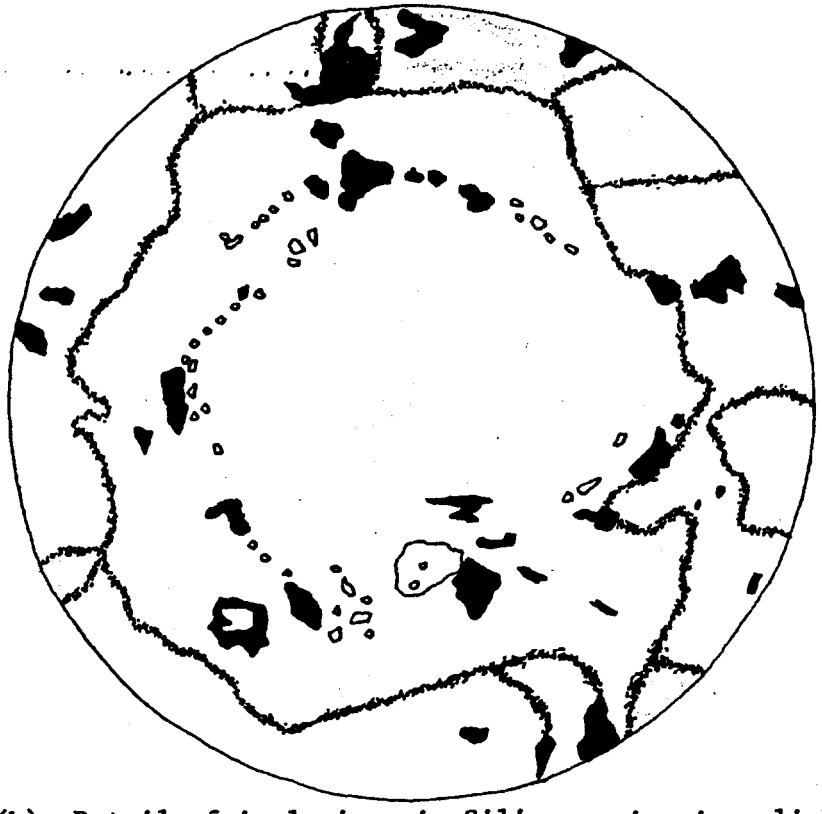

FIG. 2.18(b) Detail of inclusions in Silica grains in polished thin section of 48225. (As for Fig.2.18(a)). Note rhombic zonal arrangement of ?carbonate inclusions. Field of view as for Fig. 218(a).

under the microscope (see Fig. 2:16). Under high magnification most of the inclusions appear dark and give the impression of being empty pits. Some pits can be clearly seen to be enclosed within the silica when the microscope focus is racked up and down. Some inclusions contain birefringent material, however. The inclusions of greatest interest are those which are commonly arranged in rectangular or rhombic groups within a silica grain (see Fig. 2:18a, b), giving the impression that they are relicts of a pre-existing mineral grains. Electron microprobe analysis of these inclusions was attempted, but without success, since in most cases they appear to be "roofed over" with silica rather than actually being exposed on the surface of the polished thin section. However, they have high birefringence colours, and their relief changes markedly as the stage is rotated in plane light. Both these features are characteristic of carbonate minerals.

Other inclusions include a crack-filling mineral which may be a White Mica, perhaps diagenetic Sericite. Electron microprobe analysis of one of these inclusions revealed a very small quantity of Alumina. Finally, tiny dark prismatic inclusions are rarely present which are reminiscent of Zircon.

The sediment contains diffuse macroscopic streaks of brown material (an Iron Oxide?).

The "holes" in the sediment are of varied angular (commonly rhombic) shapes, having straight to slightly uneven edges. Their sizes range from 2mm or less up to 10mm diameter, and although most

of the holes are empty a few show the remanents of an infilling of anhedral quartz grains with a mosaic fabric. The quartz infillings have only a few inclusions, giving a "clean" appearance to the quartz.

The age of these rocks cannot be more closely defined than to say that they are pre-Permian, since they occur downslope from the Permo-carboniferous unconformity on Coal Hill and Chestermans Road.

The inclusion-rich nature of these rocks, their lack of obviously detrital silica grains, and the presence of their problematical "holes" imply that these sediments are not simply primary clastic quartz arenites. It is suggested below that they may instead be a silica replacement of a carbonate rock.

The siliceous rocks are similar to sediments referred to as "Rhomb-bearing Cherts" by Carozzi (1960, p. 335). Carozzi considers the silica-infilled rhombs to be pseudomorphs after carbonate crystals, usually dolomite. Although dolomite rhombs do not commonly grow as large as the rhombic holes in 48225, the angular nature of these holes strongly suggests that they are pseudomorphs after pre-existing soluble crystals of some sort.

According to Carozzi (*ibid.*, p. 336), "The problem of the origin of the rhomb-bearing cherts is whether they were pseudomorphs after rhomb-bearing limestones, or whether the crystals were formed from a mass of gelatinous silica containing carbonate in solution. Both hypotheses seem to be valid, as rhomb-bearing cherts occur in

limestones containing similar rhombs, or in limestones entirely devoid of them."

That 48225 is a silica replacement of a pre-existing non-siliceous (carbonate?) sediment is strongly suggested by the presence of minute inclusions of what may be relicit carbonate. The occurrence of unaltered limestone on Creekton Road (see section 2:3), immediately east of the area of siliceous rocks, suggests that the area may be underlain by Ordovician limestones, some of which have been silicified to produce the problematical siliceous sediments. If these rocks are silicified carbonates, they are more likely to be replaced Ordovician limestones than replacements of the nearby Precambrian dolomite, since calcite is much more easily pseudomorphed than dolomite. (Carozzi 1960, p. 336).

Because the large areas of limestone elsewhere in the Ida Bay area have only undergone minor silicification of fossils and formation of chert nodules, rather than wholesale silica replacement of the rock, it is evident that the silicification of rocks in the Coal Hill area must be related to those rocks having at some stage been in a markedly different diagenetic environment to that of the surrounding limestones.

The most promising mechanism to account for the silicification is the process known as "meulerization" (Larsen and Chilingar 1967, p. 72). This is a process believed to be related to the formation of "Silcrete" horizons. The formation of silcrete horizons, which is presently occurring in hot arid environments in South Africa,

Australia, and other places, appears to result from silica-rich solutions rising to the ground surface, there to precipitate as a cement, and partial replacement, of the soil or weathering horizon. According to Williamson (1957, p. 23), silcretes may form somewhat below as well as at the ground surface.

The process of meulerization refers to the replacement of limestones by silica, and is thought to be a process similar to silcrete formation (Larsen and Chilingar 1967, p. 72). In the process of meulerization silica patches grow and coalesce in limestones often leaving irregular relict carbonate patches whose later dissolution turns the rock into a spongy network of silica (Carozzi 1960, p. 315).

If such "meulerization" had at some stage gone virtually to completion in the Coal Hill area, perhaps drawing on the small silica content of the limestone as a whole to silicify a surface layer of unknown thickness, then a homogeneous siliceous rock would have resulted. The rhombic holes in the sediment are probably too angular to result from dissolution of relict limestone patches, and it is also doubtful that they represent rhombic crystals in the original limestone, since such features are not seen in primary limestones elsewhere in the Ida Bay region. Rather, it is suggested that the holes represent crystals which grew in the silicified sediment. Although authigenic carbonate crystals do not normally grow as large as the rhombs in 48225, it is entirely possible that these rhombs *could* have been authigenic carbonates, or better still, evaporite crystals growing in near-surface materials in a hot

climate of the sort conducive to silcrete formation. (Williamson (1957, p.27) records sparse rhombohedral carbonate crystals of authigenic origin in modern silcretes). These crystals must later have been pseudomorphed by silica. (Since the rhomb-filling silica is largely free of relict inclusions, this probably occurred after dissolution of the original crystals, during vadose diagenesis, produced empty holes.)

An alternative explanation of the rhombic pseudomorphs is that they result from autobrecciation of silcrete during an early phase of its formation. James *et al* (1968, p. 72-75) describe Precambrian silcretes from Michigan which formed by silicification of dolomite. These silcretes are characterised by a breccia structure which is ascribed to resilicification of earlier formed silcrete that has been brecciated during denudation. However, the angular patches in 48225 are infilled by clean coarse mosaic quartz, unlike the cherty breccia fragments described by James *et al* (1968, see Figs. 43 a,c). The coarse infillings suggest weathering out of a relatively soluble material, which is unlikely if the angular patches were originally chert.

A silcrete or "meulerization" origin for the problematical siliceous sediments on Coal Hill is preferred, since it appears to account not only for the abundant minute inclusions, but also for the presence of rhombic pseudomorphs in the sediment.

Since the limestone in the Ida Bay region is directly truncated by the Permo-carboniferous unconformity, it is clear that

at some time in the palaeozoic the present upper limits of the Ordovician limestones would have been subaerially exposed, and potentially subject to vadose diagenesis. It is therefore suggested that the meulerization believed to have taken place in the Coal Hill area may have occurred during a hot, arid period in the (middle?) palaeozoic, probably at the time of the Tabberabberan Orogeny when areas of Tasmania were being uplifted and eroded. It is, however, difficult to explain why only one area of limestone was silicified, although a much larger area must have been subaerially exposed. One possible explanation is that the silicification occurred early in the Tabberabberan Orogeny, to be followed by tectonic movements (the evidence for which is hidden by the poor outcrop in the area) which caused the silicified horizons to be eroded off in all except the Coal Hill area. Certainly, there is evidence for Thrust faulting in the Ida Bay area during the Tabberabberan Orogeny (see section 2:12).

Alternative origins for the sediment as a whole are also possible, of which the most promising is that it represents a recrystallisation of a pre-existing chert, perhaps related to the nearby precambrian dolomites. Although the siliceous sediments are unlikely to be primary quartzites, it is possible that parts of the Coal Hill area have primary quartzite bedrock stratigraphically beneath the postulated limestone bedrock.

Proof of the siliceous sediments being replaced carbonates would require identification of pseudomorphed carbonate structures such as oolites or flat-pebble conglomerates. Such structures have

not been identified in the specimens examined. The lack of bedrock outcrop is also a handicap in determining the origin of these rocks - if the bedrock was shown to consist of regions of unsilicified limestone passing into silicified material then this would indicate a replacement origin for the siliceous sediment. The fact that only siliceous material occurs in the surface deposits may result from the more soluble nature of unsilicified limestone. Thus, future drilling or location of good outcrops should clarify the origin of the siliceous sediments.

2.5 Siluro-Devonian Sediments

No rocks of Siluro-devonian age are known in the Ida Bay area, where the Ordovician limestones are invariably overlain unconformably by Permo-carboniferous rocks. This situation is considered anomalous since Ordovician limestones are overlain by Siluro-devonian clastics of the Eldon Group in most other parts of Tasmania. This anomaly may be the result either of non-deposition in the Siluro-devonian, or of unusually deep erosion (at least on the Tabberabberan anticlines) prior to the deposition of Permo-carboniferous sediments.

2.6 Permo-Carboniferous Sediments

The angular unconformity separating Ordovician and earlier sediments from overlying Permo-carboniferous sediments was not observed on Marble Hill by the present writer. It is poorly exposed and occurs in dense scrub above Newlands Quarry, but its position can be inferred from the occurrence of large blocks of tillite, and a marked change in the slope of the Hill.

The tillite is a dark grey-green sediment with large clasts (up to tens of centimetres) in an open framework. The tillite is only a thin layer, and Forsyth and Green (1976) describe it changing upwards into crudely bedded sandstone, with grey silty mudstone cropping out only seven metres above the base. Thirty metres above the unconformity near Newlands quarry a float of richly fossiliferous sandy siltstone was found by Forsyth and Green (1976) which contained dropstones and *Trigonetreta strokesi*. Forsyth and Green correlated this with the Bundella mudstone.

The unconformity at the base of the Permo-carboniferous sediments is also exposed on Mesa Creek, where it changes height by about forty metres over a horizontal distance of 200 metres (see section 2:13, Fig. 2:13). The tillite appears to grade up into a yellow-green mudstone after only a few metres, judging by the abundance of mudstone fragments at the foot of the cliff on which the upstream exposure (DM84809562) occurs.

Similar tillite is exposed on Chestermans Road at DM891958, and on Coal Hill Road at about DM897958. The basal unconformity is presumed to occur close beneath these outcrops, and the thinness of the tillite unit is indicated by the fact that the next outcrop north of the tillite outcrop on Coal Hill Road at DM897962, is of a marine mudstone dipping at fourteen degrees towards 290 degrees magnetic.

Poor outcrops of flat-lying tillite and mudstone occur on a side road off the South Lune Road, at DM88859065. These appear to be

bedrock, but slope deposits consisting dominantly of tillite and mudstone of presumed Permo-carboniferous age occur upslope, at about DM884906 on the South Lune Road. The abundance of mudstone fragments in roadside cuttings along western parts of the South Lune road indicates that mudstone bedrock of presumed Permo-carboniferous age occurs on the hillslopes above and to the west. (See Figs. 2:1, 2:2).

On the north side of Lune Sugarloaf, a very poor outcrop of shales and sandstones occurs on the South Lune Road at DM89958855, just west of ?Triassic carbonaceous sediments. The shales and sandstones are thought to be Permo-carboniferous, since they occur just downslope from sandstones and siltstones containing spiriferids on the Ida Bay Railway (Forsyth and Green, 1976). These sediments are thought to be separated from the adjacent carbonaceous sediments by a large fault (see Fig. 2:1). The extent of Permo-carboniferous rocks on the north side of Lune Sugarloaf is not known, but Forsyth and Green (1976) have produced evidence for a fairly thick Permian sequence in-between the Jurassic dolerite above and the Ordovician limestone below. Magnetometer results (*ibid.*) are consistent with the 345 metre contour being the base of the dolerite sheet on Lune Sugarloaf, so that there may be in excess of 150 metres of Permo-carboniferous sediments beneath this.

A fine yellow-white mudstone which is massive but somewhat fissile, and lacks fossils or dropstones outcrops on Gleichenia Creek at about DM848932. It dips at ten degrees towards 200 degrees magnetic, and is tenatively regarded as Permo-carboniferous on

account of its lithological similarity to other Permo-carboniferous rocks in the region.

Another outcrop of a yellow-brown sandstone having no fossils and apparently dipping 25 degrees towards 140 degrees magnetic outcrops in a small quarry on the Hastings Road at DM88009557, just east of the Springs Creek Bridge. This sandstone most closely resembles Marine sandstones of Permo-carboniferous age elsewhere in the region, although such an age implies emplacement by faulting, since this outcrop occurs well downslope of the Permo-carboniferous basal unconformity, and some of the Precambrian dolomites in the Hastings area. (see Fig. 2:1).

2.7 Triassic Sediments

As is the case in many parts of Tasmania, a clear differentiation between Permian and Triassic sediments cannot be made in the Ida Bay area. However, for the present purposes it is sufficient to regard marine sediments of the Parmeener Super Group as being of Permo-carboniferous age, while terrestial sediments are of Triassic age.

On this basis, the sandstones, red-beds, coal and carbonaceous siltstones with Sphenopsid stems (Forsyth and Green 1976) which outcrop on the South Lune Road at DM90058860 and DM90358880 are regarded as Triassic.

Sandstones outcropping on the Catamaran Road at DM92259160 are also considered to be Triassic. A dip of 23 degrees towards

280 degrees magnetic which was measured on this outcrop may actually be the dip of large scale planar crossbeds.

The only other probable Triassic rocks examined in the course of this mapping project are the sediments exposed on Creekton Road. The best bedrock outcrop occurs in a road cutting at DM918965 and comprises yellow-brown mudstones and sandstones with dark brown shale laminations 1-5mm thick spaced 1-5mm apart. The shale laminations often contain dark carbonaceous fragments interpreted as plant fragments, which imply a terrestial origin for the sediments. The finely laminated, shaly, and apparently crossbed-free nature of the sediment suggests a lacustrine origin.

Everard (1957) and Farmer (1975) record Triassic sandstones immediately to the east of Lune Sugarloaf, and a small coal mine was apparently operative in the area at one time.

Davidson (1969) has discussed the Late Permian and Early Triassic sediments of the Moonlight Hills area. (See Fig. 2:1).

2.8 Jurassic Dolerite

A near-horizontal sheet of medium grained dolerite intrudes Permian sediments on the slopes of Moonlight Flats, west of Marble Hill. Although the exact thickness of the sheet is unknown because of poor outcrop it is probably well over one hundred metres thick, and appears to have its base at about 360 metres altitude. Since there is no evidence for dolerite at similar, or higher, levels on the adjacent Marble Hill, this gives further reason to suspect that

a major fault may pass through the saddle between Marble Hill and the slopes of Moonlight Flats (see also section 2:3).

Nevertheless, Lune Sugarloaf is capped by a sheet of medium grained (2mm grainsize) dolerite which was probably originally continuous with the dolerite sill below Moonlight Flats. A magnetometer survey (Forsyth and Green 1976) suggests a base for the dolerite sheet at 345 metres on Lune Sugarloaf.

A fine-grained basic igneous rock outcrops along the eastern part of the South Lune Road (see Fig. 2:1) and has been regarded as Tertiary Basalt by, e.g., Farmer (1975). However, Forsyth and Green (1976) considered this rock to represent a second intrusion of (fine grained) Jurassic dolerite. In the absence of evidence (ratiometric, palaeomagnetic or petrologic) one way or the other, it is probably safest to accept the latter interpretation.

The contact between this fine-grained dolerite and the country rock is exposed in a roadside quarry at DM905887, where the western part of the quarry reveals an irregular intrusive contact, dipping gently eastward, between dolerite and underlying Triassic Coal measures (Forsyth and Green 1976).

Both medium and fine-grained dolerites also outcrop north of the Lune River. (See Fig. 2:1). Medium-grained dolerites outcrop on the Coal Hill Road and the southern part of Tughanah Road, while fine-grained ?Dolerites occur in a quarry at DM91859315. It is not known whether these outcrops represent separate intrusive bodies or whether they are part of the same intrusion.

2.9 Tertiary Basalts

As noted above, there is some difficulty in distinguishing between basalts and fine-grained dolerites in the field. Only one outcrop regarded as clearly an extrusive basalt was observed during the present. This basalt is a dark fine-grained rock with amygdales, which outcrops in a road cutting on Creekton Road at DM913954, and a quarry just north of the road cutting. The southern part of the road cutting consists of ?Triassic sediments, but weathering has resulted in rather poor outcrop of the basalt/sediment contact. The basalt is regarded as Tertiary purely by analogy with similar basalts elsewhere in Tasmania.

Tertiary basalts also occur southeast of Lune Sugarloaf (Everard 1957, Forsyth and Green 1976), but were not examined by the present writer.

2.10 Tertiary Sediments

Everard (1957) attributes a Tertiary age to thick gravel deposits on the north side of Marble Hill, but the present writer knows of no evidence supporting such an age.

Plant fossils, apparently of Tertiary age, have been recovered from the area of the Lune River, but the location these specimens came from is not known to the present writer.

Bedded and well-indurated sediments occur as fissure fillings in Newlands Quarry. The age of these sediments is problematical, but since they occur in the upper part of the quarry, close to the

pre-quarrying ground surface, it is possible that they are of Tertiary or Quaternary age. These sediments are discussed in Appendix Two.

2.11 Quaternary Geology and Geomorphology

Recent alluvial sediments cover large areas of the plains surrounding the Lune and D'entrecasteaux Rivers. These sediments are exposed in places where the rivers have cut through earlier fills, and exposures also occur on the West and East branches of the North Lune Road.

The slope of most of the Hills in the study area are covered with Talus and possibly also periglacial slope deposits (see Fig. 2:2). Magnetometer results (Forsyth and Green 1976) indicate that dolerite talus on Lune Sugarloaf, above Newlands Quarry, is generally about three metres thick, and includes 7m x 7m blocks. Thick deposits consisting of blocks and fragments of siliceous sediment (see section 2:4) occur on the southern slopes of Coal Hill. These slope deposits may contain blocks over one metre in diameter, commonly set in an open framework matrix giving the deposits the appearance of a Till (see Fig. 2:7).

The geomorphology of the Entrance-Exit Cave System beneath Marble Hill (See Fig. 1:4) has been discussed by Goede (1969). It is possibly significant that the main chambers and the general trend of the Cave system correspond with the axis of the main north-south trending anticline into which the limestones are folded. (See Fig. 2:1, Section 2:3). Perhaps tension resulting from folding

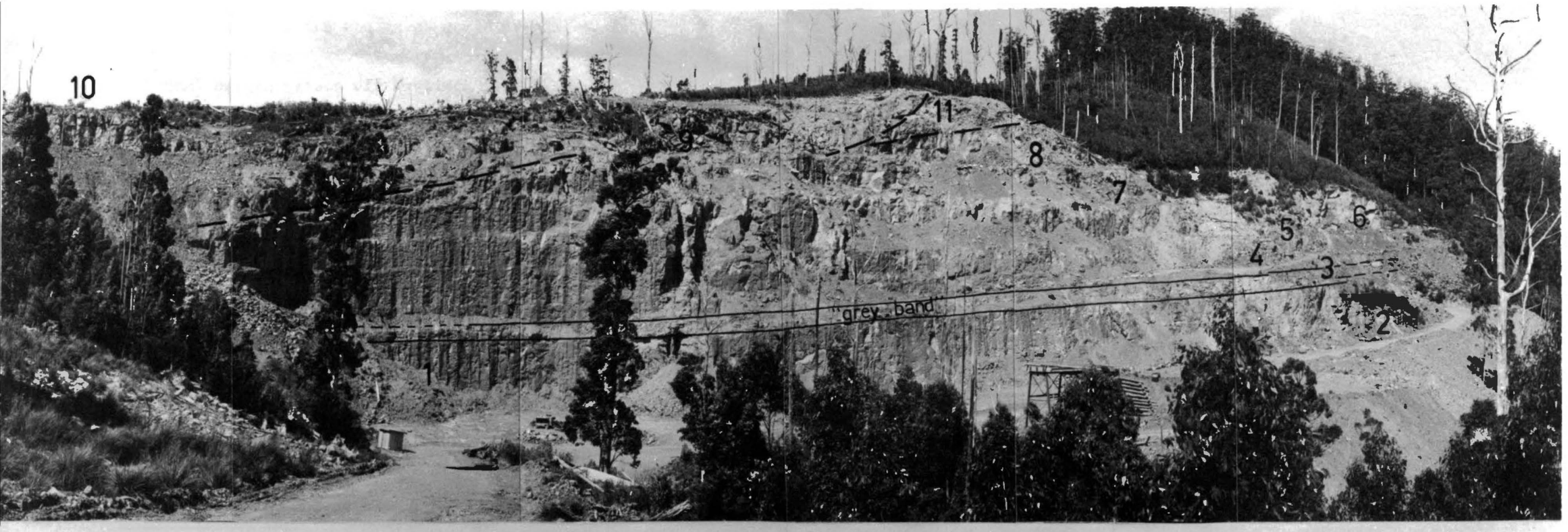

FIG.2.20 View of Newlands Quarry from the NE, looking SW towards Marble Hill. Numbers refer to location numbers in text. Birdseye limestone unit ("Grey Band" of Forsyth and Green 1976) shown for reference.

View taken Jan 1979; parts of quarry have since been altered.

: Fault and fault zone boundaries.

produced fracturing on the anticline axis which in due course provided a line of weakness along which the caves could form.

A thermal spring exists off Hastings Caves Road, at DM89559305, where it discharges heated waters into Hot Springs Creek (see Fig. 2:1). Little work appears to have been done on the geology and geochemistry of this spring, but it is generally thought to be related to a major fault which allows heated waters to rise from depth. No information is known to the present writer as to the location or nature of such a fault. The fault shown south of Hastings Caves by Farmer (1975) would be a suitable fault to explain the springs, but the present writer knows of no evidence for the existence of that particular fault. (See also Section 2:3, part 4).

2.12 Structural Geology

1. Tabberabberan Folding.

As described in section 2:3, the limestones on Marble Hill are folded into a north-south trending anticline, which is warped into a somewhat domal form by northwards and southwards dip of the anticline axis on the north and south sides of Marble Hill, respectively. This folding must be post-Ordovician, and is also pre-Permian since it is truncated by the nearly flat-lying Permo-carboniferous sediments on the top of Marble Hill. Since the only major orogeny in Tasmania between Ordovician and Permian times was the Devonian Tabberabberan Orogeny, the folding of the limestones is regarded as a Tabberabberan event. (As is the folding of other Ordovician limestones in Tasmania.)

The axis of the anticline formed in Early Ordovician quartzites at the Hogsback is on strike with the axis of the anticline in the limestones, and hence the two anticlinal structures are regarded as portions of the same large north-south trending anticline (see Fig. 2:1). The Early Ordovician quartzites on the North Lune Road (DM87759325) and near the South Lune Road (at around DM882908) are probably on the eastern limb of this anticline.

The folding is much tighter, with steeper dips, in the quartzites than it is in the (overlying) limestones. This suggests that the folding of the anticline becomes tighter downwards, in the fashion characteristic of "parallel folding". An alternative possibility is that the anticline narrows and steepens northwards along its axis.

2. Normal Faulting.

Everard (1957) postulated a large north-south trending fault to the east of Lune Sugarloaf, and having a downthrow to the east. The location of this fault can be fairly accurately located in outcrops on the South Lune Road and the Ida Bay Railway, near DM900886, where outcrops of Permian rocks occur immediately west of probable Triassic rocks.

Everard postulated a second north-south trending fault between Marble Hill and Lune Sugarloaf, also downthrowing to the east. This fault has not been located in outcrop, but its existence seems necessary in order to explain the probable occurrence of Permo-carboniferous rocks on Lune Sugarloaf (see section 2:6), at the same

topographic height as the limestones on Marble Hill. Extrapolation of limestone units north of Lune S.L. towards Marble Hill cannot presently be used to test the existence of the fault, since it is not presently possible to demonstrate a correlation between limestone horizons in the two areas. (see Section 2:3).

The present writer regards the existence of an east-west trending fault north of Marble Hill, and downthrowing to the North (see Fig. 2:1), to be necessary in order to explain the fact that Permo-carboniferous sediments seem to occur there at lower levels than the limestones on Marble Hill. (Judging by the occurrence of poor Permian outcrops at DM88859065 and a predominance of mudstone fragments in roadside cuttings - see Fig. 2:2). The fault is shown on Fig. 2:1 crossing the South Lune Road at DM885889. This location is inferred from the presence of a straight east-west trending stream channel at this point (fault controlled?) and the fact that white quartzite fragments (?Early Ordovician) cease to occur in roadside cuttings at approximately this point. (see Fig. 2:2).

There is clear evidence for another fault further north on the Lune River (see section 2:3, part 2), but in the absence of clear evidence as to its position it is not shown on Fig. 2:1.

Finally, as mentioned in section 2:3, a N-S trending fault has been postulated between Marble Hill and Moonlight Flats, with down-throw to the west. Such a fault would explain the non-occurrence of a dolerite cap on Marble Hill, the top of which seems to be horizontally equivalent to the dolerite sill below Moonlight

Flats. It would also account for steep dips in the limestone west of Blaney's Quarry as being drag on the fault, but in the absence of clearer evidence for its existence, such a fault is not shown on Fig. 2:1.

3. Thrust Faulting.

A large thrust fault runs through Newlands Quarry (see Figs. 2:19, 2:20), and has a throw of about twenty metres and a heave of 80m or more. It flattens considerably towards the eastern side of the quarry, and may disappear into a bedding plane east of the quarry exposures. In the western part of the quarry the fault passes into a wide fault breccia zone whose upper boundary steepens considerably to reach an angle of about 45 degrees to the horizontal (see Fig. 2:19). The fault breccia zone contains large rotated and disrupted blocks of lithofacies X limestones (see Ch. 3), together with large quantities of finer material in the form of pebbles, muds, and clays (see Fig. 2:21).

The disruption and rotation of limestone masses to form the fault breccia zone is regarded as the result of imbrication associated with the thrust faulting, as shown diagrammatically in Fig. 2:22. In this model, the single low-angle thrust fault splits into several higher angle faults, giving an "imbricate" structure. Differential movements along these high angle faults results in coupling, causing the intervening blocks to rotate and brecciate. As a result of this faulting, silt bands within the Lithofacies X blocks in the fault breccia zone are extensively slickenslided.

Thrust faulting normally results from compression, and the only compressional event known to have occurred after the deposition of the limestones is the Tabberabberan Orogeny. If that orogeny produced the thrust fault as well as the folding of the limestones, then the strike of the thrust fault should be parallel to the axis of the folding (i.e., north-south). Because the thrust fault is only exposed on the face of Newlands Quarry, it has not been possible to determine its strike.

At location 11, the beds immediately east of the fault zone have been warped in a sense which is opposite to that which one would expect from fault drag (see Fig. 2:19). The most reasonable explanation for this anomaly is that it represents a small fold which formed prior to failure and thrusting of the rock.

Immediately below the fault breccia zone, a large block of lithofacies X limestone has dropped down into a position stratigraphically lower than the lithofacies X horizon (see Figs. 2:19, 2:24). Since the downthrow of this block could not have occurred under the compressional regime responsible for the thrust faulting, its downthrow is probably related to some other geological event. One obvious possibility is that the enlargement of an underlying cave chamber might have resulted in collapse when one of disrupted blocks in the fault breccia zone was sufficiently undermined to become unstable, for instance.

A small thrust fault with a displacement of only a few metres occurs within Exit Cave (A. Goede, *pers. comm.*1979), but its exact location and orientation are uncertain.

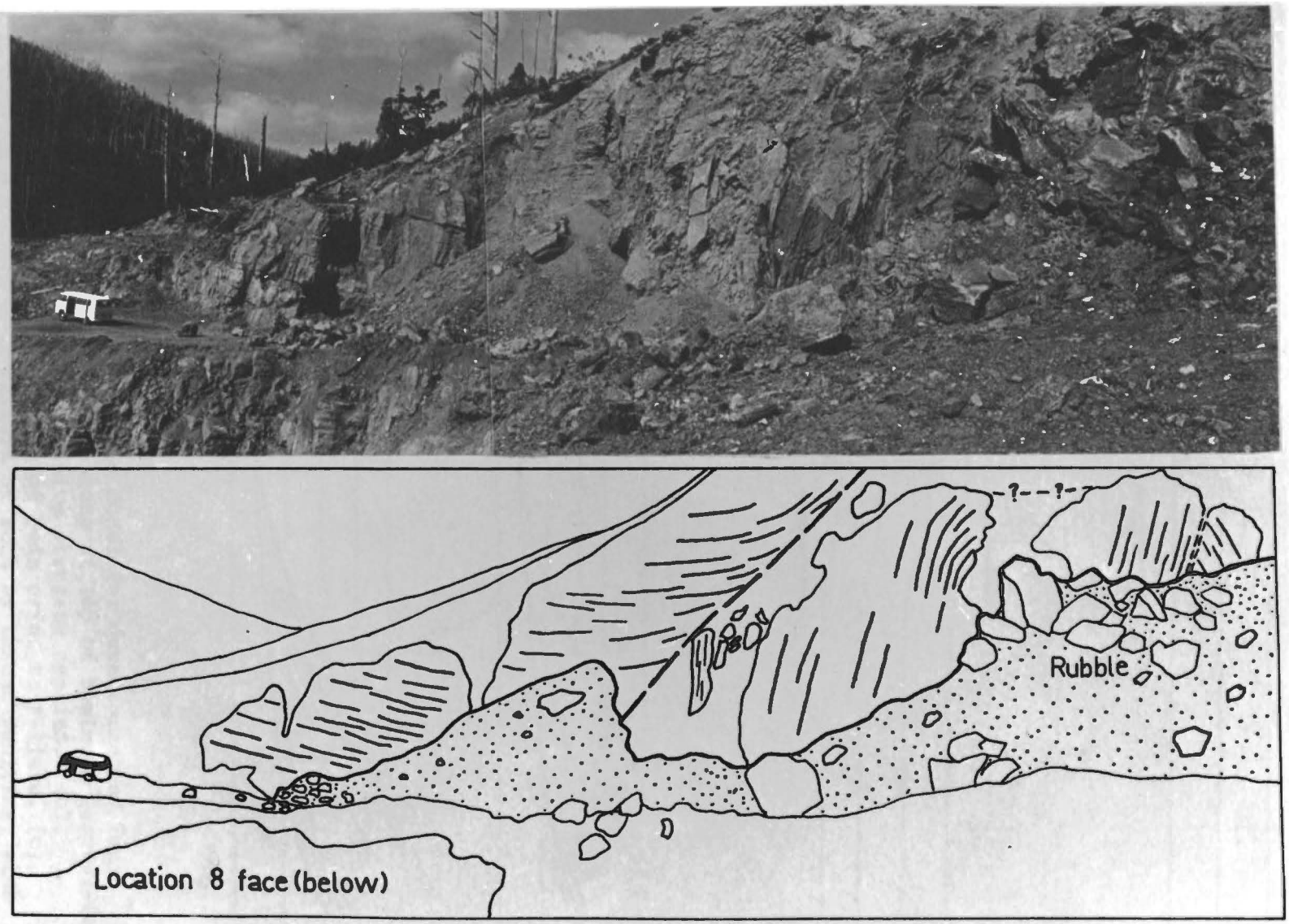

FIG. 2.21 At location 11, Newlands Quarry: view looking SE, showing rotated and disrupted blocks in the fault zone. Eastern limit of fault zone indicated in line drawing.

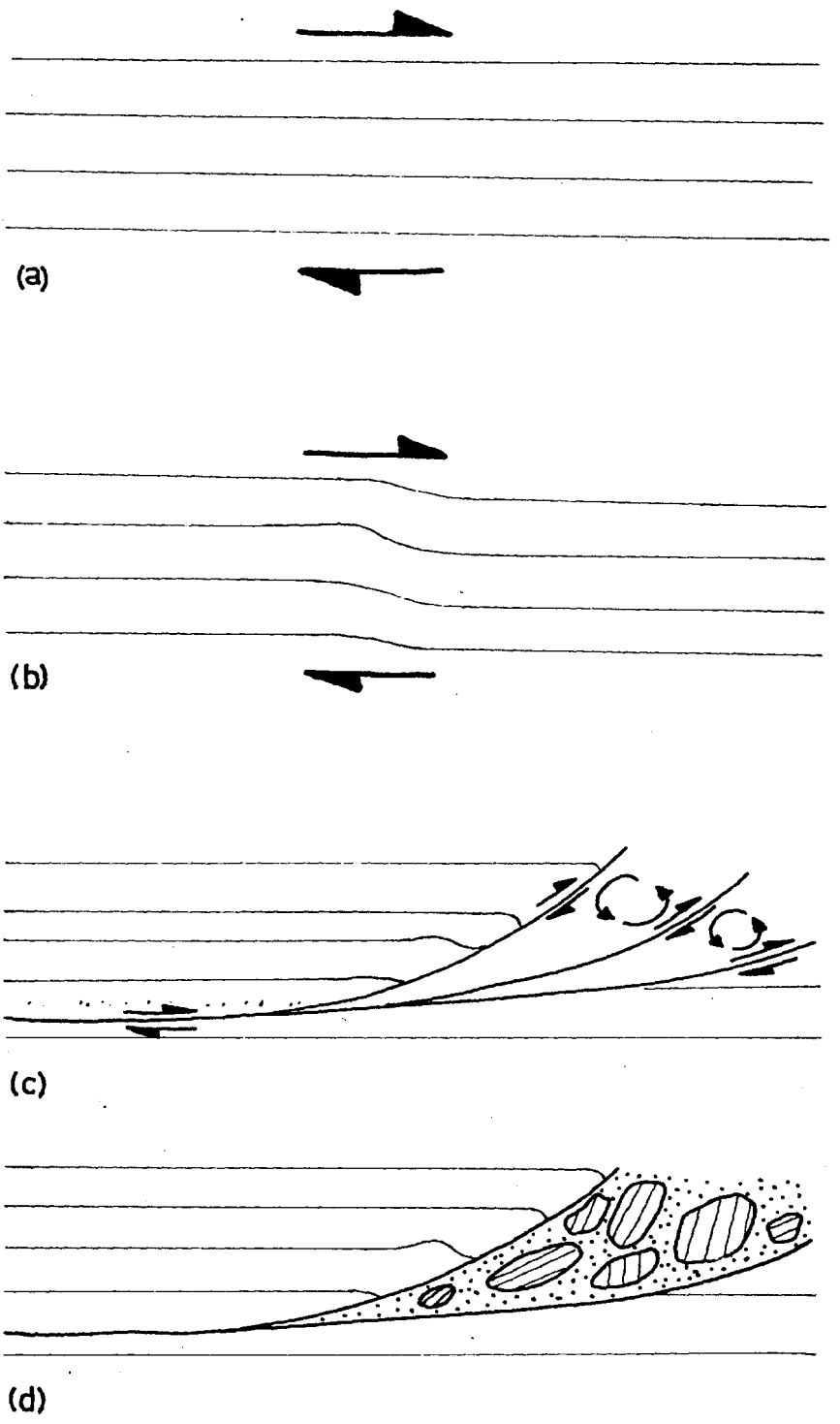

FIG. 2:22 Proposed model for development of fault breccia zone at top of Newlands Quarry:-(a), Compressive stresses applied. (b), Warping of beds prior to failure. (c), Failure of rock by thrust faulting, with development of imbricate zone. Coupling of rock masses in imbricate zone causes rotation of blocks. (d), Post-tectonic situation, with rotated blocks and finer material in fault zone.

FIG. 2:23 Top bench and 4WD tracks at top (southern side) of Newlands Quarry (c.f. Fig.4:7), showing bedrock exposed on top sides of the cuttings (arrows indicate location of sections on plan). East-west trending face exposes fault breccia zone, and beds to east of it. North-south trending cutting shows warping and disruption of beds immediately east of thrust fault. Note downthrown biomicrite block. Disruption may be related to the thrust fault, which probably strikes North-South, parallel to and behind N-S trending cutting.

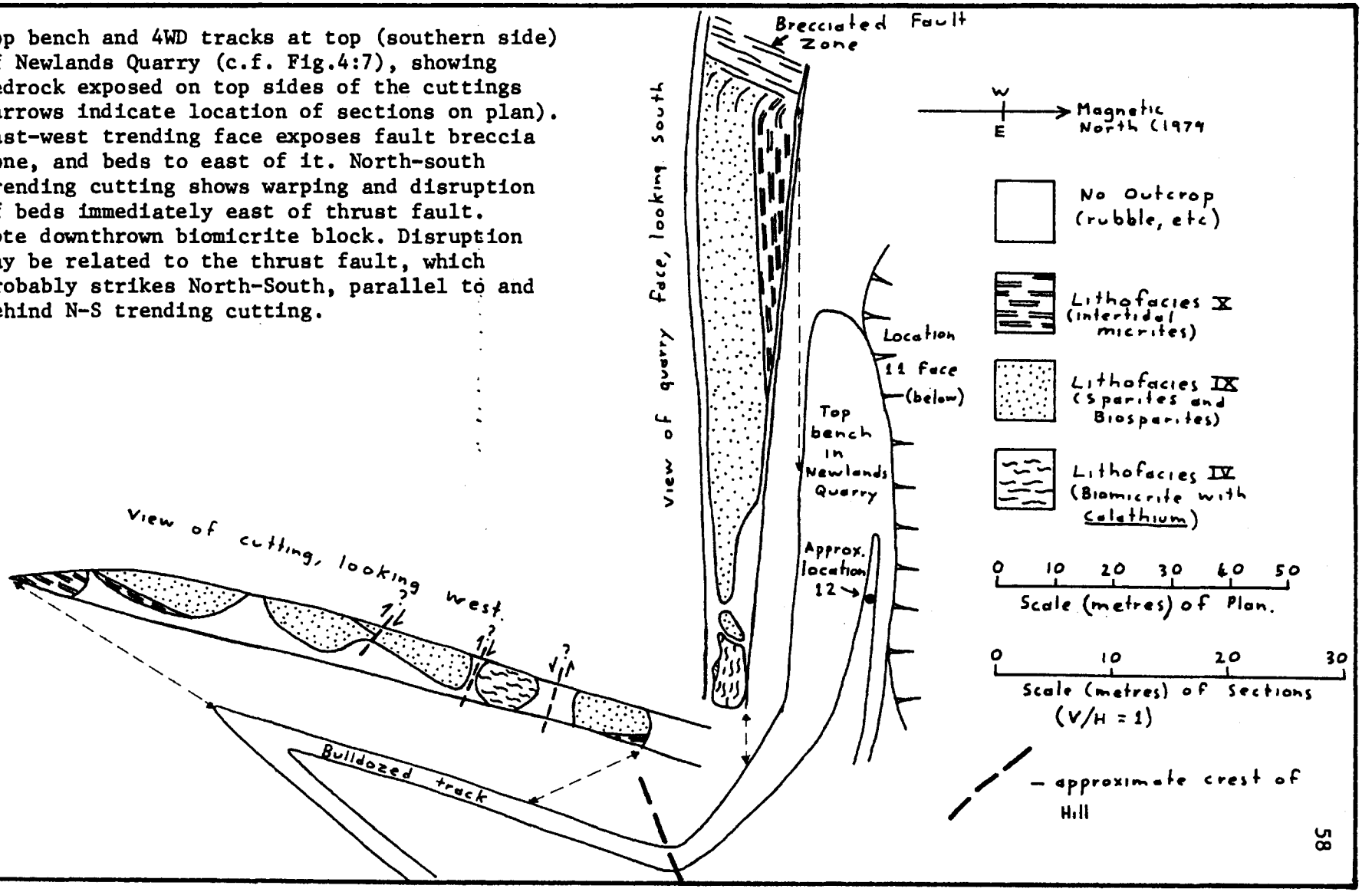

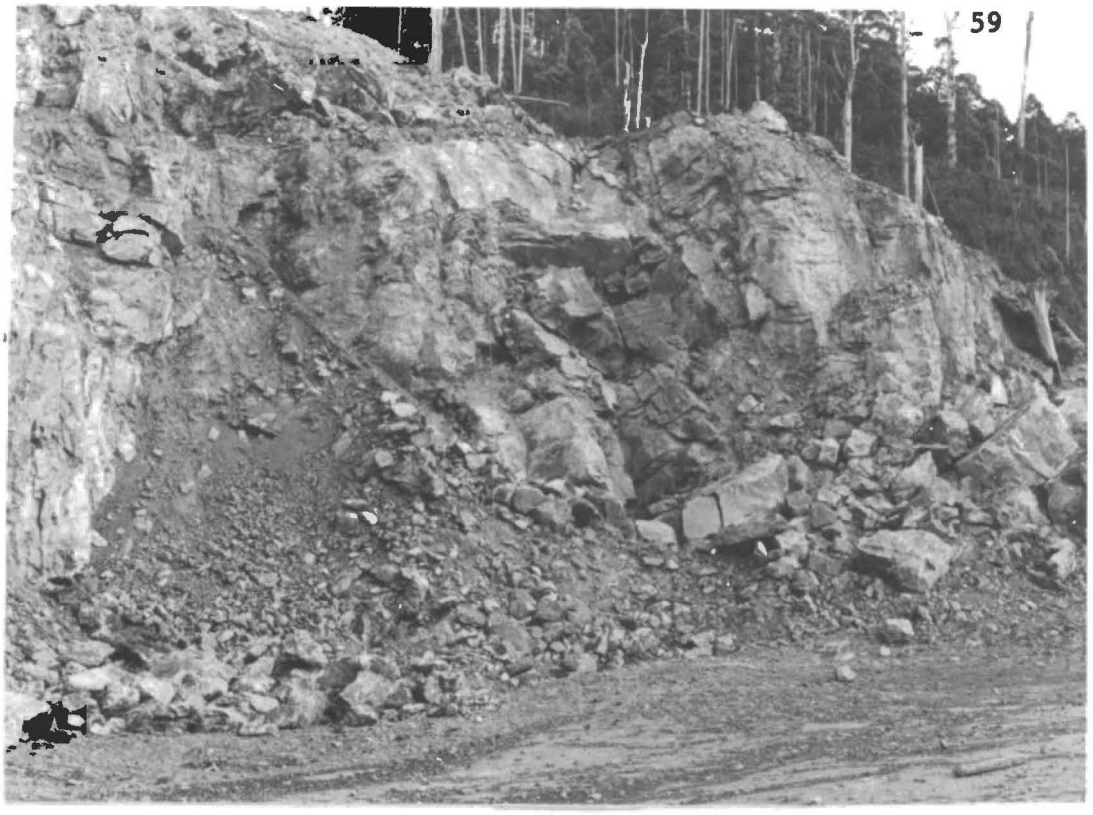

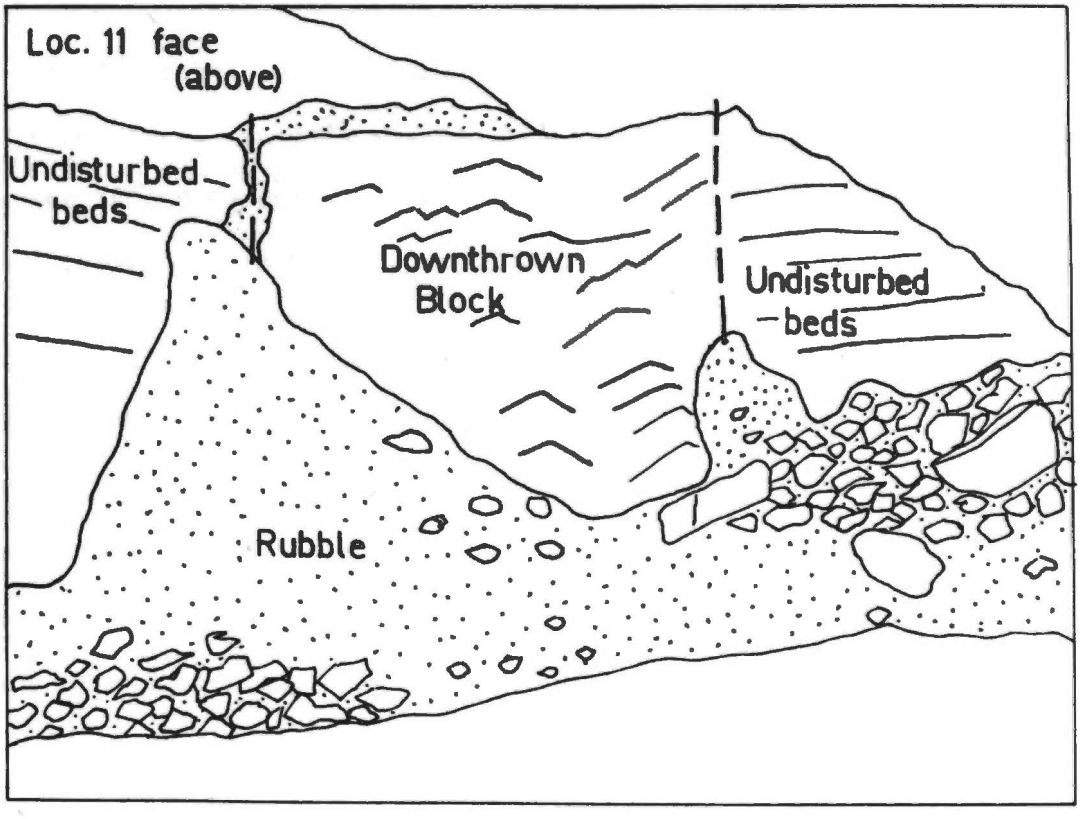

FIG.2.24 View of Loc. 8 face (In April 1979) looking SW, showing downthrown block.

Approx. 18 metres from quarry floor to top of face.

CHAPTER THREE

SEDIMENTOLOGY

3.1 Methods Employed

Detailed sedimentological work was only carried out on the limestones exposed on Marble Hill. Stratigraphic sections were measured using an Abney Level and a Jacobs Staff, and dips and dip directions were measured with a Brunton Compass. Changes in lithology were noted, and specimens collected at intervals through each lithological unit determined in the field. In most cases the lithofacies described in this chapter correspond to lithofacies determined on field criteria, although in a few cases (e.g. Lithofacies IV and V) units thought to be the same lithofacies in the field turned out to be quite different under the microscope.

About 150 Acetate peels were prepared (by the method of Katz and Friedman, 1964) for sedimentological study of field specimens, these being supplemented by a small number of thin sections. Some of these specimens were photographed with a Wild Heerbrugg M400 Photomakroscop, on Ilford FP4 black and white film, using a transmitted light stage to hold and illuminate the specimens. Field and department numbers, and collection localities, of specimens referred to or photographed in the following pages are tabulated in Appendix Seven.

3.2 Environmental Interpretation

The primary objective of the sedimentological work was to attempt to determine the environments in which the various lithofacies were deposited. The limestones at Ida Bay are in many ways similar to Ordovician limestones in most other parts of Tasmania, and as is the case with the latter, appear to represent sediments deposited in a wide tidal flat environment. Weldon (1974) has summarised the sedimentary environments envisaged in a carbonate tidal flat sequence, with particular reference to the sedimentary environments of the Benjamin Limestone of the Florentine Valley. This model is broadly applicable to the limestones at Ida Bay, which are approximately contemporaneous. Weldon (1974), Calver (1977), Page (1978) and others have discussed the sedimentary criteria used in determining the sedimentary environments of Tasmanian Ordovician limestones, and the reader is referred to the above works for a more detailed discussion of this subject. The principles discussed by the above workers have been largely adhered to in the present work, although they have been supplemented by further relevant work, as mentioned in the appropriate places in the present chapter.

In delineating lithofacies, the present writer has attempted to recognise associations of sediments which are characteristic of a fairly broad environment. For this reason, minor Flat-pebble conglomerates, channel calcarenites and so on have not been recognised as individual lithofacies. Such units, which generally only occur as interbeds 10-20 centimetres thick,

are regarded as being a micro-facies formed within the overall framework of a broader sedimentary environment. Similarly, when early diagenetic features, particularly dolomitisation, appear to characterise a particular environment, these features are taken into consideration together with the primary depositional features.

3.3 Lithofacies Analysis

The following section is a description and environmental analysis of each of the ten limestone lithofacies which have been set up on field and laboratory criteria. Where particular stratigraphic heights are given as simple heights in metres, these refer to the height above the base of the section measured in Entrance Cave, and are the heights given in Fig. 4:1, which is the combined stratigraphic section measured at a number of localities on Marble Hill. The localities at which various parts of this stratigraphic column were measured are shown on Fig. 4:1, and their actual locations on Marble Hill recorded in Appendix Six. The stratigraphic heights shown in Fig. 4:1 for particular units are dependant on the units in Blaney's Quarry and those below Newlands Quarry having been placed in the correct stratigraphic relationship, of course. (see Ch. 2:3).

Lithofacies I - Birdseye Micrites and Birdseye Oosparites

This lithofacies crops out as a pale blue-grey limestone with abundant randomly distributed birdseyes ("fenestrae"). Tubular, irregular and laminoid birdseyes all occur (Grover and Read, 1978),

FIG. 3:1 Typical field appearance of Lithofacies I (Birdseye Limestone). Note regularly spaced stylolites. Scale graduated in centimetres.

FIG. 3:2 Vertical burrows in birdseye-rich limestones of Lithofacies VIII. Scale graduated in centimetres. (N.B. Photograph printed upside down).

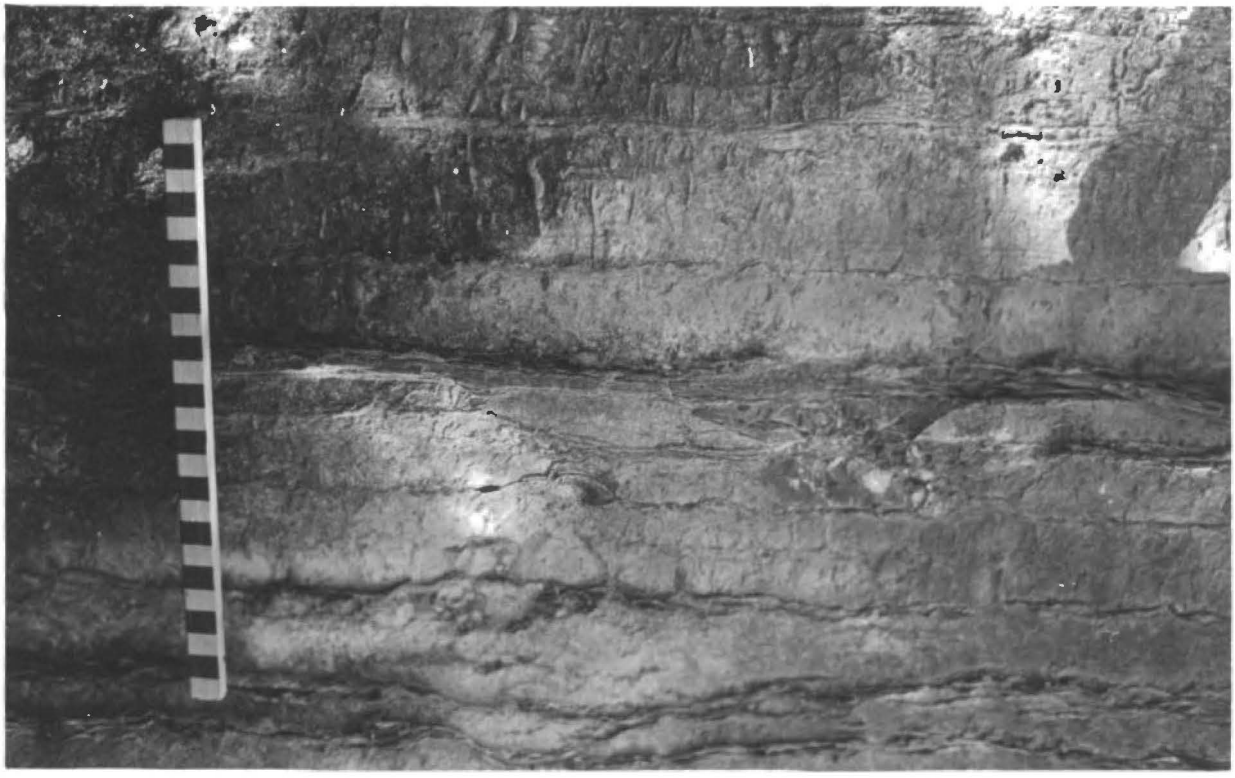

FIG. 3:3 Lithofacies I sediments in Entrance Cave, showing algal-laminated band at base overlain by flat-pebble band. Irregular and laminoid birdseyes visible as dark blebs. Note thin band of shelly material above flat pebbles. Scale graduated in centimetres.

FIG. 3:4 Lithofacies I sediments in Entrance Cave, showing a long flat-pebble to the right of scale. Shelly band includes cephalopod (*?Mysterioceras*) at right hand side of photo. Scale graduated in centimetres.

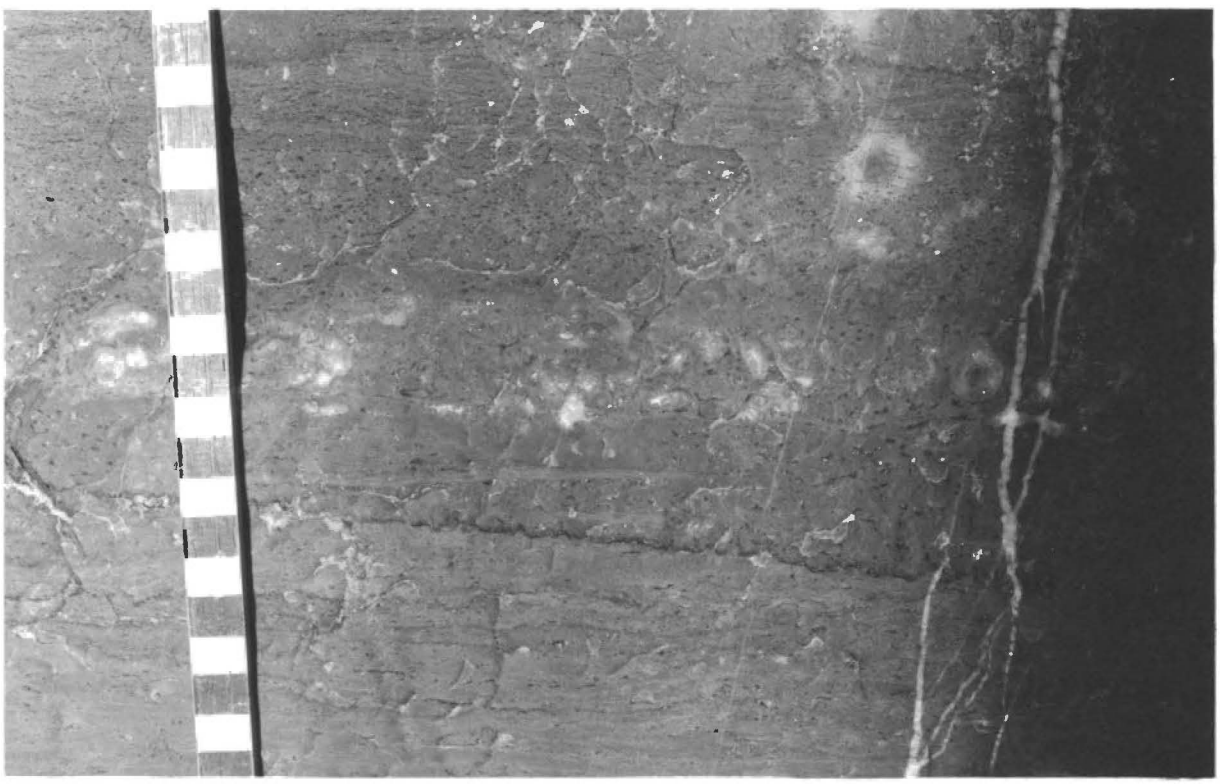

although the irregular type is predominant. With the exception of certain interbeds, this lithofacies shows no bedding planes, although an appearance of bedding is given by horizontal stylolites spaced an average of 0.1-0.2m apart (see Fig. 3:1).

The bulk of the birdseye limestones comprise dismicrites (Folk 1962). Typical examples include 48229 and 48230. Irregular birdseyes make up about twenty per cent of the rock by volume, and average 0.5 - 6.0mm diameter, and the micrite matrix is featureless apart from rare shell fragments (usually less than one per cent). Most of the birdseyes are completely infilled by sparry calcite, but in some cases, dolomite has partially replaced the calcite, as indicated by cross-cutting relationships, and by the fact that dolomite rhombs may sometimes surround remnant calcite masses. The dolomite occurs in equigranular aggregates varying from idiotopic rhombs to xenotopic masses, and dedolomitisation has commonly occurred. Individual grains average 0.1 - 0.2mm diameter.

Bands up to 0.05-0.2m thick of algal-laminated limestones commonly occur as minor interbeds within the birdseye units, and often have laminoid birdseyes. (Thicker algal-laminated units commonly occur above and/or below birdseye limestones, but are treated separately as lithofacies II, despite the obvious close relationship to birdseye limestones).

Typical examples of algal-laminated interbeds within birdseye limestones are represented by 48231 and 48232. Algal-laminated limestones are described more fully under the heading of

Lithofacies II, but it is noteworthy that algal-bands within birdseye limestones differ from true Lithofacies II sediments in having a greater abundance of birdseyes and a micritic, rather than pelmicritic, matrix.

48232 has laminoid birdseyes averaging 0.5mm thick and 2.20mm long, elongated parallel to the algal laminations (see Fig. 3:7). Tabular birdseyes also occur in 48232. They are very fine (0.05-0.1mm thick by 0.5-1.0mm high) and are oriented perpendicularly to the algal laminations. On these counts , it is probable that they represent upward migrating gas bubbles derived from decay of organic matter such as algae.

Vertical ("tubular") birdseyes are not only developed in algal-laminated interbeds, but also occur in non-algal dismicrites, in which they are usually larger (48235 contains tubular birdseyes averaging 0.6mm wide by 2.3mm high).

Flat- (and spherical- to irregular-) pebble conglomerates were observed in birdseye limestones in Entrance Cave and Newlands Quarry (see Figs. 3:3, 3:4, 3:8). The pebbles are usually 2-10mm thick and 10-20mm long (but may be up to 0.12 m long) and have rounded to sub-rounded boundaries. Many of the pebbles are probably fragments of algal-laminated material, and indeed the conglomerates commonly lie directly above algal-laminated bands.

Fossils are rare, with the exception of a unit in Entrance Cave discussed below. The only persistent fauna is a high spired gastropod (c.f. *Hormotoma* - see also Appendix Three) which occurs

at random as relatively undamaged specimens. *Tetradium* (including *T. bowanense*) occurs in a birdseye unit at 250 metres, which may represent a slightly less harsh environment than other birdseye units.

Vertical dolomitised burrows occur in a few of the birdseye units and are often associated with vertical ("tubular") birdseyes, which lends support to the theory of Grover and Read (1978) who feel that most tubular birdseyes are burrows. Fig. 3:2 shows vertical burrows in a unit below Newlands Quarry, at 210 metres. This unit contains birdseyes but cannot strictly be grouped within Lithofacies I since it also contains features characteristic of other lithofacies, and so is discussed under Lithofacies VIII.

In a few birdseye units, rare laminae up to 10mm thick, of angular quartz grains set in argillaceous matrix (e.g. 48236) indicate rare and brief periods of terrigenous influx. The clastic lamination in 48236 has an apparently tectonic cleavage, in contradistinction to the enclosing carbonates.

An unusual subfacies of the birdseye limestones occurs in the lower part of the birdseye unit in Entrance Cave (location 21), where the birdseyes are often confined to irregular bands and lenses 0.02-0.2m thick, interbedded with featureless limestones. Although indistinguishable from dismicrite in the field, these sediments are seen to be oosparites when examined microscopically. A typical example (48234) comprises laminoid to irregular birdseyes averaging 7 x 1.5mm in size, rounded to subangular intraclasts up to 10mm

FIG. 3:5 Lithofacies I. Typical dismicrite fabric, showing irregular spar-filled birdseyes, with partial dolomite replacement. Note rare gastropod fragments.
48229 Mag. x 4

FIG. 3:6 Lithofacies I. Unusual subfacies, showing birdseyes in oosparite. Probable skeletal fragment at upper left.
48234 Mag. x 10

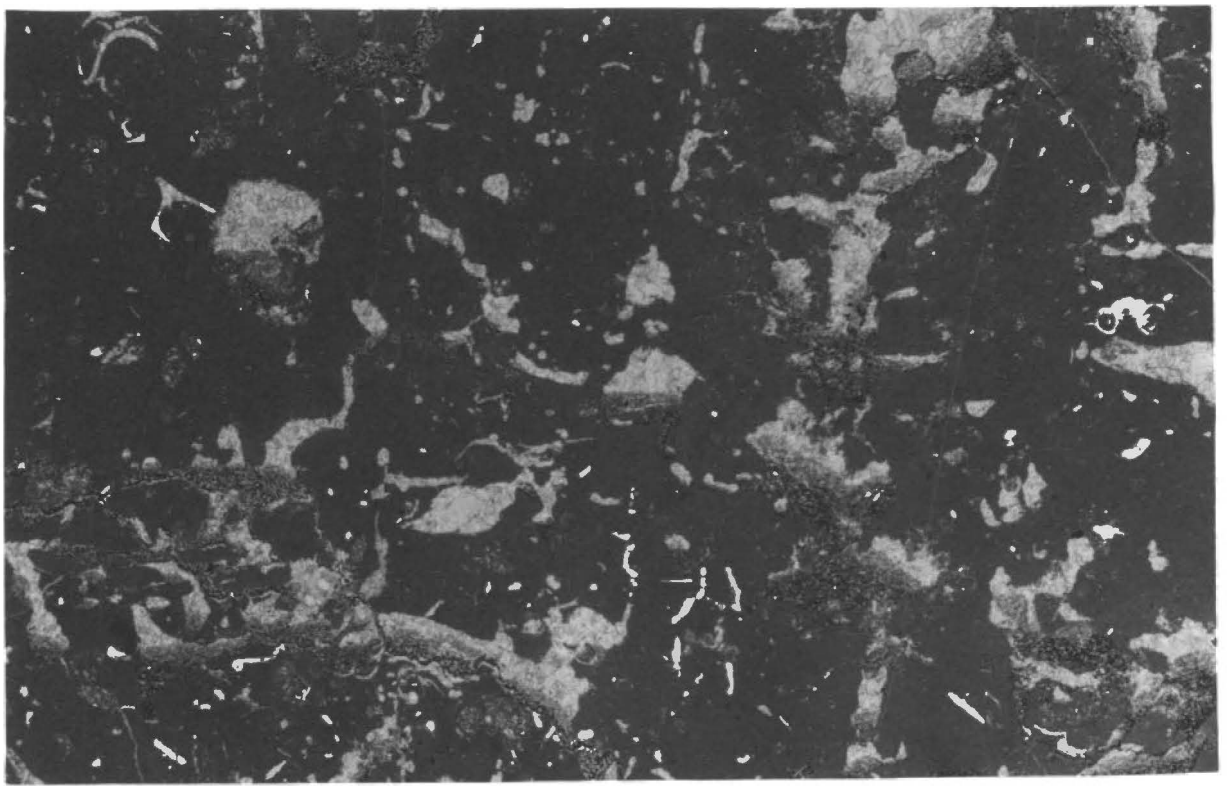

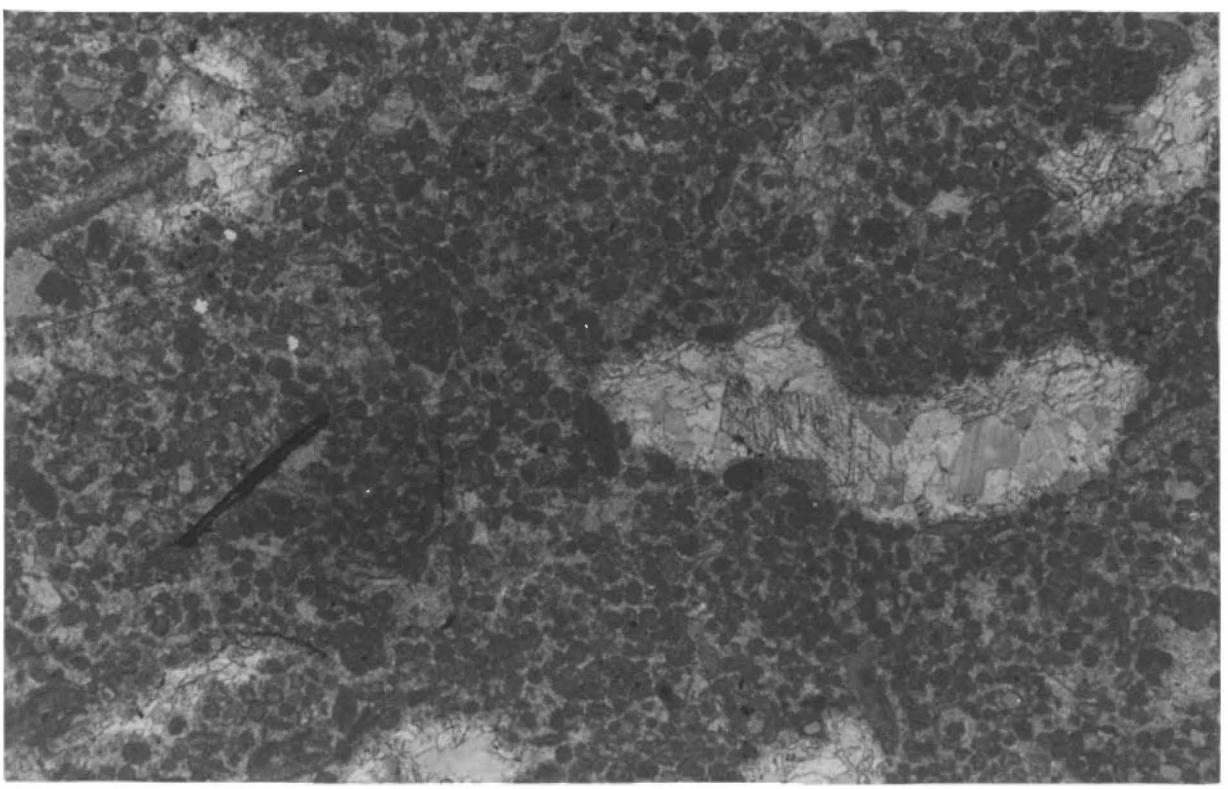

FIG. 3:7 Lithofacies I. Birdseyes in algal-laminated interbed. Note horizontal dolomitic layers. (Coarser dark bands). Coarse tubular and laminoid birdseyes visible, as well as very fine tubular (vertical) birdseyes.
48232 Mag. x 18

FIG. 3:8 Lithofacies I. Intraformational conglomerate, showing micritic intraclasts in spar.
48233 Mag. x 4

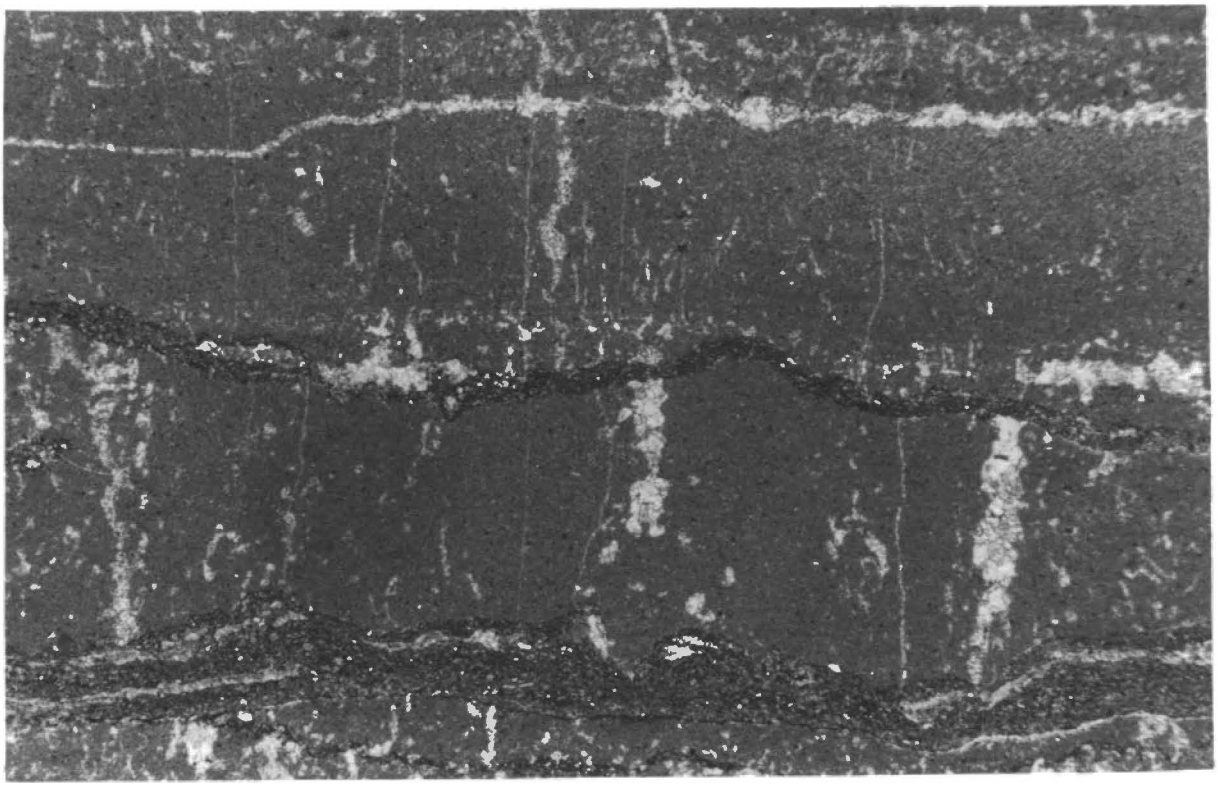

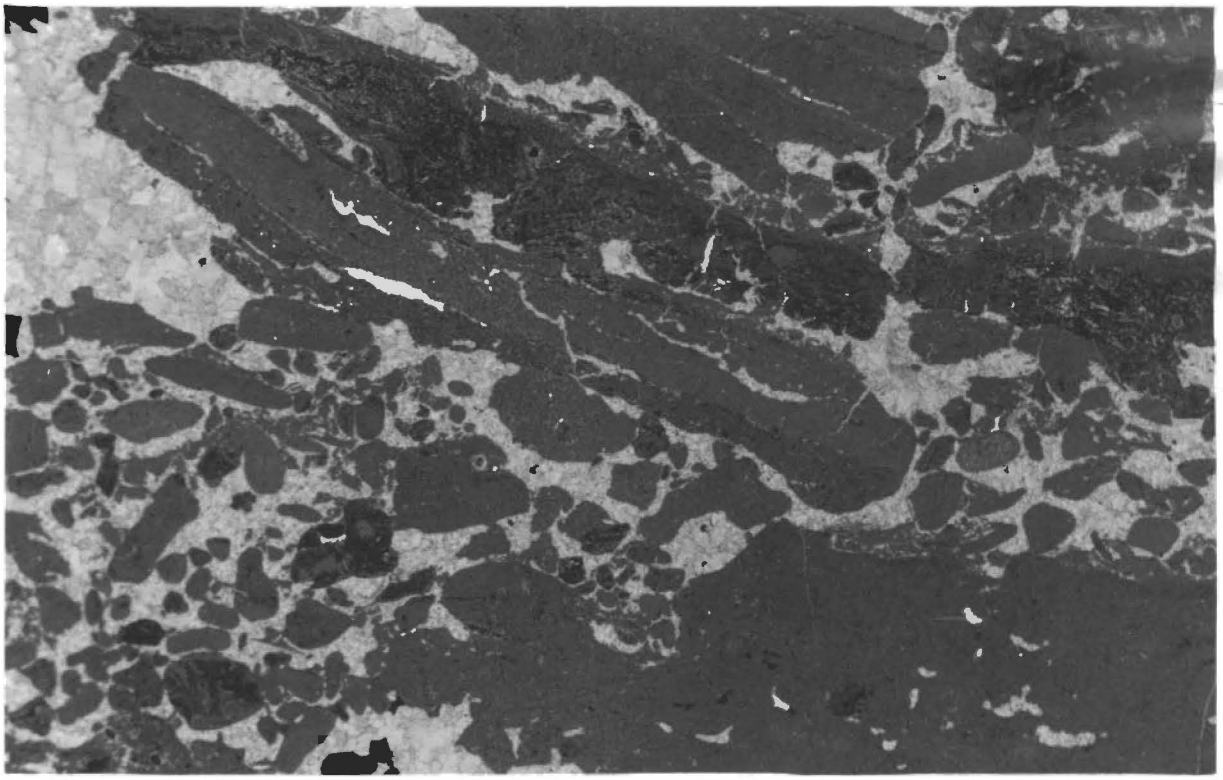

FIG. 3:9 Lithofacies I. Fossiliferous birdseye limestone at the bottom of Entrance Cave, with broken *Maclurites* specimens.
Scale graduated in centimetres.

FIG. 3:10 Lithofacies II, subfacies 2. Typical exposure in Blaney's quarry, showing thin anastomosing dolomitic stringers in two size ranges. (Thicker below, thinner above).
Scale graduated in centimetres.

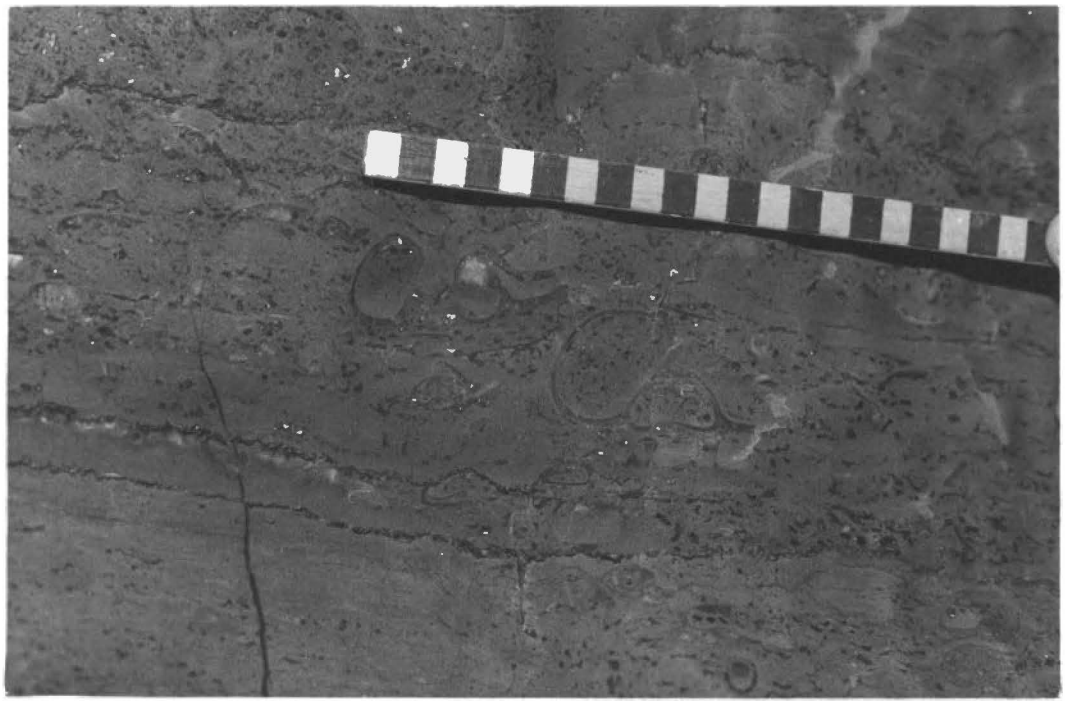

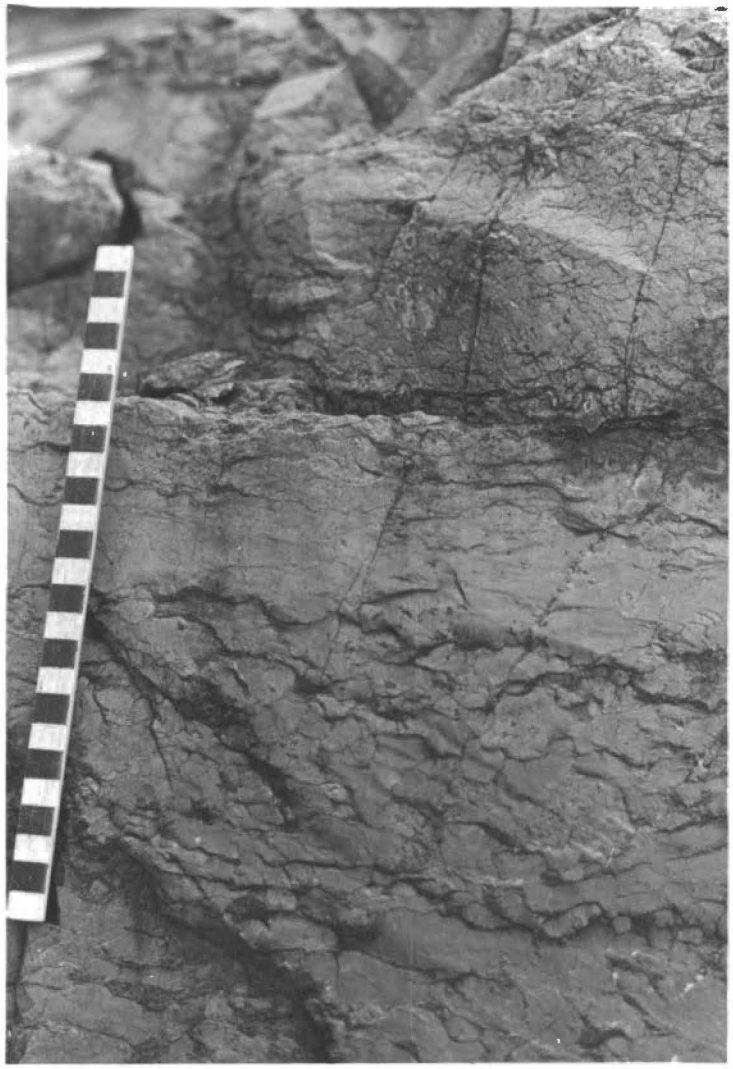

diameter, and a few fossil fragments (brachiopods?), all set in an oosparite matrix (see Fig. 3:6).

The oolites are round to somewhat oval, averaging 0.3mm diameter, and comprise over fifty per cent by volume of the sediment. They are cemented by a sparry calcite matrix. The intraclasts themselves composed of an oosparite with smaller oolites.

These oosparite birdseye limestones contain cross-bedded calcarenite bands (without birdseyes), and abundant flat-pebble and "round-pebble" intraformational conglomerates (Figs. 3:3, 3:4). Fossils are especially abundant in this unit, although mainly confined to bioclastic bands 10-60mm thick. The fossils are commonly broken, and include abundant gastropods (small low and high spired forms, together with large specimens of *Maclurites* - see Fig. 3:9), together with brachiopods, *Calathium*, small rolled colonial corals, and cephalopods. A bed containing large numbers of *Mysterioceras australe* has been reported from Entrance Cave (Teichert and Glenister 1953), and although it was not relocated in the present investigation it presumably occurs within this lithological unit. Rare oncolites are found, and conodonts have previously been found in limestones from the bottom of Entrance Cave (Burrett 1978).

Interpretation

The model put forward herein for Lithofacies I is one of deposition in supratidal to (?) upper intertidal environment, as inferred from the dominating birdseye fabric, which is regarded as

a dessication feature (Shinn 1968, Grover and Read 1978). Lime muds washed up during storm (Ball *et al* 1972) would develop a birdseye fabric as a result of dessication.

The high-spired gastropods (c.f. *Hormotoma*) found in this lithofacies are regarded as being indigenous thereto on the grounds that they occur as whole specimens randomly distributed (rather than being confined to bioclastic bands, which include organisms brought in from elsewhere), and also because, although they occur in several birdseye units, they are absent in interbedded lithologies.

At times conditions briefly became favourable for the growth of algal mats, possible as a result of minor transgressions increasing the amount of water available for algal growth, or for some other reason.

The occurrence of vertical burrows is evidence of upper intertidal conditions, since vertical burrows have been interpreted as providing more protection from fluctuating upper intertidal conditions than is provided by horizontal burrows (Rhoads 1967).

Although the use of burrow morphology as an environmental indicator can be criticised, in this case the occurrence of vertical burrows in birdseye and algal-laminated limestones is good corroboration of an upper intertidal environment.

Mudcracking and penecontemporaneous erosion of the sediments (particularly the algal-laminated material) provided intraclastic material which would have been reworked by storms and high tides to produce the flat-pebble conglomerates.

The bioclastic bands and oosparites found in Entrance Cave are unusual sub-facies for birdseye limestones. The bioclastic bands contain subtidal organisms, such as cephalopods, corals and *Calathium*, as well as a few oncolites, and must thus represent material carried into supratidal regions by storms or exceptional high tides. Why such beds are absent in other birdseye limestones units is not clear. A further puzzle is presented by the fact that whereas robust fossils such as *Maclurites* are generally broken, as is to be expected from high energy deposition, delicate forms such as *Calathium* commonly appear to be intact.

The oosparite is interpreted as a channel deposit on the grounds that oolite formation is thought to result from intermittent current transport and repeated burial and exhumation from sediments (Blatt *et al* 1972, p. 420). These requirements are fulfilled by tidal channels in high intertidal regions where the channels would often dry out for long enough for birdseyes to form.

Although few samples of the birdseye limestone unit in Entrance Cave were taken, the oosparite (48234) is from the lower part thereof, which is characterised by discontinuous lenses of birdseyes. The patchiness of the birdseyes may result from the fact that they would only have had a chance to form when the channels were dry for long periods; at other times more regular filling of the channels would have inhibited the formation of birdseyes, resulting in patches of non-fenestral oosparite.

The formation of birdseyes in the oosparite is noteworthy, since birdseyes generally do not form in sediments coarser than micrite.

Lithofacies II - Algal-laminated micrites and pelmicrites

This lithofacies has been divided into three subfacies on the grounds of matrix type, lamination size and degree of irregularly of the laminae.

Subfacies 1

In the field this subfacies crops out as a pale blue/grey micfite with flat or slightly irregular laminae 1-10mm thick, defined by thin brown laminae interpreted as the remains of algal mats (see Fig. 3:11). Well developed polygonal mudcracks may occur (see Figs. 3:14, 3:15), but birdseyes are rare, in contrast to algal-laminated bands with Lithofacies I. Fossils are rare, and stylolites are rarely discernable in the field except at contacts with other lithofacies. Stromatolite heads were not seen.

Microscopically, the thin laminae are flat to slightly undulose laminae of dark bituminous material, are 0.05-0.5mm thick, and are commonly surrounded by microspar. Idiotopic to xenotopic dolomite grains 0.1-0.2mm in diameter occur commonly within the bituminous laminae, but are sometimes distributed through the interlaminar material as well. Angular quartz grains occur sporadically within the laminae, and may be of aeolian origin.

FIG. 3:11 Lithofacies II, subfacies 1. Field appearance of Lithofacies (N.B. photo printed upside down). Scale graduated in centimetres.

FIG. 3:12 Lithofacies II, subfacies 1. Mudcrack, showing upwarping of laminae around crack. Note "Lumpy" nature of sediment between dark algal laminations. 48239 Mag. x 4.5

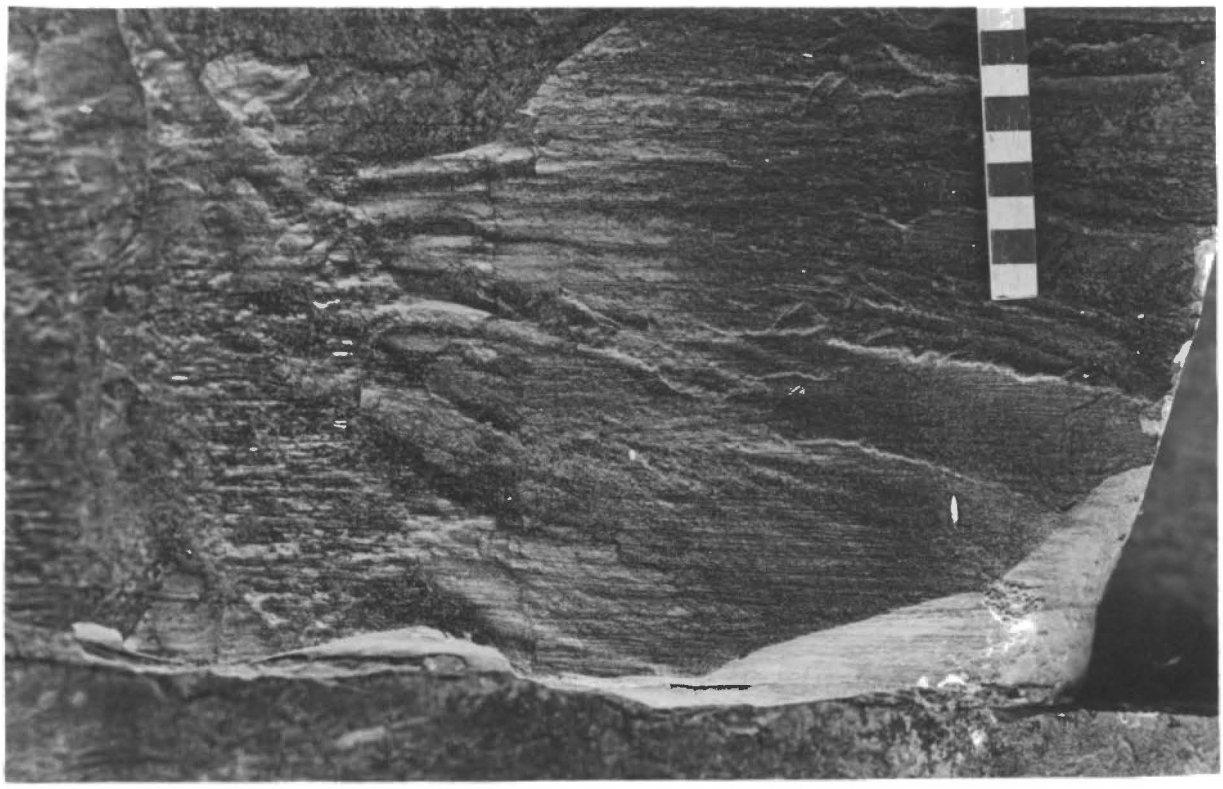

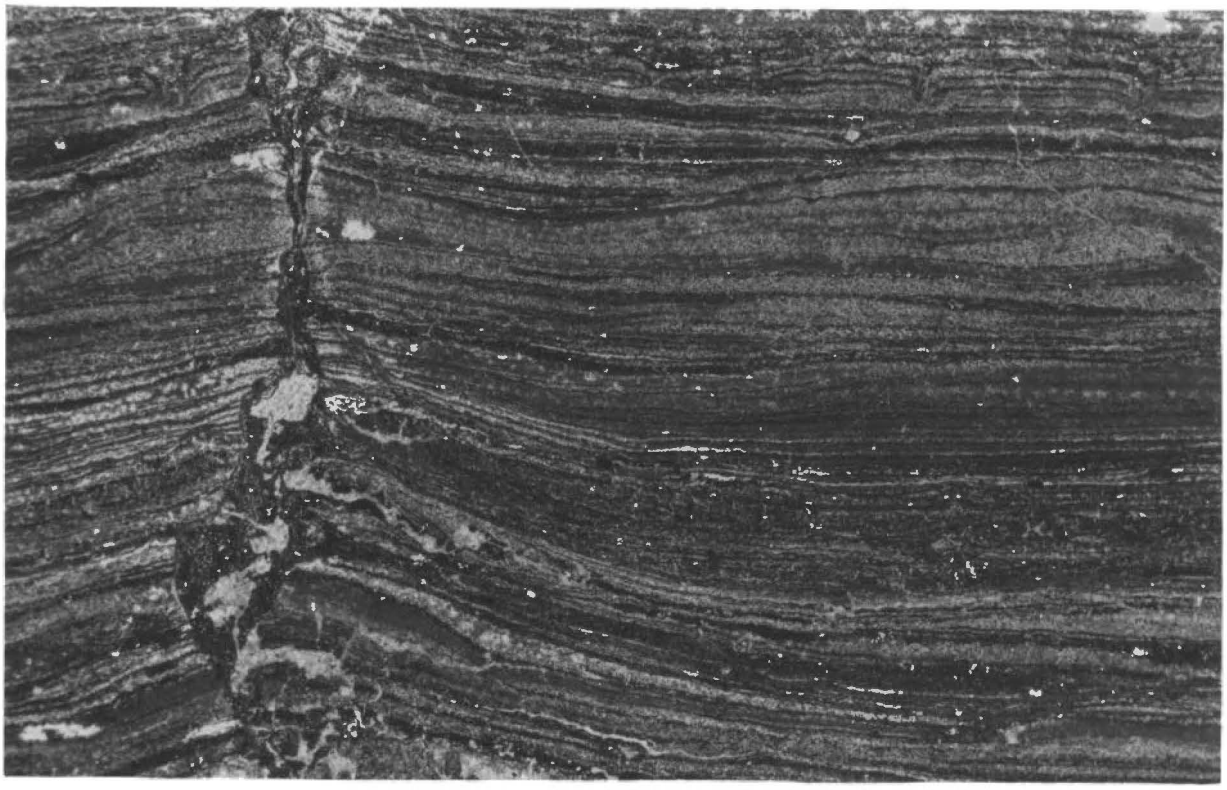

FIG. 3:13 Side-view of mudcracks in algal-laminated limestone (Lithofacies II, subfacies 1) in Blaney's Quarry. Scale graduated in centimetres.

FIG. 3:14 Top view of mudcracks. (Same as Fig. 3:13). Polygonal cracks can be discerned above scale. Scale graduated in centimetres.

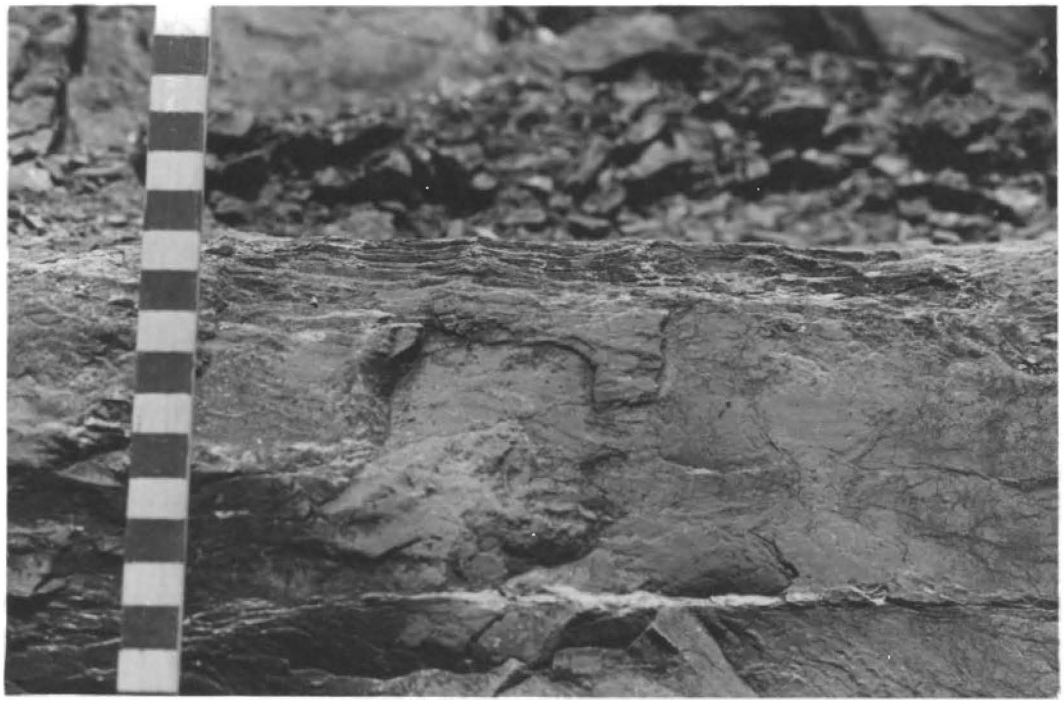

The interlaminar material usually consists of "lumpy" micrite with patches of microspar. This fabric, which is similar to the *structure grumeleuse* (Bathurst 1976, p. 512), is common in modern algal sediments (*ibid.*, p. 513). The micrite lumps average 0.2mm diameter and are interpreted as faecal pellets set in an originally micritic matrix, whose partial recrystallisation produced the microspar.

Minor stylolites occur within and bordering the algal laminae, and mudcracking is evident in 48239, in which dessication has produced cracking and concave-upwards curling of the laminae. Although this lithofacies usually occurs in association with birdseye micrites, there is not always a sequence of birdseye micrites overlain by algal-laminated limestones overlain by intrabiosparites, such as has been noted elsewhere in Tasmania for limestones of similar age (Page 1978, p. 55).

Interpretation

Algal-laminations (Logan *et al*, 1964), mudcracking, rarity of fossils, and association with birdseye limestones are regarded as indicators of intertidal-supratidal environments. The lack of stromatolite heads indicates a protected intertidal mud-flat environment (Bathurst 1976, p. 228), and this factor together with the general lack of birdseyes and high-energy conglomerate or bioclastic bands indicates a lower intertidal environment (as opposed to the higher energy upper intertidal regime suggested for algal-laminated bands within birdseye units).

The model envisioned is one of algal growth in a protected middle-lower intertidal environment trapping layers of pelletal muds accumulated by tidal action. The algal mats would trap wind-blown quartz grains, and on decay would have provided sites for dolomitisation as a result of the high Mg-content of the algal material. Occasional periods of dessication resulted in mudcracking.

Subfacies 2

This subfacies, represented by 48240 occurs interbedded with birdseye limestone units and algal-laminated units of subfacies 1. In the field subfacies 2 is characterised by a network of irregular horizontal anastromosing dolomitic stringers averaging 1-2mm thick, and rarely reaching 5mm thickness (see Fig. 3:10). Birdseyes are sparsely present, and interbedded bands of subfacies 1 type algal-laminations commonly occur. Fossils are rare, with only gastropod fragments being recognisable.

Microscopically this subfacies has the same pelmicritic matrix as subfacies 1, and it is on this ground, as well as the intimate associations of the two subfacies, that subfacies 2 is regarded as an algal-laminated sediment.

The dolomitic laminae are spaced an average of 10mm vertically apart in subfacies 2, and as a result subfacies 2 has a much lower dolomite content than subfacies 1 - perhaps 15 per cent of the subfacies 2 sediment is taken up by dolomitic algal layers, as compared to about 40-50 per cent in subfacies 1.

Irregular birdseyes are present in 48240, and microscopic stylolites are common.

Interpretation

Subfacies 2 accumulated in essentially the same fashion as subfacies 1, although an upper intertidal environment is implied by the presence of birdseyes in the sediment. The thicker and more widely spaced nature of the algal layers, resulting in a more pronounced heterogeneity of the sediment than was the case with subfacies 1, probably induced differential compaction resulting in the irregular anastomosing nature of the algal "laminations".

Subfacies 3

This subfacies occurs in two units (at 15 metres and 204 metres), interbedded with supratidal and intertidal sediments.

Subfacies 3 (eg, 48244) is characterised by thick (up to 3-8mm) flat to slightly dolomitic layers spaced 20-30mm apart in a featureless micrite (rather than the pelmicrite characteristic of subfacies 1 and 2). See Fig. 3:15.

Microscopic examination shows that the dolomitic layers contain idiotopic to rarely xenotopic dolomite in an argillaceous and bituminous groundmass. The dolomite has sometimes dissolved out, leaving rhombic pores (e.g. 48241, 48242).

The micrite is featureless apart from a few irregular to tubular birdseyes (e.g., 48242), and fossils are almost completely absent (although a single recrystallised corallite occurs in 48242).

FIG. 3:15 Field appearance of Lithofacies II (Subfacies 3) sediments. Note thin horizontal dolomitic layers. Scale graduated in centimetres.

FIG. 3:16 Possible macroscopic evaporite pseudomorphs in Lithofacies II (subfacies 3) sediments. View looking down on bedding plane. Scale graduated in centimetres.

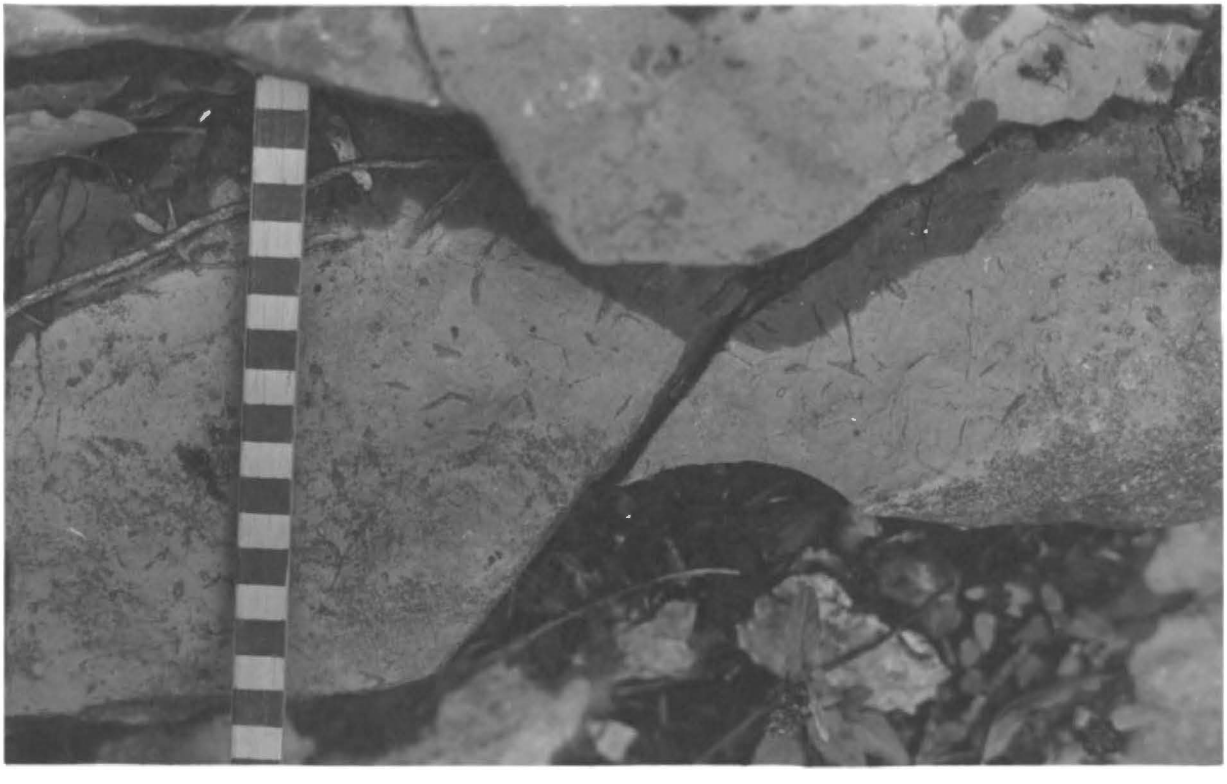

Possible macroscopic evaporite pseudomorphs were noted in the field (see Fig. 3:16), but their lack of distinctive features such as re-entrant angles and twinning precludes a definite identification.

The dolomitic bands may rarely grade into very thin laminae of dolomite and bituminous matter (c.f. subfacies 1), although these are still associated with a featureless micrite matrix (e.g. 48243).

Interpretation

A supratidal or upper intertidal environment is indicated by the occurrence of birdseyes and possible evaporite pseudomorphs, as well as the lack of fossils and the association with other supratidal or intertidal sediments. The sporadic gradations to subfacies 1 algal-laminae implies that the thick dolomitic layers may be large algal layers. An alternative possibility is that they represent dolomitisation resulting from evaporation of pore fluids from the upper layers of sediment during dessicating phases (see also Lithofacies VI).

Diagenesis in the vadose zone has resulted in development of porosity by dissolution of some of the dolomite.

Lithofacies III - Oncolitic limestones

Oncolitic limestones occur as rare thin beds (maximum four metres thick) and occupy horizons transitional between subtidal and intertidal or supratidal sediments. They are characterised by a decrease in oncolite size and a change in sediment type towards the subtidal horizons, resulting in two distinct oncolite subfacies.

Furthest away from the subtidal horizons the oncolites take the form of moderately well-sorted spherical to irregular lumps about 30-40mm diameter, formed around a core often consisting of skeletal fragments (see Fig. 3:20). The oncolites consist of concentrically stacked hemispheroids of micrite and microspar, in which bituminous patches and algal filaments (*Girvanella*) are commonly visible.

The oncolites are set in a brown dolomitic matrix (see Figs. 3:18, 3:20) which makes up 50-60 per cent of the rock. Microscopically, this matrix comprises forty per cent dolomite (generally idiotopic rhombs about 0.1mm diameter) and five per cent fossil fragments in a poorly washed xenotopic spar groundmass (55 per cent). The rock is a poorly washed dolomitic oncobiosparite.

Fossil fragments present include gastropods, trilobites, brachiopods, bryozoans and stromatoporoids. Although *Maclurites* has been previously reported from *Girvanella*-bearing beds at Ida Bay (Banks and Johnson, 1957), the gastropod fragments found within these units could not be positively assigned to *Maclurites*.

Towards the subtidal horizons an abrupt change occurs to a subfacies characterised by smaller oncolites in a calcarenite sediment (see Figs. 3:17, 3:19). The oncolites average 5-8mm diameter and make up between five per cent and fifty per cent of the sediment. The calcarenite is a poorly washed intrabiopelsparite whose dominant constituents are rounded, poorly sorted intraclasts up to 1.5mm diameter. Fossil material is common and comprises many forms in

FIG. 3:17 Small oncolites in poorly washed intrabiopelsparite. Note *Solenopora* lump on right hand side of photograph. Lithofacies III. Scale graduated in centimetres.

FIG. 3:18 Lithofacies III. Band of Large Oncolites in dolomitic sediment overlying band of small oncolites. Lithofacies VII sediments overlie the large oncolites, and Lithofacies IV sediments (subtidal Biomicrites) underlie small oncolites. Scale graduated in centimetres.

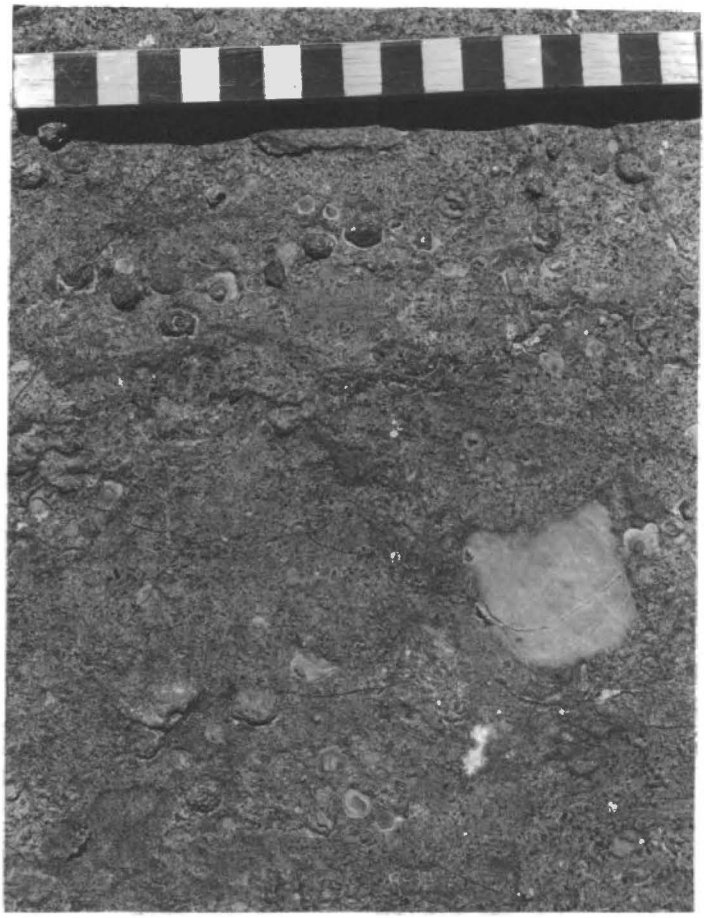

FIG. 3:19 Lithofacies III. Small oncolites in intrabiopelsparite.
48246 Mag. x 4.5

FIG. 3:20 Lithofacies III. Large irregular oncolites in dolomitic matrix. (Dark dolomite rhombs visible in matrix).
48245 Mag. x 4.5

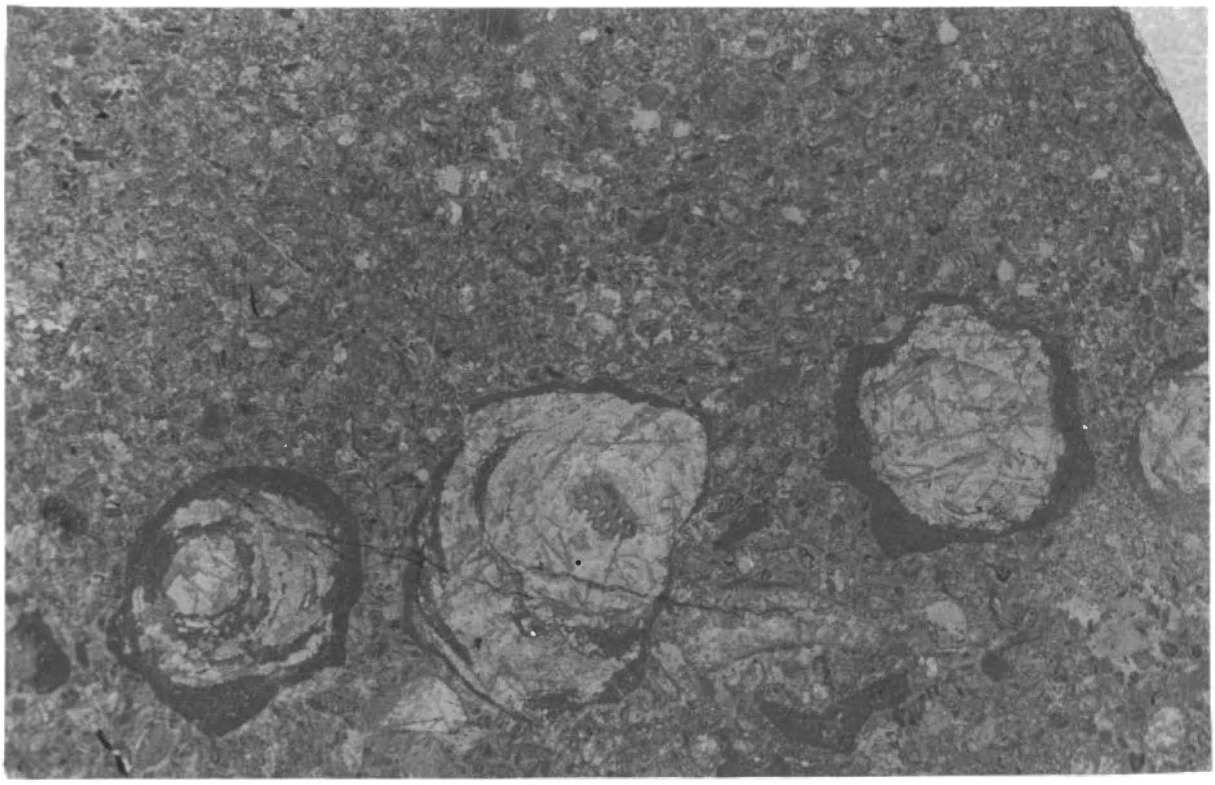

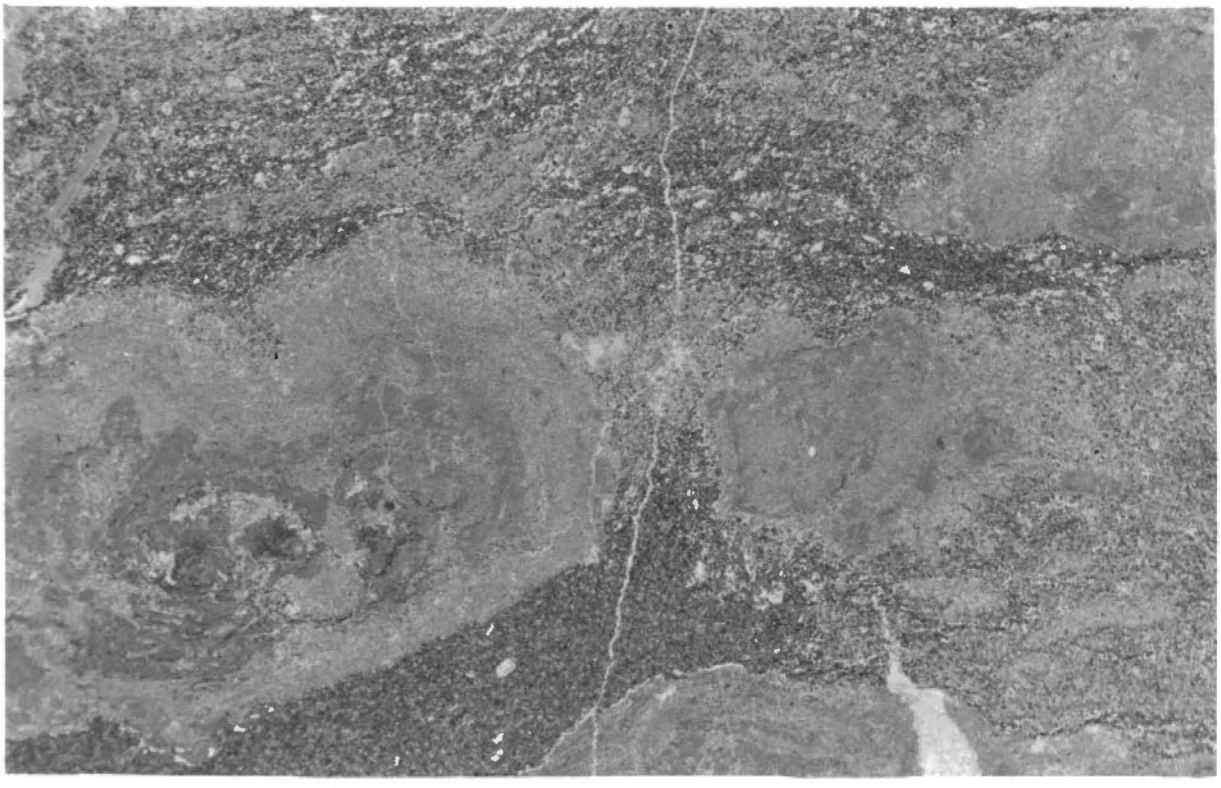

common with the adjacent subtidal beds. It may include shell fragments (often in graded bioclastic bands), corals, bryozoans, *Solenopora* and *Calathium* (in Newlands Quarry), as well as *Girvanella* filaments.

Bedding is massive in both subfacies, and burrowing is rare or absent. Only the small-oncolite subfacies is present below the subtidal Calathium-rich bed at 397 metres, but both subfacies occur at the other oncolite horizons.

Interpretation

Oncolites are considered to form where the original "substrate" (bioclast or intraclast) is free and mobile, so that algal material can grow all round the nucleus to give the familiar spheroids (Bathurst 1976). This requirement, as well as the high spar to micrite ratio in the sediments and the well rounded nature of most of the intraclasts, requires a moderately energetic environment in which bioclasts and intraclasts were in near-constant agitation. The occurrence of subtidal fossils in oncolite beds, and their stratigraphic position between subtidal and intertidal lithologies, indicates that the environment most likely to have satisfied these conditions would be a lower intertidal or upper subtidal environment above wave base in the zone of wave agitation.

The existence of two oncolitic subfacies is probably related to position within this general sedimentary environment, since the sequence of subfacies indicate that the large oncolites (in the dolomitic oncobiosparite) formed in a shallower environment within

the zone of wave agitation than did the small oncolites (in the intrabiopelsparites). Perhaps the formation of the larger oncolites is related to conditions in a lower intertidal environment where dolomitisation could take place more readily in the sediment matrix, whilst the small oncolites formed in moderately energetic conditions closer to wave base.

Dahanayake (1978) in a study of French Upper Jurassic oncolites found that increasing oncolite size was correlated with increasing dolomitisation of the sediment, and with decreasing energy of the environment. This model appears to be applicable to the Ida Bay oncolites, with the larger oncolites forming in a less energetic lower intertidal environment on the upper margins of the zone of near-constant wave agitation.

In one case (at 242 metres) small oncolites are associated with graded bioclastic bands (e.g. in 48247), perhaps representing lower intertidal conditions. Unless the small oncolites formed in lower intertidal channels, it is possible they were washed inshore by storms or strong tidal currents.

Lithofacies IV - Burrowed Biomicrites

Grouped within this lithofacies are units which are sedimentologically similar, but comprise at least two distinct biotic associations (see below). This biotic variation presumably mainly represents environmental or palaeoecological controls rather than evolutionary changes, since some of the genera involv ed (e.g.

FIG. 3:21 *Calathium*-rich burrowed biomicrite (lithofacies IV) in Newlands Quarry. Scale graduated in centimetres.

FIG. 3:22 *Palaeofavosites*/bryozoan-rich biomicrite (lithofacies IV) on floor of Newlands Quarry. View looking down on bedding. Scale graduated in centimetres.

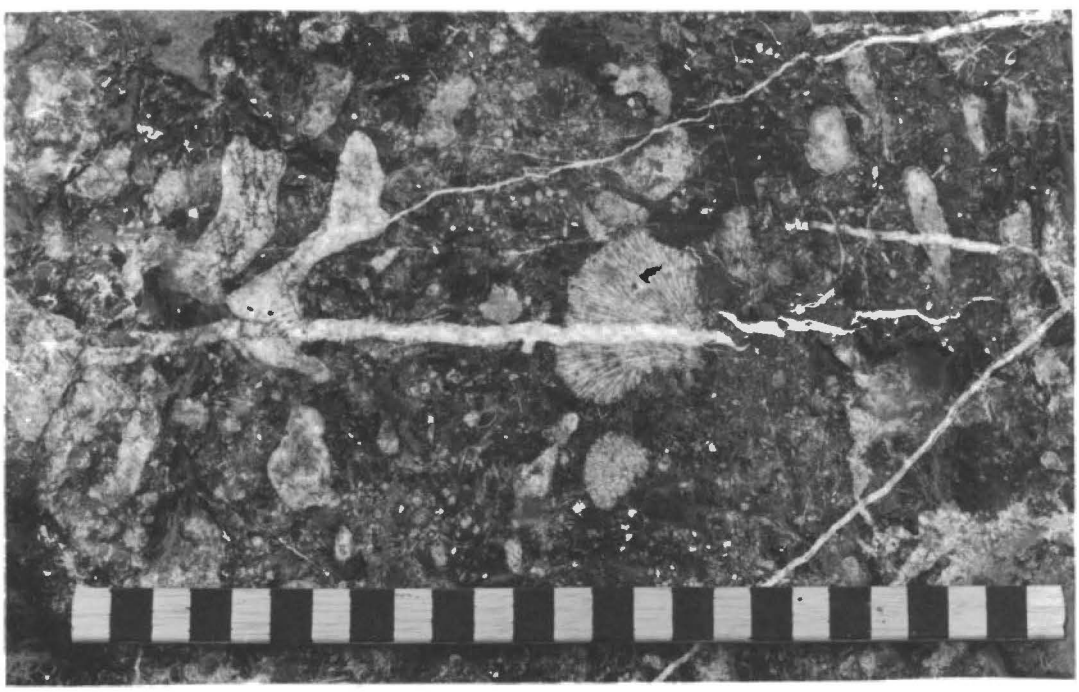

FIG. 3:23 Lithofacies IV. Detail of biomicrite.
48249 Mag. x 4.5

FIG. 3:24 Lithofacies VIII. Field appearance of unit, showing vertical burrows.
Scale graduated in centimetres.

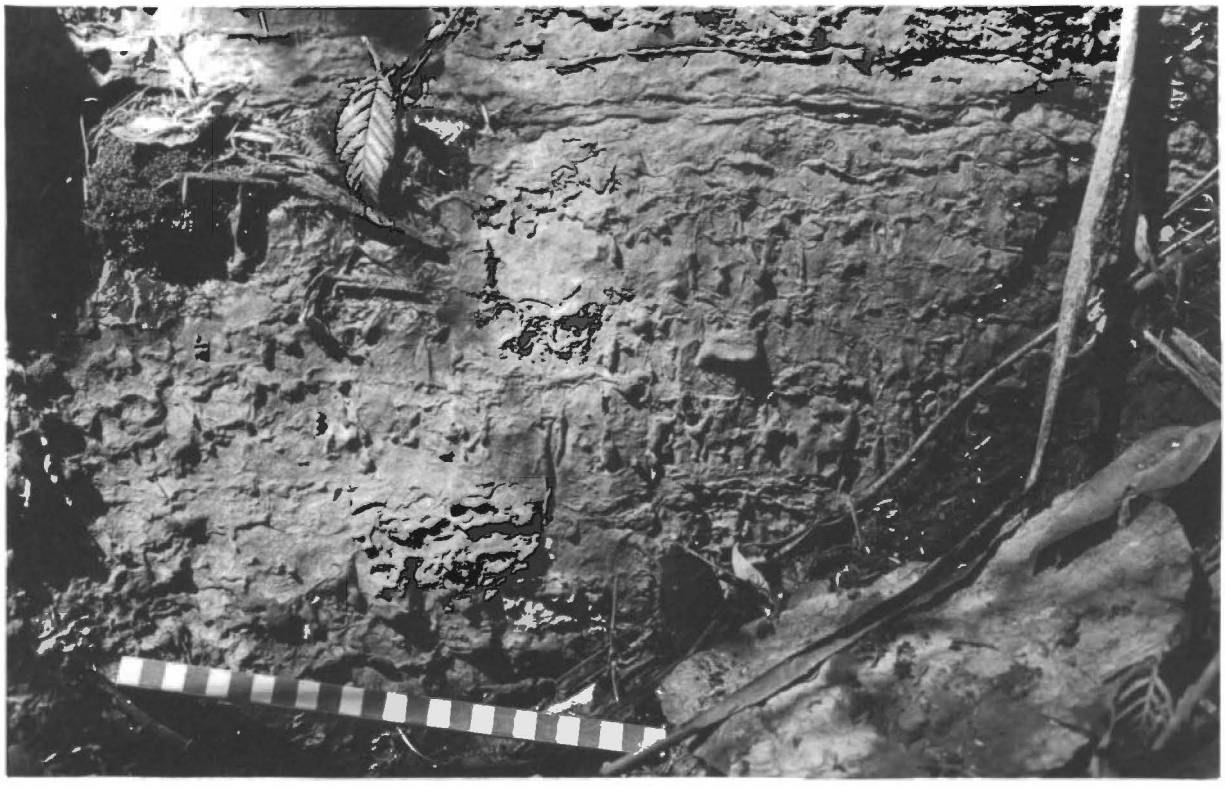

Calathium) have ranges overlapping Lithofacies IV beds in which they are rare or absent.

In the field this lithofacies is a dark micrite whose dominant features are an abundance of fossils and of random or horizontal dolomitised burrows, usually brown or grey in colour, up to 10-20mm thick and irregular to tubular in shape.

At 245 metres this lithofacies has bioclastic bands near the base, passing up into a sediment with a *Tetradium* dominated biota. Stromatoporoids, bryozoans, gastropods, possible cephalopods, crinoid ossicles and other shelly fragments also occur.

Three units in Newlands quarry are dominated by a Coral/bryozoan/*Solenopora*/*Calathium* biotic association. A unit on the floor of Newlands Quarry (at 265 metres) has only rare *Calathium* (e.g. 98319), but an unusual abundance of cephalopods. At 300 metres, another unit has abundant *Calathium*, as well as common stromatoporoids. Chert nodules up to 0.1m diameter occur in this unit, apparently as replacements of colonial corals and *Solenopora*. A similar unit occurs at the top of the quarry, at about 345 metres.

Microscopically the sediment varies from sparsely fossiliferous micrites with less than ten per cent fossil fragments in a sediment of featureless micrite and dolomitic burrows (e.g. 48248), to packed biomicrites with over fifty per cent fossils in a micrite sediment, often with dolomitised patches and complex stylolites (e.g. 48249; see Fig. 3:23). In some specimens (e.g. 48250) pellets

and small rounded intraclasts are discernable in a matrix of microspar, which may represent recrystallised micritic matrix, or slight washing of the sediments during deposition. A mottled appearance in some specimens is indicative of bioturbation.

Dissolution of specimens in Acetic Acid revealed authigenic pyrite and other metallic minerals in the insoluble residues implying reducing conditions at or below the sedimentary interface. The pyrite is not as abundant as in lithofacies V, however.

Interpretation

The high biotic diversity and micritic nature of the sediment are indicative of a subtidal environment below wave base. The *Tetradium*-rich unit is similar to "*Tetradium* wave-baffle communities" described by Walker (1972) in the Ordovician of New York State, North America. By analogy, it is probable that this unit represents an accumulation of sediments in and near the seaward edge of the zone of impingement of wave action on the substrate.

Lithofacies V - Burrowed Intrapelsparite and minor oosparite

This lithofacies is exposed in Entrance Cave above Supratidal-Upper intertidal beds, but the best exposure is in Blaney's Quarry where it crops out in a thick unit between two birdseye limestone horizons.

The lithofacies has a field appearance of a thickly bedded blue/grey limestone overlying supratidal and upper intertidal beds on a scoured erosional surface (see Fig. 3:25). Brown or grey

dolomitised burrows comprise about ten per cent of the sediment by volume and are horizontal to randomly oriented. The burrows appear abnormally short on vertical surfaces (see 3:26), and exposures on bedding planes (see Fig. 3:27) show this to result from the fact that the burrows have a radiating habit. In some cases more continuous horizontal stringers of dolomitic material occur.

The biota is rather restricted. In the unit in Blaney's quarry it consists mainly of large stromatoporoid and *Foerstephyllum* coralla. Other fossils are rare: a few endocerid cephalopods and rare bryozoans are seen in the field, but other shelly fragments are only distinguished under the microscope.

Stylolites are seen in the field, and a few 0.1-0.2m thick interbeds of fine non-burrowed unfossiliferous laminated calcarenite (e.g., 48251).

Microscopically, the burrowed lithofacies (represented by 48252 and 48253) consists largely of intraclasts and pellet-sized intraclasts in a poorly washed spar/micrite matrix. Oolites, which are largely recrystallised, comprise at least five per cent of the sediment, and an unknown proportion of the pellet-sized intraclasts are probably faecal pellets.

The intraclasts are rather poorly sorted, ranging from over 1mm to less than 0.1mm in diameter. They are sub-angular to rounded and elongate to spheroidal in shape. Most intraclasts are composed of micrite, but in 48253 a large proportion consist of

FIG. 3:25 Scour at base of thick Lithofacies V unit in Blaney's Quarry. Pale sediment below is Birdseye limestone (Lithofacies I). Scale graduated in centimetres.

FIG. 3:26 Lithofacies V, showing discontinuous expression of burrows on a vertical surface. Scale graduated in centimetres.

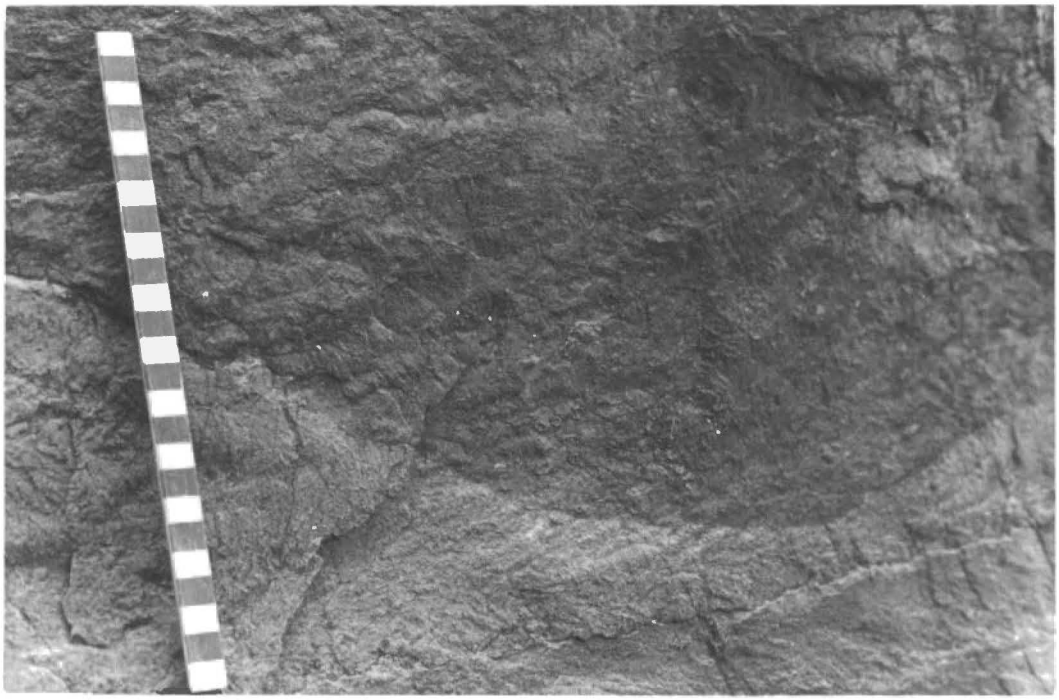

FIG. 3:27 Lithofacies V, view looking down on a bedding plane. Radiating habit of horizontal burrows is visible to left of Brunton Compass. Compass face approximatel y 5 centimetres diameter.

FIG. 3:28 Lithofacies V, view looking down on a bedding plane. Two Labechid Stromatoporoids and a *Foerstephyllum* corallum (left of compass) visible. Compass face is approximately 5 centimetres diameter.

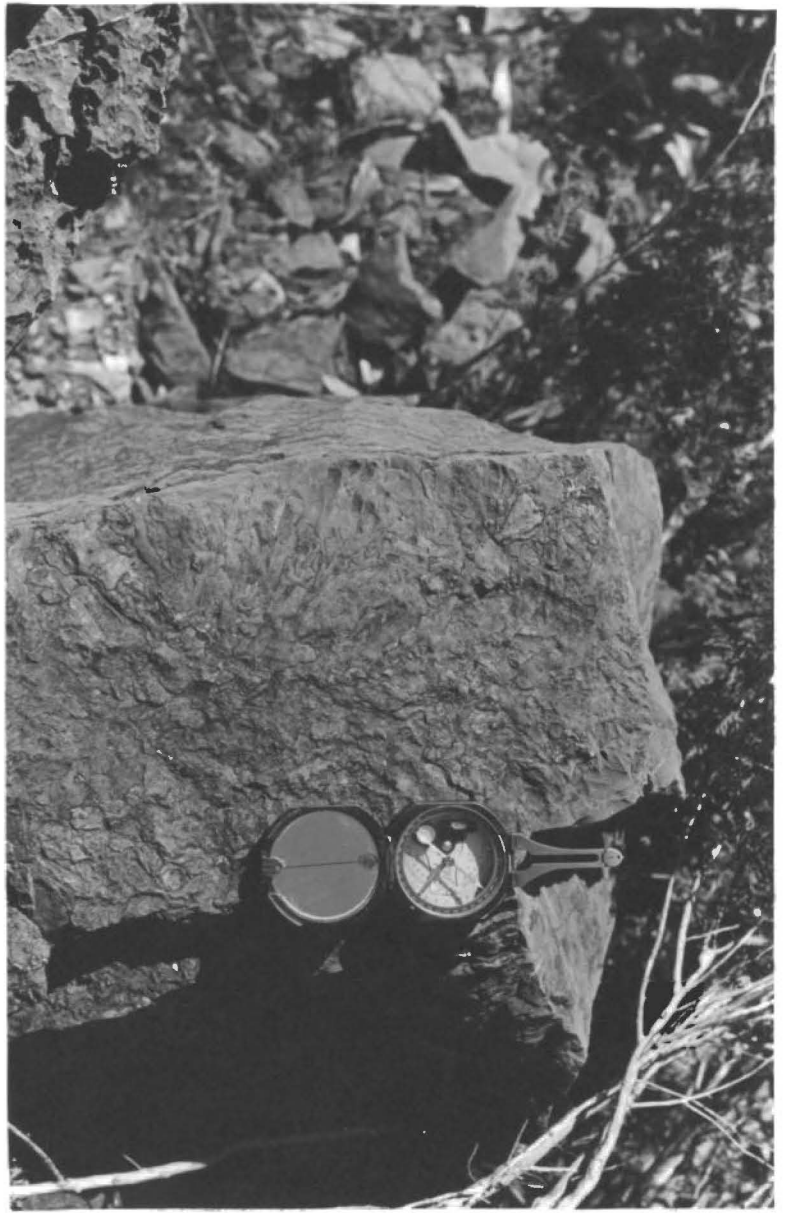

FIG. 3:29 Lithofacies V. Laminated oosparite, showing well washed lamination in centre of photo, with poorly washed laminations above and below.
48251 Mag. x 11

FIG. 3:30 Lithofacies V. Typical microscopic appearance of unit, showing uneven washing of sediment.
48252 Mag. x 18

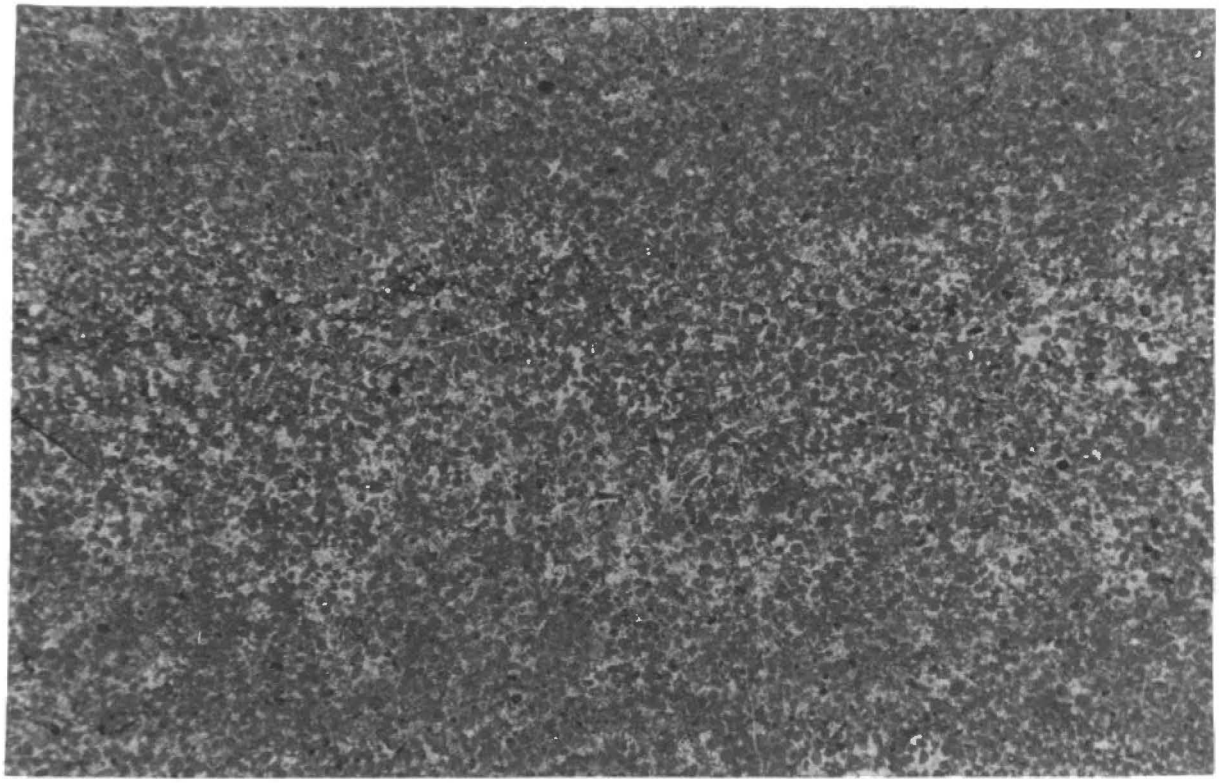

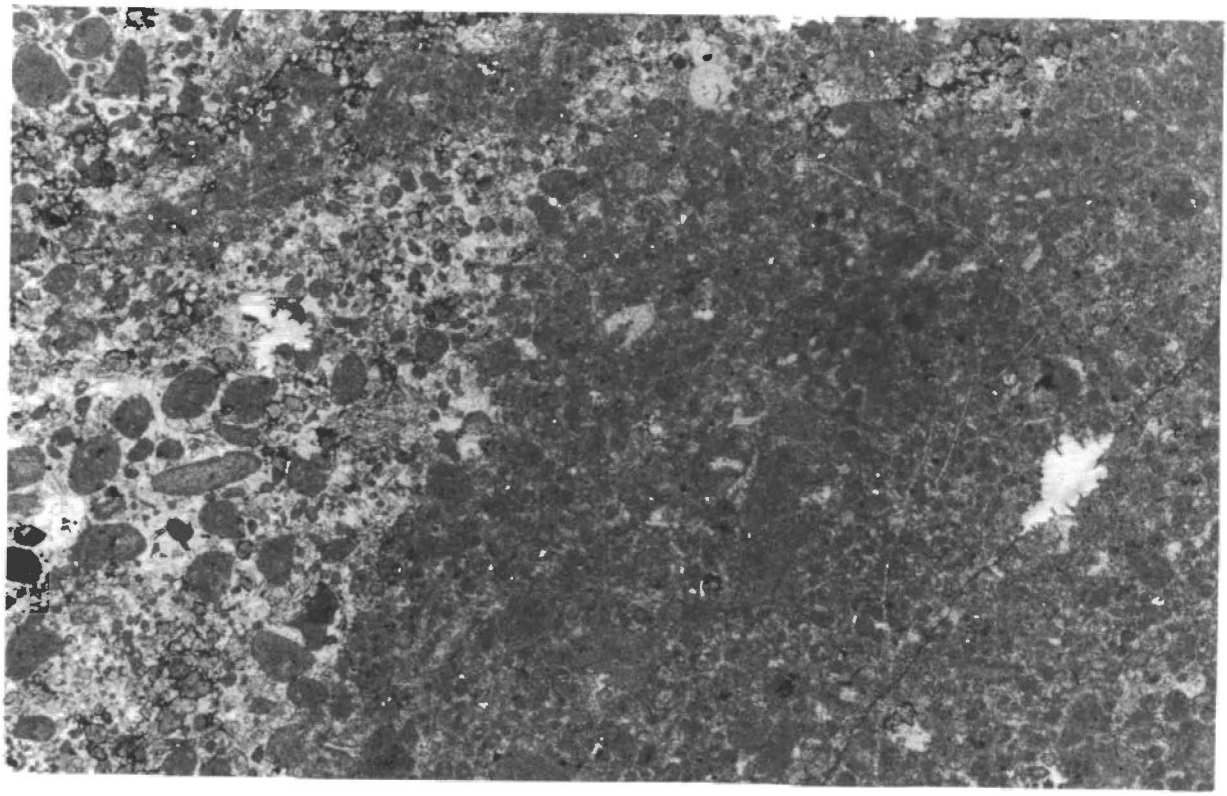

dolomite rhombs in a matrix of micritic and organic material. The latter intraclasts would have been derived from reworking of sediments with dolomitic burrows.

Fossil material comprises perhaps seven per cent of the sediment, and consists of bryozoan, gastropod, brachiopod and other shell fragments, as well as the macroscopically visible stromatoporoids and corals.

Microscopically, the dolomitised burrows appear as irregular horizontal patches of equigranular idiotopic (rarely xenotopic) dolomite rhombs set in dark bituminous material. Dissolution of specimens of this lithofacies in acetic acid yielded abundant pyrite cubes in the insoluble residues.

The non-burrowed laminated calcarenite bands, represented by 48251, comprise abundant well sorted partially recrystallised oolites, and possibly a few pellets, both averaging 0.07-0.1mm diameter, and set in a spar matrix. The sediments are thus oosparites. Laminations of 1-4mm thickness are produced by alternating layers of well-washed and poorly washed oosparite.

Interpretation

Intraclasts result from reworking of partially consolidated supra- and intertidal sediments, and may accumulate in any tidal environment. The poorly washed nature of the matrix and the poorly sorted nature of the allochems, taken together with the occurrence of oolites and the restriction of the fauna to robust coral and

stromatoporoid forms, indicate a low to moderately energetic regime. Corals and stromatoporoids were dominant reef builders in the Ordovician (Copper 1974), which suggests an energetic environment for any biotic association restricted to these forms.

A lower intertidal or subtidal environment within the zone of near-constant wave action is probably ruled out by the presence of burrows, since constant wave action would prevent preservation of burrows. In view of the poor washing and sorting, the presence of oolites, and of scouring at the base of the unit in Blaney's Quarry, this lithofacies was probably formed in an intertidal region subject to intermittent wave action and associated with intermittent, perhaps channel-switching, tidal channels. Bridge and Leeder (1976) have documented analogous modern tidal channel sediments on clastic mudflats wherein burrowing is common in tidal channel point bars, and small domal stromatolites occur high on cut-banks of channels.

The unfossiliferous laminated oosparite bands probably represent higher energy channel sediments associated with a major channel. Alternatively they could be shoal deposits resulting from minor transgressions causing extension of the intertidal environment into the subtidal environment as tongues of sediment (Reineck and Singh 1975, p. 318).

Lithofacies VI - Micrite and Biomicrite with thin dolomitic layers

In the field this lithofacies crops out above or below supratidal limestones as a dark micrite, in thin beds 20-100mm thick delineated by irregular horizontal stringers of brown-weathering dolomite which are usually only a few millimetres thick but may reach 30mm thickness (see Figs. 3:31, 3:32). A few vertical burrows occur (see Fig. 3:32). Bands 50-100mm thick of intrasparrudite and graded intrasparenite bands are common; these rest on scoured surfaces. Occasional chert nodules occur in some units.

Macroscopic fossils are rare. A few bryozoan, gastropod and other shell fragments can be seen in outcrop, but the only significant occurrences of macroscopic fossil material are in a thin "*Tetradium* horizon" at 275.5 metres (at location 1) and a dolomitic biomicrite band at 288 metres (at locations 1 and 4).

Microscopically, the micrite bands range from almost featureless micrites (e.g. 48254) to fossiliferous micrites (e.g. 48255) and biomicrites (e.g. 48256) in which large quantities of fossil materials (and angular spar fragments interpreted as comminuted fossil material) are present as small fragments 0.1-1.0mm or more in size (see Fig. 3:34). Identifiable fossils include whole Ostracod shells, sponge spicules, crinoid ossicles, trilobite and brachiopod fragments.

Ill-defined patches of spar and microspar give the sediment a mottled appearance and probably result from bioturbation (see

Fig. 3:34). Probable pseudomorphs after evaporite crystals occur as elongate subhedral laths (av. 0.2 x 0.07mm) which have grown displacively in patches of equigranular xenotopic spar (e.g. in 48256-see Fig. 3:35).

The horizontal to irregular dolomite stringers comprise two distinct types. The first type is the common case of dolomite grains in a hypidiotopic fabric with dark interstitial organic and/or argillaceous matter. Of a more unusual nature is the occurrence of idiotopic dolomite rhombs dispersed in a spar matrix (see Fig. 3:36). In the latter case the dolomite comprises no more than twenty per cent of the stringer, whereas in the former case it comprises 80 or 90 per cent.

Rare tubular birdseyes and hinds of mudcracking (in the form of v-shaped nicks on micrite/dolomite stringer interfaces) occur in the sediment (both features are visible in 48257).

The intrasparite bands consist of rounded to sub-rounded irregular shaped intraclasts, ranging in size from 30mm long to only 0.2mm diameter, in a spar matrix (see Fig. 3:37). The matrix is rarely dolomitic (e.g. 48259). The intraclasts are usually of micrite, and are spar supported. Ostracods (commonly unbroken) and bryozoan fragments are common in the intrasparite bands.

Two thin but anomalous interbeds occur within units of Lithofacies VI. The first, at 275.5 metres (at location 1) consists

FIG. 3:31 Field appearance of Lithofacies VI, showing horizontal dolomitic stringers. Scale graduated in centimetres.

FIG. 3:32 Detail of Lithofacies VI, showing vertical burrows and intrasparenite band. Scale graduated in centimetres.

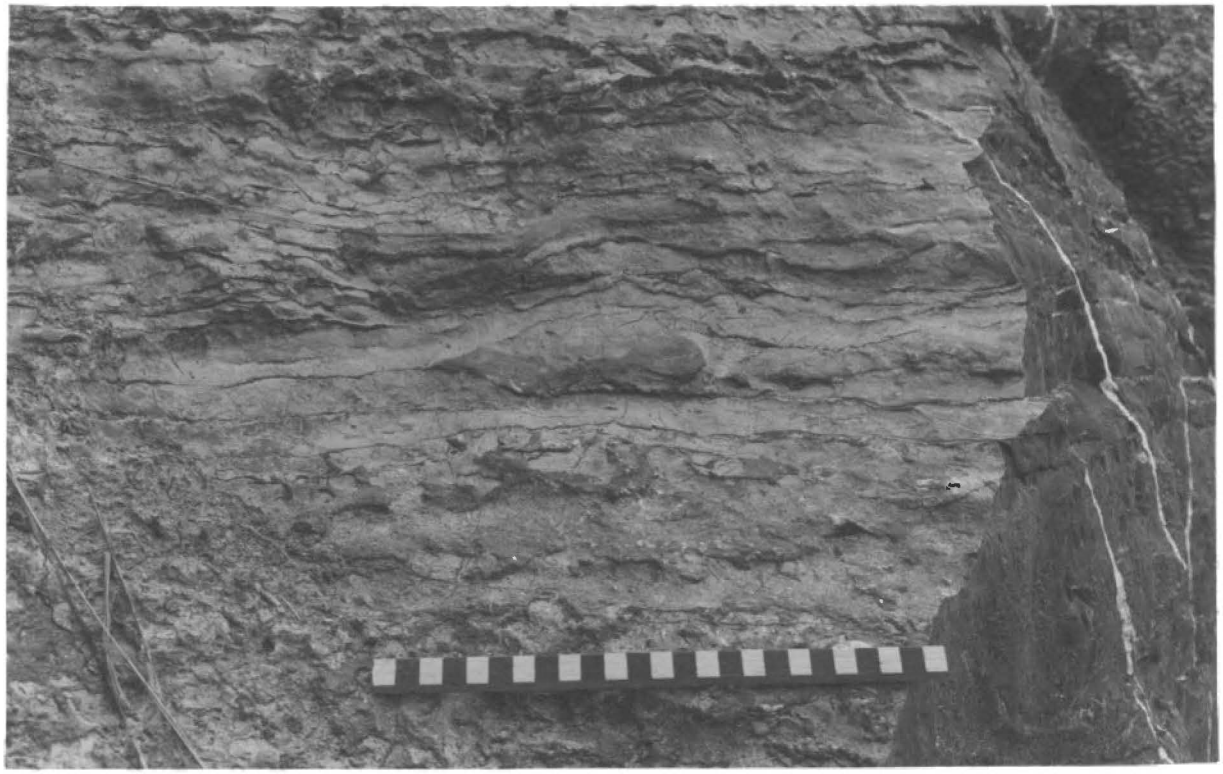

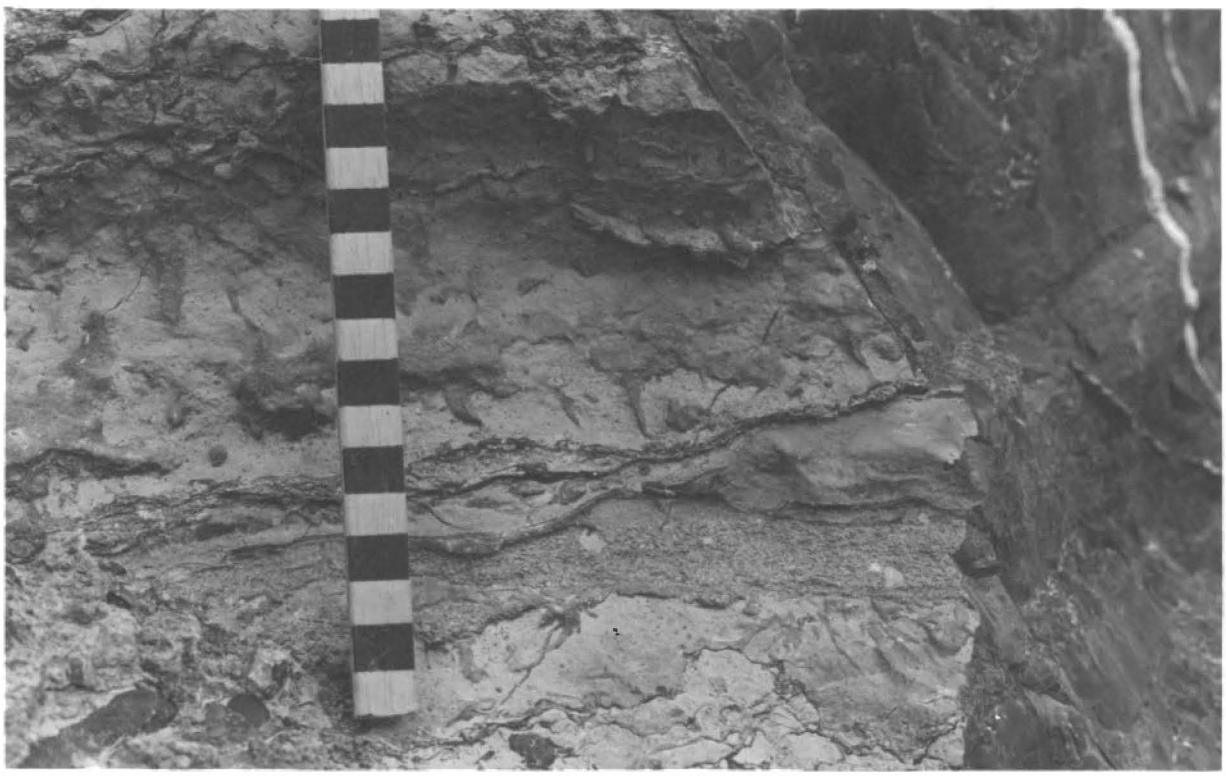

FIG. 3:33 Lithofacies VI. *Tetradium c.f. syringoporoides* corallum in Tetradium-rich interbed. (see text). Scale graduated in centimetres.

FIG. 3:34 Lithofacies VI. Microscopic appearance of sediment, showing abundant comminuted fossil material and mottled nature of sediment, indicating bioturbation. 48255 Mag. x 15

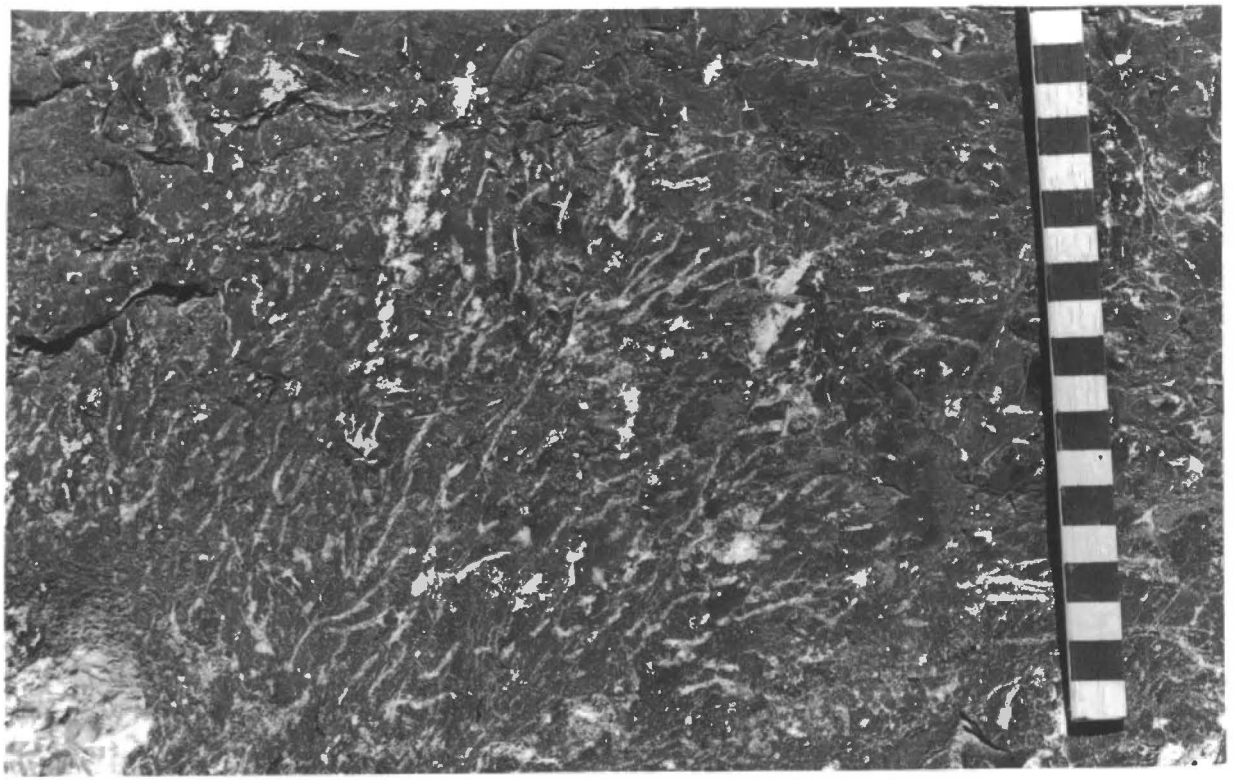

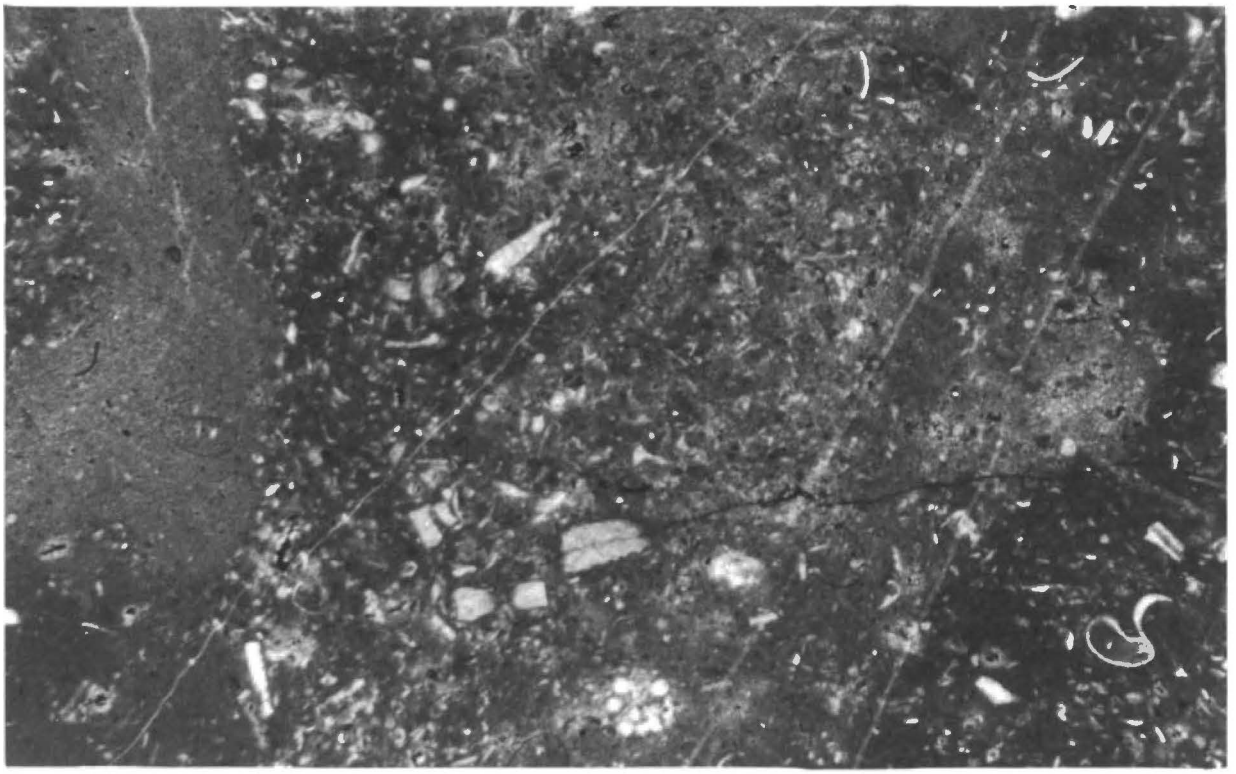

FIG. 3:35 Lithofacies VI. Elongate laths of spar in coarse spar matrix. Elongate laths probably represent evaporite pseudomorphs.
48256 Mag. x 21

FIG. 3:36 Lithofacies VI. Dolomite rhombs dispersed in spar matrix. (Spar grain boundaries hardly visible due to poor acetate peel).
48257 Mag. x 60

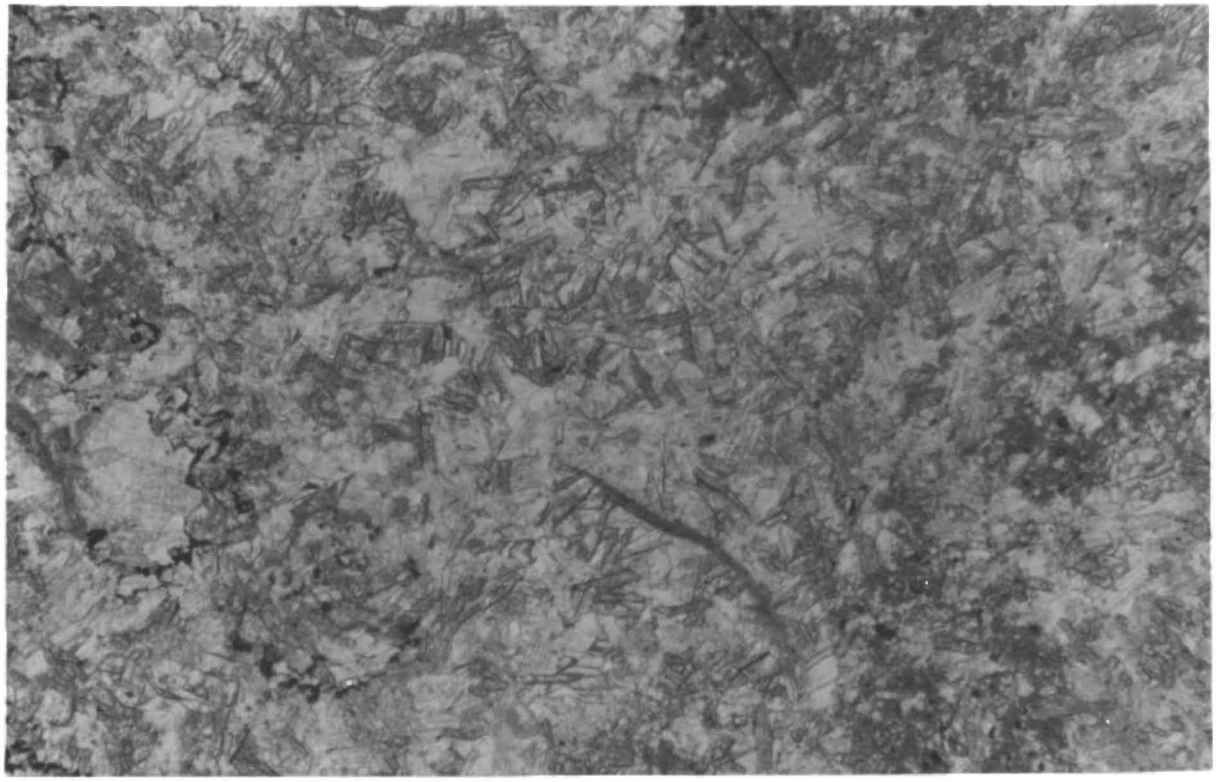

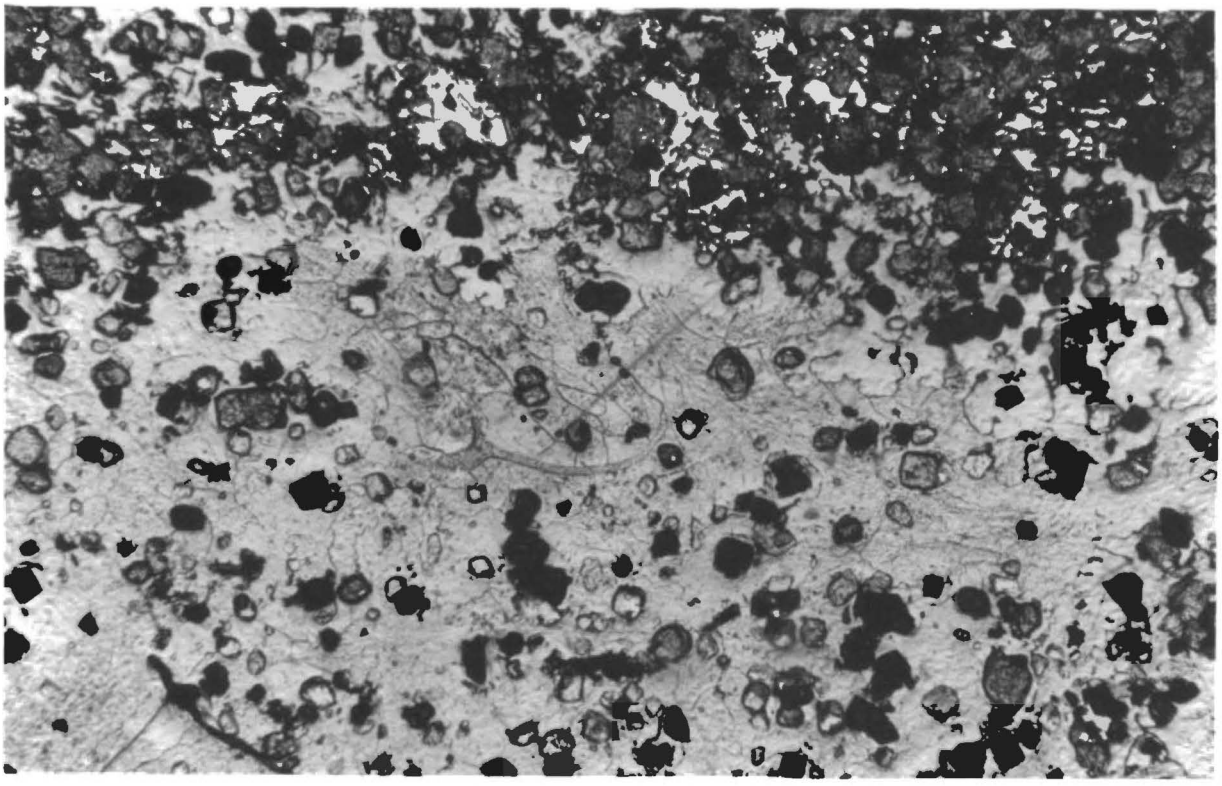

FIG. 3:37 Lithofacies VI. Intrasparite band, showing micrite intraclasts in partially washed matrix. (Sparry at bottom, micritic in centre of photo). A few ostracod shells are visible (e.g. at bottom centre).
48258 Mag. x 4.5

FIG. 3:38 Lithofacies VI. Probable collapse breccia, showing large irregular dolomite patch (lefthand two thirds of photo). *Solenopora* lump (bottom) and bryozoan (right) visible.
48261 Mag. x 5

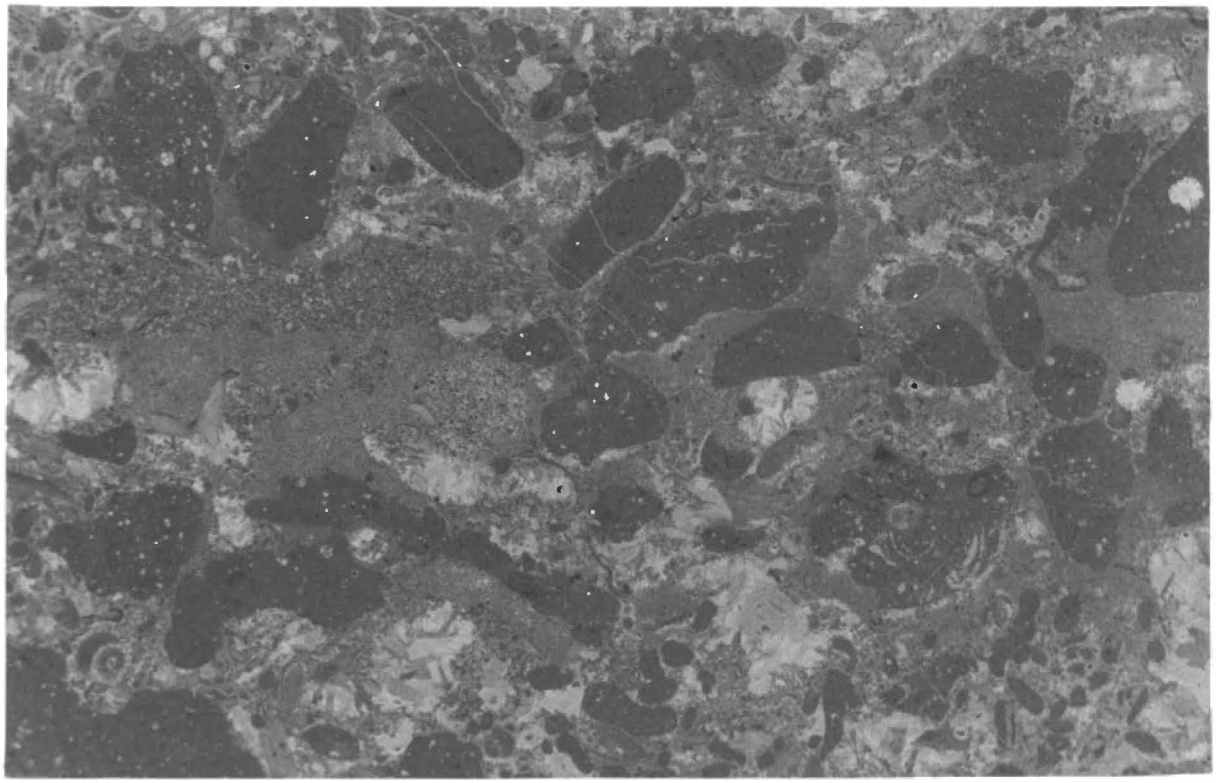

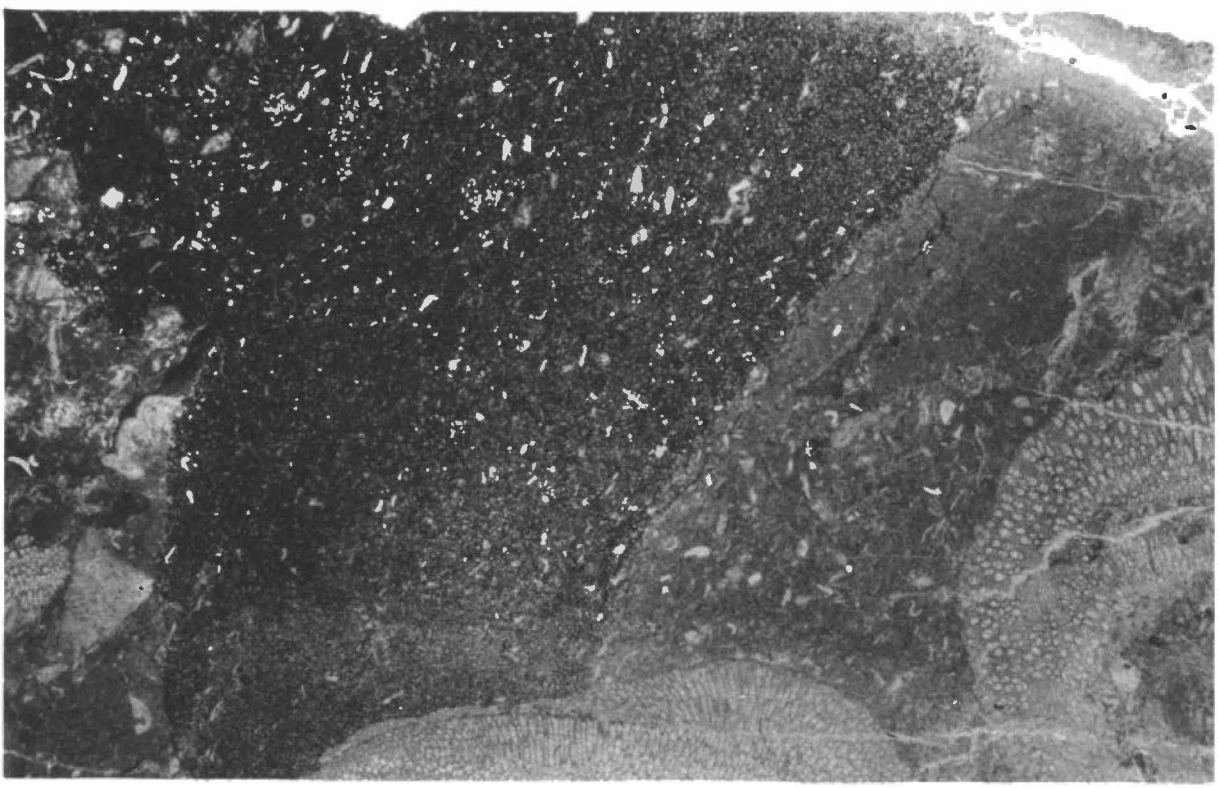

of a 0.6 metre thick horizon consisting of domal colonies of *Tetradium c.f. syringoporoides* (e.g. 98354) in growth position (see Fig. 3:33). The colonies average 0.2m by 0.5m wide at the base, and occur in the mottled micrite rich in comminuted fossil material which is typical of Lithofacies VI. *Tetradium* corallites comprise less than twenty per cent of the sediment, and little broken *Tetradium* material has accumulated in the bed.

The second anomalous interbed outcrops at 288 metres (at locations 1 and 4), and is characterised by an abundance of relatively undamaged macrofossils (notably *Solenopora*, corals such as *Bajgolia caespitosa*, *Pycnolithus*, other Heliolitids and Rugose corals, Bryozoans and aulacerid stromatoporoids). The sediment in which the fossils occur is the micrite rich in comminuted fossil material which is characteristic of Lithofacies VI. In thin section ostracods and probable evaporite pseudomorphs are visible in some specimens (e.g. 48260).

The other feature characteristic of this second interbed is the presence of large patches of dolomite which comprise between twenty per cent and eighty per cent of the sediment. These patches may be o.1m or more thick, are randomly oriented and have angular irregular shapes (see Fig. 3:38).

Interpretation

The occurrence of this lithofacies above or below birdseye limestone units, the rarity of unbroken fossils, the occurrence of sparse birdseyes, vertical burrows and mudcracking together with

the occurrence of evaporites indicate a dessicating upper intertidal environment. The horizontal dolomitic stringers, particularly those with bituminous interstitial material, may be related in part to the decay of algal mats. Alternatively, periods of dessication may have caused evaporation of pore-fluids from the upper layer of sediment and upward capillary movement of saline waters from below, with dolomitisation resulting from the consequent concentration of salts in the surface layer of sediment (Ginsburg 1972, p.65). Burrowing, sometimes vertical, must also account for some of the dolomitic patches.

The dominant fauna preserved in Lithofacies VI is the ostracod fauna. Ostracods inhabit a wide range of environments from marine through brackish to fresh water (Moore et al 1952, p. 526), and their occurrence as the major fauna in the upper intertidal lithofacies VI could simply result from them being washed up from more seaward environments. However, the fact that most other fossil material in the facies is comminuted raises the possibility that the ostracods may have been indigenous to the upper intertidal environment, perhaps living in restricted backflat lagoons which were too brackish for other organisms.

Bioturbation features and vertical burrows indicate the presence of other hardy organisms, perhaps including gastropods. The activities of these organisms are probably responsible for the comminution of fossil material washed up with lime muds from lower intertidal or subtidal regions. The grade of intrasparite bands

result from deposition of coarse material during intermittent storms or high tides.

The *Tetradium* interbed may represent an incipient *Tetradium*-boundstone wave baffle (Walker 1972) which began to develop as a result of a minor transgression but whose development was terminated (by a return to upper intertidal conditions).

The fossiliferous dolomitic interbed a little higher in the sequence also represents a minor transgression, on the grounds of the abundance of relatively undamaged macrofossil forms in it. The major problem with this interbed is explaining the presence of large irregular dolomitic patches. These probably result from regions of greater porosity in the original sediments. The most attractive theory to account for these patches is that a minor transgression, with increased wetting of the sediments, caused dissolution of evaporites in and beneath the biomicrite, leading to the development of a collapse breccia with patches of differing porosity as a result. Evaporite pseudomorphs occur within the biomicrite interbed (see 48261, 48260), although this fact is difficult to explain if the interbed was formed in a lower intertidal or subtidal environment as is implied by the biota. It is probable that the evaporites are derived from reworking of underlying sediments during the minor transgression, or from occasional drying of the sediment in a lower intertidal environment.

Lithofacies VII - Micrite and Biomicrite with thick dolomite layers

This lithofacies outcrops as a dark micrite containing thick irregular horizontally oriented dolomite patches and layers averaging 10-50mm thick (see Figs. 3:39, 3:40). Units of this lithofacies rest on abrupt scoured bases, and have graded intraclastic and bioclastic bands and laminated clacarenite layers (see Fig. 3:39). Macroscopic fossils are not abundant, but gastropods, cephalopods, stromatoporoids, *solenopora* lumps and other shell material does occur more frequently than in Lithofacies VI.

Microscopically, the sediment is typically a micrite, featureless apart from scattered dolomite rhombs, but with large irregular patches of hypidiomorphic to xenomorphic dolomite (e.g. 48262). Commonly the micrite varies to a biomicrite containing up to 25 per cent or more by volume of fossil fragments and angular spar patches interpreted as comminuted fossil material (e.g. 48263, 48264). Small calcite laths (about 0.3 x 0.1mm) which occur in some specimens (e.g. 48264) are interpreted as evaporite pseudomorphs.

The intrabiosparite layers (e.g. 48265) show fining upwards and comprise poorly sorted, rounded clasts of micrite ranging from 0.2 - 3.0mm diameter, together with broken shell fragments in a spar matrix (see Fig. 3:42).

The laminated calcarenites (e.g. 48266) are better sorted with no vertical gradation in grainsize. The comprise ostracod shells and fragments up to 1mm long (about 15 per cent by volume)

FIG. 3:39 Field appearance of Lithofacies VII. Note thick laminated calcarenite band near base and thin graded intrasparite higher up. Scale graduated in centimetres.

FIG. 3:40 Appearance of Lithofacies VII on a fresh vertical surface. Dolomite shows as lighter coloured areas of sediment. Scale graduated in centimetres.

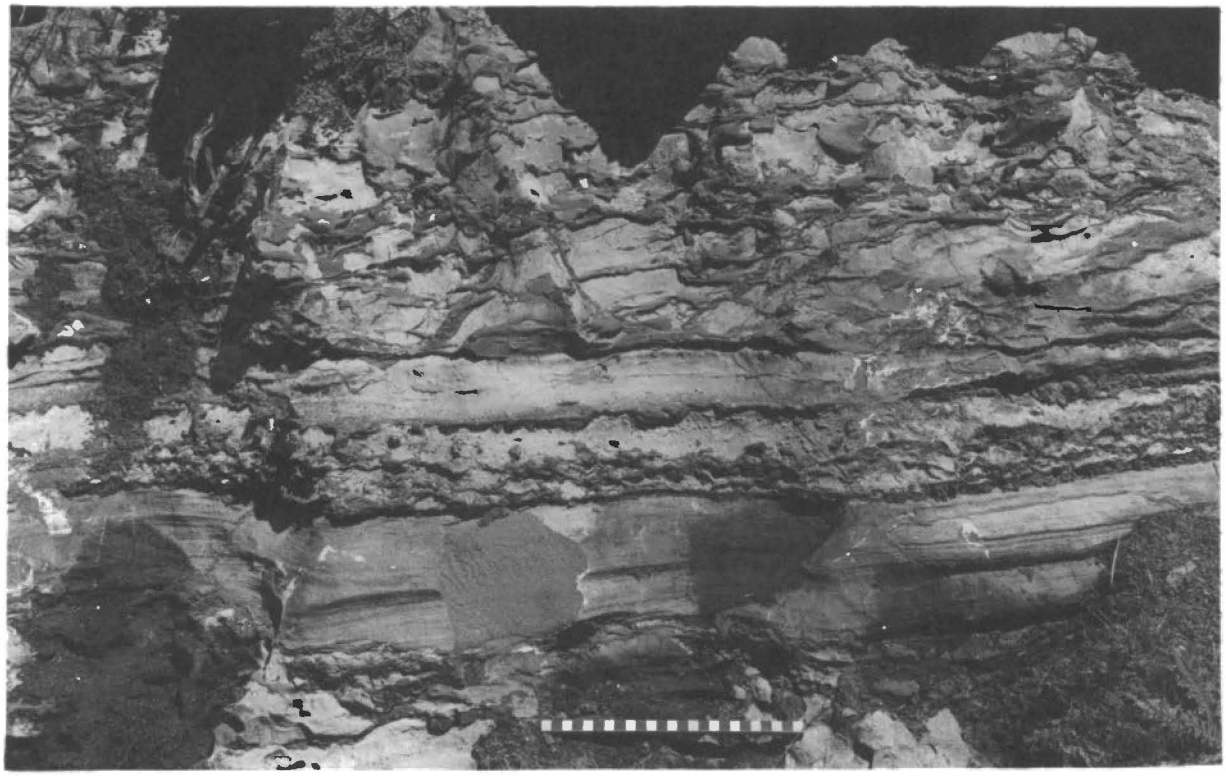

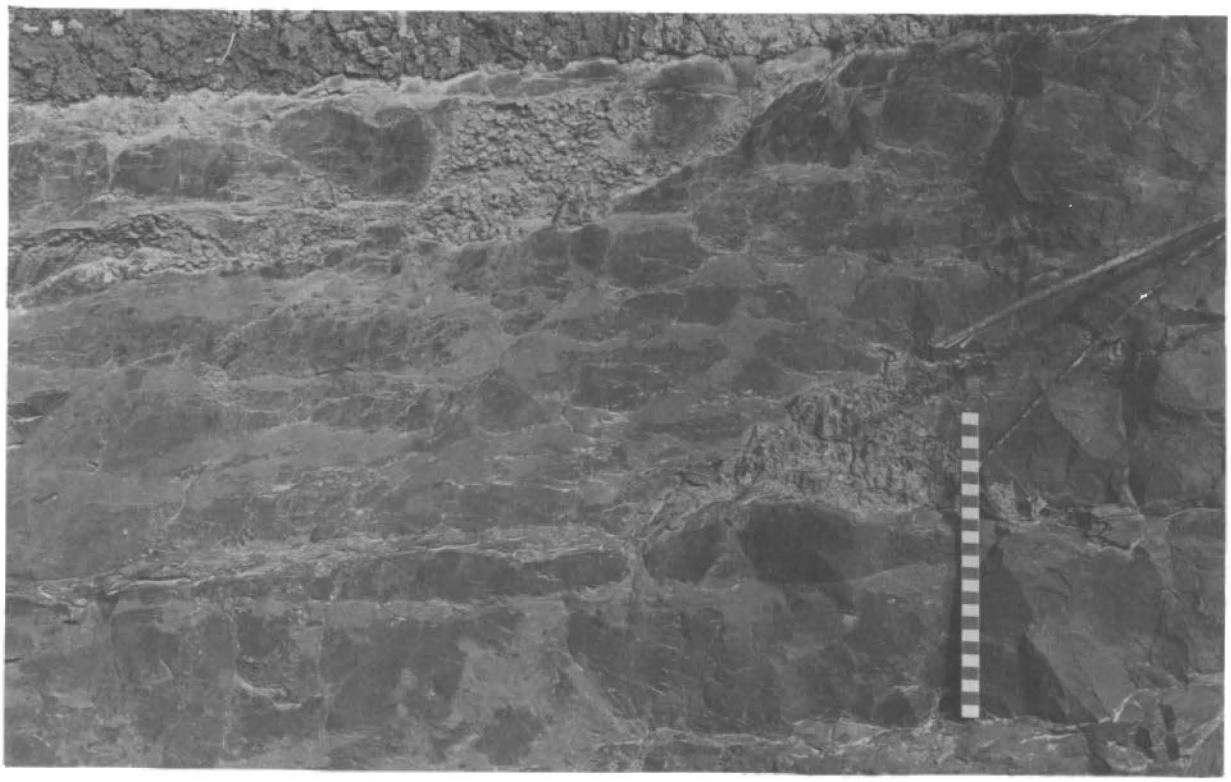

FIG. 3:41 Lithofacies VII. Detail of laminated calcarenite, showing intraclasts in spar matrix. Note abundant ostracod shells (mostly unbroken).
48266 Mag. x 12

FIG. 3:42 Lithofacies VII. Graded Intrasparite layer, overlying micrite and dolomitic layer.
48265 Mag. x 4

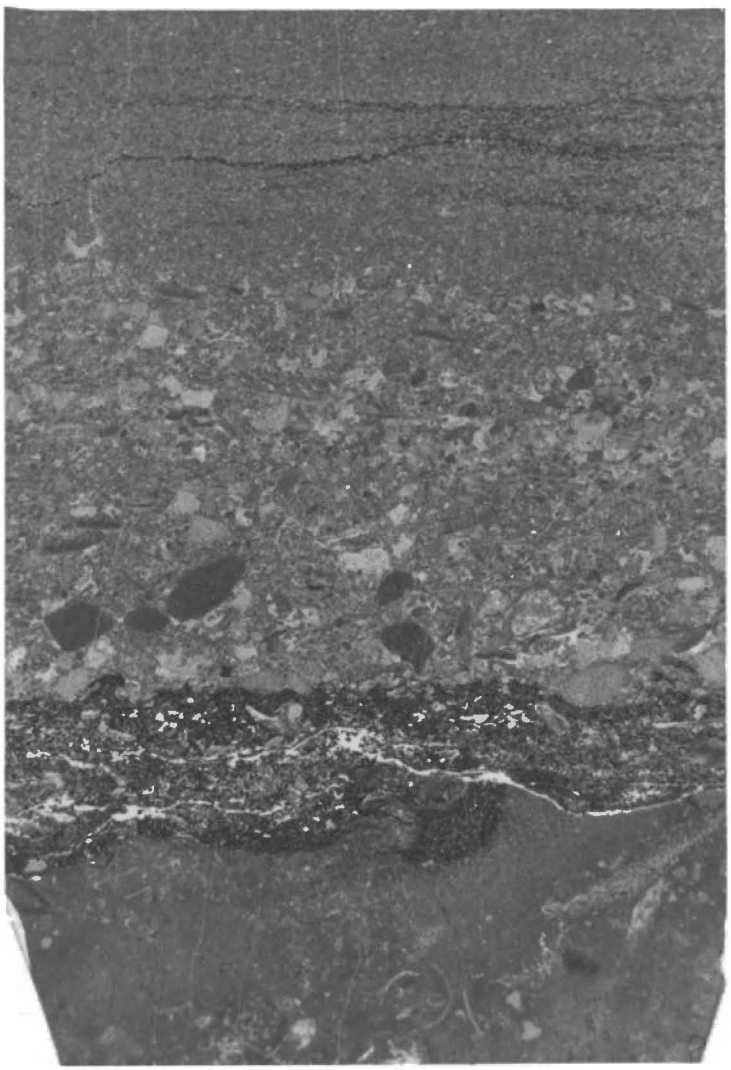

and rounded to sub-sangular micrite intraclasts averaging 0.3mm diameter (about 40 per cent by volume) in a spar matrix (see Fig. 3:41).

Interpretation

This lithofacies is similar to lithofacies VI, and commonly crops out immediately above or below units of the latter. In the field Lithofacies VII is differentiated from lithofacies VI in having thicker dolomite stringers and greater quantities of macroscopic fossil material.

Lithofacies VII is therefore regarded as having a similar origin to lithofacies VI in that it results from the accumulation of lime muds in an intertidal environment, with periodic drying out resulting in the formation of irregular horizontal dolomite patches. However, a lower intertidal environment is envisaged for lithofacies VII on the grounds of its lack of birdseyes, mudcracks and vertical burrows, its scarcity of evaporite pseudomorphs, and the greater abundance of fossil material washed up from subtidal regions. Graded intrabiosparite bands have been deposited by high tides and/or storms, while tidal channels have deposited intraclasts and ostracods presumably derived from upper intertidal regions.

Lithofacies VII can probably be regarded as a transitional facies between the upper intertidal lithofacies VI and the subtidal lithofacies IV.

Lithofacies VIII - Vertically burrowed Micrites

This lithofacies is set up to accommodate a single unit at 210 metres (at location 20) which shows transitions between a number of sediment types. It is overlain by birdseye limestones and underlain by upper intertidal-supratidal lithofacies II (subfacies 3 sediments).

The sediment is a burrowed micrite with horizontal stringers of dolomite and argillaceous material about 20mm thick. Some stringers (e.g. in 48268 contain angular ?quartz grains up to 0.1mm diameter. At the bottom of the unit the burrows have random orientations, but vertically oriented burrows are common through most of the unit (see Fig. 3:24).

Thin bands of mudcracked algal-laminations (lithofacies II, subfacies 1) are present and birdseyes (often tubular) are common, particularly in the upper part of the unit. Microscopical (e.g. 48267) the sediment is a dismicrite with thin dolomite stringers. The birdseyes are commonly replaced by dolomite and the large size of the tubular birdseyes (1-2mm diameter) suggests a vertical burrowing origin.

Fossils are rare and seem to consist mainly of gastropod fragments. One 0.15m thick band of Tetradium occurs in the unit.

Interpretation

This unit has all the earmarks of a supratidal upper intertidal environment - mudcracking, birdseyes, vertical burrows,

algal-laminations and low faunal diversity. In view of the increased frequency of these characteristics towards the top of the unit, it is probable that a transition from an upper intertidal environment at the base to a supratidal environment at the top is recorded. The horizontal dolomitic and argillaceous stringers may represent periods of terrigenous influx, or may be algal-laminations containing windblown terrigeneous material trapped by the algal mats.

Lithofacies IX - Intrasparite and Intrabiosparite

This lithofacies comprises beds 0.05-0.5m thick of a pale brown to grey sparry sediment. Grainsize is highly variable, ranging from thin micritic interbeds through to coarse sparites with grainsizes in excess of 2mm diameter. Intraclasts are commonly visible in the field, ranging up to rudite-grade clasts several centimetres long. The intrasparites are usually richly fossiliferous; near the top of Newlands Quarry they contain brachiopods, trilobites, gastropods, bryozoans, *Solenopora*, solitary corals and crinoid ossicles.

Units of Lithofacies IX occur interbedded between supra- or intertidal and subtidal micrite units. One unit of lithofacies IX near the top of Newlands Quarry grades up into a unit of lithofacies X.

Microscopically a typical specimen (48269) contains well rounded and sorted spar-supported micrite intraclasts in a well

FIG. 3:43 Field appearance of Lithofacies IX on a fresh surface. Scale graduated in centimetres.

FIG. 3:44 Lithofacies IX. Fine-grained intrasparite. Note well sorted and spar-supported nature of most of the intraclasts. 48269 Mag. x 20

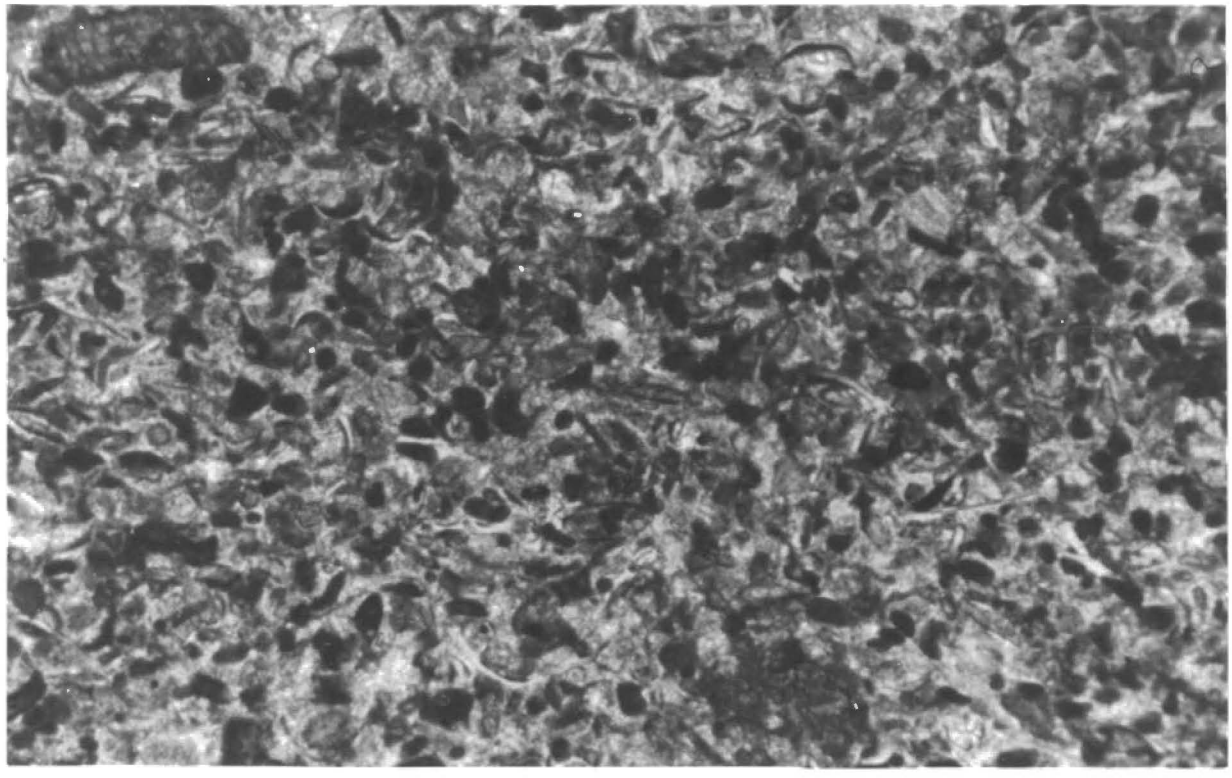

FIG. 3:45 Lithofacies IX. Problematical intrasparite. Fine-grained mass at right is part of a rudite-grade intraclast of microspar sediment.
48274 Mag. x 5

FIG. 3:46 Lithofacies IX. Coarse-grained Intrabiosparite, showing poorly sorted clasts and fossil fragments, including *Stictopora* (upper right).
48270 Mag. x 5

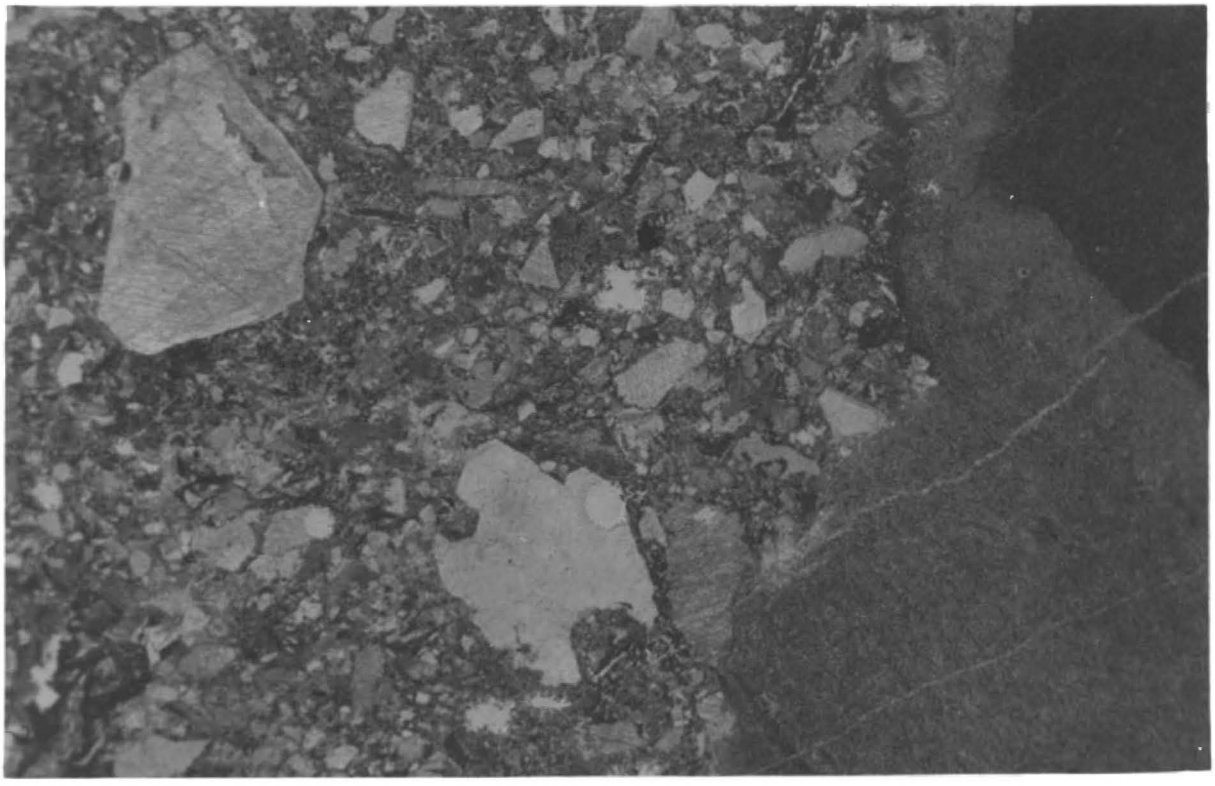

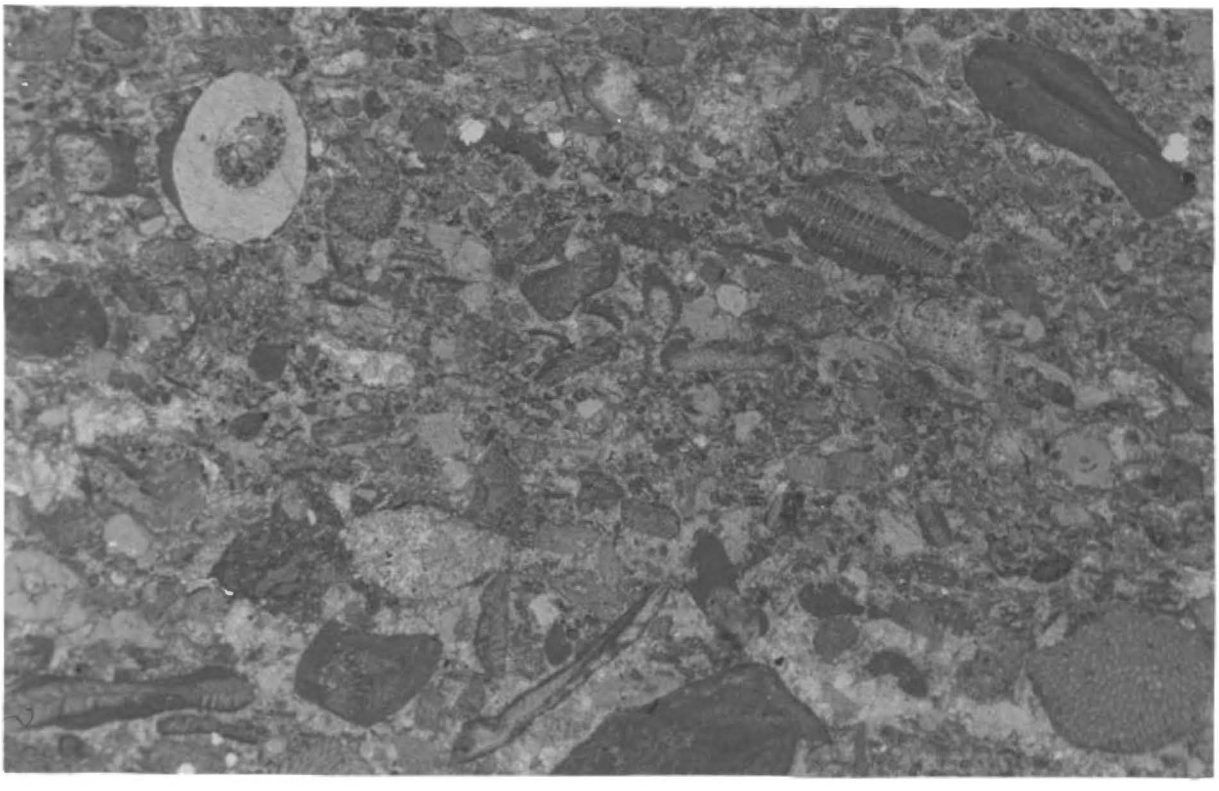

washed matrix (see Fig. 3:44). The intraclasts are usually in the range of from 0.1mm to 0.3mm diameter, and some may be of faecal origin. About fifteen per cent of the sediment consists of broken bryozoans and shell fragments averaging 0.8mm long, and ooliths occur rarely.

In other specimens (e.g. 48270 - See Fig. 3:46) the intraclasts are larger (up to 8mm diameter) and are sub-rounded but poorly sorted. The intraclasts include micrite clasts, spar grains (often with syntaxial over-growth rims - eg, in 48271) and spar grains containing probable evaporite pseudomorphs (e.g. in 48270).

In exceptional cases (e.g. 48272) the sediments are biosparites comprising bryozoan and crinoid fragments (about 25 per cent of sediment), together with a few spar intraclasts with syntaxial overgrowths, supported in a coarse-grained spar matrix.

Interpretation

The abundance of fossils, the absence of dolomite and burrowing, the well-washed sparry matrix and the occasional presence of ooliths indicate an energetic subtidal or lower intertidal environment. The sediment was probably deposited in an environment where wave base impinged on the substrate so that currents were continually winnowing out mud particles, and rounding and sorting allochems. The ?evaporite-bearing intraclasts were derived from shoreward regions.

Sediments of problematical origin occur in beds transitional from Lithofacies IX to Lithofacies X near the top of Newlands Quarry. These sediments are described here in view of their possible interest. Specimen 48275 contains a poorly-washed brachiopod-rich biosparite layer in-between dolomitic biomicrites, and probably represents a lower intertidal deposit. Specimen 48274 is an intrasparite containing a rudite-grade (30mm diameter) angular clast of a microspar-grade sediment (see Fig. 3:45). Both the clast and the spar matrix have dark material (bituminous?) filling interstitial spaces. Specimen 48273 is an apparently in situ specimen of the microspar sediment (grading into spar) of which the large clast in 48274 is composed. The spar/microspar occurs in a 10-20mm thick layer and is very clean, containing neither fossils nor intraclasts and micrite patches. Because of the absence of any micrite the microspar is regarded as being os syn-depositional origin. Specimen 48273 also has irregular horizontal bands of idiotopic to hypidiotopic dolomite rhombs set in a dark ?bituminous matrix. An irregular layer at the bottom of 48273 consists of angular spar fragments ranging from 3mm to 0.1mm in diameter, set in a dark ?bituminous matrix.

Lithofacies X - Biomicrite with Biosparite and Silt Layers

One unit of this lithology occurs near the top of Newlands Quarry, interbedded between two lithofacies IX units. Dislocated blocks of this lithofacies X bed also occur as rotated blocks in the fault zone at location 11, and in a downthrown block at location 8 (see Ch. 2).

This lithology consists of micrite, biomicrite and sparite beds averaging 50-100mm thick, separated by silty and bituminous laminae 10-30mm thick (see Figs. 3:47, 3:48). The silt layers have been extensively slickenslided by the thrust fault which they outcrop in and adjacent to (see Ch. 2). A typical silt band (in 48276) has a distinct cleavage (Tabberabberan?) at an angle of about 30 degrees to the bedding, and consists of angular quartz grains averaging 0.08mm diameter (60 per cent of sediment) in a fine grained argillaceous or bituminous groundmass. Dolomite rhombs about 0.1mm diameter rarely occur dispersed through bands of argillaceous material (e.g. 48278).

Some thick micrite beds (up to 0.5 metres thick) have grey irregular horizontal to randomly oriented burrows. The micrite is rich in pyrite, both in the form of microscopic disseminated cubes (revealed by dissolution of the limestone in acid) and as nodules up to 30mm diameter. The pyrite is indicative of reducing conditions at or just below the depositional interface.

Microscopically, a typical micrite bed (e.g. 48276) consists of micrite with sparse macrofossils (trilobite fragments, etc.) and with minute angular spar fragments (probably comminuted fossil material) making up about fifteen per cent of the sediment. In 48283, the micrite contains rounded or subrounded clasts, averaging 0.7mm diameter, of a dark ?bituminous and silty material, probably derived from reworking of silty laminae.

Specimen 48277 is a typical graded biomicrite band between two laminae of silty material. Macrofossils are confined to the lower portion of the band, and the micrite again contains sparry fragments representing comminuted fossil material. The upper part of the band has a mottled appearance indicating bioturbation.

Some biomicrites are more densely packed; 48280 contains over fifty per cent macrofossil material, much of which is relatively unbroken, while 48282 contains at least forty per cent comminuted fossil fragments.

Sparry interbeds up to 100mm thick occur commonly within the lithofacies X unit, and represent both brachiopod rich biosparite bands, and laminated calcarenites (both types of interbed shown in Fig. 3:48). These interbeds commonly rest on undulating scoured interfaces.

Microscopically, the biosparite bands consist of abundant shelly fragments in a rather poorly washed spar matrix (e.g. 48279- see Fig. 3:52) or a matrix of spar with diffuse micrite lumps about 0.1 - 0.2mm diameter which are interpreted as probable faecal pellets (e.g. 48278). Commonly, the biosparite bands are interbedded between silt layers, and in 48281 (see Fig. 3:51) a bioclastic band 10mm thick consists of shell fragments in a silt matrix.

Fossils commonly occur in the micrite layers too, although usually in concentrated bands showing grading and resting on

FIG. 3:47 Field appearance of Lithofacies X (at location 12 - now quarried away). Staff graduated in 0.1 metre units.

FIG. 3:48 Detail of Lithofacies X field appearance. Note thin silt bands (dark), biosparite bands (upper half of photo) and laminated calcarenite band. Note vertical stylolite 9 cm from right end of scale; such stylolites are noted in several places on Marble Hill, and presumably result from lateral compression (Tabberabberan tectonism?). Scale graduated in centimetres.

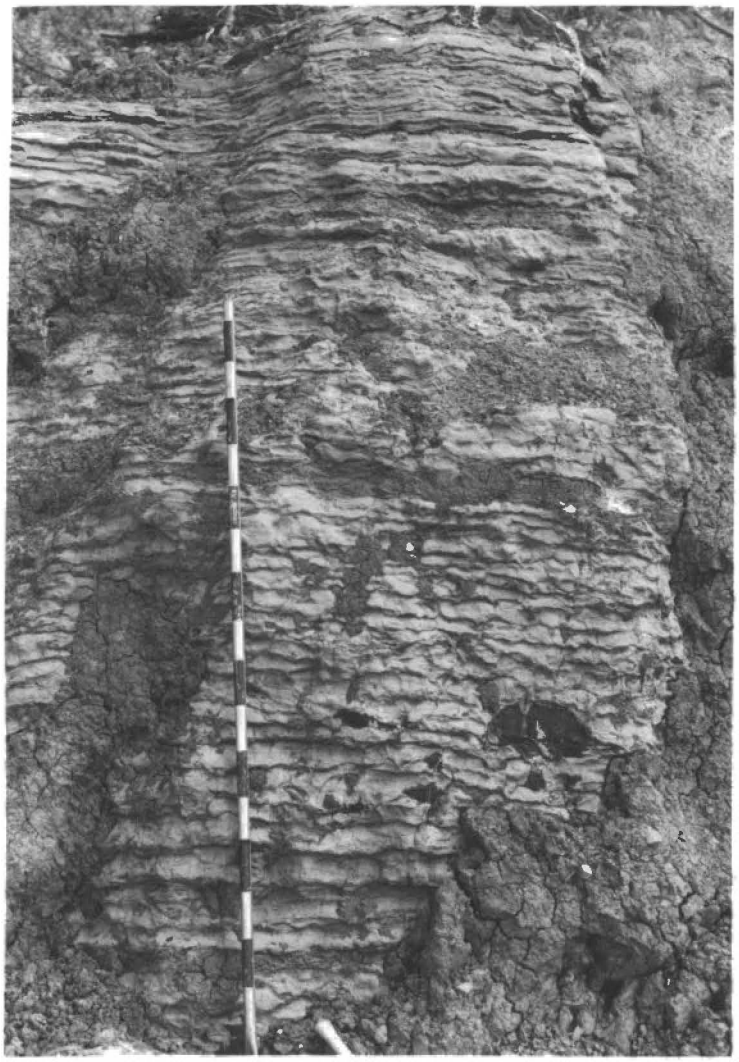

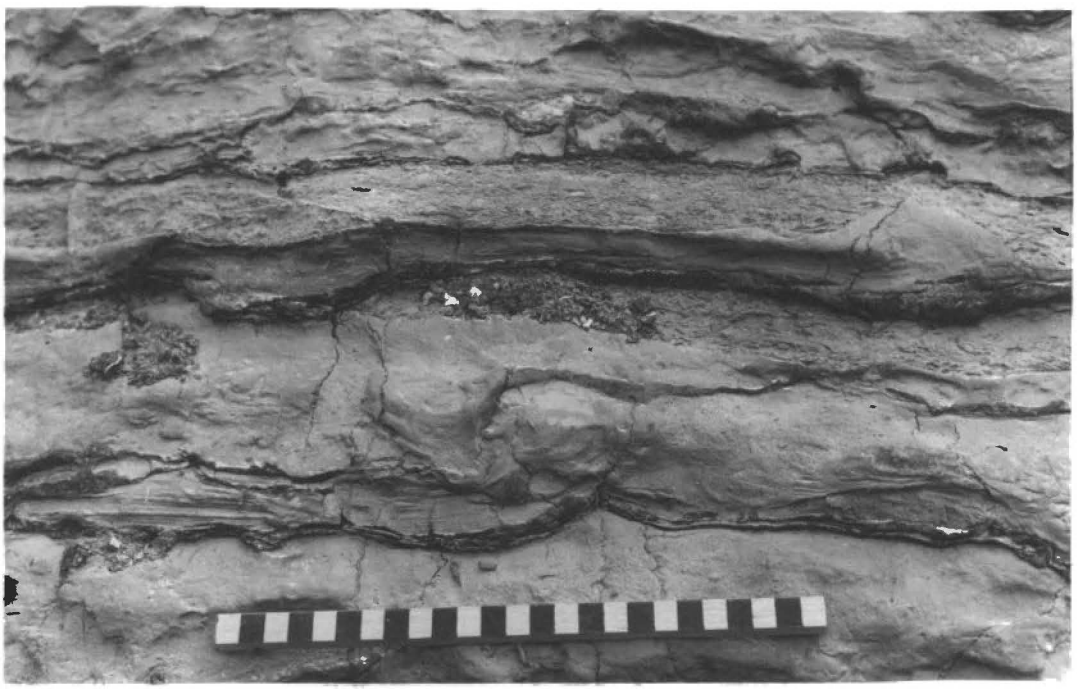

FIG. 3:49 Lithofacies X. Problematical shelly fossil. Possibly fossil is a gastropod, with opening at lower right representing slit generating a selenizone.
98321 Mag. x 4.5

FIG. 3:50 Lithofacies X. Oblique section of problematical tubular fossil. May be a sponge-delicate surficial appearance reminisent of spicules.
98322 Mag. x 7

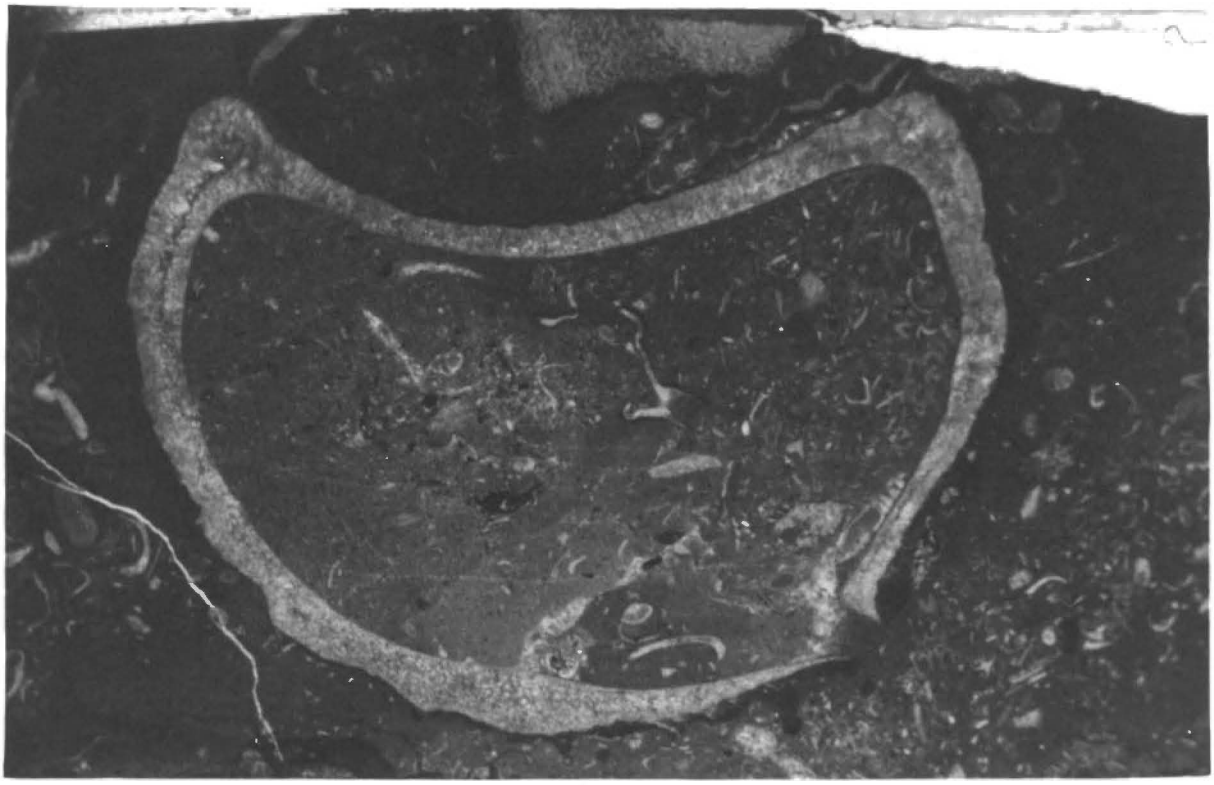

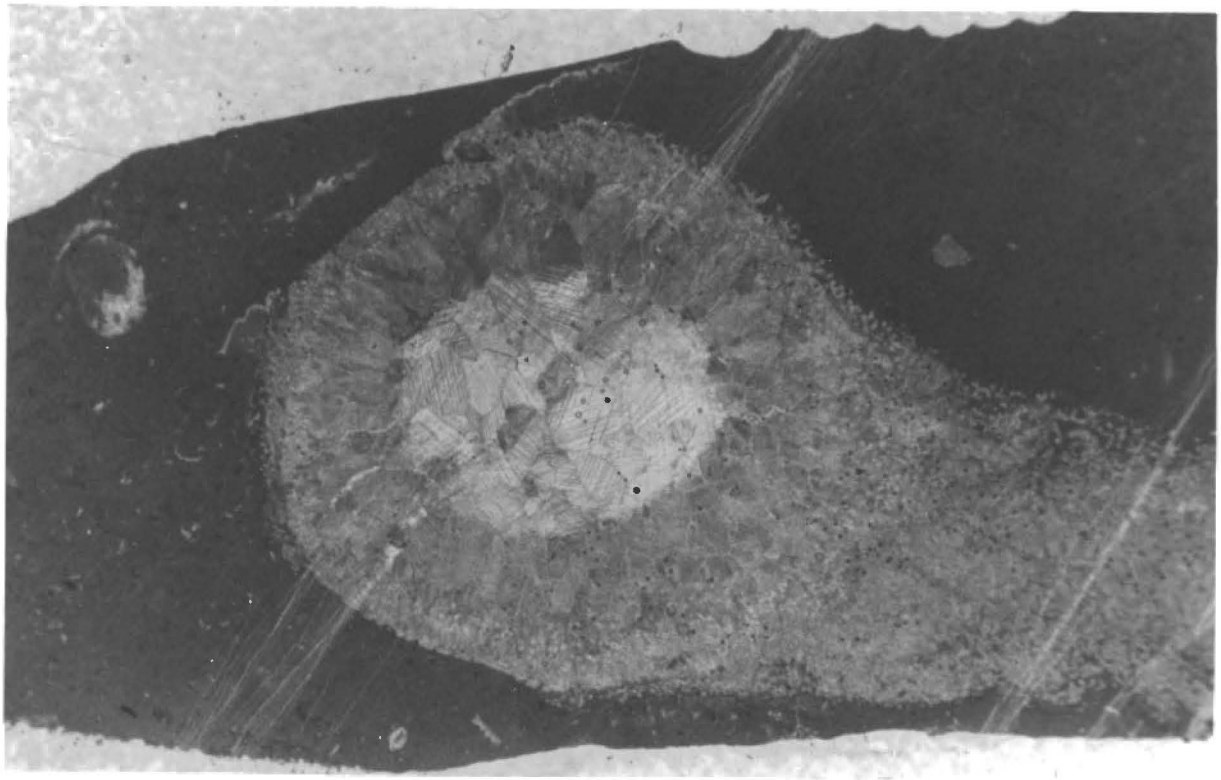

FIG. 3:51 Lithofacies X. Silt band (dark) overlain by micrite with a vertical stylolite (see also Fig. 3:48). Silt band is rich in dolomite and probable fossil fragments which are silicified and hence not properly reproduced by acetate peel.
48281 Mag. x 4.5

FIG. 3:52 Lithofacies X. Bioclastic band overlying silty band. Bioclastic band is fossil fragments in a poorly washed spar matrix (patches of unwashed micrite visible).
48279 Mag. x 4.5

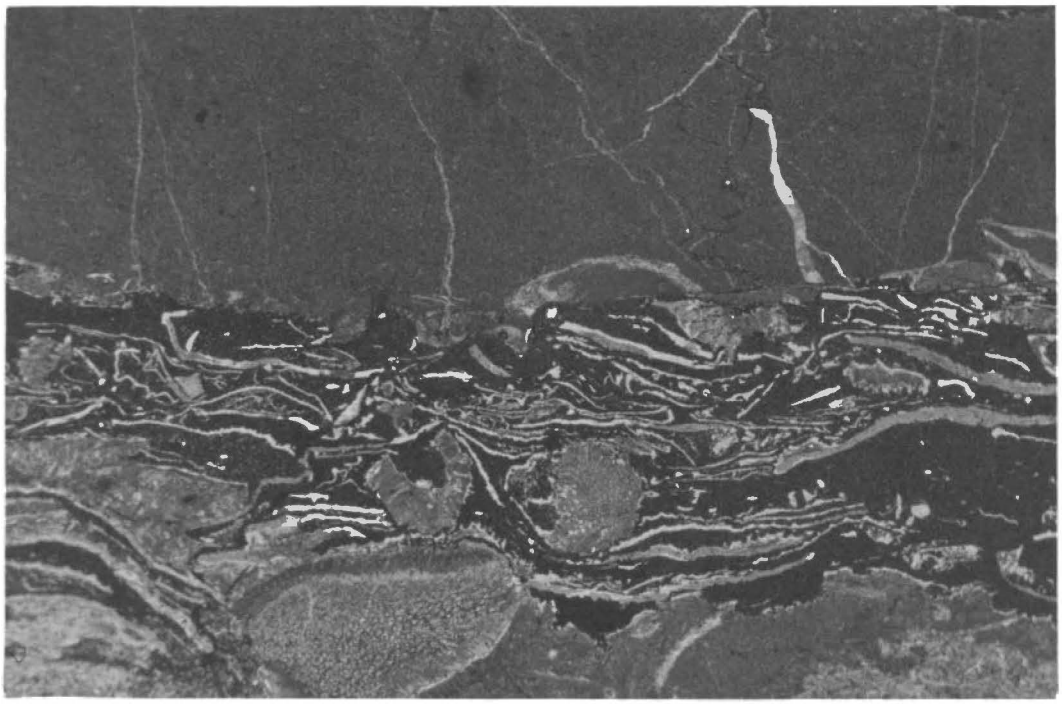

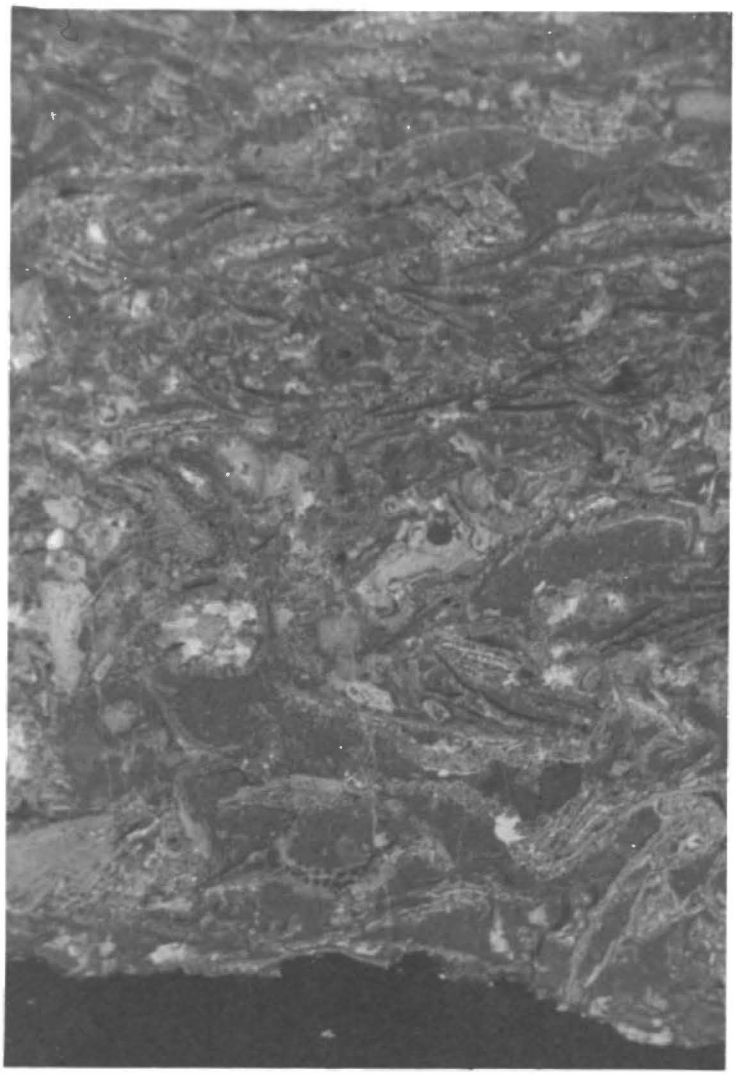

scoured bases. Fossils present include bryzoans, problematic branching tubular structures (sponges? - see Fig. 3:50), *Solenopora*, *Bajgolia c.f. furcata*, *Tetradium*, crinoid and trilobite fragments, and other shelly fragments including the problematic structure in 98321 (see Fig. 3:49).

Interpretation

The thin bedding and presence of graded biomicrite bands as well as biosparite and laminated calcarenite bands indicate fluctuating tidal and channel activity, which implies an intertidal environment. The abundance of biota and apparent absence of dissication features imply a lower intertidal environment.

The thin silt laminae represent short bursts of terrigenous input. That these bursts are related to changing conditions in the source area, rather than to a changing local sedimentary environment, is implied by the rarity of silt beds elsewhere in the Ida Bay limestone sequence.

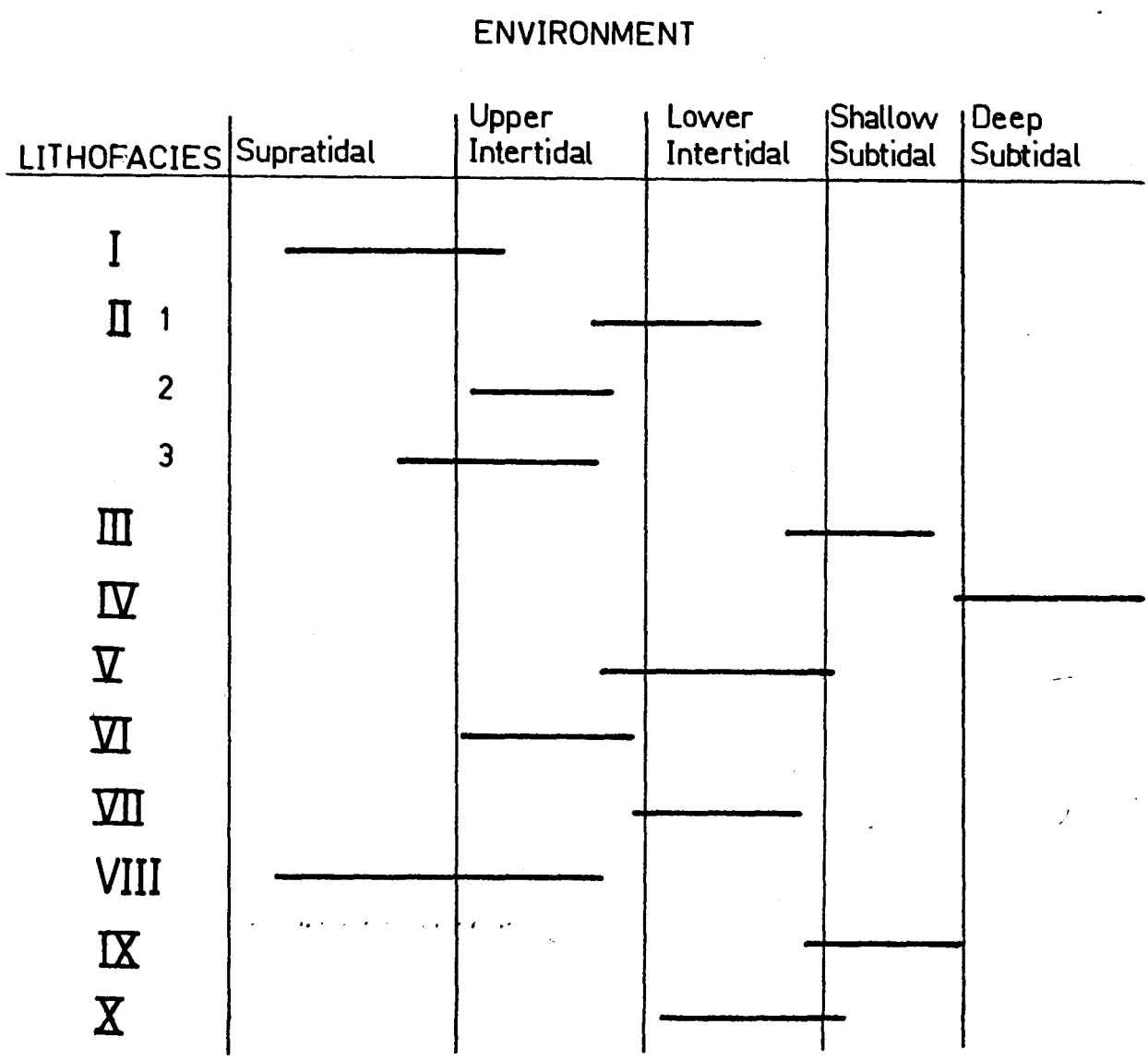

FIG. 3:53 Environmental Distribution of Lithofacies, in terms of onshore-offshore position.

CHAPTER FOUR

STRATIGRAPHY AND SEDIMENTOLOGICAL SYNTHESIS

4.1 Age and Correlation of Ida Bay Sediments

The limestones at Ida Bay have long been known to be correlates of the Gordon Limestone (Gordon Sub-group-Corbett and Banks 1974) which outcrops elsewhere in Tasmania, and is of Middle-Late Ordovician age. Correlation with the Gordon Limestone is made on the grounds of sedimentological and biotic similarity, as well as similar stratigraphic position.

(I) Clastic Sediments

Clastic sediments occur beneath the Gordon Sub-group in other parts of Tasmania, in a similar stratigraphic position to the quartzites beneath the limestones at Ida Bay. However, whilst the earliest known carbonate sediments in the Ida Bay area are probably upper Chazyan in age (see below), carbonate sedimentation is known to have begun as early as Late Canadian times (Crobett and Banks 1974) in the Florentine Valley, 90 kilometers north of Ida Bay. The quartzites at Ida Bay cannot be accurately dated, although the Helicotomide gastropods found in them are probably Early Ordovician (Moore 1960, p. 189). Since the nature of the transition from the quartzite at Ida Bay to the overlying limestone is unknown, several interpretations of the Early-Middle Ordovician geology of the Ida Bay Region are possible.

a) Clastic sedimentation continued in the Ida Bay Area after it had ceased in the Florentine Valley area.

b) Clastic sedimentation ceased at about the same time in the Ida Bay area as in the Florentine Valley area, but a period of non-deposition and/or erosion intervened before carbonate sediments began being preserved.

c) Unknown structural complications have hidden or destroyed a large portion of the Early-Middle Ordovician stratigraphic record.

(II) Carbonate Sediments

Figure 4:2 is a stratigraphic range chart showing the range, in the Ida Bay limestones, of most of the fossils noted during the present project. This information, combined with previous work on the Ida Bay area (see Chapter 1), can be used to draw some conclusions about the age of the limestones and their stratigraphic relationships to the Gordon Limestone elsewhere in Tasmania.

The oldest limestone beds examined on Marble Hill are those at the bottom of Entrance Cave. (Beds containing *Tetradium c.f. syringoporoides* on the old Lune Tram at about DM889878 have previously been thought to be of a similar age to the Entrance Cave beds (Banks 1957, 1962), but on structural considerations the present writer feels they are probably somewhat younger, and approximately equivalent to the beds at the bottom of location 20 (200 metres Fig. 4:1)).

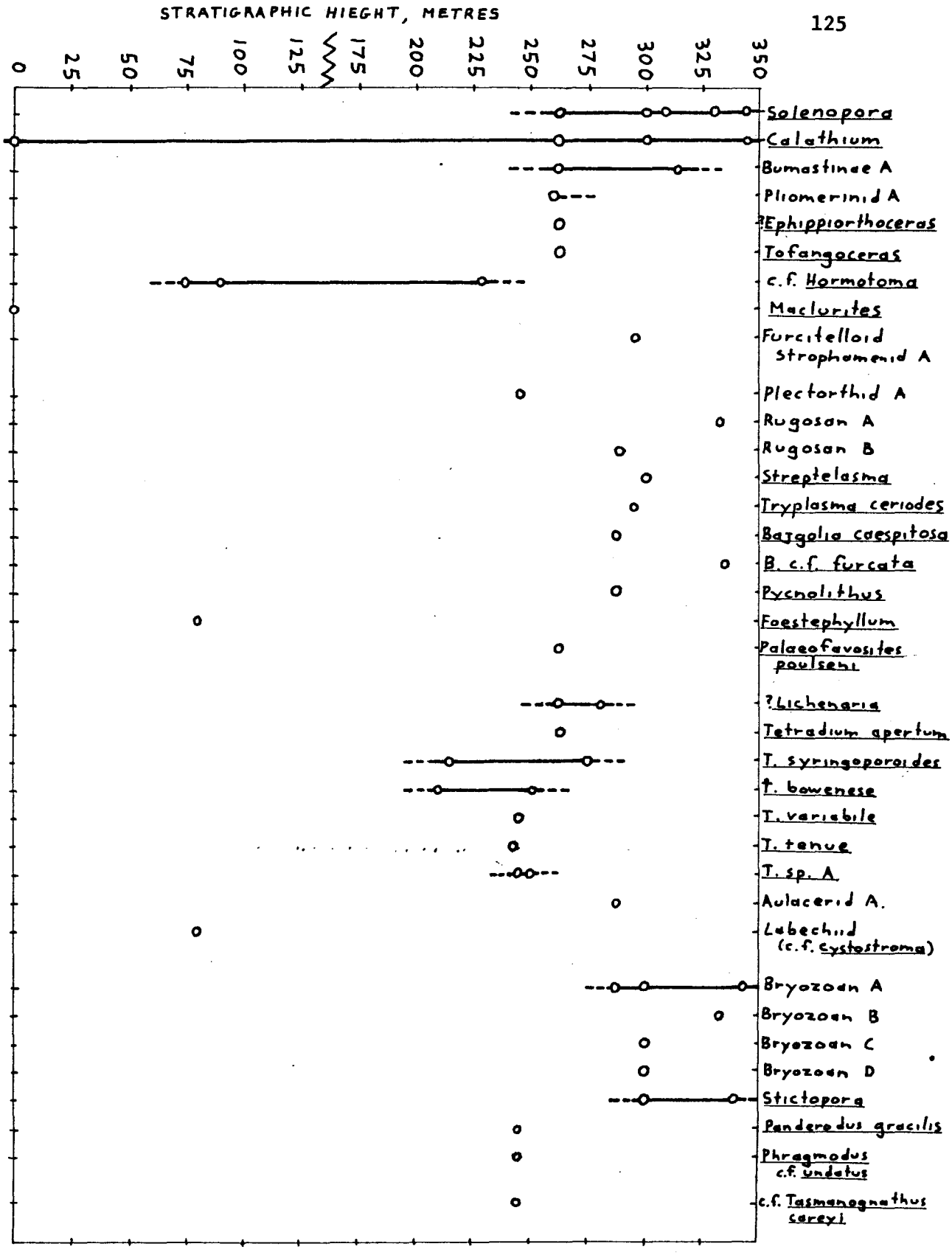

FIG. 4:2 Stratigraphic range chart for fossils identified in limestones on Marble Hill during present study. Stratigraphic heights correspond to heights on Fig. 4:1. Circles represent known occurrences of fossil, lines represent interpolated range of fossil.

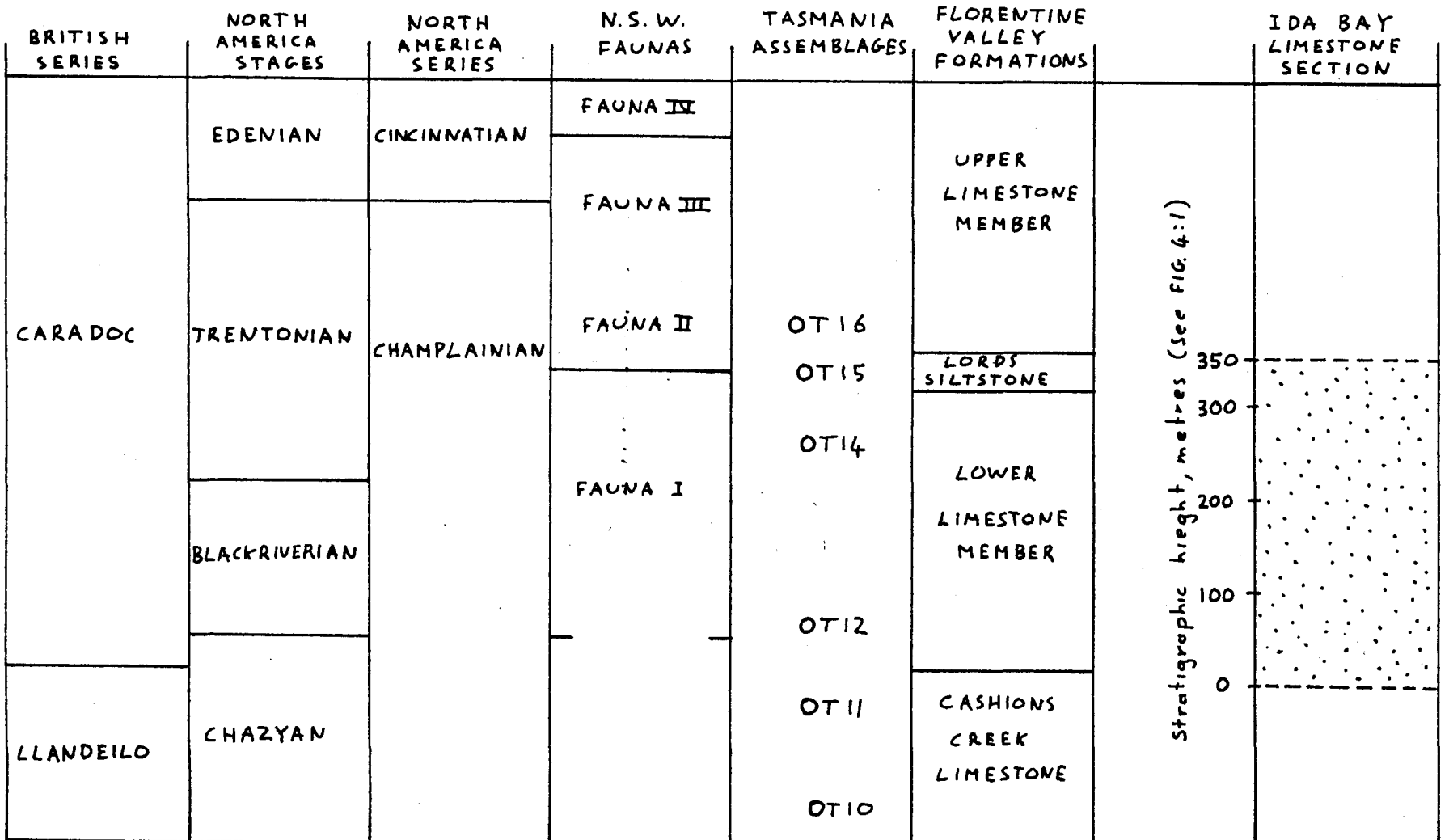

FIG. 4:3 Correlation chart showing probable chrono-, bio- and lithostratigraphic correlation of limestones at Ida Bay. Correlations shown for Ida Bay are tentative only. Chart is not drawn to any uniform scale, but is intended to convey possible relationships only.

Maclurites is found at the bottom of Entrance Cave, and conodonts including *Panderodus serpaglii* and *Belodina alabamensis* have previously been obtained from the same location (Burrett 1978). Both *Maclurites* and *B. alabamensis* are characteristic of the Chazyan assemblage OT10 of Banks and Burrett (*in press*). Teichert and Glenister (1953) described *Mysterioceras australe* and *Trocholitoceras idaense* from a slightly higher horizon in Entrance Cave. The occurrence of *Trocholitoceras* seemed to indicate an upper Canadian age for these beds, but the identification of *Trocholitoceras* now seems to have been in error (B. Stait, *pers. comm.*, 1979).

The beds in Entrance Cave are probably Late Chazyan in age, because of their relatively small stratigraphic distance below probable Blackriverian beds.

The next higher beds, those in Blaney's Quarry, contain *Foerstephyllum*, rare endocerid cephalopods (*Hecatoceras longinguum* has been described from this quarry by Teichert and Glenister 1953), and a stromatoporoid similar to *Cystostroma*, which is characteristic of the Blackriverian assemblage OT12 of Banks and Burrett (*in press*).

The section measured at location 20, below Newlands Quarry, appears to comprise beds equivalent to part of the Lower Limestone Member of the Florentine Valley (Corbett and Banks, 1974). Burrett (1978) found *Plectodina aculeata, Belodina compressa, Panderodus gracilis* and *Phragmodus undatus* 10 metres above the base of the location 20 section, and a similar fauna also including *Bryantodina abrupta* near the top of the location 20 section. In the present

study, *P.gracilus*, *P.undatus*, c.f.?*Tasmanognathus careyi* and *"Plectodina"* or *"Aphelognathus" florentina* have been found at 243 metres (see Fig. 4:1). Plectorthid brachiopods have also been recovered from the latter position, and are similar to brachiopods spanning the middle half of the Lower Limestone Member (J. Laurie, *pers. comm.*, 1979). The location 20 section is also characterised by an abundance of *Tetradium*, comprising at least six species (see Fig. 4:2).

These faunas have a number of elements in common with assemblage OT14 of Banks and Burrett (*in press*) although *Foerstephyllum* is not present. *Tetradium bowanense* is common, as it is in the Lower Limestone Member (Corbett and Banks 1974). *Tetradium variabile* is present, and *T. apertum* occurs in beds immediately above (at the bottom of Newlands Quarry). These species occur in Fauna I of Webby (1969) which is Blackriverian or Trentonian in age (Webby and Semeniuk, 1971). In view of the faunas present, the beds at location 20 are probably Blackriverian/Early Trentonian in age.

The highest beds exposed on Marble Hill are those in Newlands Quarry, immediately above the location 20 section. Subtidal beds on the floor of Newlands Quarry contain *Tetradium apertum*, *Palaeofavosites poulseni*, a few specimens of *Calathium*, cephalopods, and fragments of ?*Bumastoides*. Higher up in Newlands Quarry, at about 295 metres (see Fig. 4:1), Furcitelloid Strophomenids are found which are similar to brachiopods occurring thirty metres below the Trentonian Lords Siltstone of the Florentine Valley (J. Laurie,

pers. comm., 1979). *Calathium*, which is characteristic of the Lower Limestone Member (under the name *Ischadites* - Corbett and Banks 1974) is particularly common in a unit at 300 metres, and also occurs in the topmost beds in the quarry.

It is therefore probable that most if not all of the beds in Newlands quarry are Trentonian in age, and equivalent to beds in the upper part of the Lower Limestone Member. A Pliomerinid and *Stictopora* occur in the upper beds in Newlands Quarry, which may therefore correlate with the Lords Siltstone of the Florentine Valley. The Lords Siltstone is characterised by a *Pliomerina* - Stictoporid assemblage (OT15 of Banks and Burrett *in press*).

On the grounds of faunas, and relative thicknesses, it appears likely that few if any at all of the beds at the top of Newlands Quarry are equivalent to the Upper Limestone Member of the Florentine Valley.

Although a Cincinnatian age has previously been suggested for beds at the top of Newlands Quarry (Hill 1955, Banks 1957), the evidence no longer seems favourable to such a view, and the oldest beds on Marble Hill are probably Trentonian in age. *Bajgolia ida* which occurs on Marble Hill is considered by Corbett and Banks (1974) to occur only in the Upper Limestone Member, which throws doubt on the foregoing speculations. However, the stratigraphic position of *B.ida* on Marble Hill is unknown, and furthermore no specimens of *Palaeophyllum*, which is common in the Upper Limestone Member

(*ibid.*) are known on Marble Hill. It is suggested herein that *B. ida* may in fact occur within the Lower Limestone Member equivalent at Ida Bay.

Other corals have been reported from the Limestones on Marble Hill, including *Heliolites*, *Favosites* (Banks, 1957), *Lichenaria ramosa*, *Tetradium ?compactum*, *Billingsaria banksi*, *Coccoseris ramosa* and *Acidolites* (Hill 1955). These were not recollected in the course of the present project, and their stratigraphic positions are unclear.

4.2 Sedimentological Synthesis

The sedimentary environments determined in chapter three for the various lithofacies present in the limestones at Ida Bay fall within the overall model of a tidal flat complex, as described by Weldon (1974). These environments are schematically depicted in Figure 4:4.

In this project, the depositional environment of each lithofacies has been described almost entirely in terms of onshore-offshore position alone (that is, in terms of whether the lithofacies was deposited in a supra-, inter-, or sub-tidal environment). Such a differentiation is clearly superficial, since several different lithofacies may occur in, say, the upper intertidal environment. In order to fully understand the differences between lithofacies it is necessary to take into account a multitude of other factors apart from onshore-offshore position, including palaeoecology, hydraulics, local topography and so on.

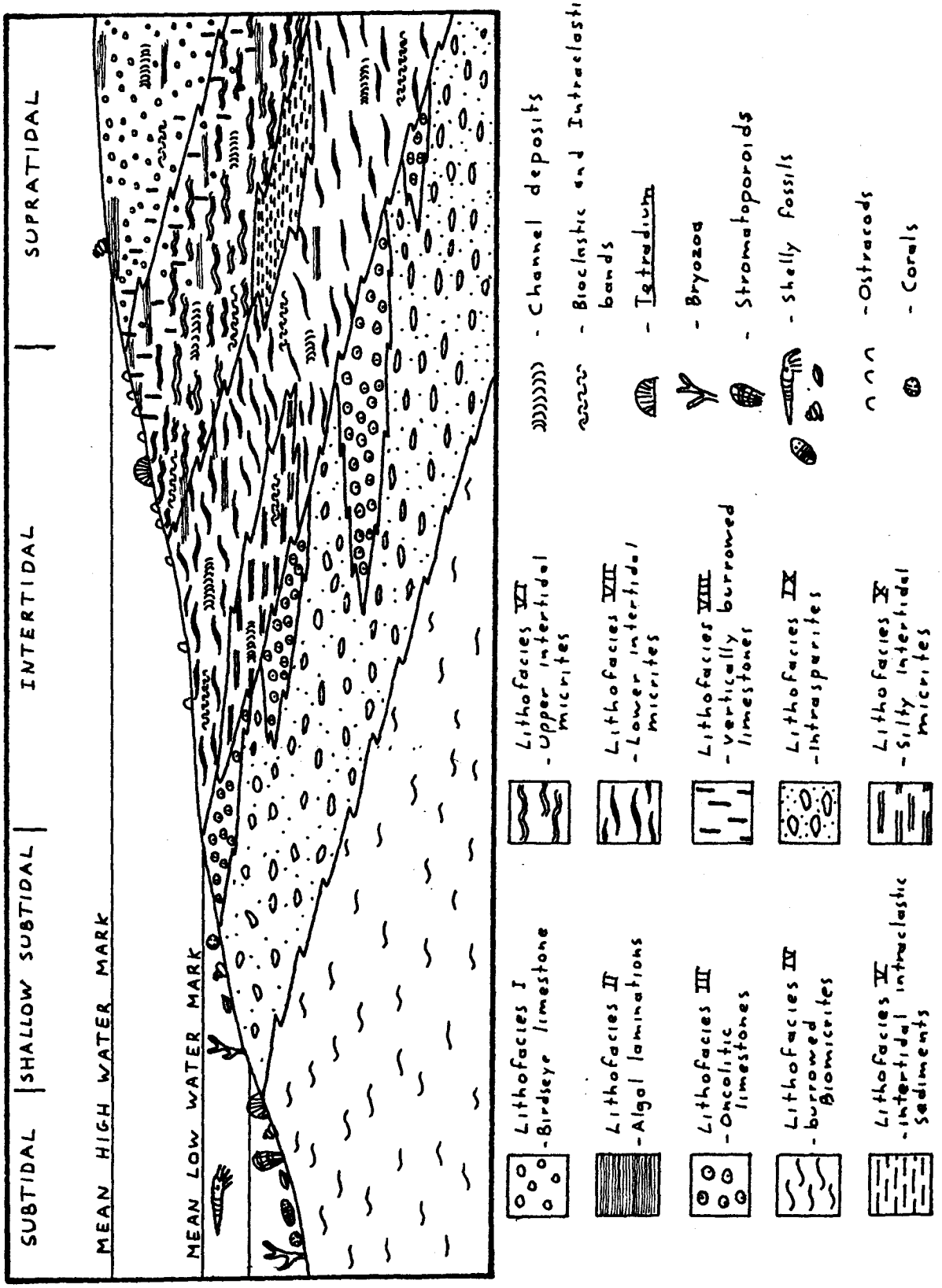

FIG. 4:4 Depositional environment proposed for Limestones at Ida Bay, depicting prograding tidal flat. Vertical scale is much exaggerated. Some of the common faunal associations are shown.

Nevertheless, valuable information can be derived from data about onshore-offshore positions of various lithofacies. Transgressive sequences can be determined from the sequence of lithofacies, and Fig. 4:5 is a representation of this information determined for the limestones on Marble Hill.

Below 240 metres, only supratidal and intertidal lithofacies occur. On faunal grounds this lower part of the limestone sequence is probably equivalent to the lower-middle part of the Lower Limestone Member of the Florentine Valley (see section 4:1). As Page (1978, p. 70) points out, deposition of sediments in the Lower Limestone Member was of a similar supratidal-intertidal nature until the latter stages of deposition of that member. Apart from supporting the correlation of units between Ida Bay and the Florentine Valley, this observation implies that the two areas were behaving in a tectonically similar fashion at the same time, such that in neither area did the depositional basin subside sufficiently to allow sedimentation to occur in subtidal conditions.

Above 240 metres in the Ida Bay section, deposition became dominantly subtidal and intertidal, with very little supratidal sedimentation taking place. Again, this is the same situation as is found in the upper part of the Lower Limestone Member, and in the Lords Siltstone and Upper Limestone Member of the Florentine Valley (Page 1978, p. 70, 72), and serves to strengthen the faunal correlations outlined in section 4:1.

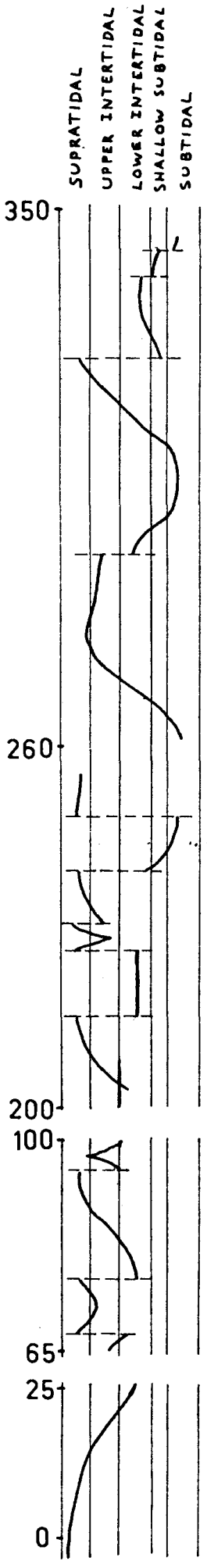

FIG. 4:5 Schematic representation of Transgression/Regression cycles in limestones at Ida Bay, as deduced from sequence of lithofacies. Scale is in metres, corresponding to stratigraphic column in Fig. 4:1.

As suggested in section 4:1, the topmost beds in Newlands Quarry may be equivalent to the Lords Siltstone in the Florentine Valley. A clastic unit equivalent to the Lords Siltstone is not present in Newlands Quarry, but the topmost beds include a Lithofacies X unit having a higher concentration of silt bands than any units elsewhere in the sequence (see Fig. 4:1). It is therefore possible that the deposition of silt bands in the Ida Bay area is related to the same events responsible for the deposition of the Lords Siltstone in the Florentine Valley.

As Fig. 4:5 shows, most of the depth change patterns in the limestones at Ida Bay comprise cycles of depositional regressions followed by erosional transgressions. This is the most common situation in the Gordon Sub-group, and the overall depositional environment at Ida Bay can be regarded as having been that of a prograding tidal flat.

Between 280 and 300 metres, and possibly also between 0 and 25 metres stratigraphic height, a major depositional transgression occurs, however. This apparently reflects basin subsidence occurring at a faster rate than sediment accumulation, and is probably a local event since virtually all depth change patterns in the Lower and Upper Limestone Members of the Florentine Valley are of the depositional regression/erosional transgression type (Calver 1977, Page 1978).

The general depositional model for the limestones can now be summarised as follows:

The limestones were deposited on a wide tidal flat which may have been many kilometres wide. Towards the bottom of the sequence, deposition of birdseye micrites and algal-laminated sediments in supratidal or upper intertidal regions took place, with occasional transgressions related to tectonic instability and/or compaction and stylolitisation, resulting in deposition of intertidal sediments associated with tidal channels.

In later times transgressions became more significant, resulting in deposition of oncolitic or intrasparite sediments in energetic shallow subtidal areas, and muddy biomicrites in deeper less energetic subtidal regions. With ongoing progradatio n and regression the sediment pile built up into the intertidal environment where micritic sediments were deposited. Although the intertidal environment supported few organisms apart from burrowers, occasional storms or high tides washed in quantities of shelly and intraclastic material which were deposited in graded bands or as tidal channel sediments. Occasional dessication of the sediments resulted in dolomitisation of the surface layers as a result of evaporation of pore fluids and concentration of salts in surface layers. At times evaporites were precipitated, usually in the form of microscopic crystals.

CHAPTER FIVE

PALAEOMAGNETIC INVESTIGATION OF IDA BAY LIMESTONES

5.1 Purpose of Palaeomagnetic Work

Little palaeomagnetic work has been done on palaeozoic rocks in Tasmania, and the only published palaeomagnetic study on the Tasmanian ordovician is Briden (1967), who found that the natural remanent magnetisations (NRM) of certain early ordovician sandstones resulted from secondary magnetisation. Briden regarded this as resulting from regional heating in the Tertiary.

Since the limestones at Ida Bay are amongst the least folded and altered Ordovician rocks in Tasmania it was hoped that they would retain the primary magnetisation recorded in them at the time of deposition, which would allow a quantitative determination of Tasmania's palaeolatitude in the middle-upper Ordovician.

In fact, as discussed below, the primary magnetisation has been destroyed, and replaced by a magnetisation of later - probably Cretaceous-age.

The laboratory work in this project was undertaken during a 3½ week visit to the palaeomagnetic laboratory of the Australian National University (ANU) in Canberra.

5.2 Palaeomagnetic Principles

Although most rock-forming minerals are non-magnetic, it is usual for most rocks to contain small amounts of magnetic material such as magnetite or haematite. If such minerals are present in a rock at the time of its deposition or cooling from a magma then the magnetic grains will line up their magnetisations with the Earth's magnetic field of the time, so giving the rock an initial *Primary Magnetisation*.

The total magnetic field of a rock is called its *Natural Remanent Magnetism* (NRM), and can be measured in oriented specimens by the use of various types of magnetometer. The magnetisation is specified in terms of its direction (comprising *Declination* - degrees clockwise from true north - and *Inclination* - degrees from horizontal, where upwards is negative and downwards positive), and its *Intensity* (usually measured in e.m.u. per cubic centimetre, which unit equals 10^3 amps per metre).

Assuming that the Earth's magnetic field always has been approximately a dipole, it is possible to use the declination and inclination to compute the position of the poles of the Earth's magnetic field at the time the magnetisation was imprinted in the rock. Thus, if we know that the NRM of a rock is its primary magnetisation we can deduce the palaeolatitude at which it formed, further assuming that the axis of the Earth's magnetic field has always been close to the axis of rotation (i.e. that the Earth's field has always been an axial geocentric dipole).

Commonly, however, rocks have undergone processes subsequent to their formation which have caused part or all of the primary magnetisation to be replaced ("overprinted") by later magnetisations. These *Secondary Magnetisations* may constitute all or only part of the NRM of a rock.

The processes by which rocks acquire their magnetisations (Primary or Secondary) include the following:-

Igneous and metamorphic rocks commonly acquire a *thermoremanent magnetisation* (TRM) by cooling from a high temperature through the Curie point(s) of the magnetic mineral(s) present. Clastic sediments may acquire a *detrital remanent magnetisation* (DRM) resulting from detrital magnetic particles aligning with the Earth's field as they are deposited. *Chemical remanent magnetism* (CRM) may result from the authigenic growth of magnetic minerals in a rock, the minerals growing with their magnetisations aligned wit h the EArth's Magnetic field.

Viscous remanent magnetism (VRM) is a form of secondary magnetism which is particularly relevant to the present study. VRM is discussed by McElhinny (1973, pp. 52-58). Magnetic viscosity is the tendancy for individual "single domain" magnetic grains to change their magnetic orientation in response to thermal fluctuations. (A *domain* is a volume wherein all atoms are magnetically aligned. If a single grain contains more than one domain its magnetic behaviour will be quite different from a single domain grain. In practice it seems that single domain grains are the only ones which need to be considered when dealing with magnetite and haematite bearing rocks (McElhinny 1973, p. 49)).

The *relaxation time* of an assemblage of such grains is the time constant of the period it takes for that whole assemblage to viscously change its magnetic orientation from one direction to another. Relaxation time is ultimately determined by the coercivity of the grains, but is also a function of the absolute temperature and the volume of the grains, the latter in its turn determining the *blocking temperature* of the grains. For a given absolute temperature there will be some grains of sufficiently small volume that the thermal fluctuations will be large enough to cause the magnetic moment of those grains to change spontaneously from one alignment to another. The relaxation time of the grains becomes shorter as absolute temperature becomes larger, and/or as grain volume becomes smaller. The *critical blocking temperature* for a grain of given volume is thus defined as the temperature at which the relaxation time of an assemblage of such grains becomes small (say 100 to 1000 secs.). This temperature may be below the curie point of the mineral.

The size of most magnetic particles found in rocks is sufficient for them to have extremely long relaxation times at room temperatures (of the order of 10" years: McElhinny 1973, p. 55). However, as temperatures rise the relaxation time of the magnetic grains in a rock may be shortened sufficiently to allow the rock to acquire a secondary VRM in geologically short times. This VRM is usually referred to as a viscous Partial Thermoremanent Magnetism (PTRM) since it only affects those magnetic particles in a rock having less than a given blocking temperature (McElhinny 1973, p.56).

A total TRM, by contrast, is the sum of the PTRMs of all magnetic particles in a rock with blocking temperatures from the curie point down to room temperature.

Because of the possibility of rocks acquiring secondary magnetisations, we might try to subdivide palaeomagnetic specimens into stable specimens - those whose magnetisation had remained unchanged since the rocks formation - and unstable specimens, whose magnetisation had changed since the rock was formed. However, since a rock will contain grains with a range of different blocking temperatures, the reality is that a specimen may contain several magnetic components of differing stabilities and directions, of which the NRM is simply the net resultant. A primary magnetisation is a highly stable component, whereas younger secondary magnetisations may be unstable components resulting from viscous re-alignment of grains with lower blocking temperatures. On the other hand, secondary magnetisations can result from alteration, or late stage diagenetic or metamorphic growth of magnetic minerals, in which case the secondary components could well be quite stable. (Zijderveld 1975, p. 24).

A common situation is for a specimen to show both a stable primary magnetisation and an unstable secondary magnetisation. Hence, few serious conclusions can be drawn from initial NRM measurements; in order to determine the nature of the magnetic components present it is necessary to progressively "clean" a sample so as to remove the less stable components first. The results of such progressive

demagnetisation are best analysed by the orthogonal vector plot method of Zijderveld (1967), as discussed in section 5:4 below.

In this study progressive thermal demagnetisation was employed, wherein the specimen is heated in a field-free space to successively higher temperatures until the curie point is reached. This allows the blocking temperature "spectrum" of the specimen to be investigated, by demagnetising components of lower blocking temperatures before those of higher blocking temperatures.

Alternatively, A.C. demagnetisation can be used to magnetically clean specimens by removing magnetically "softer" components first. However, A.C. cleaning was not employed in this study, and so concepts relating to A.C. demagnetisation are not discussed here.

5.3 Field and Laboratory Procedures

Samples were collected from throughout the exposed limestone section (in and below Newlands Quarry, and in Blaney's quarry) on Marble Hill. Three specimens were collected at each site, a "site" being a single stratigraphic horizon (to within a metre or so), and extending no more than one or two metres along. (Such precise positioning of sites was later shown to be unimportant, but would have been relevant if a primary magnetisation had been found).

Specimens were chosen which were in situ, but could be removed with relative ease and which had a flat surface which could be oriented accurately with a Brunton compass.

In the lab up to four 25mm diameter cores were drilled from each specimen. Cores were sliced into 23mm lengths and numbered as, for instance:- SIB266.11

The specimen field number precedes the decimal point. The first digit succeeding the decimal point refers to the number of the core drilled from the specimen, while the second succeeding digit refers to the number of the core sliced from the original drill core. 189 final cores were prepared in this way.

After preparation of cores, the facilities at ANU provide a "black box" system wherein measurement of specimens and calculation of results is almost fully automated. The NRM of each core was measured, in a field-free space, with a Cryogenic Magnetometer (Model C102, built by Superconducting Technology Inc., California) interfaced with a Hewlett-Packard 2116B minicomputer. To carry out the measurement, each core is rapidly placed within the magnetometer in a number of standard orientations, and the components of the magnetic field in the X, Y and Z directions were measured. From this the declination, inclination and total intensity of magnetisation are computed and recorded on paper tape and printed copy.

The NRM directions were corrected according to the field data, so as to give directions of NRM relative to the present horizontal plane at the collection sites, and were then plotted on a stereographic projection and found to cluster near the present field direction at Ida Bay (see Fig. 5:4) indicating a strong secondary component of magnetisation. If the NRM had been a primary

(ordovician) magnetisation, previous work (Embleton 1973) indicates that a lower inclination and an approximately east-west declination would be expected.

Forty-eight of the cores - one from each field specimen - were selected for an initial progressive thermal demagnetisation run. For each thermal demagnetisation step, the cores were placed in an electric coil furnace situated in a field-free space provided by three perpendicular Helmholtz coils whose fields can be adjusted to cancel all external fields with an accuracy of a few gammas. The cores were heated to the required temperature (measured by thermocouples within the furnace) and allowed to remain at that temperature for a few minutes before the furance was turned off and the cores cooled in the field-free space. During heating, argon gas was injected into the furnace in an effort to avoid oxidisation of minerals in the limestone.

The cores were then transferred to steel carrying boxes, which provided a field-free space, and from thence to the magnetometer. After measurement of field directions and intensities the cores were returned to the furnace for the next heating step. The steps used on the first demagnetisation run were 150, 200, 250, 300, 350, 400, 450, 475, 485, 500, 510, 520 degrees Celsius.

Cleaning was discontinued at 520 degrees C., since by this stage intensities were very low (0.01 - 0.02 emu x $10^{-6}/cm^3$) and varying in a fashion which indicated that they were probably in the noise level.

Subsequently a second demagnetisation run was performed on a further 45 cores, with smaller steps in the 450-500 degrees C. range. (In the two runs a total of 93 cores were cleaned, but the results were given for 99 components. This is an error resulting from the fact that in some cores, the main component was originally regarded as two separate components. This discrepancy in no way affects the final results, however.) Results differed somewhat from the first run in this range, possibly due to repeated heating causing mineralogic changes with resultant aberrant magnetic behaviour.

5.4 Analysis of the Data

The data obtained in the demagnetisation run was processed by computer, using standard programmes developed at ANU, to give a list of field-orientation corrected magnetisation directions and magnetic intensities. This information was plotted in three forms:-

1. Intensity Plots. The magnetic intensity remaining after each thermal cleaning step is represented on an intensity versus temperature plot, where the initial intensity is "normalised" to a value of one. Space prohibits the reproduction of plots for all 93 cleaned cores, but fig. 5:1 gives intensity plots for a number of representative samples.

2. Stereographic Plots. These plots show the change of direction of the remaining magnetisation after each cleaning step. Figure 5:2 shows a number of representative examples, illustrating the near constant direction of magnetisation most samples showed at low temperatures, and the instability shown at higher temperatures. (see below)

3. Orthogonal (Zijderveld) Plots. These are the most useful plots since they combine intensity and direction data. A representative example is given as Figure 5:3. The principles involved in these plots are explained in Zijderveld (1967) and (1975). Since the plots used at ANU are slightly different to the original Zijderveld plots, a brief explanation is given below:-

The demagnetisation of a specimen can be represented in three dimensional space as a line joining endpoints of the vector representing the magnetisation intensity and direction after each cleaning step. (Where distance of vector endpoint from co-ordinate system origin equals magnetic intensity and direction of vector from origin equals direction of magnetisation.)

The path so obtained can be represented in two dimensions by plotting the three orthogonal projections of the line on a single set of axes. This differs from the original Zijderveld plots, wherein only two of the three projections are plotted - the projection to the horizontal plane and one only of the vertical planes.

The orthogonal plots allow one to visually assess the number and nature of the magnetic components present in a sample. As Zijderveld (1967, p. 258) explains, "In general, when the end point of the resultant magnetisation vector changes along a straight-line during the treatment, it is plausible that during this demagnetisation interval only one single magnetisation is affected. The direction of this straightline, which can easily be calculated

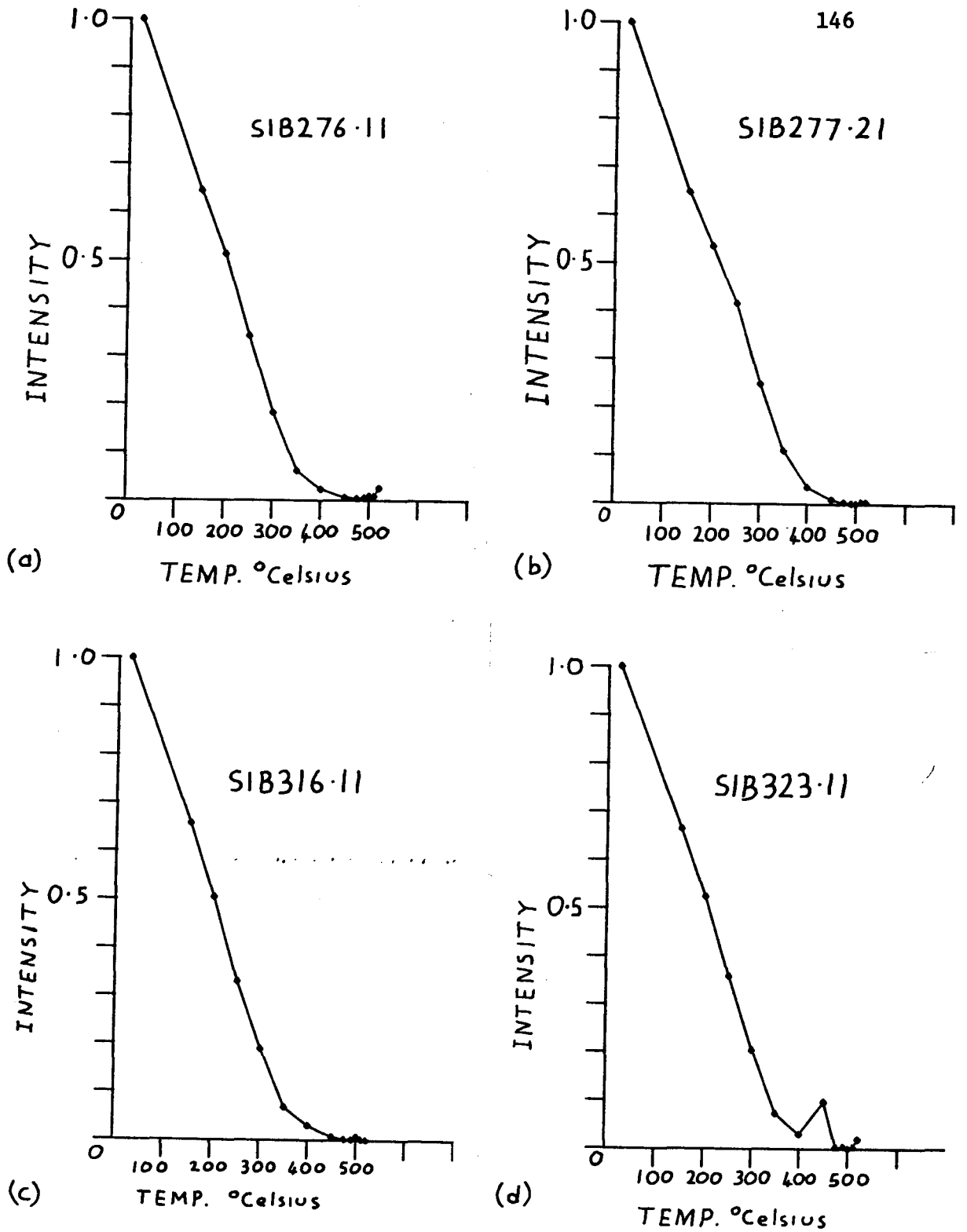

FIG. 5:1 Sample intensity plots. In these plots the initial (NRM) intensity is normalised to one. The plot shows the decay of intensity as the specimen is thermally cleaned to successively higher temperatures. The shape of the curve is similar for all four examples above, and this is true for most of the specimens cleaned.

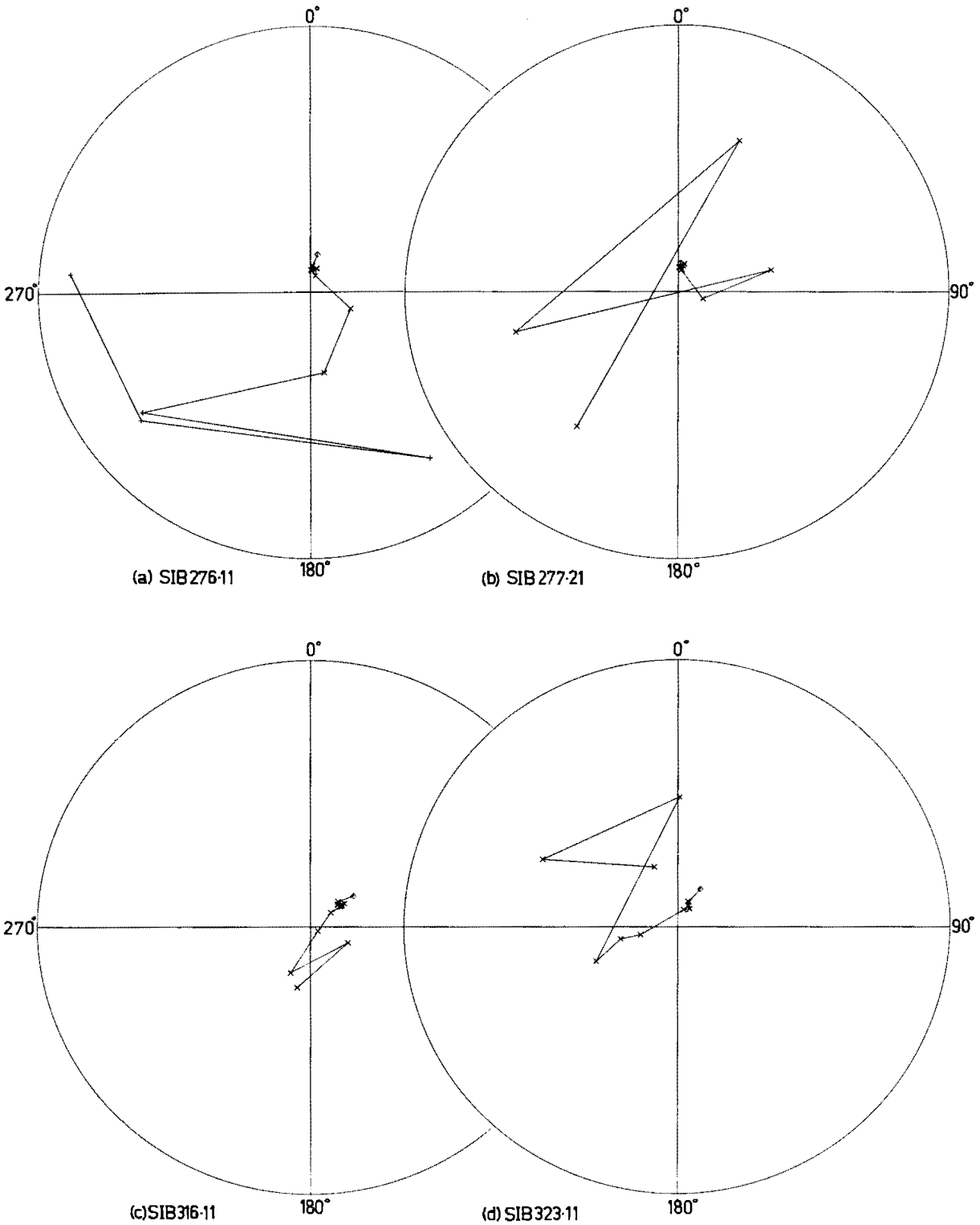

FIG. 5:2 Sample stereographic projections (oriented with respect to true north) of the change of direction of the magnetisation in selected specimens with increased cleaning temperatures (Each x represents a cleaning step, and ◇ the NRM direction.). Note stable low temperature directions and instability at high temperatures. (c) and (d) show a trend towards the southwest before becoming unstable

FIG. 5:3 Zijderveld plot of Thermal demagnetisation of SIB316.11. The three lines are projections onto three orthogonal planes of a line traced in three dimensions by endpoints of vectors representing magnetisation intensity and direction after each cleaning step. Lines of + symbols represent projection onto East-West vertical plane, diamond symbols onto North-South vertical plane, and x symbols onto the horizontal plane.

Numbers placed beside vector endpoints represent temperature in degrees celsius to which specimen was heated before measurement of vector. The straight-line segment representing the secondary component of magnetisation is obvious (and in a slightly different direction to the NRM direction).

The plot is scaled at 0.588965 e.m.u. x $10^{-6}/cm^3$/axis cm.

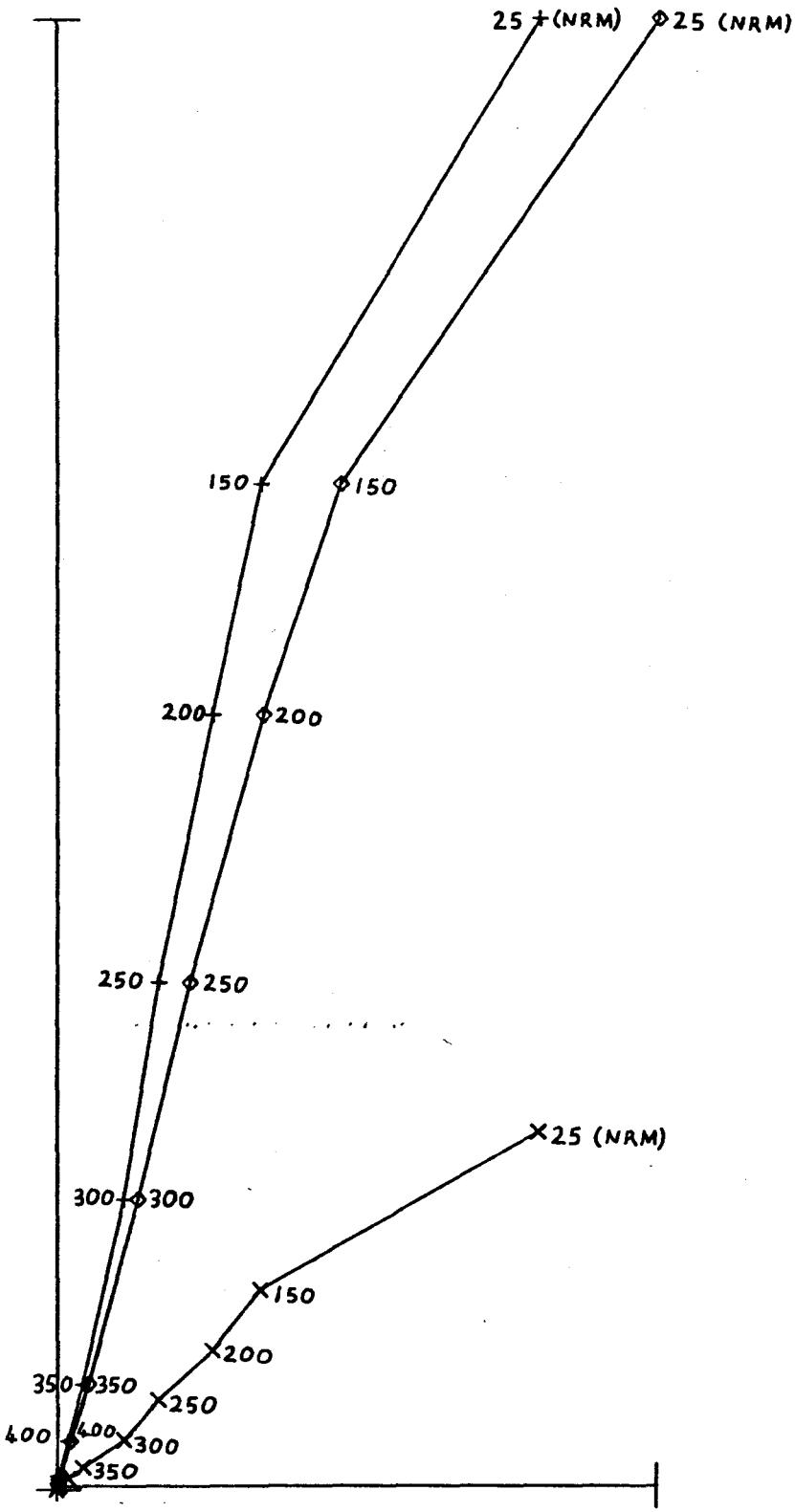
25 + (NRM)
◇25 (NRM)
150 +
◇150
200 +
◇200
250 +
◇250
×25 (NRM)
300 +
◇300
×150
×200
350 +
◇350
×250
400 +
◇400
×300
×350

from the diagram, is the direction of the magnetisation that is eliminated. A straight line, however, is only proved strictly by at least three points (mind measuring errors!) and may arise when, e.g., two magnetisations are affected simultaneously in a constant ratio.

From the moment that the resultant vector no longer changes its direction, but decreases along a straight line exactly to the centre of the co-ordinate system, this magnetisation must be one single component. By a "component" we understand here a group of magnetisations with the same direction and polarity."

The declination and inclination of each component can be measured off the horizontal and vertical orthogonal projections, respectively, with a protractor. For accuracy, however, they should be calculated from the primary data.

In a simple example, a specimen with both a primary magnetisation, and a secondary magnetisation in a different direction, will yield an orthogonal plot showing the two separate components as two lines joining at an angle to each other.

Examination of the orthogonal plots obtained for each magnetically cleaned core showed only one component of magnetisation, which was revealed during thermal demagnetisation from 150 to about 400-450 degrees celsius. This component is close to, but not quite identical to, the NRM direction. At higher temperatures this component is cleaned out and the magnetisation becomes unstable. (see Figs. 5:2, 5:3).

It appears that any primary magnetisation was long ago cleaned out, and that later the magnetic domains with lower blocking temperatures were remagnetised to give the lower temperature component. The Tabberabberan Orogeny and the Jurassic dolerite intrusion are obvious explanations for the cleaning out of the primary magnetisation, but no attempt has been made to test these possibilities by a more detailed examination of the data. That the lower temperature component is not a primary component is almost certain for reasons discussed in sections 5:3 and 5:6.

The data on the cleaning intervals during which the component was measured in each core was fed into the computer, and the mean direction calculated from all the individual components. Finally the resulting palaeopole position, and the statistical parameters for the component (R, K, *alpha* 95 circle) were calculated by computer. Statistical parameters were not calculated for individual cleaning steps by the standard computer programmes, and time limitations have since prevented this being done either manually or automatically.

Since the above variables were all calculated automatically it is not necessary to go into detail about them here, other than to state their significance.

The mean direction of the magnetic components measured in each sample is calculated as detailed in McElhinny (1973, p. 81). The position of the palaeomagnetic pole corresponding to this mean direction is computed by the method given in McElhinny (1973,pp.23-25).

If the consistent magnetic component in each sample is considered as a vector, then the vector sum of these vectors in all the samples has length R. Effectively, R is the resultant component of magnetisation calculated from the individual components measured in each specimen. The calculation of R is detailed in McElhinny (1973, p. 78), and R can in turn be used to calculate K (ibid., p. 79). "The parameter K is called the *precision parameter* and determines the dispersal of the points. If K=0 they are uniformly distributed (the directions are therefore random), and when K is large the points cluster about the true mean direction." (*ibid*, p. 78).

The *alpha* 95 angle is the semi-angle subtended by the cone around the resultant vector of magnetisation (R) within which there is a 95 per cent probability that the true mean direction lies. (Fisher 1953, in McElhinny 1973, p. 79).

5.5 Results

The 189 NRM directions measured are tabulated in Appendix four. Fig. 5:4 is a stereoplot of the NRM directions after application of a field correction. (See section 5:3).

Ninety-three cores were treated by thermal cleaning, and the directions measured in each core for the consistent component of magnetisation (see section 5:4) are given in appendix five. Fig. 5:5 is a stereoplot of these directions, and table 5:1 gives the palaeopole and other statistics calculated from the directions

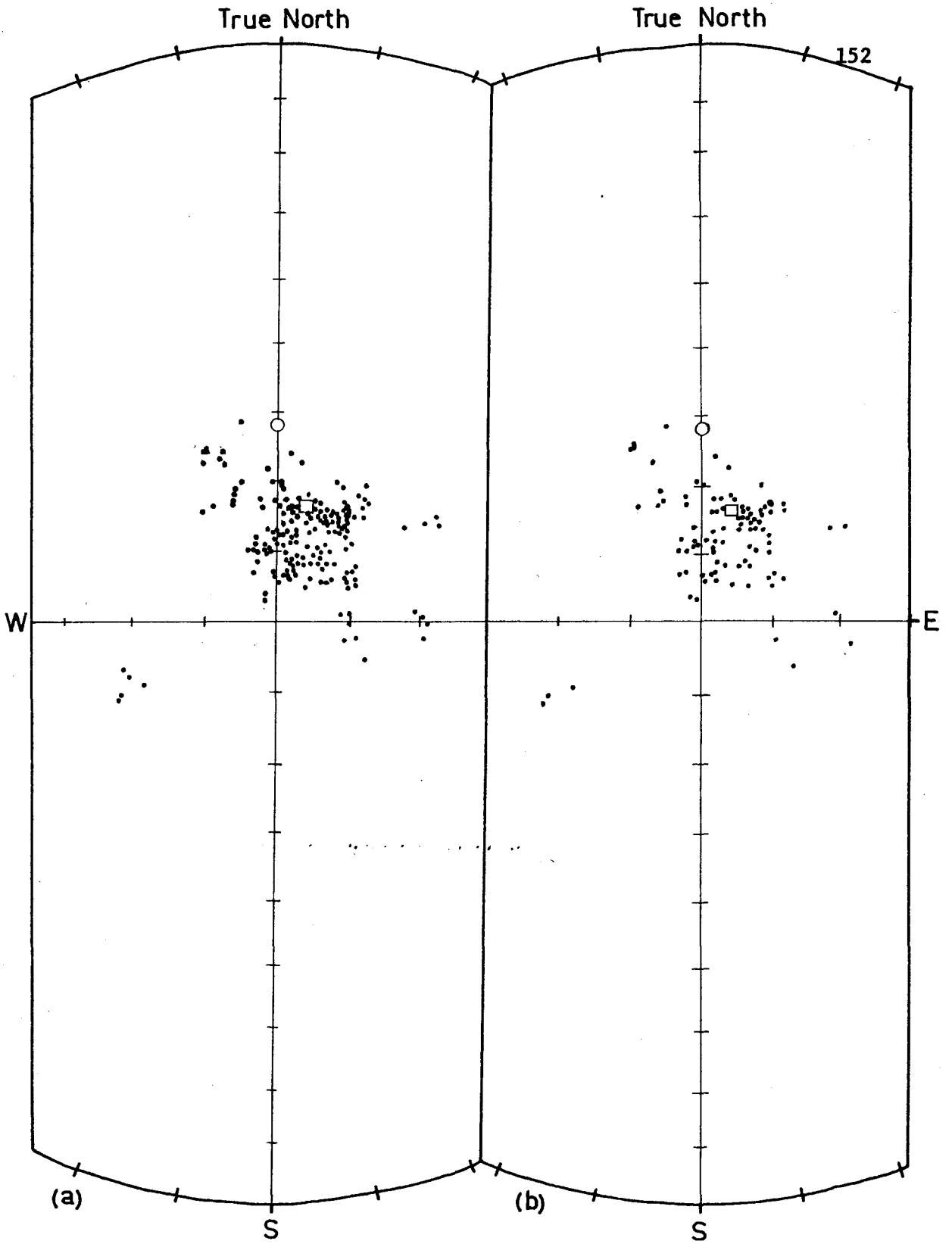

FIG. 5:4 Stereoplot of NRM directions in Ida Bay limestones (a) All 189 specimens measured. (b) Only those specimens which were later cleaned, and whose secondary component directions are shown in Fig.5:5.
(Equal-area nets)

○ Present axial dipole field at Ida Bay
□ Present magnetic field at Ida Bay
• NRM Directions

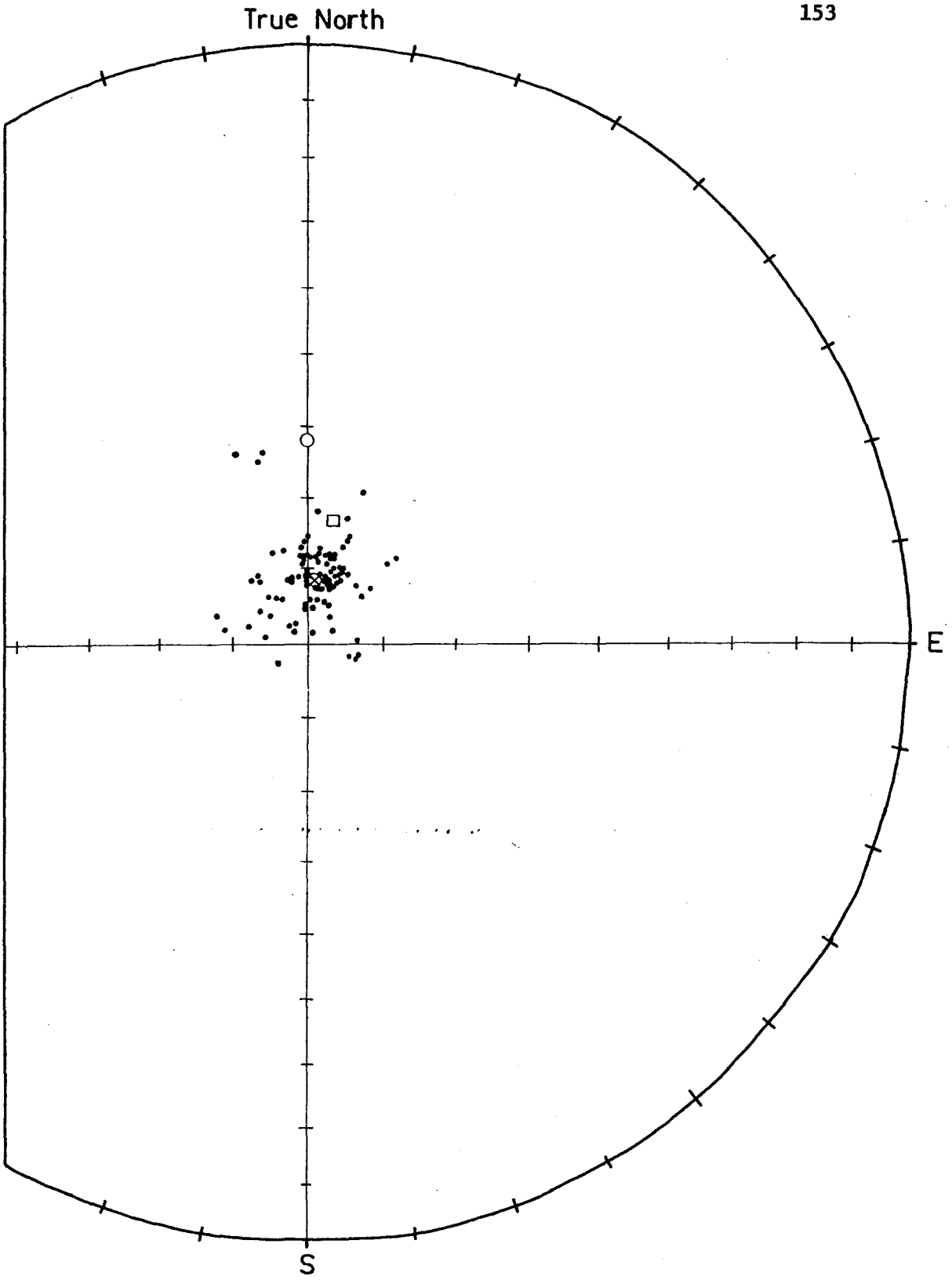

FIG. 5:5 Stereoplot showing directions of secondary component in specimens measured. (Equal-area net)

- ○ Present axial dipole field at Ida Bay.
- □ Present magnetic field at Ida Bay.
- • Secondary component directions.
- ⊗ Mean secondary component direction.

S	N	D	I	K	R	alpha 95	Long.P.P.	Lat.P.P.	Palaeolat.
48	99	5.52	-81.63	85.1	97.85	1.55	143.81E	59.74S	73.60S

TABLE 5.1 Results obtained from Secondary Component of Magnetisation in Ida Bay limestones.

S : number of samples

N : number of cores

D : mean Declination (degrees clockwise from north)

I : mean Inclination (degrees upwards negative)

K : Precision Parameter (see McElhinny 1973, p.78)

R : Sum unit Vectors (see McElhinny 1973, p. 78)

alpha 95 : Semi-angle (degrees) of 95% circle of confidence

Long.P.P. : Longitude of palaeopole (degrees)

Lat.P.P. : Latitude of palaeopole (degrees)

Palaeolat. : Palaeolatitude of site (Ida Bay) at time of secondary magnetic overprinting, in degrees.

of this component. Since the inclination of the mean direc tion of the component is negative, it therefore represents a normal, rather than reverse, magnetisation.

The samples from Newlands quarry and Blaneys quarry are from the eastern and western limbs, respectively, of the anticline into which the Ordovician sediments on Marble Hill are folded. (see Ch. 2). Visual comparison of stereoplots of the directions of magnetisation in specimens from either limb indicates no appreciable grouping of palaeomagnetic directions according to which limb the specimens are taken from. Hence, the magnetic directions measured appear on this evidence to be a post-folding overprint, and so it was not necessary to apply a correction to the data for bedding dip.

The total NRM direction is usually in a slightly different direction to the main magnetic component, which most probably is the result of minor overprinting due to viscous re-alignment with more recent fields.

NRM intensities are generally in the range 19.0 - 4.0 emu x $10^{-6}/cm^3$. Between the cleaning steps of 150 degree celsius to 400 degrees celsius intensities generally decay from about 13.0 - 3.0 to 0.8 - 0.06 emu x $10^{-6}/cm^3$. (See Fig. 5:1).

The remainder of this chapter is devoted to a discussion of the consistent magnetic component represented in Fig. 5:5 and Table 5:1.

5.6 Age of Magnetic Overprinting

The palaeomagnetic pole obtained from these measurements (Table 5:1) falls at 143.81 degrees east longitude and 59.74 degrees south latitude. This is close to the Cretaceous part of the apparent polar wander path for Australia, as most recently determined by Peirce and Klootwyk (*in press* 1979). (See Fig. 5:6). Palaeomagnetic poles falling on the same part of the apparent polar wander path have previously been obtained from rocks yielding radiometric ages of 70 to 98 m.y. (*ibid.*). From its position, the palaeopole determined in the present study probably represents an overprinting event between 90 and 98 m.y., most likely about 95 m.y. (mid-Cretaceous).

5.7 Speculations on Cause of Magnetic Overprinting

One explanation for the overprinting is that it results from regional heating associated with the intrusion of Cretaceous Syenites which outcrop in the Port Cygnet region, 30 kilometers northeast of Ida Bay. These syenites have been radiometrically dated at 98 m.y. (McDougall and Leggo 1965), but although they are thus in the right age range it is unlikely that they would have caused the overprinting while younger tertiary basalts only a few kilometers from the limestones have had no appreciable effect. The country rocks adjacent to the syenites show little metamorphic alteration (R. Ford *pers. comm.* 1979) implying that the intrusions would not have been a sufficient source of heat for the long period necessary to account for the overprinting. (see below).

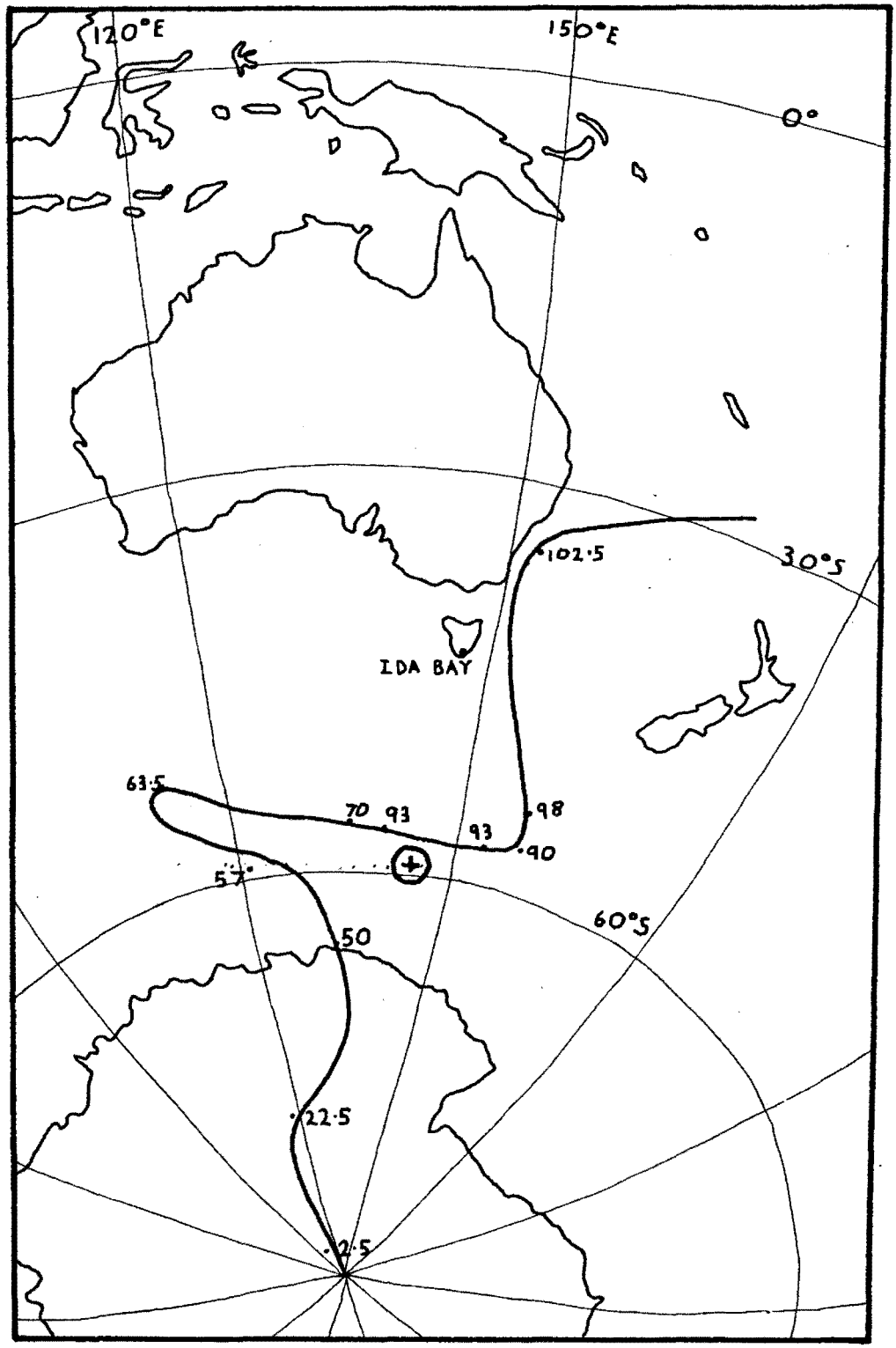

FIG. 5:6 Apparent Polar wander path for Australia in Cretaceous -Tertiary times. (Pierce and Klootwyk, in press), with palaeopole determined for overprint component in Ida Bay limestones indicated. α-95 circle shown, together with ages previously determined for parts of polar wander path (in m.y.)(Ibid.).

Palaeomagnetic work on the syenites (Robertson and Hastie 1962) has yielded a primary magnetisation (Declination 314°, Incl.-85°) which is significantly different in declination from that determined in the present study.

An alternative hypothesis is that the overprinting results from burial of the sediments and heating related to increased geothermal heat flow prior to the rifting of the Tasman Sea. Subsequent uplift and cooling resulting from the rifting, with erosion of overburden, would have allowed the overprinting - a viscous P.T.R.M. - to be preserved in the limestones.

A similar mechanism is proposed for overprinting in rocks of the Sydney Basin. (B.J.J. Embleton, *pers. comm.* 1979).

The sampled limestones show no petrological evidence of heating, and the only information available on the temperatures they have been exposed to comes from observations on the colour of conodonts. (Epstein *et al* 1977) extracted from other Ida Bay limestone specimens. These observations indicate that the limestones have been subjected to temperatures not exceeding 100 degrees Celsius (C.F. Burrett, *pers. comm.* 1979).

Since the overprinting is not cleaned out until the rocks are heated to 400 or 450 degrees Celsius for about five minutes, an estimate of the time required to produce such an overprint with the relaxation times resulting from heating to no more than 100 degrees Celsius can be obtained using the relationships between

temperature and relaxation time given in McElhinny (1973, sections 2.3.3, 3.4.2). These indicate that a period of the order of 10^7 years is required to produce the observed overprinting.

This is a reasonable result, and implies that heating to near 100 degrees Celsius can explain the observed overprinting if the overprint is a viscous P.T.R.M. acquired over a long period around 95 m.y. If so, the overprint does not represent the Earth's magnetic field at any one point in time, but rather is the net affect of P.T.R.M.s acquired over a period of some millions of years.

It does not appear that heating due to simple burial (with a "normal" geothermal gradient) could have produced temperatures in the limestones approaching 100 degrees. It is not possible to determine the thickness of rocks overlying the limestones in the mid-cretaceous, but a probable maximum thickness of overburden can be "guesstimated" by totalling the present thickness of overlying units, and adding to this an estimated thickness of sediments which would have accumulated if sedimentation had continued at Permo-triassic accumulation rates until the mid-cretaceous. The thickness of presently exposed overlying rocks (Permo-carboniferous sediments, lower triassic sediments, Jurassic dolerite sill) measured from Marble Hill to the Mt La Perouse area (DM790830) total 860 metres. (Davidson 1969, Farmer 1975, Present Study). Sedimentation until the mid-cretaceous, at the averaged lower Permian - lower Triassic rate of 11.83 metres per million years (calculated from approximate ages and thicknesses of the aforementioned exposed sediments) would

have yielded a further 1600 metres of sediment, giving a total of 2460 metres maximum overburden depth, assuming no unknown structural complications. This figure is probably a gross over-estimate, since there is no evidence for sedimentation having continued uninterrupted into the cretaceous in Tasmania.

The average geothermal gradient in the earth's crust near the surface is at present 0.03 degrees Celsius per metre (Smith 1973, p. 102). Using this value and assuming an average surface temperature of ten degrees Celsius (Verhoogen *et al* 1970, p. 638) we get a temperature of 10+ (2460 x 0.03) = *83.8 degrees Celsius* for rocks buried to a depth of 2460 metres. This is significantly below the 100 degrees to which the limestones may have been subjected, and the true temperature is probably far lower again, since the 2460 metre estimate of overburden thickness is probably much exaggerated. It is clear that simple heating due to burial is insufficient to account for the temperatures needed to produce a PTRM overprint of the observed magnitude.

It is probable that abnormally high heat flow associated with the initiation of the rifting which formed the Tasman Sea was responsible for heating rocks at Ida Bay (and presumably much of Eastern Australia) to the level at which the observed PTRM could be acquired.

It is well known (e.g. Smith 1973, p. 126, 128) that mid-ocean spreading ridges have some of the highest heat flow values recorded near the Earth's surface, as a result of upwelling of

magmas in the asthenosphere would have provided high heat flow values in the crust near the site of incipient rifting for several millions of years before the onset of continental breakup.

The continental shelf off the eastern side of Tasmania is quite narrow (see: Griffiths and Varne, 1972), so that Ida Bay would have been no more than one hundred kilometers or so from the site of rifting. The limestones at Ida Bay can be expected to have undergone heating as a result of the incipient rifting of the Tasman Sea, together with the effects of burial to at least 860 metres. (Known overburden thickness; see above).

Because the zone of high heat flow around spreading ridges is restricted to only a few hundred kilometres. (Smith 1973, p.128), it is to be expected that the eventual onset of rifting would have led to rapid cooling of the rifted continental crust as it moved away from the spreading zone, allowing the acquired PTRM to be "frozen" in the limestones. Alternatively, faulting prior to and associated with the onset of breakup would have caused relative "uplift" of the limestones and erosion of much overburden, causing cooling. This latter possibility is the more enticing of the two, since the magnetic overprint appears to have been "frozen" into the limestones prior to the actual breakup at about 80 m.y.

5.8 Site of Magnetisation in the Limestones

No attempt was made to determine the nature of the magnetic minerals responsible for the magnetisation of the limestones. However,

dissolution of limestone samples for the extraction of conodonts also revealed the presence of small quantities of metallic minerals. Non-magnetic Pyrite was the most common of these minerals, but there were also black and reddish crystals of what may be Magnetite and Haematite. These minerals occur as well-formed cubic crystals, and are thus probably authigenic.

5.9 Further Work

If crustal regions in and near Tasmania did in fact experience higher-than-normal heat flow values in the mid-cretaceous it is to be expected that mid-cretaceous magnetic overprinting would be common as a secondary component in any pre-cretaceous Tasmanian rocks which were at the time buried to a moderate depth, comparable to the burial depth of the limestones of Ida Bay. The only later events which might have imprinted a PTRM in Tasmanian rocks would be similar high heat flow values related to the rifting of Tasmania from Antarctica at about 50 m.y., and regional heating associated with the Tertiary basalts.

By careful palaeomagnetic studies of suitable Tasmanian rocks, using progressive cleaning techniques and Zijderveld-plot analysis of the data, it should be possible to confirm (or otherwise) the occurrence of a magnetic overprinting event in Tasmania in the mid-cretaceous. If the rifting of Antarctica from Tasmania also resulted in an overprinting event, it is entirely possible that a late-cretaceous overprinting resulting from this event would be dominant in western and southern Tasmania, while the mid-cretaceous

event may be dominant in eastern Tasmania. (Since these are the areas adjacent to the two rift zones involved).

The present study, and the abovementioned possibilities indicate the potential value of studying not only the primary magnetisation of rocks, but also their secondary magnetisations.

As has been explained, the present study could not determine a direction of primary magnetisation because no stable endpoint was reached after the secondary component of magnetisation was cleaned out of the limestones. However, an examination of stereograms recording the demagnetisation of some of the specimens cleaned (see Fig. 5:2) reveals that prior to becoming unstable, the magnetisation vectors obtained after each cleaning step changed direction slightly, in a fashion that appeared to define an arc of a great circle. This "Remagnetisation Circle" (Halls, 1976), is probably due to the higher temperature components of the secondary component's blocking temperature spectrum overlapping with the remnants of the blocking temperature spectrum of an earlier component. This earlier component no longer has a stable high temperature endpoint, [redacted], since the high temperature spectrum measured in the laboratory consists of components having extremely low intensities (less than 0.8 - 0.06 emu x $10^{-6}/cm^3$) which are probably in the noise level.

It is worth investigating the possibility that this earlier component represents a pre-folding magnetisation. Since the folding of the Tasmanian ordovician rocks results from the Devonian

Tabberabberan Orogeny, a pre-folding component of magnetisation would in all probability be a primary ordovician magnetisation.

Halls (1976) presents a method of using partial remagnetisation circles determined from rocks in structurally disoriented areas to determine the pre-folding direction of magnetisation. In a nutshell, his method involves taking samples from, say, both limbs of a fold. The arcs of the remagnetisation circles obtained from these samples are plotted on a stereonet, and are extrapolated as great circles until they intersect. The intersection represents the direction of the secondary component. The fold is then structurally unfolded, resulting in the great circles intersecting at a new point representing the direction of the pre-folding (Primary?) component. (See Halls 1976, fig. 2).

Although partial remagnetisation circles appear to have been obtained from the limestones at Ida Bay, the folding in the area is probably insufficient to warrant an attempt at using Hall's method. Instead, it is suggested that there may be potential in attempting to use this method in an area of limestone which has been folded into steeper folds (although still without significant metamorphic alteration of the rocks). The Florentine Valley is suggested as a suitable location for such a study, if it were deemed worthwhile.

CHAPTER SIX

SUMMARY AND CONCLUSIONS

The bulk of the Ordovician rocks in the Ida Bay area occur in a north-south trending Tabberabberan anticline. Pure quartzarenites and siliceous conglomerates of presumed Early Ordovician age are exposed in the anticline at the Hogsback, and south of the Lune River. A gastropod fauna is found sparsely preserved at both localities.

Stratigraphically above the quartzites, about 350 metres of Gordon Sub-group limestones occur on Marble Hill, where their anticlinal structure is warped into a domal form by northward and southward dip components on the north and south sides of the hill, respectively. The limestones comprise sediments laid down in a prograding tidal flat environment, and range in age from Late Chazyan to Trentonian. The bulk of the limestone is probably a time-equivalent of the Lower Limestone Member of the Florentine Valley, and a silty limestone at the top of the Marble Hill section may be equivalent to the Lords Siltstone in the Florentine .

Further outcrops of Ordovician limestone occur in a belt extending north from Mesa Creek towards the Hastings Caves Area, in a small area on the Lune River, and probably on the south-western side of Coal Hill (north of the Lune River). The structural relationships between these outcrops and the main anticline through Marble Hill and the Hogsback are unknown.

Regional mapping in areas north of the Lune River has demonstrated substantially different distributions of Permo-Carboniferous and Triassic sediments, and of Jurassic dolerites, to the distribution previously postulated (Farmer 1975).

White siliceous sediments occurring on the southern slopes of Coal Hill, and having a superficial resemblance to a quartzite, may be silicified limestones. These rocks are characterised by microscopic inclusions of a birefringent mineral similar to calcite or dolomite, by an abundance of microscopic pits (leached out inclusions?), and by angular macroscopic holes which may represent large (leached out) carbonate or evaporite crystals. A model of silicification of surface layers of limestone by a process related to silcrete horizon formation is proposed for these rocks. The silicification may have occurred in a hot arid climate as long ago as the mid-Palaeozoic.

Palaeomagnetic measurements indicate that the primary magnetisation of the limestones (which was probably a chemical remanent magnetism resulting from authigenic growth of magnetic mineral grains) has been overprinted by later secondary magnetisations. Apart from minor recent viscous remagnetisation, the main overprint component of magnetisation is one yielding a palaeopole which falls near the mid-cretaceous part of the apparent polar wander path for Australia. This overprint magnetisation may be associated with burial and increased heat flow just prior to rifting of the Tasman Sea.

A new form of the Receptaculitid *Calathium* has been found in the limestones on Marble Hill, which has three walls instead of the usual two.

BIBLIOGRAPHY

Aitken, J.D., 1967. Classification and environmental significance of cryptalgal limestones and dolomites, with illustrations from the Cambrian and Ordovician of southwestern Alberta. J. Sed. Pet., 37 : pp. 1163-1178.

Alberstadt, L.P. and Walker, K.R., 1976. A receptaculitid-echinoderm pioneer community in a middle Ordovician reef. Lethaia, 9 : pp. 261-272.

Ball, M.M., Shinn, E.A., Stockman, K.W., 1972. Geologic record of Hurricanes. In Ginsburg, R.N. (ed.), South Florida Carbonate Sediments: Sedimenta II, University of Miami, Florida.

Banks, M.R., 1957. Stratigraphy of Tasmanian Limestones. In Limestones in Tasmania, Tas. Geol. Surv. Miner. Res. 10

_____ and Johnson, J.H., 1957. The occurrences of *Maclurites* and *Girvanella* in the Gordon Limestone (Ordovician) of Tasmania. J. Paleont., 31 : pp. 632-640.

_____, 1962. Ordovician System. In Spry, A. and Banks, M.R. (eds.). The Geology of Tasmania, J. Geol. Soc. Aust., 9 : pp. 107-362.

_____ and Burrett, C.F., *in press*. A preliminary statement on the Biostratigraphic succession in the Ordovician System of Tasmania. J. Geol. Soc. Aust.

Bathurst, R.G.C., 1976. Carbonate sediments and their diagenesis. Elsevier, Amsterdam, 658p.

Blatt, H., Middleton, G. and Murray, R., 1972. Origin of Sedimentary Rocks. Prentice-Hall Inc., New Jersey, 634p.

Briden, J.C., 1967. Secondary Magnetisation of some Palaeozoic rocks from Tasmania. Pap. Proc. Roy. Soc. Tasm., 101 : pp. 43-48.

Bridge, P.H. and Leeder, M.R., 1976. Sedimentary model for intertidal mudflat channels, with examples from the Solway Firth, Scotland. Sedimentology, 23 : pp. 533-552.

Burrett, C.F., 1978. Middle-Upper Ordovician conodonts and stratigraphy of the Gordon Sub-group, Tasmania, Australia. Unpubl. Ph.D. Thesis, Uni. of Tasmania.

Calver, C.R., 1977. Palaeoecology of the Lower Limestone Member, Benjamin Limestone, Florentine Valley. Unpubl. Hons. Thesis, Uni. of Tasmania.

Carey, S.W. and Banks, M.R., 1954. Lower Palaeozoic unconformity in Tasmania. Pap. Proc. Roy. Soc. Tasm., 88 : pp. 63-70.

Carozzi, A.V., 1960. Microscopic Sedimentary Petrography. John Wiley and Sons, Inc., New York, 485p.

Collins, B.R., 1968. Ida Bay area. Speleo-spiel, No. 24 : p. 4 (Tas. Caverneering Club Newsletter).

Copper, P., 1974. Structure and development of Early Palaeozoic reefs. In Cameron, A.M. (ed.), Proc. Second. Internat. Coral Reef Symp., Gt. Barrier Reef Comm., Brisbane, 1 : pp. 365-386.

Corbett, K.D. and Banks, M.R., 1974. Ordovician stratigraphy of the Florentine Synclinorium, Southwest Tasmania, Pap. Proc. Roy. Soc. Tasm., 107 : pp. 207-229.

Dahanayake, K., 1978. Sequential position and environmental significance of different types of oncoids. Sediment. Geol., 20 : pp. 301-316.

Davidson, J.K., 1969. Upper Permian and Lower Triassic sedimentation and palynology of the La Perouse area. Unpubl. Hons. Thesis, Uni. of Tasmania.

Dickenson, D.R., 1945. Limestone Quarries at Ida Bay. Unpubl. Rep. Dep. Mines, Tasm., 1945, pp. 46-63.

Embleton, B.J.J., 1973. The palaeolatitude of Australia through Phanerozoic time. J. Geol. Soc. Aust., 19 : pp.475-482.

Epstein, A., Epstein, J. and Harris, L.D., 1977. Conodont Color Alteration - an index to conodont metamorphism. U.S. Geol. Surv. Prof. Paper 995 : pp. 1-27.

Everard, G.B., 1957. Ida Bay. In Limestones in Tasmania, Tas. Geol. Surv. Miner. Res. 10 : pp. 132-137.

Farmer, N., 1975. Geological Atlas I:250000 series, sk55/8. Dept. Mines, Hobart, Tasmania.

Folk, R.L., 1962. Spectral subdivision of limestone types. In Ham, W.E. (ed.), Classification of Carbonate Rocks : a symposium. Am. Assoc. Pet. Geol., Memoir 1.

_____, 1968. Petrology of Sedimentary Rocks. Austin, Texas: Hemphill's Bookstore, 170p.

Forsyth, S.M. and Green, G.R., 1976. Investigation of Limestone deposits at Ida Bay. Unpubl. Rept. Dept. Mines., Tasm. 1976/58

Ginsburg, R.N. (ed.), 1972. South Florida Carbonate Sediments (Sedimenta II). Comparative Sedimentology Laboratory, Uni. of Miami.

Goede, A., 1969. Underground Stream Capture at Ida Bay, Tasmania and the relevance of cold climatic conditions. Aust. Geographical Studies, 7 : pp. 41-48.

Griffiths, J.R. and Varne, R., 1972. Evolution of the Tasman Sea, Macquarie Ridge and Alpine Fault. Nature Phys. Sci., 235 : pp. 83-86.

Grover, G. and Read, J.F., 1978. Fenestral and associated vadose diagenetic fabrics of tidal flat carbonates, Middle Ordovician New Market Limestone, Southwestern Virginia. Jour. Sed. Petr., 48 : pp. 453-473.

Halls, H.C., 1976. A least-squares method to find a remanence direction from converging remagnetisation circles. Geophys. J. Roy. Astr. Soc., 45 : pp. 297-304.

Hill, D., 1955. Ordovician Corals from Ida Bay, Queenstown and Zeehan, Tasmania. Pap. Proc. Roy. Soc. Tasm., 89 : pp. 237-254.

James, H.L., Dutton, C.E., Pettijohn, F.J. and Wier, K.L., 1968. Geology and Ore deposits of the Iron River - Crystal Falls District, Iron County, Michigan. U.S. Geol. Surv. Prof. Paper 570, 134p.

Johnson, J.H. and Høeg, O.H., 1961. Studies of Ordovician Algae. Quarterly of the Colorado School of Mines, 56, no. 2.

Katz, A. and Friedman, G.M., 1964. The preparation of stained acetate peels for the study of carbonate rocks. J. Sed. Petr., 35 : pp. 248-249.

Larsen, G. and Chilingar, G.V., (eds.), 1967. Diagenesis in Sediments. Developments in Sedimentology 8, Elsevier, Amsterdam, 551p.

Logan, B.W., Rezak, R. and Ginsburg, R.W., 1964. Classifi cation and environmental significance of algal stromatolites. J. Geol., 72 : pp. 68-83.

McDougall, I. and Leggo, P.J., 1965. Isotopic age determinations on granitic rocks from Tasmania. J.Geol.Soc.Aust., 12 : pp. 295-332.

McElhinny, M.W., 1973. Palaeomagnetism and Plate Tectonics. Cambridge Uni. Press.

Miagkova, Ye. I., 1965. Soanity-novaja gruppa organizmov. (English translation in Internat. Geol. Rev., 8 (1966) : pp. 795-802).

Moore, R.C., Lalicker, C.G., Fischer, A.G., 1952. Invertebrate Fossils. McGraw-Hill Book Company, Inc., New York, 766p.

_____ (ed.), 1960. Treatise on Invertebrate Palaeontology, Part I, Mollusca 1. Geol. Soc. Am. and Uni. of Kansas Press, 351p.

Nitecki, M.H., 1972. North American Silurian receptaculitid algae. Fieldiana Geol., 28 : pp. 1-108.

Nye, P.B., 1926. The Limestone Quarries at Ida Bay. Unpubl. Rep. Dept. Mines. Tasm., 1926, pp. 203-211.

Opik, A.A., 1951. Notes on the stratigraphy and palaeontology of Cambrian, Ordovician and Silurian rocks in Tasmania. Bur. Min. Res. Geol. and Geophys. Recs., 1951-55.

Page, M.G., 1978. Sedimentology and Palaeoecology of the Upper Limestone Member, Benjamin Limestone. Unpubl. Hons. Thesis, Uni. of Tas.

Pierce, J.W. and Klootwyk, C.T., 1979 (*in press*). Discrepancies between the Indian and Australian Tertiary apparent polar wander paths.

Reineck, H.E. and Singh, I.B., 1975. Depositional Sedimentary Environments. Springer-Verlag, Berlin, 439p.

Rhoads, D.C., 1967. Biogenic working of intertidal and subtidal sediments in Barnstable Harbour, Massachussetts. J. Geol., 75 : pp. 461-476.

Robertson, W.A. and Hastie, L., 1962. A Palaeomagnetic study of the Cygnet Alkaline Complex of Tasmania. J. Geol. Soc. Aust., 8 : pp. 259-268.

Shimer, H.W. and Shrock, R.R., 1965. Index fossils of North America. Massachussetts Institute of Technology Press, Cambridge Massachussetts, 837p.

Shinn, E.A., 1968. Practical significance of birdseye structure in Carbonate Rocks. J.Sed.Petr., 38 : pp. 215-223.

Smith, P.J., 1973. Topics in Geophysics. MIT Press, Cambridge, Mass., 246p.

Spry, A., 1957. The precambrian dolomites of Tasmania. In Limestones in Tasmania, Tas. Geol. Surv. Miner. Res. 10 : pp. 32-38.

Teichert, C. and Glenister, B.F., 1952. Fossil nautiloid faunas from Australia. J. Paleont., 26 : pp. 730-752.

Teichert, C. and Glenister, B.F., 1953. Ordovician and Silurian cephalopods from Tasmania, Australia. Bull.Amer. Paleont., 34 (144).

Twelvetrees, W.H., 1915. The Catamaran and Strathblane Coalfields, and Coal and Limestone at Ida Bay. Tasm. Geol. Surv. Bull., 20.

Verhoogen, J., Turner, F.J., Weiss, L.E., Wahrhaftig, C., Fyfe, W.S., 1970. The Earth : an introduction to Physical Geology. Holt, Rinehart and Winston, Inc., USA, 748p.

Walker, K.R., 1972. Community ecology of the Middle Ordovician Black River Group of New York State. Geol. Soc. Am. Bull., 83 : pp. 2499-2524.

Webby, B.D., 1969. Ordovician stromatoporoids from New South Wales. Palaeontology, 12 : pp. 637-662.

_____ and Semeniuk, V., 1971. The Ordovician coral genus Tetradium Dana from New South Wales. Proc. Linn. Soc. N.S.W., 95 : pp. 246-259.

_____ and Banks, M.R., 1976. Clathrodictyon and Ecclimadictyon (Stromatoporoidea) from the Ordovician of Tasmania. Pap. Proc. Roy. Soc. Tasm., 110 : pp. 129-138.

Weldon, B.D., 1974. Carbonate Lithofacies and Depositional environments of the Gordon Limestone Subgroup, Florentine Valley. Unpubl. Hons. Thesis, Uni. of Tasmania.

Williamson, W.O., 1957. Silicified Sedimentary rocks in Australia. Am. Jour. Sci., 255 : pp. 23-42.

Wray, J.L., 1977. Calcareous Algae. Elsevier, Amsterdam, 185p.

Zijderveld, J.D.A., 1967. A.C. Demagnetisation of Rocks: analysis of results. In Collinson, D.W., Creer, K.M. and Runcorn, S.K. (eds.), Methods in Palaeomagnetism, Elsevier, Amsterdam, pp. 254-286.

Zijderveld, J.D.A., 1975. Palaeomagnetism of the Esterel Rocks. Doctoral Thesis, Rijksuniversiteit Utrecht., Krips Repro BV, Meppel, Netherlands, 199p. ("A palaeomagnetic picture-book").

oOo

APPENDIX VOLUME

CONTENTS

APPENDIX ONE

ECONOMIC GEOLOGY

No serious study of the limestones from an economic point of view was made during the present study, but since limestone is presently being quarried at Newlands Quarry the following observations suggested by the present study are offered for their potential usefulness.

It appears that limestone grade (i.e. percentage of $MgCO_3$ and $CaCO_3$ in a sample) is at least partially controlled by limestone type (lithofacies), as is intuitively to be expected. Forsyth and Green (1976) note that "drilling results in the main face show some continuity of zones of contrasting limestone grade, sub-parallel to the bedding." The fact that zones of a particular chemistry are not always strictly co-incident with lithological boundaries may result from the movement of diagenetic fluids through the sedimentary pile subsequent to deposition, but it is nevertheless clear that lithofacies distribution is at least a rough guide to the distribution of different economic grades of limestone.

The most obvious control on the grade of limestone is the amount of dolomite (Ca, $MgCO_3$) in them. Dolomite usually occurs in the limestones at Ida Bay in the form of burrow fillings, or as horizontal stringers and bands which are recognisable in the field

by their reddish or brown colour (sometimes grey on fresh surfaces) and their tendency to stand out on weathered surfaces because of their greater resistance to weathering (e.g. see Fig. 3:39). In principle, therefore, it should be possible to estimate the grade of limestone by visually estimating the percentage of dolomite in the rock.

For instance, Forsyth and Green (1976) record a low grade limestone in what they call "the Grey Band", which is a unit occurring just below 280 metres in the limestone section on Marble Hill (see Fig. 4:1). Although this band is a birdseye limestone unit (lithofacies I), it contains abundant algal-laminations. Algal-laminated limestones contain large quantities of dolomite (e.g., see Fig. 3:12) in the algal laminations, which explains the low $CaCO_3$ grade of the "grey band", and probably of other algal-laminated units.

On the grounds of visual estimation, then, it should in principle be true to say that limestones of lithofacies II, VII and perhaps sometimes IV and VI (see ch. 3, and Fig. 4:1) should have the lowest $CaCO_3$ grades, since they have the greatest volumetric proportions of dolomite. Conversely, lithofacies IX and X should have the highest $CaCO_3$ grades, since these beds have comparatively little dolomite. On this basis, the beds at the top of Newlands Quarry, being predominantly of lithofacies IX and X, should be of a high grade (see Figs. 4:1, 2:19).

In view of these possibilities it is suggested that it would be worthwhile conducting systematic analyses of limestones by lithofacies, to determine whether or not a correlation between lithofacies and chemical composition exists, and is sufficiently good to be of practical use in delineating areas of probable high grade limestone on field criteria. If a good correlation does exist, it could be expected to apply in other areas of Gordon Sub-group limestones in Tasmania as well.

It is probable that any correlation will be complicated by diagenetic phenomena, of which the most important is dedolomitisation. In the latter process dolomite is replaced by calcite ($CaCO_3$), but still retains the crystal form and macroscopic colour of dolomite. This means that much of the "dolomite" seen in the field may actually be dedolomite, so that the $CaCO_3$ grade of some limestones may be higher than the field appearance would lead one to suspect. Diagenetic phenomena such as dedolomitisation probably account for the fact that zones of constant limestone grade only approximately coincide with lithofacies distribution in Newlands Quarry, as noted by Forsyth and Green (1976).

A second chemical consideration which will be of importance for some uses of limestone relates to the occurrence of authigenic pyrite (FeS_2) in the limestone. Although it is always only present in low concentrations, it is more abundant than usual in the main lithofacies V unit at Blaneys Quarry, and in the lithofacies X unit at the top of Newlands Quarry, where it sometimes forms nodules up

to several centimetres diameter. Thus, whereas some beds may have a high $CaCO_3$ grade, their usefulness for some purposes may be reduced by their relatively high sulphur content, in the form of pyrite.

A final economic consideration concerns the thrust fault in Newlands Quarry (see section 2:12 of this thesis). In the upper, western parts of Newlands Quarry this fault has produced a wide zone of disrupted limestone blocks set in masses of clay and mud. Hence, this area of the quarry is difficult to work, and if future expansion of the quarry could avoid following the fault zone then quarry development would probably be rather cheaper than would otherwise be the case. Since the fault is only exposed on the face of Newlands Quarry, the strike of the fault is unknown. It appears likely, however, that the fault zone will extend southwards through the crest of the hill, since it is probably a Tabberabberan thrust developed with the folding of the limestones on Marble Hill. As such, the strike of the fault should parallel the north-south trending axis of the fold (see also section 2:12).

If this is the case, the cheapest means of expanding the quarry would be to follow high grade limestone beds southwards through the crest of the hill, staying to the east of the fault zone rather than trying to quarry west through it. In any case, since the beds in Newlands Quarry dip eastwards, and since the Permo-carboniferous unconformity is immediately above the western part of Newlands Quarry, it follows that any attempt to follow high

grade limestone beds by quarrying up-dip and towards the west would soon peter out when the high grade unit "ran up into" and was truncated by, the unconformity (see Fig. 2:10).

Drilling or exposure of further outcrops in the area south of Newlands Quarry should clarify the direction in which the thrust fault breccia zone extends.

APPENDIX TWO

FISSURE-FILLING SEDIMENTS IN LIMESTONE

The purpose of this appendix is to record the existence of a fissure-filling sediment in the limestones exposed in Newlands quarry. (Time limitations have precluded a proper study of these sediments, but they may be of interest to later workers). These sediments were noted at locations 7 and 11 in early 1979, and although both these outcrops have since been quarried away, similar deposits probably still exist nearby.

The sediments consist of red and pale green deposits, whose bedding varies from about 4cm thick to fine laminations less than a millimetre thick. Red and green beds may occasionally alternate. The sediment fills narrow fissures in the limestone, and the bedding of the sediment is essentially horizontal although somewhat undulose, and rises markedly against the Ordovician limestone enclosing the fissures. The sediment appears to have filled fissures which opened in response to movement of blocks of limestone, as is clearly indicated in Figure 7:2:1.

A typical specimen (48227 - See Figure 7:2:2) is a hard indurated rock consisting of fine reddish laminae intercalated between lighter coloured laminae of fine-grained calcite spar. The sparry laminae commonly lense out markedly over a centimetre or two, and show grading. It is probable that the reddish laminae represent

accumulations of insoluble material ("Terra Rossa"?) from the surrounding limestones, while the sparry laminae represent periods, perhaps brief as implied by their grading, when the fissures contained carbonate-saturated waters in which little insoluble material from the limestones was present, or in which it was abnormally diluted by water filling the fissures. Post-depositional bands of relatively coarse calcite have grown in the sediment, disrupting some of the depositional laminae. (As shown in Figure 7:2:2).

Specimen 48228 (see Figure 7:2:3) is a four centimetre thick coarsely graded bed in which large fragments of reddish and yellow-greenish sediment occur in a groundmass of fine to coarsely crystalline spar and other fragments. The large fragments have irregular shapes and ragged edges indicating a short distance of transportation. The fragments appear to be of the fissure-filling sediment, and so perhaps 48228 represents an intraformational conglomerate formed when an earth tremor or movement of loose country rock blocks around the fissure caused minor brecciation of the fissure-fill sediments.

A model which may explain this sediment is of a fissure, damp or with carbonate-saturated waters actually lying in it, wherein insoluble residues derived from the weathering of the surrounding and overlying limestones gradually accumulate. Occasional abnormally large influxes or accumulations of water would dilute the suspended insoluble residues, enabling deposition of a purer sparry calcite band. The alternation between greenish and reddish

layers of sediment may reflect alternating reducing and oxidising conditions, such that iron oxides formed under oxidising conditions would give a reddish colour to the red beds in the sediment.

There is no evidence presently available as to the age of the fissure-filling sediments. An interesting possibility, however, is that they may contain pollens, spores or even bones which would allow the dating of the sediments as well as perhaps furthering knowledge of the terrestial floras and faunas of Tasmania during whatever period the sediments do in fact represent.

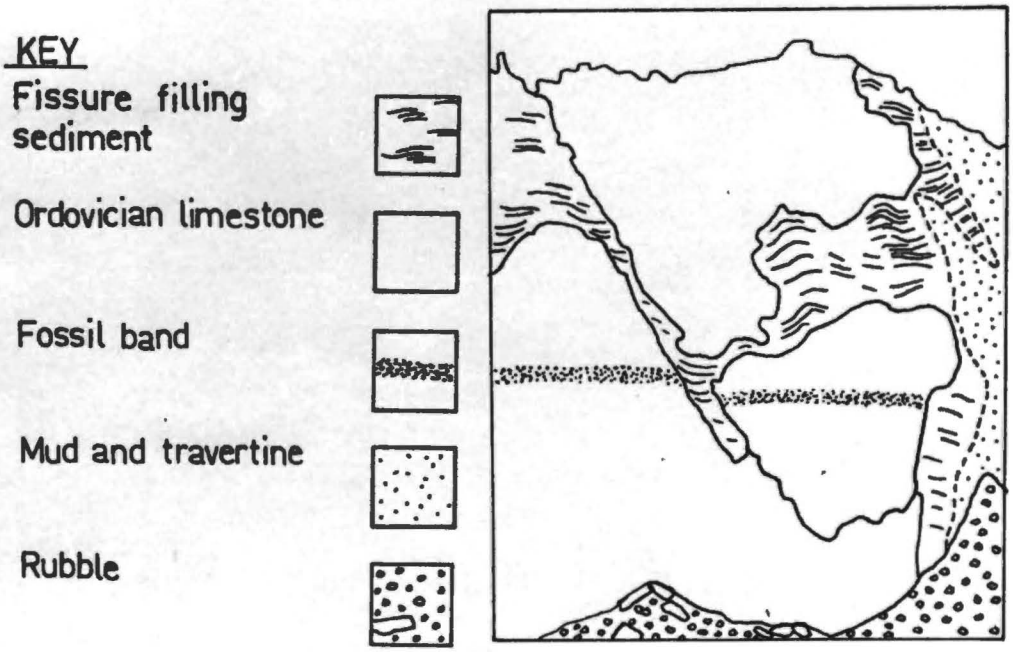

FIG. 7.2.1 Fissure-filling sediments, at location 7 in Newlands Quarry. Staff graduated in 10cm units. Note block which has slipped down, as indicated by fossil band.

FIG. 7:2:2 Laminated fissure-filling sediments from location 7. Dark laminae are composed of red sediment-probably insoluble residues from weathering of enclosing limestones - while pale laminations and lenses are composed of fine-grained spar. Note grading visible at top of spar laminations.
Note post-depositional spar band which has disrupted a dark lamination.
48227 Mag. x 4.5

FIG. 7:2:3 Intraformational conglomerate in fissure-filling sediment from location 7. Note fining upwards and irregular "ragged" shapes of intraclasts.
48228 Mag. x 3.5

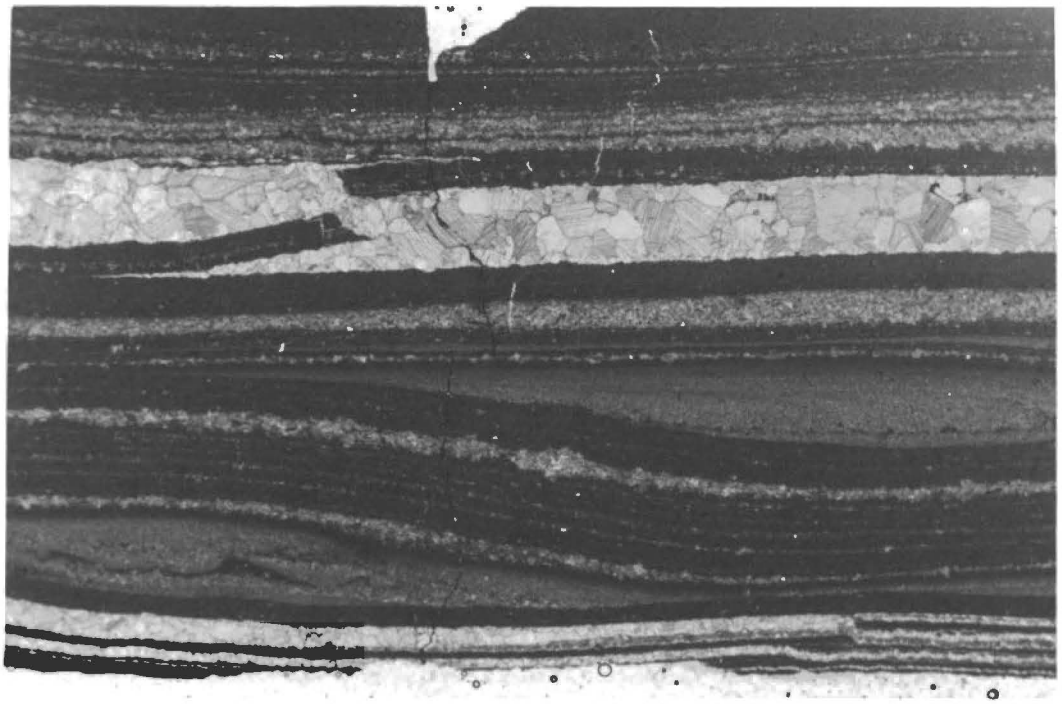

APPENDIX THREE

SYSTEMATIC PALAEONTOLOGY

Preparation of Material

Since palaeoecological analysis was not an aim of this project, no attempt was made to collect an unbiased cross-section of the biota present in the limestones and quartzites at Ida Bay.

Limestone samples from subtidal and intertidal beds were dissolved in 0.1N acetic acid, and the residues sieved through a 30 or 40 mesh sieve to catch large particles, and a 100 or 120 mesh sieve to catch conodonts and fine particles. Silicified macrofossils were sometimes obtained from these specimens, but only rarely was a specimen dissolved specifically to obtain silicified macrofossils. Hence, brachiopods and molluscs are poorly represented in the faunas documented herein.

Rubber moulds of Early Ordovician gastropods in quartzite were prepared by coating the gastropod casts with latex. Since the quartzites were not first impregnated with a binding substance, removal of the rubber moulds commonly caused quartz grains to be pulled away from the rock, resulting in a lack of fine detail in the moulds, and partial destruction of the original specimens. Impregnation of sandy sediments prior to preparation is strongly recommended to future workers for this reason.

Cephalopods and some Calathids were slabbed and polished, but the majority of specimens studied were examined in thin section. (In a few cases, acetate peels prepared by the method of Katz and Friedman (1964) were used). As a result, a large proportion of the fossils studied are Corals, Algae, Bryozoans and Stromatoporoids.

Photography

A fine coating of Magnesium oxide was applied to silicified specimens and rubber moulds by holding the specimens in MgO produced by burning magnesium ribbon. Non-silicified specimens were similarly coated after cleaning with chisels and vibro-tools.

Photographs of specimens were taken with a Wild Heerbrugg M400 Photomakroscop, with illumination being provided by an Intralux 150H Volpi goose neck fibre optics unit, and a fibre optics ring illuminator. Ilford FP4 black and white film was used, and specimens larger than 2cm x 2cm were photographed in sections.

Thin sections and Acetate peels were photographed with the same microscope and film, using a transmitted light stage to hold and illuminate the specimens.

Identification

Gastropods, cephalopods, brachiopods, trilobites, corals and stromatoporoids were identified by the use of the Treatise of Invertebrate Palaeontology, volumes J, K, H, O, F. B. Stait, J. Laurie and K. Kenna assisted with identification of cephalopods,

brachiopods and corals, respectively. Coral identification was assisted by the use of Hill (1955), Webby and Semeniuk (1971), and a manuscript by Dr M.R. Banks, Key to Australian Ordovician Corals.

Calcareous algae were identified with the assistance of Johnson and Hoeg (1961), and Receptaculitids with the assistance of written communication with M. Nitecki (Field Museum of Natural History, Chicago). Miagkova (1965), Alberstadt and Walker (1976) and Wray (1977) were also consulted regarding the Receptaculitids. The classification scheme used herein for the Receptaculitids is mainly based on Nitecki (1972, in Wray 1977, p. 102). The classification of the Receptaculitids is still in a state of flux, but M. Nitecki (written communication, 1979) has placed Tasmanian Ordovician Receptaculitids in the genus *Calathium*, rather than the genera *Receptaculites* and *Ischadites* into which they have variously been placed by previous workers in Tasmania.

Shimer and Shrock (1965) was also consulted in regard to gastropods, and Webby (1969) in regard to stromatoporoids.

Brief descriptions of fossil forms studied in the Limestone and underlying quartzite at Ida Bay are given on the following pages, with reference to photographic plates found within this appendix.

Notes on Fossils

With the exception of Prosobranch A (c.f. *Hormotoma*), all gastropods described in this appendix were obtained from Early Ordovician Quartzites on the Hogsback and at Location 14.

The two trilobites described herein are from loose specimens: Bumastinae A was found loose at the top of the exposures of location 10, while Pliomerinid A was found in a large block on the floor of Newlands Quarry (about 265 metres - see Fig. 4:1), and must therefore be derived from somewhere in the section above that point.

Conodonts were only identified in one specimen (98372), which contained *Panderodus gracilis*, c.f. *Tasmanognathus careyi*, *"Plectodina"* or *"Aphelognathus" Florentina* sp. nov., and *Phragmodus* c.f. *undatus*. Identification was carried out by Dr C.F. Burrett.

A few scolecodonts and sponge spicules were found in limestone residues dissolved to extract conodonts.

PHYLUM RHODOPHYTA

Class RHODOPHYCEAE

Order CRYPTONEMIALES

Family SOLENOPORACEAE

genus Solenopora 98316 PLATE I (A,B)

Rounded nodular to basally elongate thalli, 20-100mm or more in diameter, with concentric growth zones. Tissue composed of closely packed radiating threads of cells. Walls of threads thicker than partitions separating cells in a thread, and partitions commonly do not occur at the same level in adjoining cell threads.

PHYLUM CHLOROPHYTA

Class CHLOROPHYCEAE

Order DASYCLADALES

Family RECEPTACULITACEAE

genus Calathium 98317, 98318, 98319, 98320 PLATE I (C,D,E,F)

(M.Nitecki (written comm., 1979) indicates that Tasmanian receptaculitaceans previously placed in the genera *Receptaculites* and *Ischadites* are in fact Calathids).

Conical thallus, having two walls separated by thin lateral rods. Lower part of outer wall forms cone diverging at smaller angle than upper part. Inner wall has circular pores arranged rhombohedrally; outer wall has pores partially covered by skeletal plates. Lateral rods attached to inner surface of outer wall and outer surface of inner wall by enlarged heads arranged rhombohedrally.

Specimen 98319 is similar to *Calathium*, and is tentatively placed in that genus.

genus Calathium new form. 98013 PLATE II (A,B)

Calathium with three walls instead of the usual two. At top of specimen, outer cone 53mm diameter, middle cone 32mm diameter, and inner cone 14mm diameter (all measured from outer wall surface to outer wall surface). Preserved part of thallus about 40mm high. Middle and inner wall appear to diverge from a single wall at base of preserved part of thallus. Lateral rods span spaces between inner and middle walls, and middle and outer walls.

PHYLUM ARTHROPODA

Class TRILOBITA
Order ILLAENIDA
Family ILLAENIDAE

Bumastinae A 98323

Only pygidium known. Pygidium smooth and convex, with no axial furrows or terrace lines on upper surface. Slight flattening at edges to form flange, upper surface and doublure mould have shallow sagittal furrow. Pygidium 40mm wide between antero-lateral corners (which is maximum width), and 34mm long.

Order PHACOPIDA
Family PLIOMERIDAE
Subfamily PLIOMERINAE

Pliomerinid A 98324 PLATE II (C)

Thorax 9.5mm wide, 10mm long, with 11 segments. Pygidium 7mm wide across antero-lateral corners, and 5mm long. Pygidium with five axial rings.

PHYLUM MOLLUSCA

Class CEPHALOPODA

Subclass MAUTILOIDEA

Order MICHELINOCERATIDA

Family PROTEOCERATIDAE

genus c.f. Tofangoceras 98326 PLATE II (D)

Longiconic orthocone, Phragmocone surficially annulated, of subcircular section. Siphuncle relatively large, between centre and venter, with central sparry calcite column representing possible siphuncular canal. Episeptal cameral deposits well developed.

genus c.f. ?Ephippiorthoceras 98325 PLATE II(E)

Longiconic orthocone. Siphuncle between centre and venter. Well developed cameral deposits, parietal deposits grow adorally to form near-complete siphuncular lining.

Class GASTROPODA

Subclass PROSOBRANCHIA

Prosobranchid A 98327, 98328 PLATE III (A)

Shell high spired, with seven or more whorls. Whorls rounded with relatively deep sutures.

This genus is comparable to *Murchisonia (Hormotoma)*. The specimens occur in birdseye limestone horizons only, and Page (1978) obtained better specimens of a similar gastropod from birdseye limestones in the Florentine Valley. He assigned his specimens to *M. (Hormotoma)*.

Prosobranchid B 98329 PLATE III (B,C)

Orthostrophic, spire very low, almost flat. Base with wide conical umbilicus. Whorls deep, flattened above acutely sub-angular periphery. Whorl profile curves inward below sub-angular periphery at upper outer edge of whorl.

Genus c.f. *Ophileta*, but umbilical sutures absent or not seen.

Prosobranchid C 98330 PLATE III (D)

Orthostrophic, low spire, subrounded angulation on central upper whorl surface.

Order ARCHaeogastropoda
Suborder MACLURITINA
Superfamily EUOMPHALACEA
Family HELICOTOMIDAE

Helicotomide A 98331, 98332, 98333, 98334, 98335, 98336 PLATE III (E,F,C,H,I)

Shell orthostrophic and conispiral. Spire a low cone. Small elevated Carina at outer edge of upper whorl surface, with concave surface just above it. Transverse growth lines sweep forward from inner part of whorl to carina on outer part of whorl. Shell diameter varies from 11mm - 28mm.

Genus c.f. *Orospira*, but tubercles not present and lower outer part of whorl not as rounded.

PHYLUM BRACHIOPODA

Class ARTICULATA

Order STROPHOMENIDA

Family STROPHOMENIDAE

Furcitelloid Strophamenid A 98337, 98338 PLATE IV (A,B,C,D)

Biconvex costellate shell. Pedicle valve with large foramen, but pseudodeltidium not seen. Brachial valve has two large cardinal process lobes projecting posteriorly. Median ridge present, transmuscle septa well developed with curved sub-median septa.

Subfamily c.f. Furcitellinae.

Order ORTHIDA

Family PLECTORTHIDAE

Plectorthid A 98339 PLATE IV (E,F)

Brachial valve unknown. Pedicle valve with large interarea and coarse plications.

PHYLUM COELENTERATA

Class ANTHOZOA

Order RUGOSA

Rugosan A 98340 PLATE IV (G)

Solitary corallite, 9.5mm outside diameter. Walls 1mm thick. Septa in two orders, 25 septa in each order. First order septa 2mm long, second order septa 0.35mm long. Two small corallites budding off outside of corallite in specimen 98340.

Similar to *Brachyelasma*, except for thick nature of walls and presence of budding corallites.

Rugosan B 98341 PLATE IV (H)

Solitary corallite 7mm outside diameter. Walls 1mm thick. Septa in two orders, 23 septa in each order. First order septa 0.7mm long, second order septa 0.3mm long. No axial structures developed.

Similar to Brachyelasma, except for thick nature of walls.

Superfamily ZAPHRENTICAE

Family STREPTELASMATIDAE

genus Streptelasma 98342 PLATE V (A)

Solitary corallite 10mm diameter, wall 1mm thick. Septa long, sometimes seen to be of two orders. First order septa coalesce to form irregular axial structure. (34 first order septa)

Suborder CYSTIPHYLLINA

Family TRYPLASMATIDAE

genus Tryplasma

species T. ceriodes 98343 PLATE V (B,C)

Ceriod corallites up to 9.5mm in diagonal diameter. Numerous (40in 8mm dia. corallite), short (0.3mm long), septal spines of a single order, spaced alternately in adjoining corallites. Tabulae usually complete and slightly up-arched, sometimes with dissepiments. Tabulae regularly spaced 2-3mm apart.

This species has been previously described from Ida Bay by Hill (1955).

Order TABULATA
Family AULOPORIDAE
Subfamily SYRINGOPORINAE

genus Bajgolia
species B. caespitosa 98344, 98345 PLATE V (D)

Corallites 1.5-2mm diameter, walls 0.4 - 0.7mm thick. Corallites in ramose branches 3-5mm thick. Corallites polygonal at branch axes.

species B c.f. furcata 98346 PLATE V (E)

Corallum forms discrete branches 5-8mm diameter. Corallites round to polygonal in axial region of corallum. Corallites 0.8-1.2mm diameter, wall of individual corallites 0.2-0.3mm thick. Diffuse dark median zone between adjoining corallite walls. Rare Tabulae.

Almost identical to *B. furcata*, except for slightly smaller size of some corallites. Similar to *B. contiqua*, but fewer tabulae.

Family HELIOLITIDAE
Subfamily COCCOSERIDINAE

genus Pycnolithus 98347, 98345 PLATE V (F)

Encrusting corallum with slender tabularia, 0.3mm diameter, separated by thick coenenchyme. Tabularia crossed by simple concave-upwards tabulae.

Family SYRINGOPHYLLIDAE
Subfamily BILLINGSARIINAE

genus Foerstephyllum 98348 PLATE V (G, H)

Corallum massive, corallites 1.5-2.0mm diameter with 18-20 spines, of one order. Walls straight or slightly curved in

transverse section. Tabulae spaced about six per 5mm, usually up-arched to occasionally flat or irregular.

Species similar to *F. minutum*, but walls insufficiently curved, and tabulae more regular up-arched form than in *F. minutum*.

Family FAVOSITIDAE
Subfamily FAVOSITINAE

genus Palaeofavosites
species P.poulseni 98349, 98350 PLATE VI (A, B)

Rare mural pores of angles of walls. Tabulae not flat, variable in form. Spines abundant and well developed. Corallites <2mm diameter.

Family CHAETETIDAE
Subfamily ?LICHENARIINAE

genus ?Lichenaria 98351, 98352 PLATE VI (C, D)

Corallites about 0.4mm diameter, of round to irregular shape with rare septum-like projections into corallite space (maximum one per corallite-probably incomplete walls). Walls slightly undulose in longitudinal section.

Subfamily TETRADIINAE

genus Tetradium
species T. apertum 98353 PLATE VI (E, F)

Corallum an irregular mesh of corallites arranged in chains and bundles. Corallites average 1.2mm diameter, are subquadrate with slight indentations of outer wall at sites of septa. Walls ~0.05 thick.

c.f. T. halysitoides group.

species T. c.f. syringoporoides 98354, 98355 PLATE VI (G,H,I)

Corallites subquadrate, 1.5mm to 2.0mm diameter, usually single, spaced approx. 5mm apart. Walls 0.2mm thick, septa about 0.15mm thick.

Corallites thicker than T. c.f. syringoporoides described by Hill (1955), but otherwise specimens are very similar.

species T. bowanense 98356, 98357 PLATE VI (J, K)

Subquadrate corallites 0.8-1.0mm diameter, in sub-rounded to sub-quadrate branches 2-4mm dia. Four to 16 corallites arranged in parallel rows within branch. Corallites with sub-quadrate outlines, varying to sub-rounded in thicker walled specimens (e.g. 98356).

Differentiated from *T. dendroides* on grounds of small branch diameter and neat arrangement of corallites in rows. Differentiated from *T. variabile* on grounds of smaller branch diameter, shorter septa, and lack of branches with more than sixteen corallites.

species T. variabile 98358 PLATE VII (A)

Corallum 6mm diameter, corallites 0.8-1.1mm diameter, with sediment-filled lacunae on periphery of branch. Corallites sub-quadrate with walls 0.1-0.05mm thick. (single corallite). Septa have marked axial taper, extend at least 2/3 of corallite radius, sometimes joining at axis. Second order septa developed rarely.

species T. tenue 98359 PLATE VII (B)

Corallum of isolated intermeshed corallites, each of which may diverge into four new corallites. Corallites sub-quadrate, or rounded immediately after divisions. Corallites usually 1.0-2.5mm diameter.

species T.sp.A. 98360, 98361, 98362 PLATE VII (C)

Corallites usually single, may occur in bundles of 2 or 4. Corallites 0.8-2.0mm diameter, subquadrate to subrounded, with walls 0.3-0.2mm thick. Septa taper rapidly, reaching inwards 1/2 to 2/3 of corallite radius.

Similar to *T. duplex*, but corallites too big and walls too thick.

Order STROMATOPOROIDEA

Family AULACERIDAE

Aulacerid A 98363 PLATE VII (D)

Coenosteum with large axial canal 8mm diameter divided into chambers by strongly arched tabulae. Canal surrounded by 5mm layer of vesicular tissue.

Family LABECHIIDAE

genus c.f. Cystostroma 98364 PLATE VII (E)

Coenosteum laminar with some hemispherical forms. Laminated appearance imparted by latilamellae of vesicular tissue alternating with pelletal or dolomitic micrites. Transverse skeletal elements composed of vesicular tissue - "cysts". Cysts average 0.8mm long, 0.2-0.3mm high. Pillars poorly developed, astrorhizae not seen.

PHYLUM BRYOZOA

Class GYMNOLAEMATA

Order TREPOSTOMATA

Bryozoan A 98365, 98366, 98367 PLATE VIII (A,B)

Zoarium ramose, 7-13mm diameter. Zooecia polygonal, with subrounded corners. Zooecia average 0.2-0.3mm diameter. Zooecia trend parallel to Zoarium axis in centre of Zoarium, but curve in exterior parts of zoarium to open laterally. Walls of zooecia thicken markedly towards exterior (varying from 0.01mm thick in zoarium axis to 0.09mm thick at exterior surface). Diaphragms usually complete and flat, but may be incomplete disseppiments. Diaphragms average 0.1mm apart along zooecium axis.

Bryozoan B 98368 PLATE VIII (C, D)

Similar to Bryozoan A, except diaphragms only present in terminal 0.7mm of Zooecia. ("Mature" part of zoarium).

Bryozoan C 98369 PLATE VIII (E, F)

Zoarium ramose, 5-7mm diameter. Zooecia average 0.2mm diameter, round to slightly irregular in cross-section. Zooecia may be in tangential contact, or up to 0.2mm apart. Zooecia open laterally to exterior. Diaphragms simple, flat or slightly up-arched, average 0.1mm apart. Acanthopores present in exterior parts of Zoarium.

Bryozoan D 98370 PLATE VIII (G, H)

Zoarium massive, irregular oval shape, 45mm across long axis. Zooecia polygonal with subrounded corners, 0.3-0.2mm diameter. Diaphragms mostly flat, complete, 0.1mm apart in longitudinal section. Diaphragms may be curved and/or incomplete in some cases.

Order CRYPTOSTOMATA

genus Stictopora 98365, 98369

Lenticular Zoarium, 2.7mm x 1.2mm overall dimensions. Zoarium bifolate, Zooecia average 1.5mm diameter.

PLATE I - ALGAE

A. Solenopora - 98316 Longitudinal section

B. Solenopora - 98316 Transverse section

C. Calathium - 98317 Transverse section

D. Calathium - 98317 Longitudinal section, showing cross-section of outer wall, and tangential section of inner wall. Note rhombohedrally arranged pores in inner wall.

E. Calathium - 98318 Transverse section, showing cross-section of outer wall. Lateral rods, and pores in outer wall, are visible. Note Crinoid Ossicle next to *Calathium*.

F. ?Calathium - 98319 Transverse section of probable *Calathium*, showing perforated inner wall, lateral rods, and recrystallised outer wall.

PLATE I - ALGAE

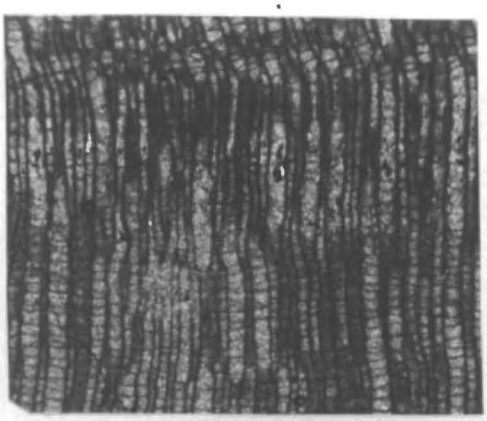

A

2mm

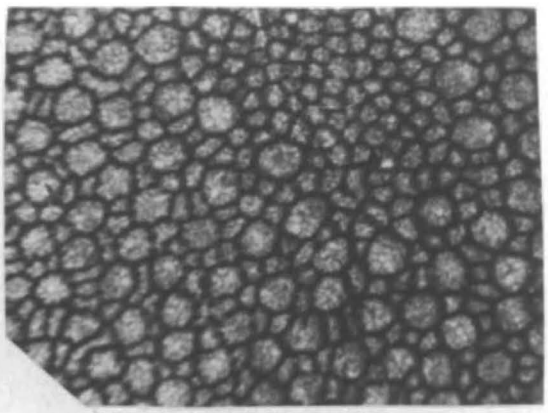

B

1mm

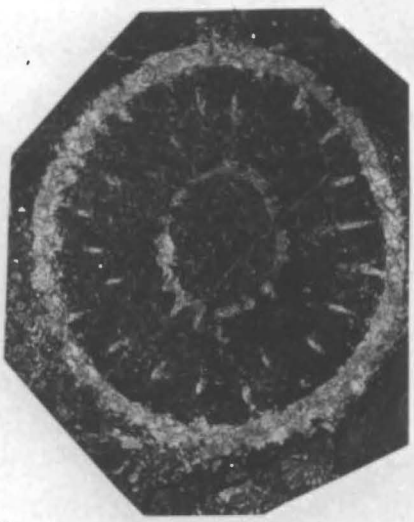

C

10mm

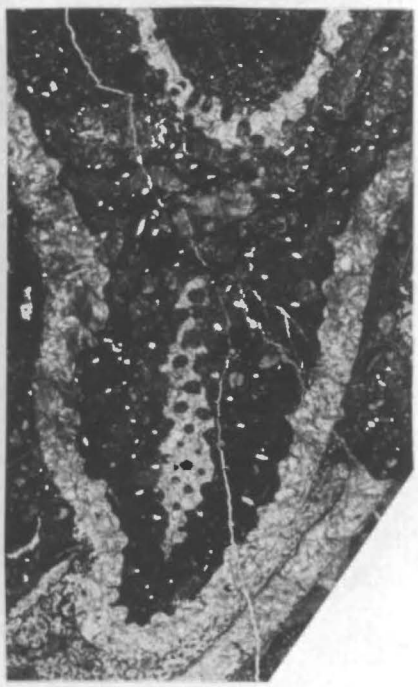

D

10mm

E

1mm

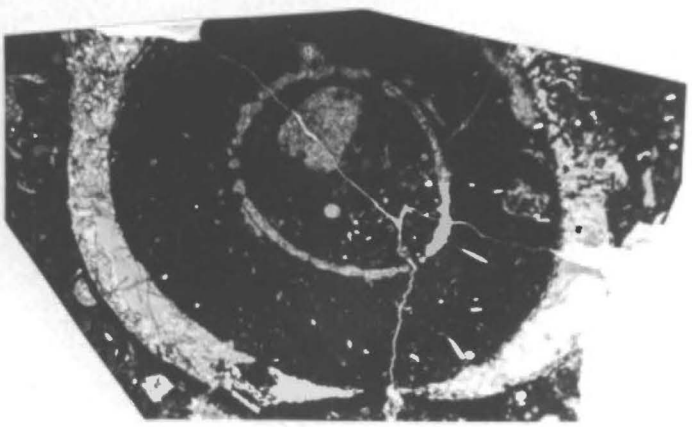

F

10mm

PLATE II - ALGAE, TRILOBITA, CEPHALOPODA

A. Calathium (new form) - 98013 Transverse section near top of specimen. Note presence of three walls, with enlarged heads on each wall for attachment of lateral rods.

B. Calathium (new form) - 98013 Transverse section near bottom of specimen. Note Lateral rods between middle and outer walls. Inner and middle walls are united into one wall at the top of this section, which is cut slightly oblique to a plane perpendicular to thallus axis.

C. Pliomerinid A - 98324 Pygidium, Thorax and small portion of Cephalon.

D. c.f. Tofangoceras 98326 Tracing of photo. Stipple represents spar deposits, including cameral deposits and ?siphuncular canal.

E. c.f. ?Ephippiorthoceras - 98325 Tracing of photo, stipple represents spar deposits. Parietal deposits indicated diagrammatically.

PLATE II - ALGAE, TRILOBITA, CEPHALOPODA

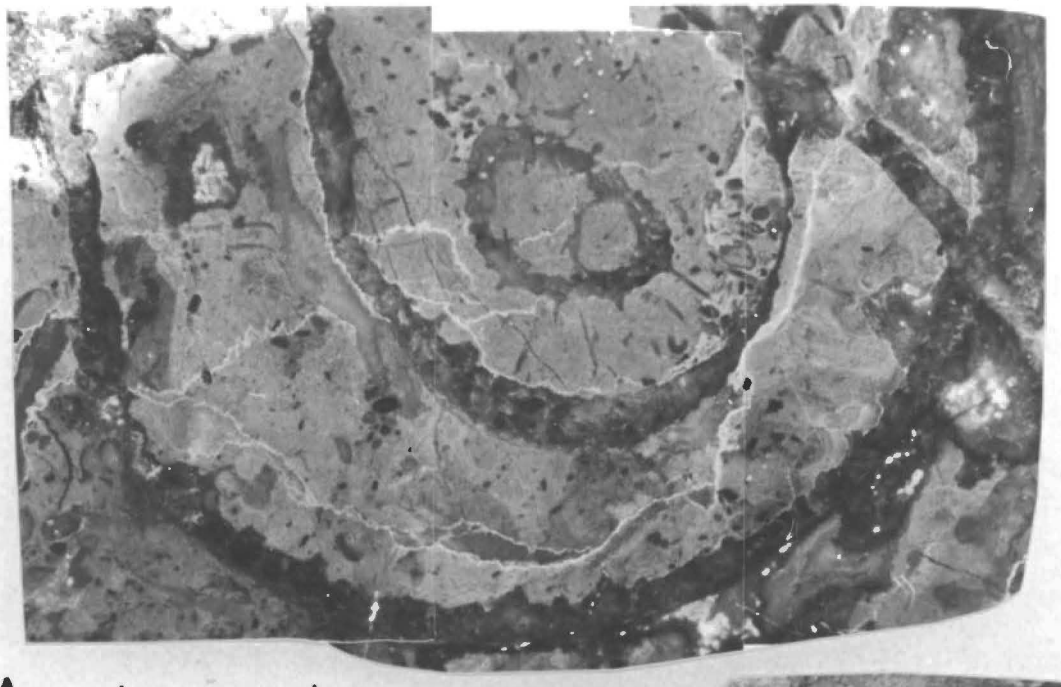

A

10mm

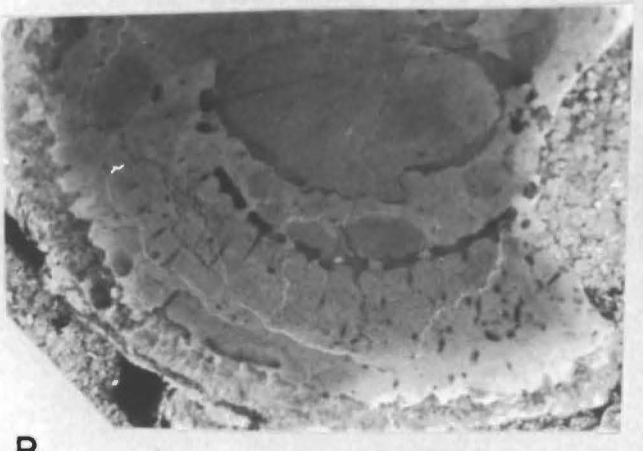

B

10mm

C

2mm

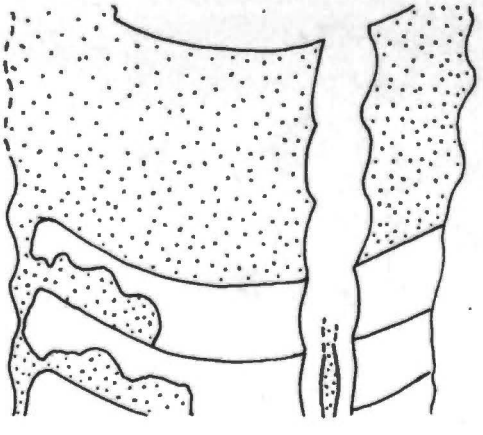

D

10mm

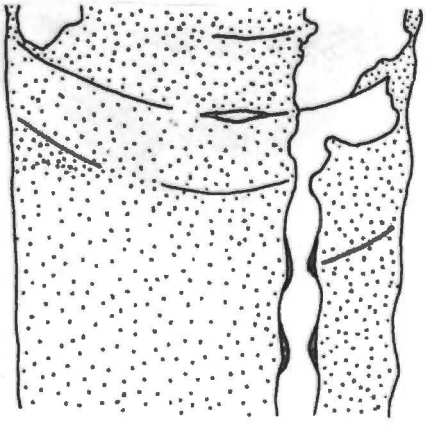

E

5mm

PLATE III - GASTROPODA

A. Prosobranch A — (c.f. Hormotoma) - 98327 Cross-section, slightly away from coiling axis.

B. Prosobranch B — (c.f. Ophileta) - 98329 Lateral view, showing very low spire and shape of whorl. Rubber mould.

C. Prosobranch B — (c.f. Ophileta) - 98329 Dorsal view. Rubber mould.

D. Prosobranch C — 98330 Dorsal view. Rubber mould.

E. Helicotomide A — 98333 Lateral view, showing carina. Rubber mould.

F. Helicotomide A — 98334 Dorsal view. Rubber mould.

G. Helicotomide A — 98334 Lateral view, showing whorl profile. Rubber mould.

H. Helicotomide A — Drawing of reconstructed shell.

I. Helicotomide A — 98332 Dorsal view of whorl surface, showing growth lines. Rubber mould.

PLATE III - GASTROPODA

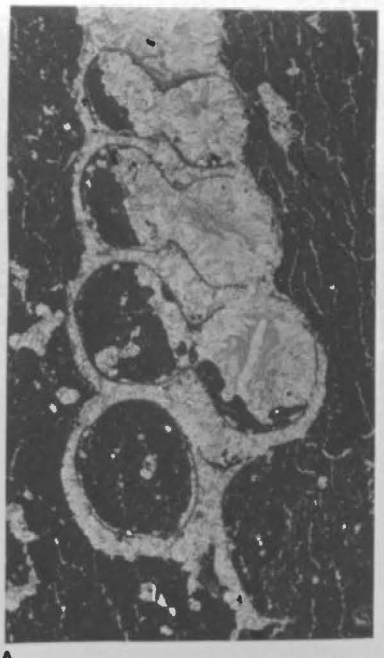

A

10mm

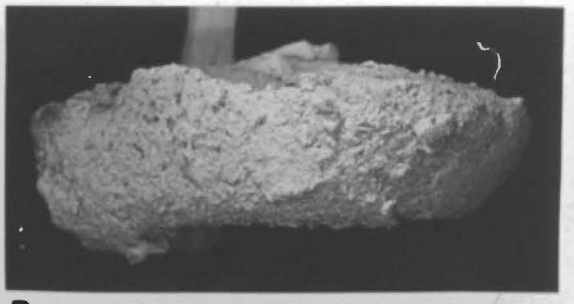

B

5mm

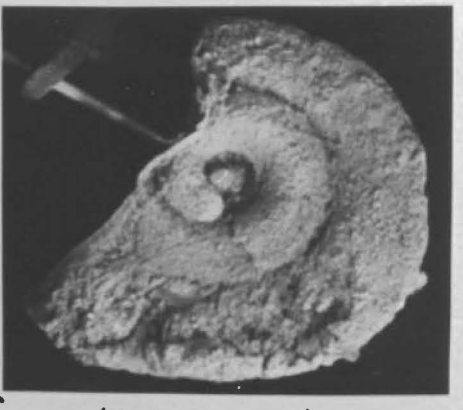

C

10mm

E

10mm

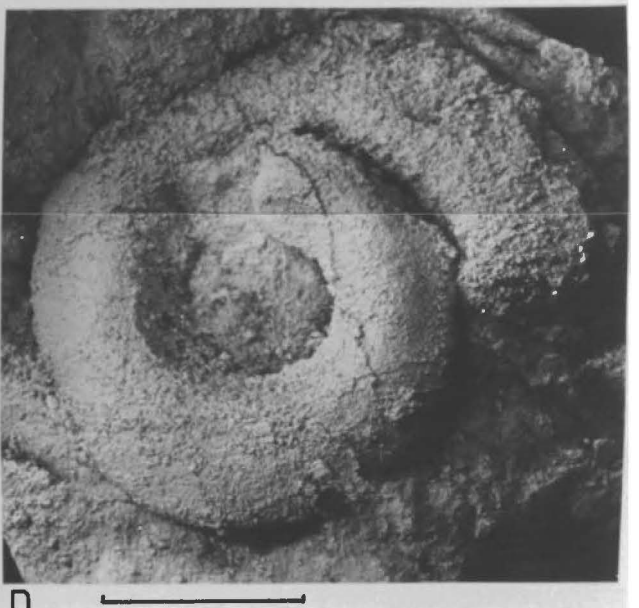

D

10mm

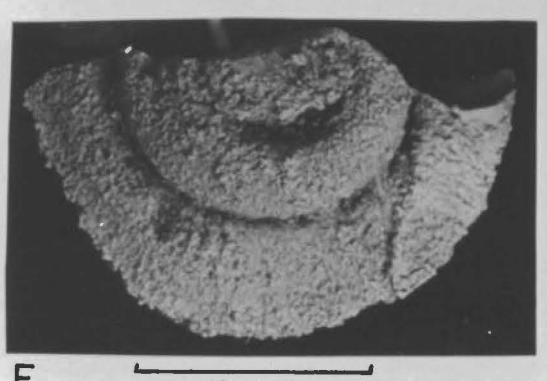

F

10mm

G

10mm

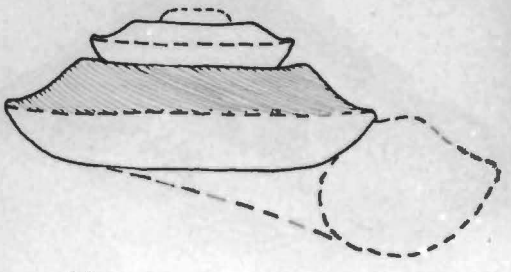

H

I

10mm

PLATE IV - BRACHIOPODA, COELENTERATA

A. Furcitelloid Strophamenid A - 98337
Brachial Valve, internal

B. Furcitelloid Strophamenid A - 98337
Brachial Valve, external

C. Furcitelloid Strophamenid A - 98337
Pedicle Valve, internal

D. Furcitelloid Strophamenid A - 98337
Pedicle Valve, external

E. Plectorthid A - 98339
Pedicle Valve, internal

F. Plectorthid A - 98339
Pedicle Valve, external

G. Rugosan A - 98340
Transverse Section, showing two budding corallites

H. Rugosan B - 98341
Transverse Section

PLATE IV - BRACHIOPODA, COELENTERATA

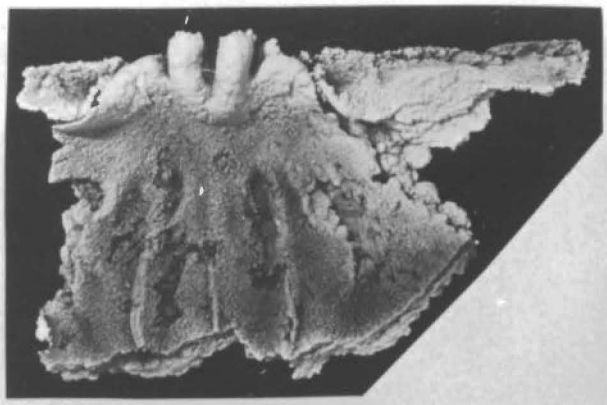

A

5mm

B

5mm

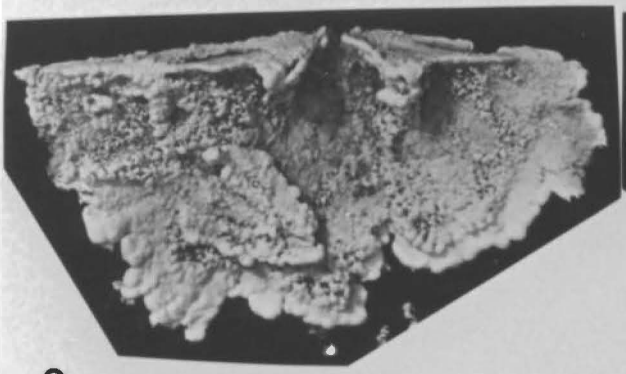

C

5mm

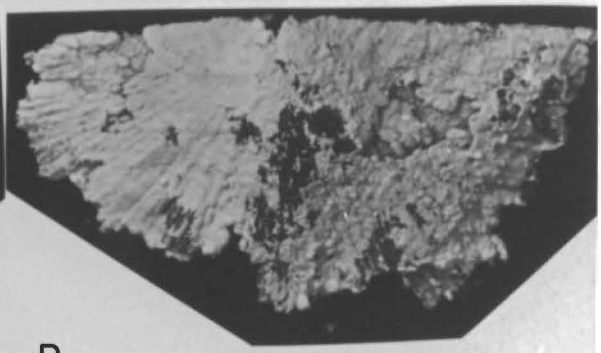

D

5mm

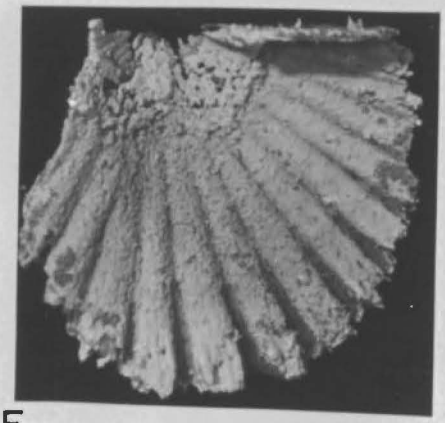

E

5mm

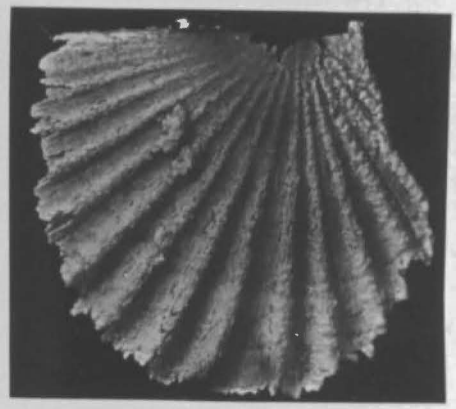

F

5mm

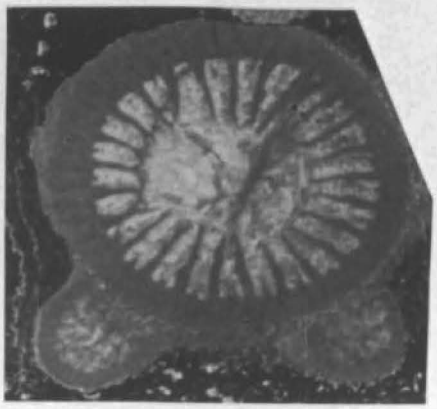

G

5mm

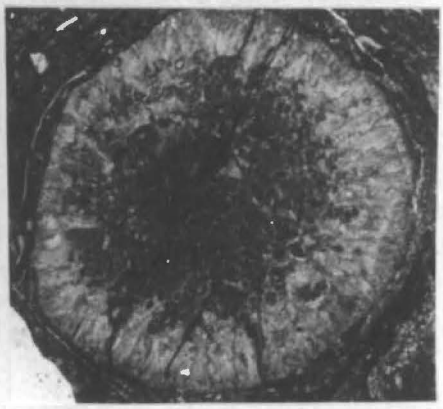

H

5mm

PLATE V - COELENTERATA

A. Streptelasma - 98342 Transverse Section

B. Tryplasma ceriodes - 98343 Transverse Section

C. Tryplasma ceriodes - 98343 Longitudinal Section. Note disseppiments near base of photo.

D. Bajgolia caespitosa - 98344 Transverse/oblique sections

E. Bajgolia c.f. furcata - 98346 Longitudinal section of corallum

F. Pycnolithus - 98347 Longitudinal section

G. Foestephyllum - 98348 Transverse section

H. Foestephyllum - 98348 Longitudinal section

PLATE V -COELENTERATA

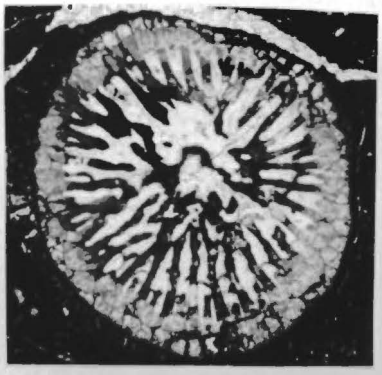

A 5mm

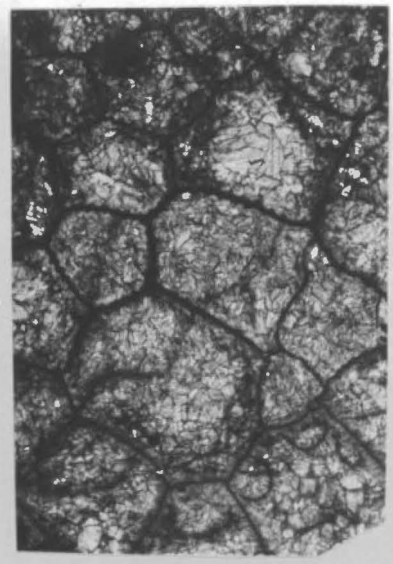

B 10mm

C 10mm

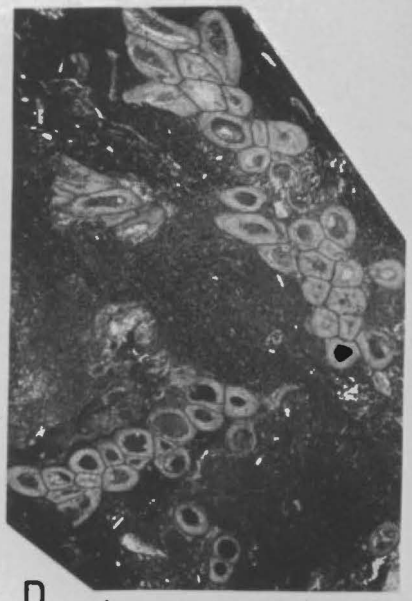

D 10mm

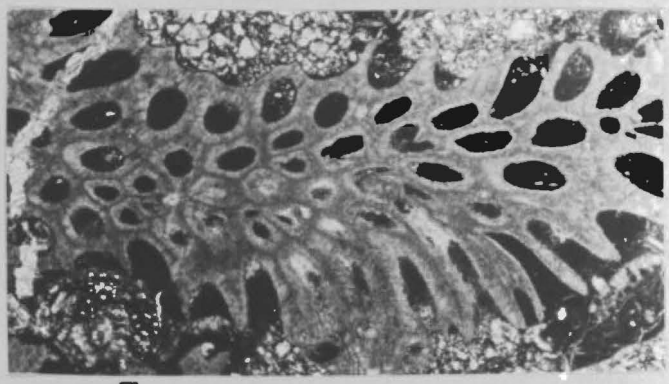

E 5mm

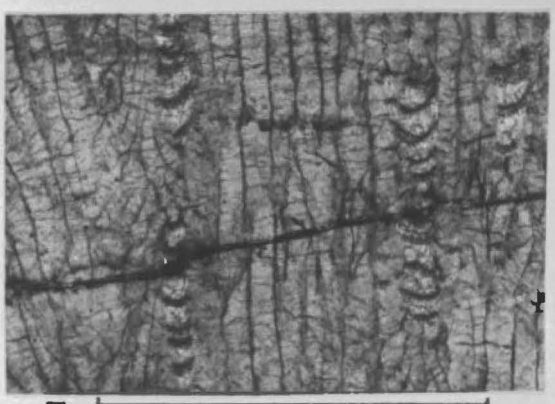

F 5mm

H 5mm

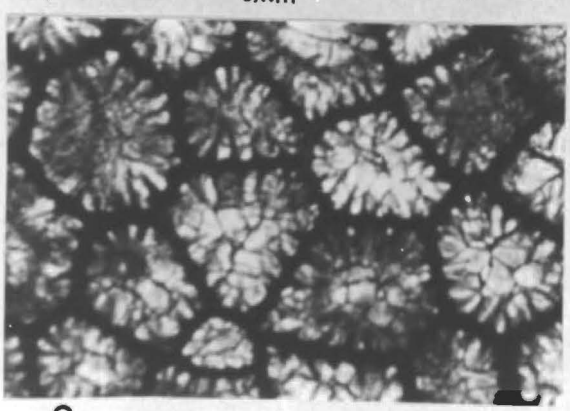

G 1mm

PLATE VI - COELENTERATA, TETRADIUM

A. Palaeofavosites poulseni - 98349 Transverse section

B. Palaeofavosites poulseni - 98350 Longitudinal section

C. ?Lichenaria - 98352 Transverse section, showing incomplete walls

D. ?Lichenaria - 98352 Longitudinal section

E. Tetradium apertum - 98353 Longitudinal section

F. Tetradium apertum - 98353 Transverse section. Note corallite at upper left, in which filling is still unrecrystallised

G. Tetradium c.f. syringoporoides 98354

H. Tetradium c.f. syringoporoides 98354 Transverse section of corallite with partially recrystallised infilling. Diagonal corallite diameter : 1.6mm

I. Tetradium c.f. syringoporoides 98355 Transverse section

J. Tetradium bowanense - 98357 Transverse section

K. Tetradium bowanense - 98356 Transverse section

PLATE VI -COELENTERATA,TETRADIUM

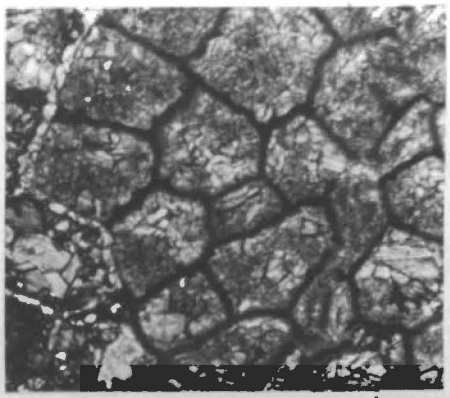

A

5mm

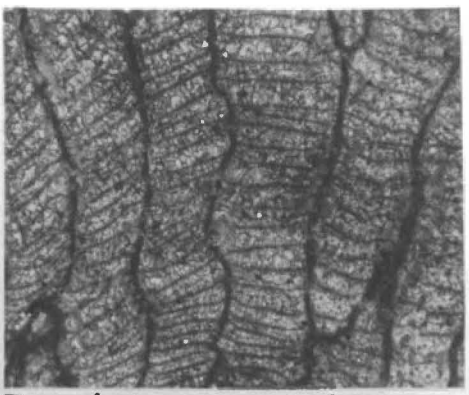

B

5mm

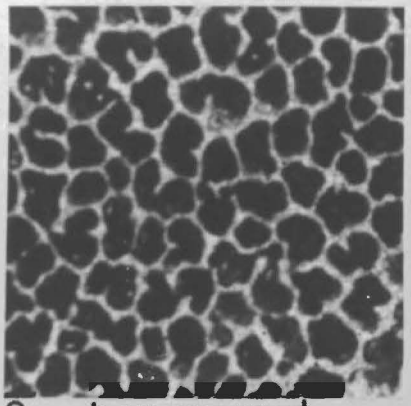

C

2mm

D

2mm

E

5mm

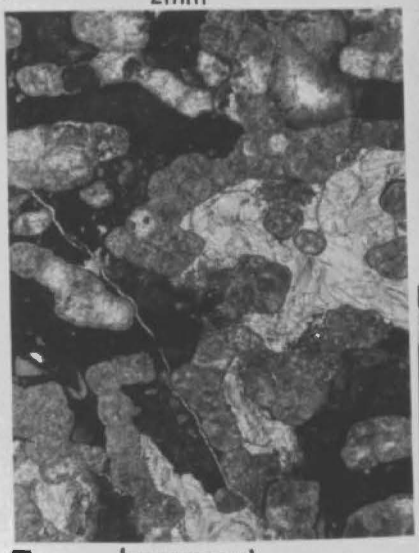

F

5mm

H

1mm

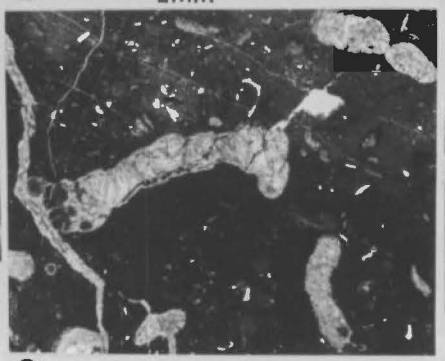

G

5mm

I

1mm

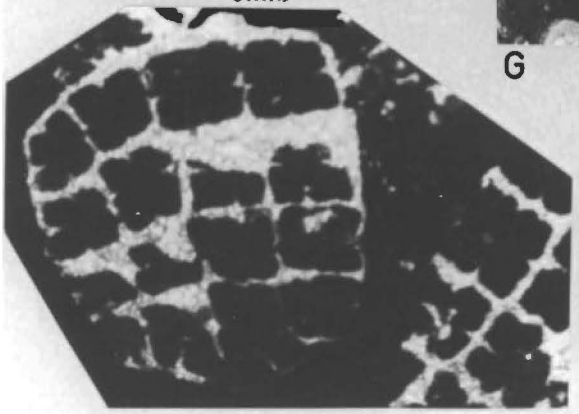

J

5mm

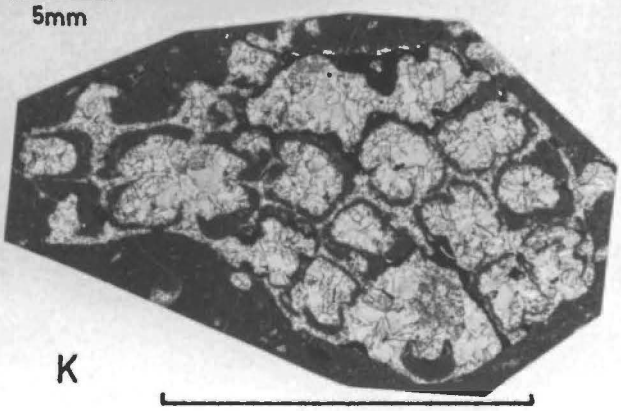

K

5mm

PLATE VII - TETRADIUM, STROMATOPOROIDEA

A. Tetradium variabile - 98358 Transverse section

B. Tetradium tenue - 98359 View of intermeshed corallites. Note subquadrate cross-section of corallites prior to division, and rounded cross-section immediately after division (e.g. upper right of photo)

C. Tetradium sp. A. - 98360 Transverse section

D. Aulacerid A - 98363 Longitudinal section of axial canal, surrounded by vesicular tissue

E. c.f. Cystostroma - 98364 View normal to latilaminae, showing cysts and lamination of pelletal mud.

PLATE VII -TETRADIUM, STROMATOPOROIDEA

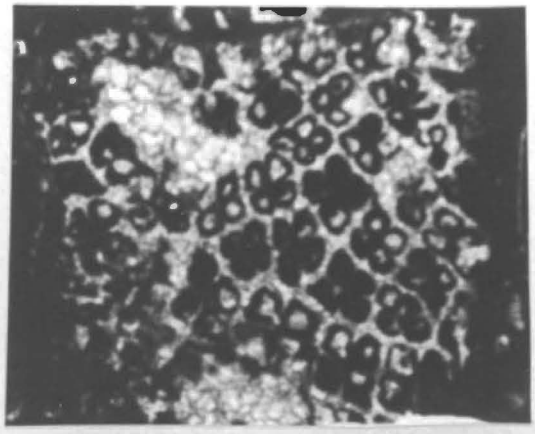

A

5mm

B

10mm

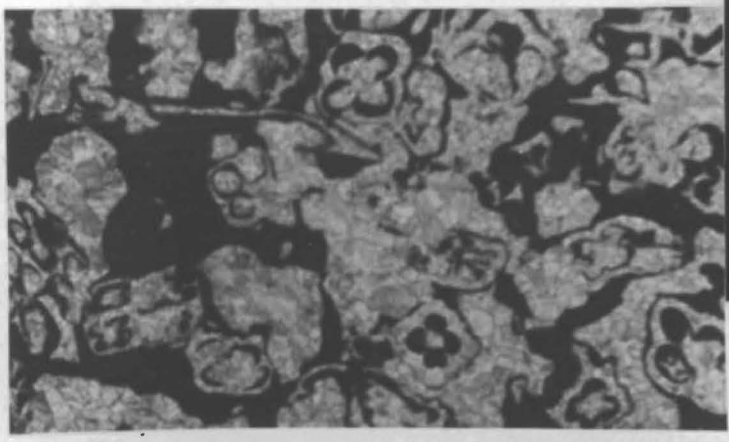

C

5mm

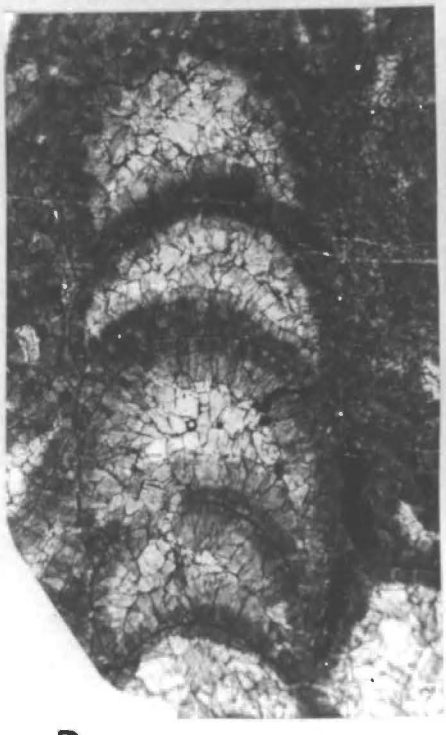

D

5mm

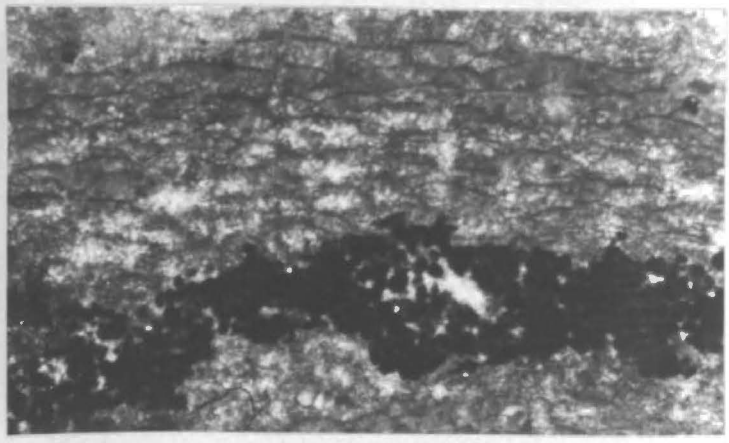

E

2mm

PLATE VIII - BRYOZOA

A. Bryozoan A - 98365 Transverse Section of Zoarium encrusted by organism similar to *Pycnolithus* or *Coccoseris*

B. Bryozoan A - 98366 Longitudinal section of Zoarium

C. Bryozoan B - 98368 Longitudinal section of Zoarium

D. Bryozoan B - 98368 Tracing of lower portion of illustration C, above

E. Bryozoan C - 98369 Longitudinal section of Zoarium

F. Bryozoan C - 98369 Oblique section of Zoarium. Note separation of Zooecia, particularly on margin of Zoarium

G. Bryozoan D - 98370 Transverse section

H. Bryozoan D - 98370 Longitudinal section

PLATE VIII - BRYOZOA

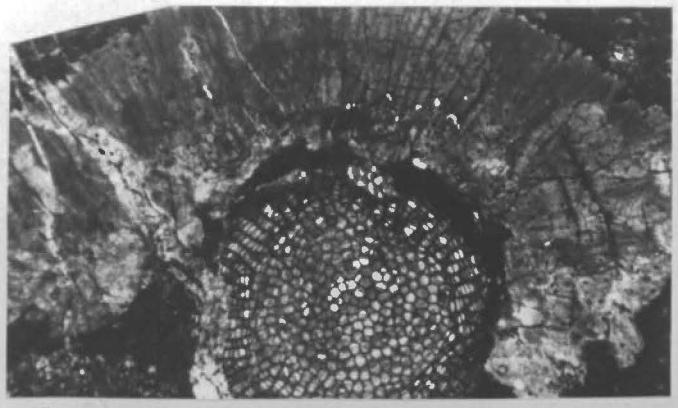

A

10mm

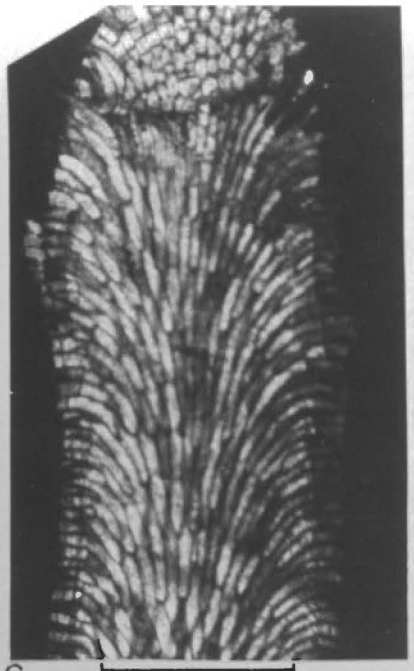

C

5mm

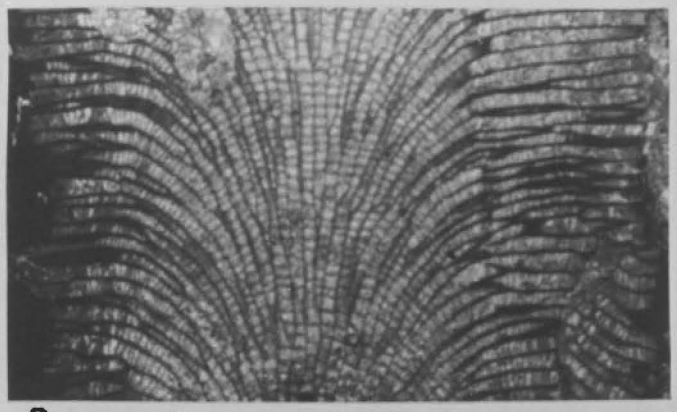

B

5mm

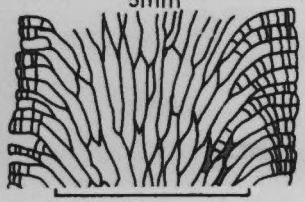

D

5mm

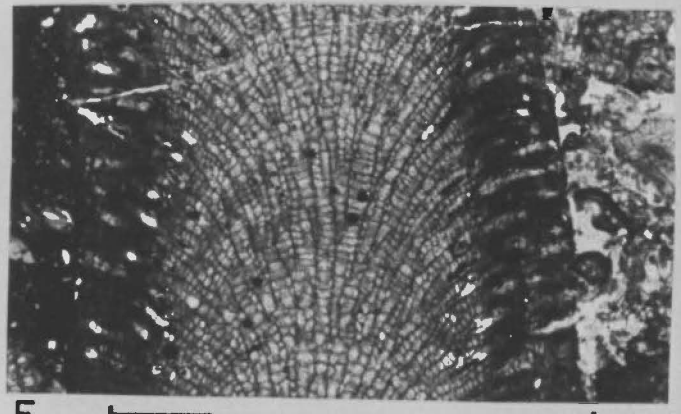

E

5mm

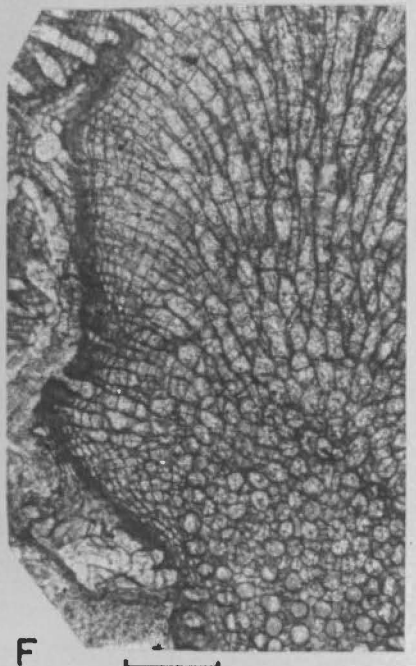

F

1mm

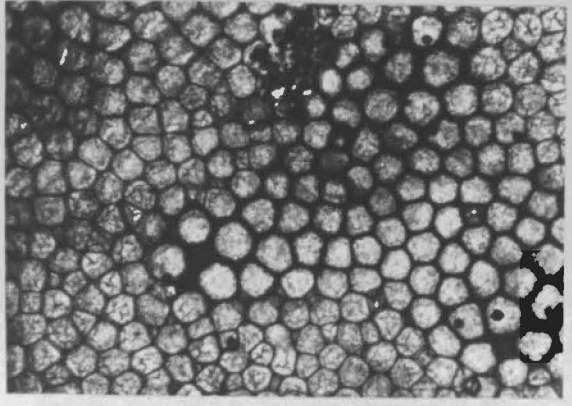

G

2mm

H

2mm

APPENDIX 4

FIELD CORRECTED NRM DIRECTIONS

The following pages are photocopies of parts of a computer printout listing the NRM directions of all cores measured. The left hand column gives an abbreviation of the specimen number (see also section 5:3 of this thesis) wherein "IB" is used instead of "SIB", and the first digit of the number is deleted. Numbers between 65.11 and 91.41 are in the 200 range (e.g. "65.11" is 265.11), while numbers between 03.11 and 24.41 are in the 300 range.

The NRM directions are specified by Declination and Inclination (DECL and INCL columns, respectively) according to the conventions specified in section 5:2 of this thesis. NRM directions are field corrected, so that they are oriented with respect to present-day horizontal and true north.

The column headed "INTENS" gives the total magnetic intensity (in e.m.u. x 10^{-6}) of the NRM in each core, while the column headed "JCM3*10^{-6}" gives the corrected intensities in e.m.u. x $10^{-6}/cm^3$. (Calculated on the assumption of a volume of 10.5 cm^3 for each core, which is close to the truth).

	DECL	INCL	INTENS	JCM3*10-6
1865.11	345.85	-77.72	142.985	13.6176
1865.21	353.44	-78.47	230.012	21.9059
1865.31	344.59	-78.78	173.603	16.5336
1865.41	350.85	-79.73	137.918	13.1351
1866.11	334.45	-82.41	212.744	20.2613
1866.21	343.35	-82.62	185.181	17.6362
1866.31	342.64	-81.18	181.361	17.2725
1866.41	343.68	-79.80	91.5491	8.7190
1867.11	336.80	-86.07	167.986	15.9987
1867.21	332.79	-86.50	199.697	19.0187
1868.11	12.18	-76.78	92.9930	8.8565
1868.21	21.62	-74.20	80.2841	7.6461
1869.11	58.77	-78.93	103.772	9.8831
1869.21	64.01	-79.07	100.407	9.5626
1869.22	51.39	-80.67	104.934	9.9937
1869.31	56.52	-78.87	81.4283	7.7551
1870.11	4.29	-84.23	90.4878	8.6179
1870.21	11.34	-83.37	100.981	9.6173
1870.31	14.81	-83.10	98.7111	9.4011
1870.41	357.52	-82.42	100.929	9.6123
1871.11	4.89	-72.79	55.3629	5.2727
1871.21	12.02	-73.42	58.0750	5.5310
1871.31	9.98	-72.55	45.9425	4.3755
1871.41	5.36	-72.47	55.8341	5.3175
1872.11	36.25	-70.31	45.2756	4.3120
1872.21	34.93	-69.02	50.6338	4.8223
1872.31	37.25	-69.25	43.4352	4.1367
1872.41	38.84	-71.28	63.2558	6.0244
1873.11	15.90	-80.33	89.6232	8.5355
1873.12	23.46	-80.22	40.3036	3.8384
1873.21	21.42	-75.55	66.7501	6.3571
1874.11	42.63	-75.01	37.1350	3.5367
1874.21	32.30	-74.41	40.5268	3.8597
1874.31	34.43	-74.91	45.9849	4.3795
1874.41	36.78	-74.01	46.8073	4.4578
1875.11	243.72	-65.35	65.1985	6.2094
1875.21	244.69	-66.11	54.5167	5.1921
1875.31	249.27	-68.03	56.5098	5.3819

	DECL	INCL	INTENS	JCM3*10-6
IB75.41	253.00	-67.54	49.9152	4.7538
IB76.11	12.03	-73.53	51.7040	4.9242
IB76.21	21.71	-75.84	45.8658	4.3682
IB77.11	9.50	-78.17	135.496	12.9043
IB77.21	6.06	-77.54	155.764	14.8347
IB77.31	1.31	-77.56	244.792	23.3135
IB77.41	10.85	-77.62	328.691	31.3039
IB78.21	352.98	-73.62	77.2415	7.3563
IB78.31	352.59	-72.44	148.652	14.1573
IB78.41	358.95	-72.71	140.065	13.3395
IB79.11	0.92	-70.67	166.319	15.8399
IB79.21	357.73	-70.30	167.912	15.9917
IB79.22	356.41	-68.22	156.376	14.8929
IB80.11	343.83	-66.26	53.1676	5.0636
IB80.12	342.10	-65.99	80.5805	7.6743
IB80.21	339.25	-63.97	79.6304	7.5839
IB80.31	336.45	-65.22	71.0481	6.7665
IB81.11	338.44	-63.76	59.4829	5.6650
IB81.21	350.69	-61.14	55.7172	5.3064
IB81.31	343.03	-66.65	53.2129	5.0679
IB81.41	343.12	-64.82	53.3396	5.0800
IB82.11	326.89	-71.57	47.0008	4.4763
IB82.21	340.48	-72.43	85.2654	8.1205
IB82.31	332.96	-71.40	44.8437	4.2708
IB83.11	63.20	-77.63	145.605	13.8672
IB83.21	56.22	-77.03	111.769	10.6447
IB83.31	55.20	-78.05	86.4852	8.2367
IB83.41	64.52	-77.70	86.9693	8.2828
IB84.11	106.53	-80.31	155.738	14.8322
IB84.21	103.42	-78.76	119.705	11.4005
IB84.22	114.78	-76.60	191.575	18.2452
IB85.11	28.77	-72.91	108.296	10.3139
IB85.21	27.41	-74.28	190.148	18.1093
IB85.31	35.26	-72.45	167.295	15.9329
IB85.41	35.73	-74.41	129.996	12.3806
IB86.11	22.79	-81.54	50.3762	4.7977
IB86.12	8.01	-80.13	50.9107	4.8486
IB86.21	12.73	-81.82	50.2821	4.7888
IB86.31	21.17	-82.68	50.2348	4.7843

	DECL	INCL	INTENS	JCM3*10-6
IB87.11	21.05	-73.56	41.0010	3.9049
IB87.21	18.02	-72.97	25.3225	2.4117
IB88.11	1.69	-83.36	47.1605	4.4915
IB88.21	32.86	-80.08	49.9369	4.7559
IB88.31	34.35	-79.55	50.5226	4.8117
IB89.11	24.16	-73.89	48.3946	4.6090
IB89.21	23.16	-73.72	43.4757	4.1405
IB89.31	27.48	-73.78	30.0965	2.8663
IB90.11	11.56	-83.15	40.8773	3.8931
IB90.21	15.98	-83.00	47.4802	4.5219
IB90.31	13.37	-81.41	45.5841	4.3413
IB90.41	10.98	-81.26	41.4426	3.9469
IB91.11	23.11	-72.82	39.9045	3.8004
IB91.21	17.74	-74.77	41.7010	3.9715
IB91.31	32.09	-73.71	40.2591	3.8342
IB91.41	26.50	-74.30	38.1163	3.6301
IB03.11	17.62	-83.02	36.2091	3.4485
IB03.21	16.01	-81.65	38.4010	3.6572
IB03.31	19.27	-82.69	36.0800	3.4362
IB03.41	13.90	-83.06	39.3292	3.7456
IB04.11	37.32	-77.49	64.0588	6.1008
IB04.21	33.08	-77.11	39.3666	3.7492

	DECL	INCL	INTENS	JCM3*10-6
IB05.11	12.39	-78.52	30.7343	2.9271
IB05.21	354.40	-79.61	24.9991	2.3809
IB05.31	21.11	-83.09	23.3254	2.2215
IB05.41	17.06	-78.24	29.5511	2.8144
IB06.11	13.85	-71.18	121.898	11.6093
IB07.11	353.33	-79.14	13.8379	1.3179
IB07.21	340.82	-79.29	41.3166	3.9349
IB07.31	7.32	-79.06	21.4563	2.0435
IB07.41	342.48	-79.42	27.7559	2.6434
IB08.11	358.59	-77.29	38.1932	3.6375
IB08.21	354.93	-76.95	47.0171	4.4778
IB08.31	355.01	-79.32	38.3353	3.6510
IB08.41	359.11	-77.95	41.9569	3.9959
IB10.11	98.20	-69.53	46.3443	4.4137
IB10.21	87.40	-71.07	58.2403	5.5467
IB10.31	89.74	-69.96	47.8336	4.5556
IB10.41	91.91	-69.24	56.4598	5.3771
IB11.11	341.00	-71.75	51.4139	4.8966
IB11.21	342.66	-70.78	47.3935	4.5137
IB11.31	346.46	-69.81	55.3078	5.2674
IB11.32	343.41	-70.69	53.9812	5.1411
IB12.11	4.71	-66.18	51.4031	4.8955
IB12.21	9.10	-67.32	53.8417	5.1278
IB12.31	2.52	-71.26	54.3671	5.1778
IB13.11	28.93	-74.79	138.755	13.2147
IB13.12	31.40	-75.14	156.735	14.9271
IB13.21	30.68	-73.75	183.938	17.5179
IB13.22	32.03	-75.49	171.286	16.3130
IB14.11	27.64	-74.50	157.947	15.0426
IB14.21	27.12	-73.89	157.933	15.0412
IB14.31	32.76	-74.85	159.015	15.1443
IB14.41	32.93	-75.31	160.622	15.2973
IB15.11	28.50	-70.89	112.861	10.7487
IB15.12	29.13	-71.74	110.820	10.5543
IB15.21	34.53	-73.62	109.543	10.4326
IB15.31	28.37	-73.60	115.369	10.9875
IB16.11	53.43	-67.93	133.139	12.6799
IB16.21	55.89	-65.32	144.985	13.8081
IB16.31	56.38	-63.65	140.557	13.3864

	DECL	INCL	INTENS	JCM3*10-6
1816.41	59.59	-63.96	129.185	12.3033
1817.11	27.08	-73.23	170.043	16.1945
1817.21	28.24	-73.76	169.036	16.0986
1817.31	25.96	-69.07	159.580	15.1981
1817.41	22.34	-74.46	168.636	16.0606
1818.11	39.72	-72.72	115.232	10.9745
1818.21	38.04	-75.34	114.088	10.8655
1818.31	38.33	-75.50	112.156	10.6815
1818.41	42.93	-76.55	97.0197	9.2400
1819.11	40.94	-83.91	204.243	19.4517
1819.21	49.92	-81.61	199.710	19.0200
1819.31	37.76	-82.89	191.304	18.2195
1819.32	51.76	-81.32	235.694	22.4470
1820.11	3.56	-74.45	245.014	23.3347
1820.21	6.97	-74.40	258.554	24.6242
1820.31	8.25	-75.53	234.555	22.3386
1820.41	4.10	-76.18	230.054	21.9099
1821.11	40.52	-79.81	261.758	24.9294
1821.21	37.90	-79.75	261.633	24.9174
1821.31	41.01	-79.13	245.305	23.3624
1821.41	45.79	-77.95	246.292	23.4564
1822.11	22.04	-76.24	114.386	10.8939
1822.21	244.48	-70.13	96.7340	9.2128
1822.31	14.95	-75.00	127.407	12.1340
1822.21	15.92	-74.74	116.474	11.0928
1822.41	9.12	-76.21	129.437	12.3273
1823.11	30.94	-71.15	45.3632	4.3203
1823.21	23.09	-68.46	46.8284	4.4598
1823.31	33.09	-68.82	38.8163	3.6968
1823.32	32.72	-66.59	43.7573	4.1674
1824.11	2.10	-78.48	59.6599	5.6819
1824.21	0.74	-77.11	45.3239	4.3166
1824.31	3.91	-76.00	45.4028	4.3241
1824.41	353.91	-79.81	57.3530	5.4622

APPENDIX 5

SECONDARY COMPONENT OF MAGNETISATION

The following is a listing of the directions of the secondary component of magnetisation measured in those cores which were subjected to thermal demagnetisation. This listing includes the rare cases in which two components were mistakenly defined in a core (see section 5:3 of this thesis). The listing is split into two groups, representing the first and second demagnetisation runs. (see Sect. 5:3).

The listing comprises specimen number, the temperatures between which the component is represented by a straight or near-straight line on the Zijderveld plots, and the direction of the component in terms of Inclination and Declination. (Field corrected as in Appendix 4). The column giving the temperature steps defining the component is headed "COMPONENT", and the temperatures are in degrees celsius. Inclination and Declination are given in degrees.

First Demagnetisation Run

Specimen	Component	Inclination	Declination
SIB303.11	250-400	-85	277
303.11	400-475	-55	300
304.11	200-250	-81	2
305.11	250-350	-83	308
306.11	350-520	-72	20
307.21	25-300	-79	16
307.21	250-350	-78	286
308.21	150-250	-81	357
310.11	150-300	-78	359
310.11	400-500	-66	175
311.11	250-350	-79	319
312.11	150-250	-78	10
312.11	400-510	-70	232
313.11	150-400	-78	14
314.11	150-400	-78	0
315.11	150-400	-77	20
316.11	150-400	-75	47
317.11	150-400	-81	21
318.31	150-400	-79	24
319.11	200-300	-88	303
320.11	150-400	-80	25
321.11	150-400	-84	13
322.11	150-300	-82	0
323.11	150-400	-79	24
324.11	150-300	-77	358
265.31	150-350	-78	0
266.21	150=250	-81	348
267.21	150-400	-83	328
268.21	200-400	-84	37
269.11	200-400	-82	108
270.11	150-300	-79	10
271.11	200-350	-80	0
272.11	150-300	-79	26
273.21	300-450	-85	228
274.21	200-350	-81	16
275.11	150-400	-76	22
276.11	200-350	-81	0
277.21	200-350	-80	20
278.21	200-400	-79	357
279.11	200-400	-78	8
280.11	150-300	-64	345
281.11	200-350	-72	6
282.31	150-250	-62	339
282.31	300-450	-73	30
283.31	150-250	-80	43
284.11	200-350	-83	90

Specimen	Component	Inclination	Declination
SIB285.11	200-350	-86	67
286.11	150-300	-82	23
287.11	200-350	-80	52
288.21	150-300	-81	10
289.11	150-300	-80	21
290.11	150-250	-82	17
291.11	150-250	-84	29
	Second Demagnetisation Run		
SIB303.21	250-350	-84	307
304.21	250-450	-87	335
305.21	250-350	-82	323
307.31	250-350	-82	282
308.31	250-350	-79	278
310.21	250-350	-79	324
311.21	250-350	-80	324
312.21	250-350	-77	340
313.12	200-430	-77.5	18
314.21	200-450	-76	1
315.12	200-350	-78	18
316.21	200-400	-73	48
317.21	250-400	-80	32
318.41	200-350	-79	27
319.32	250-400	-87	314
320.21	250-400	-80	29
321.21	250-430	-82	10
322.21	200-430	-81	3.5
323.21	250-400	-78	18.5
324.41	200-350	-77	348
265.41	250-400	-81	0
266.11	250-400	-81	346
267.11	250-400	-83.5	334
268.11	300-440	-88.5	48
269.21	300-400	-83	112.5
270.21	200-430	-81	12.5
271.41	250-400	-81	347
272.21	200-250	-75	23
273.21	250-350	-85.5	3.5
274.31	250-350	-81	18.5
275.21	200-400	-74.5	23
277.11	250-400	-82.5	11
278.31	250-430	-76.6	0
279.21	300-430	-77	9.5
280.21	200-350	-63	348
281.21	200-400	-68	21
282.21	250-430	-78	4.5
283.11	200-400	-78.5	51

Specimen	Component	Inclination	Declination
SIB284.22	250-430	-82.5	106
285.21	200-400	-85	54.5
286.12	200-350	-84	18.5
287.21	200-400	-79	33
288.11	200-350	-81.5	21
289.21	200-350	-81	28
290.21	200-350	-85.5	3
291.21	250-440	-85	19.5

APPENDIX SIX

NUMBERED LOCATIONS

During the course of field work certain locations were numbered, and some of these are referred to by their numbers in this thesis. The following is a listing of the numbered locations, giving the number, grid reference (see chapter 1) and comments about each location. The locations in Newlands Quarry are also marked on Figs. 2:20 and 4:7. Some of these locations (in quarries) have been marked in the field by a yellow number spray-painted onto the rock.

Location 1 DM88808732
Section measured up from eastern end of Newlands Quarry floor.

Location 2 DM88488737
Section measured up from western end of Newlands Quarry floor.

Location 3 DM88478736
Section at western end of Newlands Quarry.

Location 4 DM88508735
Section at western end of Newlands Quarry.

Location 5 DM88578732
Section at western end of Newlands Quarry.

Location 6 DM88458732
Westernmost part of Newlands Quarry.

Location 7 DM88528730
Section in western part of Newlands Quarry.

Location 8 DM88588726

Section in upper western part of Newlands Quarry.

Location 9 DM88728729

Section in upper middle part of Newlands Quarry.

Location 10 DM88848731

Section in uppermost exposure on eastern side of Newlands Quarry.

Location 11 DM88608724

Section across thrust fault breccia zone on upper western side of Newlands Quarry.

Location 12 DM88608720

Section immediately above and to south of Location 11. In early 1979 this was the uppermost working face in Newlands Quarry, but it has since been quarried away.

Location 13 DM87759325

Outcrop of ?Early Ordovician quartzite on west branch of the North Lune Road.

Location 14 DM88249082

Quarry on South Lune Road, exposing ?Early Ordovician quartzites with gastropods.

Location 15 DM88009185

Outcrop of Ordovician limestone on the Lune River.

Location 16 DM87549458

Small quarry in ?Early Ordovician quartzites on the north west side of the Hogsback.

Location 17 DM87328765

Section measured up western part of Blaneys Quarry.

Location 18 DM87458766

Section measured up eastern part of Blaneys Quarry.

Location 19 DM87378765

Section measured in middle of upper part of face at Blaneys Quarry.

Location 20 DM88688767 to DM88758745

Section measured up the access road to Newlands Quarry. Upper end of section is immediately below level of main floor of quarry.

Location 21 DM87658752 to DM87608778

Section measured through about 300 metre length of Entrance Cave. (i.e. from near cave bottom to entrance).

APPENDIX SEVEN

SPECIMEN CATALOGUE

The following is a listing of specimens submitted with this thesis. These specimens are housed in the rock and fossil collections of the Geology Department of the University of Tasmania.

The following abbreviations refer to preparations submitted with the specimens:-

TS : Thin Section

AP : Acetate Peel

H : Hand specimen only

R : Rubber mould

Department Number	Field Number	Description	Collection Location	Preparations
48221	SIB129	?Early Ordovician quartzite	DM87759325	TS
222	331	Ordovician limestone	88009185	AP
223	255	" "	84909540	TS
224	257	" "	"	TS
225	145	Problematic siliceous sediment	89209505	TS
226	155	" " "	89409500	H
227	87	Fissure Filling sediment	88528730	TS
228	86	" " "	"	TS
229	220	Lithofacies I	88738755	AP
230	245	"	87578763	AP
231	212	"	88788766	AP
232	25	"	88808732	AP
233	29	"	"	AP
234	243	"	87658752	AP
235	181	"	87458766	AP
236	211	"	88788766	TS
237	216	"	88788766	AP
238	164	Lithofacies II	87328765	AP
239	195	"	88688767	AP
240	167	"	87328765	AP
241	248	"	87568770	AP
242	247	"	"	AP
243	246	"	87568767	AP
244	198	"	88688767	AP
245	221	Lithofacies III	88768746	AP
246	68	"	88478732	AP
247	225	"	88768746	AP
248	226	Lithofacies IV	"	AP
249	2	"	88808732	TS
250	83	"	88528730	AP
251	175	Lithofacies V	87458766	AP
252	170	"	87328765	AP

Department Number	Field Number	Description	Collection Location	Preparations
48253	SIB250	Lithofacies V	DM87608778	AP
254	15	Lithofacies VI	88808732	AP
255	11	"	"	AP
256	55	"	88508735	AP
257	39	"	88808732	AP
258	37	"	"	AP
259	12	"	"	AP
260	54	"	88508735	AP
261	42	"	88808732	TS
262	58	Lithofacies VII	88478732	AP
263	207	"	88778770	AP
264	84	"	88528730	AP
265	62	"	88478732	AP
266	60	"	"	AP
267	199	Lithofacies VIII	88688767	AP
268	204	"	"	AP
269	94	Lithofacies IX	88588726	TS
270	295	"	88608724	AP
271	299	"	88608720	AP
272	300	"	"	AP
273	97	"	88588726	AP
274	97	"	"	AP
275	98	"	"	AP
276	101	Lithofacies X	88588726	AP
277	116	"	88608724	TS
278	120	"	88608720	AP
279	100	"	88588726	AP
280	297	"	88608724	AP
281	100	"	88588726	AP
282	115	"	88608724	TS
48283	99	"	88588726	AP
98013	106	*Calathium* (new form)	88848731	H
98316	42	*Solenopora*	88808732	TS

Department Number	Field Number	Description	Collection Location	Preparations
98317	SIB66	*Calathium*	DM88478732	TS
318	341	*Calathium*	88608715	TS
319	240	*?Calathium*	88488737	TS
320	262	*Calathium*	88848731	TS
321	114	problematic shell	88608724	TS
322	114	?Sponge	"	TS
323	309	Bumastinae A	88848731	H
324	242	Pliomerinid A	88808732	H
325	239	*?Ephippiorthoceras*	88488737	H
326	160	*Tofangoceras*	"	H
327	168	c.f.*Hormotoma*	87328765	AP
328	193	c.f.*Hormotoma*	"	AP
329	138	Prosobranch B	88249082	H, R
330	138	Prosobranch C	"	H, R
331	329	Helicotomide A	87549458	H
332	138	"	88249082	H, R
333	138	"	"	H, R
334	138	"	"	H, R
335	138	"	"	H, R
336	138	"	"	H, R
337	80	Strophamenid A	88458732	H
338	353	"	89308820	H
339	224	Plectorthid A	88768746	H
340	117	Rugosan A	88608724	TS
341	54	Rugosan B	88508735	AP
342	76	*Streptelasma*		
343	103	*Tryplasma Ceriodes*	88848731	TS
344	54	*Bajgolia caespitosa*	88508735	TS
345	252	" " *Pycnolithus*	89308820	TS
346	332	*Bajgolia c.f. furcata*	88608715	TS
347	54	*Pycnolithus*	88508735	TS
348	180	*Foerstephyllum*	87328765	TS
349	1	*Palaeofavosites poulseni*	88808732	TS
350	47	" "	88488737	TS

Department Number	Field Number	Description	Collection Location	Preparations
98351	SIB 2	*?Lichenaria*	DM88808732	TS
352	50	"	88478736	TS
353	124	*Tetradium apertum*	88488737	TS
354	17	*T. syringoporoides*	88808732	TS
355	206	"	88758760	AP
356	234	*T. bowanese*	88758745	AP
357	203	"	88688767	TS
358	228	*T. variabile*	88768746	TS
359	224	*T. terue*	"	H
360	230	*T. sp. A.*	"	TS
361	229	"	"	AP
362	233	"	"	TS
363	54	Aulacerid A	88508735	TS
364	172	c.f. *Cystostroma*	87328765	TS
365	78	Bryozoan A, *Stictppora*	88478732	TS
366	342	Bryozoan A	88608715	TS
367	54	"	88508735	TS
368	117	Bryozoan B	88608724	TS
369	72	Bryozoan C, *Stictopora*	88478732	TS
370	78	Bryozoan D	"	TS
371	82	?Sponge	88528730	TS
372	224	Conodonts	88768746	

FIG. 2.1 REGIONAL GEOLOGY OF THE IDA BAY AREA

0 1000 2000 3000

Scale – metres
(Scale = 1:25,000)
Contour Interval 200 feet

Grid lines on the margin of this map are 1000 metre intervals of the Australian Map Grid. Full co-ordinates are given only in the southwest corner of the map, and all grid references from this map should be prefixed by the letters DM.

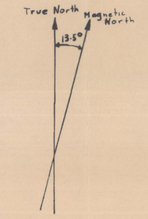

Magnetic North is true for 1977.

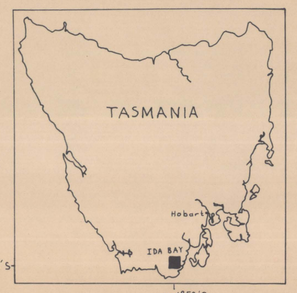

42°26'S — 146°52'E

LOCALITY

KEY

- Qa — Quaternary Alluvium
- Tb — Tertiary Basalt
- Jdl — Jurassic Dolerite
- Rl — Triassic La Perouse Formation
- Ru — Triassic Undifferentiated
- Pcm — Permian Cygnet Coal Measures
- Pt — Permo/Carboniferous Tillite
- Pu — Permo/Carboniferous undifferentiated
- Ss — Problematical Siliceous Sediment
- Ogl — Ordovician Gordon Sub-group Limestone
- Oqt — Ordovician Quartzite
- pEd — Precambrian Dolomite

- Main road (Unsealed)
- Minor road (Unsealed)
- Railway
- Walking Track
- Geological boundary
- Geological boundary (Approximate)
- Geological boundary (Inferred)
- Normal Fault, downthrown side indicated
- Normal Fault (inferred)
- Reverse or Thrust Fault, upper block indicated
- Anticline, plunge direction indicated
- Anticline, concealed
- Dip and Strike of bedding, dip in degrees given.
- Bedding Horizontal
- Quarry or cutting
- Depression

RESPONSIBILITY MAP Scale 1:250,000

1 Present Study Mapping
2 Davidson (1969)
3 Mines Dept. 1:250000 Map (Farmer, 1975)
4 Inferred from present study mapping and previous mapping.

Main roads
Minor roads

FIG. 2:2 OUTCROP MAP OF THE IDA BAY AREA

0 1000 2000 3000

Scale - metres

Contour interval = 200 ft.

This map shows the field mapping data used in the preparation of FIG. 2:1 (Interpretation map). Dips are shown on FIG. 2:1 only. FIG. 2:2 does not show outcrop data for areas not examined in the present mapping project. Refer to FIG. 2:1 for geographical nomenclature, etc.

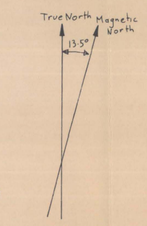

Magnetic North is true for 1977.

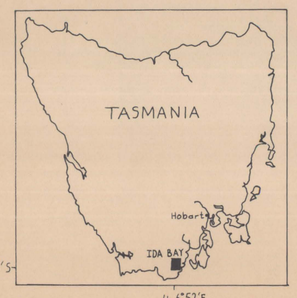

43°24'S 147°26'S

LOCALITY 146°52'E

KEY

Bedrock Outcrop	Loose fragments; Unconsolidated deposits.	
Qa	a	Quaternary Alluvium
Tb	b	Tertiary Basalt
Jdl	x	Jurassic Dolerite
Rl		Triassic La Perouse Formation
Ru	+	Triassic Undifferentiated
Pcm		Permian Cygnet Coal Measures
Pt	t	Permo/Carboniferous Tillite
Pu	p	Permo/Carboniferous Undifferentiated
Ss	s	Problematical Siliceous Sediment
Ogl	g	Ordovician Gordon Sub-group Limestone
Oqt	o	Ordovician Quartzite
pЄd		Precambrian Dolomite

- Main road (Unsealed)
- Minor road (Unsealed)
- Railway
- Walking Track
- Reverse or thrust fault, upper block indicated
- Quarry or cutting
- Depression
- Approximate boundary of areas of known outcrop.

5184000mN

+81000mE 46' 82 83 48' 84 85 86 146°50'E 87 88 89 52' 90 91 54' 92 93 94

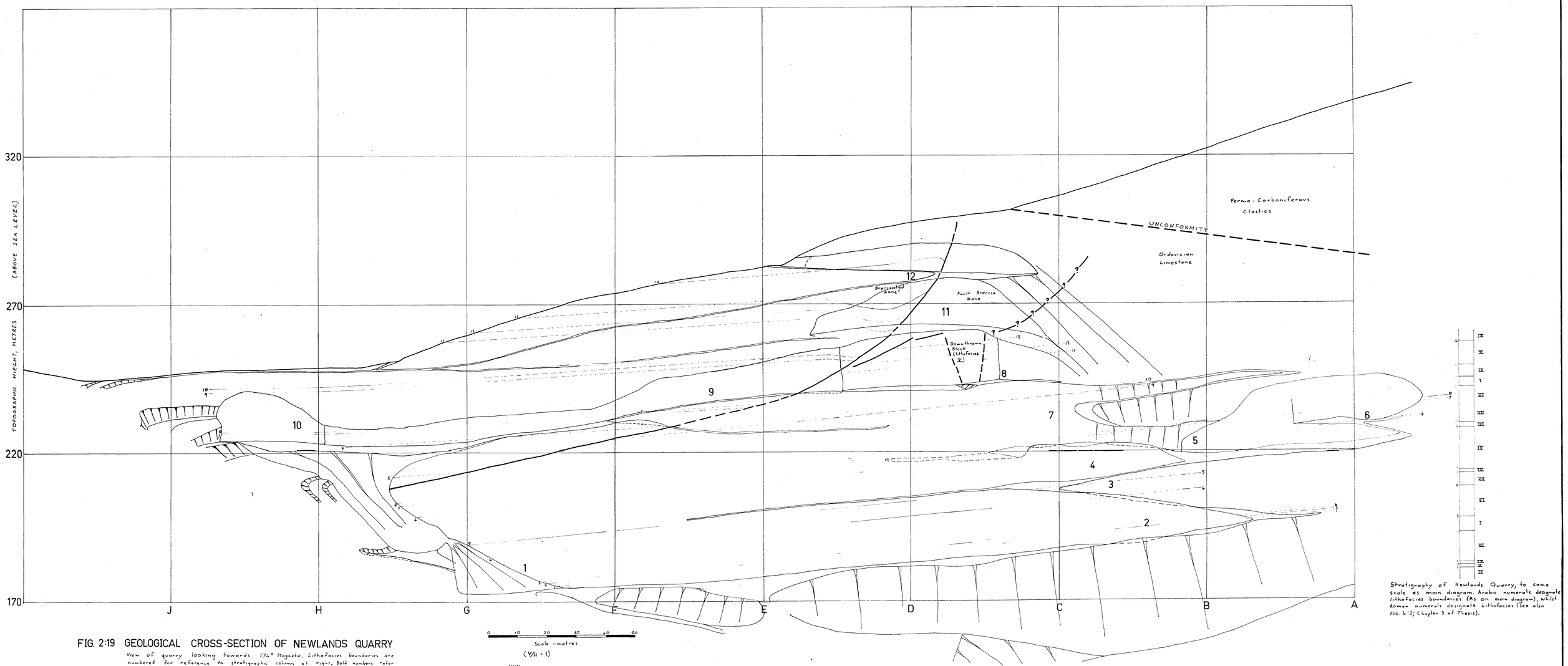

FIG. 2:19 GEOLOGICAL CROSS-SECTION OF NEWLANDS QUARRY

View of quarry looking towards 174° Magnetic. Lithofacies boundaries are numbered for reference to stratigraphic column at right. Bold numbers refer to numbered locations (see Appendix 6), and Letters across bottom of section refer to grid used in FIG. 6:7.
View accurate as of mid-1979

Stratigraphy of Newlands Quarry, to same scale as main diagram. Arabic numerals designate lithofacies boundaries (As on main diagram), whilst Roman numerals designate Lithofacies (See also FIG. 4:1; Chapter 3 of Thesis).

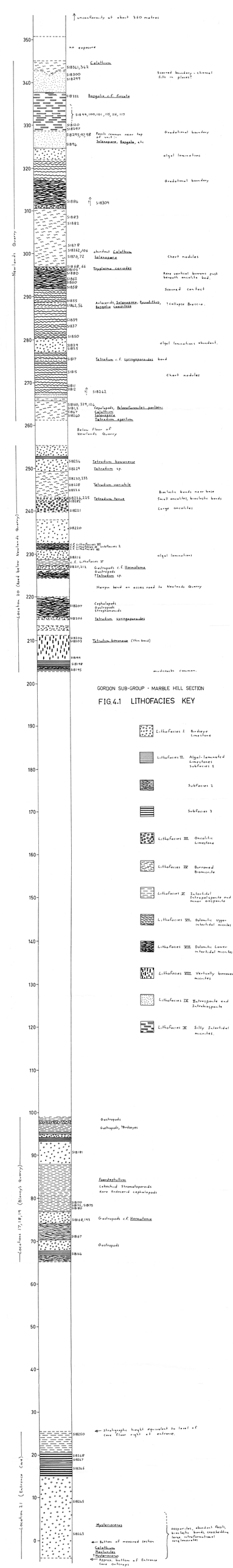
Location 21 (Entrance Cave)
Location 17, 18, 19 (Storey's Quarry)
Location 20 (East bster Newlands Quarry)
Newlands Quarry
unconformity at about 360 metres
no exposure
Calathium
Scoured boundary - channel fills in places?
Bolgalia c.f. forsete
Gradational boundary
Fossils common near top of unit
Solenopora, Bolgalia, etc
algal laminations
Gradational boundary
Tetradium c.f. syringoporaeides band
Chert nodules
Below floor of Newlands Quarry
Tetradium howeanum
Tetradium sp.
Tetradium verticillo
Tetradium tenue
Large oncolites
c.f. Lithofacies IV
Gastropods c.f. Hormotoma
Gastropods
Tetradium sp.
Horizon band on access road to Newlands Quarry
Cephalopods
Gastropods
Stromatoporoids
Tetradium syringoporaeides
Tetradium himmaense (thin band)
mudcracks common.
Gastropods
Gastropods, Thordeyes
Favositothallum
Labechiid Stromatoporoids
Gastropods c.f. Hormotoma
Gastropods
Stratigraphic height equivalent to level of cave floor right at entrance.
Mystieridrerus
Bottom of measured section
Calathium
Manlaxites
Hydnoceras
Approx. bottom of Entrance Cave (estimate)
GORDON SUB-GROUP - MARBLE HILL SECTION
FIG. 4.1 LITHOFACIES KEY
Lithofacies I Birdseye Limestone
Lithofacies II Algal-laminated Limestones Subfacies 1
Subfacies 2
Subfacies 3
Lithofacies III Oncolitic Limestone
Lithofacies IV Burrowed Biomicrite
Lithofacies V Intertidal Intraspelsparite and minor wackestone
Lithofacies VI Dolomitic Upper-intertidal micrites
Lithofacies VII Dolomitic Lower-intertidal micrites
Lithofacies VIII Ventually laminated micrites
Lithofacies IX Intrasparite and Intrabiosparite
Lithofacies X Silty Intertidal micrites.

FIG. 4:6 GEOLOGICAL CROSS-SECTION OF BLANEY'S QUARRY

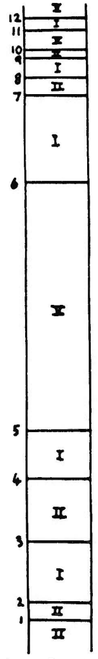

Stratigraphy of Blaney's quarry, scale : 2cm = 5 metres vertically. (See also FIG. 4:1 to compare stratigraphy). Arabic numerals refer to bed boundaries on main diagram, Roman numerals refer to lithofacies (See Chapter 3 and FIG. 4:1)

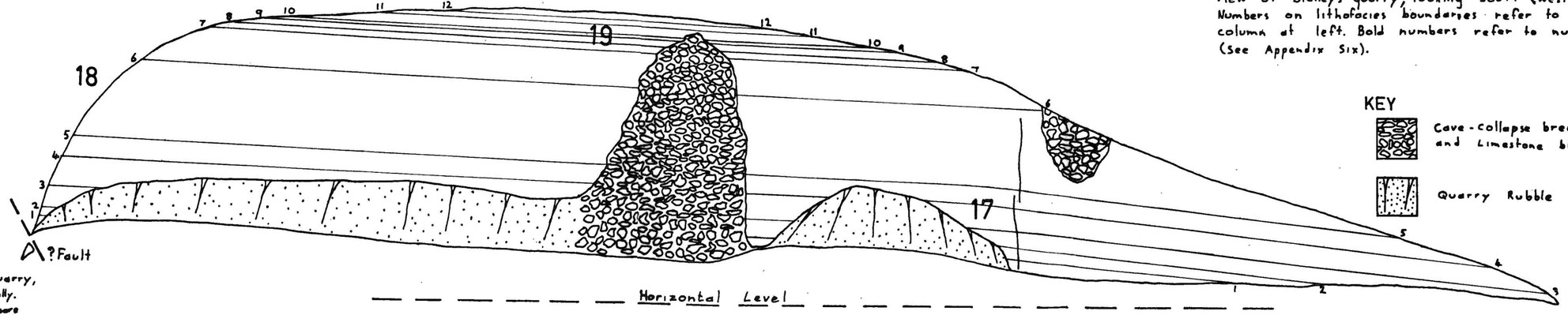

0 10 20 30 40

Scale – metres (V/H = 1)

View of Blaney's quarry, looking south (west is to right). Numbers on lithofacies boundaries refer to stratigraphic column at left. Bold numbers refer to numbered locations (See Appendix Six).

KEY

Cave-collapse breccias (Travertine and Limestone blocks)

Quarry Rubble

FIG.4:7 PLAN OF NEWLANDS QUARRY

(Accurate as of mid-1979, although some parts undergoing change)

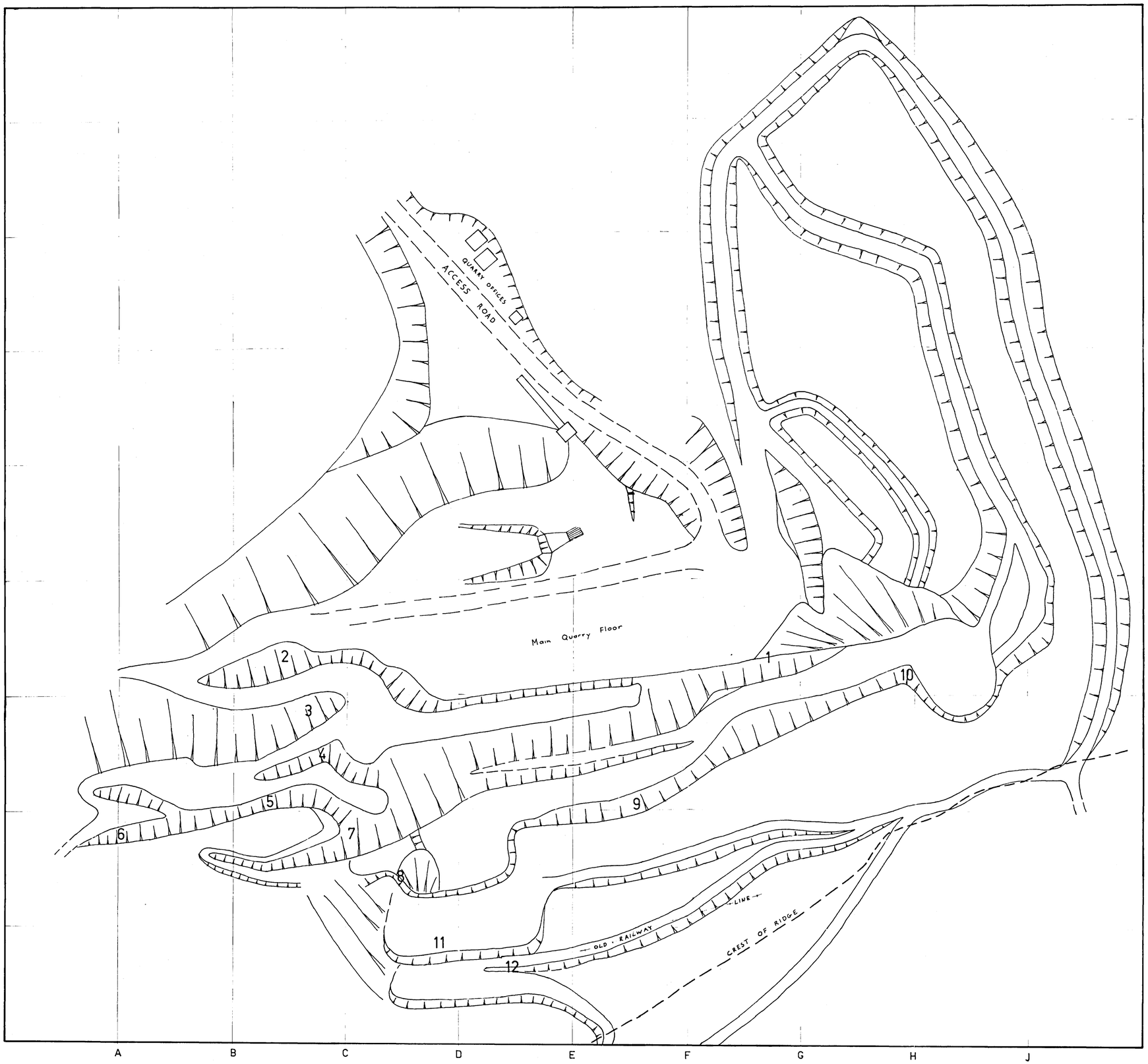

0 50 100

Scale - metres

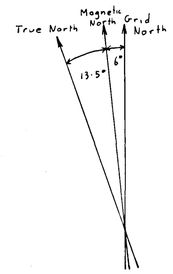

KEY

5 - Numbered locations (See Appendix Six)

- Quarry faces, cuttings, rubble piles
- Roads, benches
- Building

Plan adapted from plan prepared by PEACOCK DARCEY & ANDERSON (20-6-75)